MEMBRANE GAS SEPARATION OF FISCHER-TROPSCH GASES

By

M. van Vuuren (B.Eng.)

Dissertation submitted in fulfillment of the requirements for the degree Masters in Engineering in the School of Chemical and Minerals Engineering at the Potchefstroom campus of the North-West University

Supervisor: Prof. S. Marx (North-west University, South Africa)
Co-supervisor: Prof. H. Neomagus (North-west University, South Africa)

Potchefstroom
South Africa
November 2005

Summary

Membrane-based gas separation has attracted considerable interest over the past few years because of its low energy consumption and cost-effective separation. Many studies have been conducted related to amorphous silica membrane. This membrane has been reported to perform well with respect to separating various gases including the Sasol Fischer Tropsch gases Hydrogen, Methane and Carbon dioxide.

This study is devoted to the investigation of the performance of a commercially available amorphous silica membrane for the separation of a typical Fischer Tropsch gas mixture.
For both single and binary permeation experiments performed, it was found that the membrane permeation of the gases Hydrogen, Methane and Carbon dioxide is independent of the trans-membrane pressure.
As far as temperature is concerned, it was established that the permeation of the three gases is inversely dependent on an increase in operating temperature. This was observed for both single and binary permeation experiments.
In general, higher fluxes were achieved if the gases were fed directly onto the support (shell side feed).
Selectivity towards Hydrogen was not significantly influenced by any of the operating parameters investigated (temperature, trans-membrane pressure, membrane orientation).

The overall conclusions that were made based on the results obtained are that this membrane can essentially be classified as a Knudsen-type membrane, since selectivity values are in the region of Knudsen transport. The selectivity values are thus not large enough to qualify this membrane as a successful gas separation membrane.

It was however, established that this membrane may perform more effectively if used for pervaporation application purposes.

Samevatting

Membraan gebaseerde gas skeiding het oor die afgelope aantal jare groot belangstelling uitgelok weens die lae energie verbruik en koste effektiwiteit verbonde aan hierdie tegnologie. Verskeie studies is uitgevoer met betrekking tot amorfe silika membrane. Daar word gerapporteer dat hierdie tipe membrane reeds verskeie gasse, insluitend die Sasol Fischer Tropsch gasse, waterstof, metaan en koolstof dioksied suksesvol kan skei.

Hierdie studie is gewy aan 'n ondersoek na die werkverrigting van 'n kommersieël beskikbare amorfe silika membraan vir die skeiding van 'n tipiese Fischer-Tropsch gasmengsel.
Vir beide enkel and binêre deurlaatbaarheids eksperimente is daar bevind dat die deurlaatbaarheid van die drie gasse waterstof, metaan en koolstof dioksied, onafhanklik is van die trans-membraan druk.

Wat temperatuur aanbetref, is daar vasgestel dat die deurlaatbaarheid ten opsigte van die drie gasse omgekeerd afhanklik van 'n toename in die bedryfs temperatuur is. 'n Hoër deurlaatbaarheid word ook behaal as die gasses direk op die steunlae gevoer word (Mantel kant voer).
Veranderinge in die bedryfstoestande het tot geen beduidende toename in selektiwiteit gelei nie.

Die algehele gevolgtrekking wat gemaak kan word is dat die membraan essentieël geklasifiseer kan word as 'n Knudsen-tipe membraan, weens die feit dat selektiwiteit waardes binne die betrokke grense val. Die selektiwiteit waardes is dus nie groot genoeg om hierdie membraan te kwalifiseer as 'n suksesvolle gas skeidings membraan nie.
Hierdie membraan mag egter meer effektief presteer indien dit aangewend word vir pervaporasie doeleindes.

Declaration

I, Marcelle van Vuuren, hereby declare that the dissertation entitled: "**Membrane Gas Separation of Fischer-Tropsch Gases**" submitted in fulfillment of the requirements for the degree Master in Engineering (M. Eng.) is my own, and that all sources consulted are shown in the references. The assistance received and provided regarding this dissertation is found in the acknowledgements.

Signed, at Potchefstroom on the 25th day of May 2006.

.....

M. van Vuuren

Acknowledgments

The following persons are acknowledged and thanked for their assistance during and upon completion of this dissertation:

- Prof. S. Marx – Project Leader and Tutor
- Prof. H. Neomagus – Assistant Tutor and Mentor
- Mr. J. Kroeze – Experimental Setup and Equipment
- All persons from the department of Chemical and Minerals Engineering who provided any assistance with respect to this study.
- Prof. H. Krieg and all persons from the department of Chemistry, who were involved in the synthesis of materials used to perform experiments.
- Mr. R. Farmer – Experimental Assistance
- Mr. J. Scholtz (project mentor) and the financial assistance and support provided by Sasol Ltd.

Table of Contents

List of Symbols And Abbreviations

Symbol	Unit	Description
$\alpha_{i/\varphi}$	-	Selectivity of membrane with respect to component *i.*
D	$mol.m^{-2}$	Diffusion Coefficient
σ	-	Variance of a set of values
σ	m	Boltzman's constant
δ	m	Membrane Support Thickness
τ	-	Tortuosity
ℓ	m	Membrane tube length
r_p	m	Mean pore radius
ε_{sup}	%	Support porosity
η	$N.s.m^{-2}$	Gas viscosity

Abbreviation	Unit	Description
R	J/mol.K	Universal Gas constant
M	$Kg.mol^{-1}$	Molecular Weight
N	$mol.m^{-2}.s^{-1}.kPa^{-1}$	Permeance
J	$mol.m^{-2}.s^{-1}$	Flux
C	$Mol.m^{-3}$	Concentration
SEM	-	Scanning Electron microscopy
GC	-	Gas Chromatograph
SS	-	Stainless Steel

List of Tables

List of Figures

CHAPTER 1 Project Definition

1.1 INTRODUCTION

Separation is an important operation in industry, and often chemical conversions in many processes are restricted by thermodynamic equilibrium. Consequently, products from a reactor or gasifier have to be separated from unconverted reactants. Typically the recovery or removal of inorganic gases from organic mixtures is quite important in practical industries. The recovery of hydrogen from off gases and removal of carbon dioxide from methane mixtures are typical examples of such separation and purification processes [Asaeda, 2001:151].
Distillation, extraction, absorption and adsorption processes are not only energy consuming but also require complicated facilities. An alternative thus needs consideration.

Increasing amount of research in the formation of gas separation membranes indicates that membrane technology is growing and becoming another alternative for industrial gas separation processes.
Membrane technology is a fairly simple and recent technology that proves to be more energy-efficient than conventional separation processes. Today membrane processes are used in a wide range of applications and the numbers of such applications are still growing.
Membrane separations are currently gaining importance, and separations based on microporous membranes such as zeolites, microporous carbons and carbon molecular sieves are becoming increasingly popular. Some researchers have developed sol-gel derived silica or modified silica membranes for separation [Asaeda, 2001:151]. For the purpose of this study, ceramic-based membranes; a NaA zeolite prepared by centrifugal casting (used as a test membrane), and amorphous industrial silica (Pervatech,B.V.®), and their efficiencies as separation alternatives is thus studied.

1.2 MOTIVATION AND STATEMENT

Most membranes for commercial separation processes are natural or synthetic, glassy or rubbery polymers. However, for high temperatures (>200 °C) or operation with chemically reactive mixtures, ceramics, metals, and carbon find applications [Seader *et al*, 1998]. Increasingly new applications of membranes in fuel cells and in catalytic membrane reactors are studied. The new application fields have high demands and expectations for the membrane material such as thermal stability for high-temperature applications, solvent and chemical stability, sterilization ability and biocompatibility. Despite their variability and the highly developed module technology, organic polymer membranes can hardly fulfill the structural and functional requirements of the application fields.

The development of new ceramic-based membranes for the dehydration of hydrocarbon mixtures and the separation of organic mixtures is of great interest to Sasol Ltd. since regeneration of any components that can be successfully separated will prove to be economical. The Fisher Tropsch (FT) process of reforming natural gas into carbon monoxide and hydrogen (syn-gas) and using this gas to manufacture liquid fuels and chemicals is well known and has been in commercial use for over 50 years [Dry, 2002]. Since the cost of syn-gas is high, it is important that the maximum amount is converted in the downstream FT reactors. This requires that the composition of the syn-gas matches the overall usage ratio of the reactions in the FT reactors. The tailgas from the FT reactors, containing unconverted syn-gas, CH_4 and CO_2 is recycled to the autothermal reformers. Recycling of CO_2 ensures the attainment of the required H_2/CO ratio for the FT reactors [Dry, 2002]. Therefore, achieving the necessary separation of the tailgas mixture from the reactor product is of great importance.

Using membrane-based gas separation in order to ensure optimum syn-gas composition for maximum conversion, could resolve in a more cost effective FT process. Since microporous ceramic-based membranes meet all the criteria for suitable separation of these gases, any further developments with regard to these type membranes could lead to a major improvement in the separation field.

The classes of membranes used for investigation are thus, microporous ceramic-based type membranes such as NaA and Amorphous Silica, because of among others, their widespread application in industry and their overall chemical stability.

1.3 OBJECTIVES

The objectives of this investigation are:

- Investigation of the effect of different process variables, such as temperature, pressure drop and membrane orientations on the flux or permeance, and/or mixture selectivity of the gases H_2,CO_2 and CH_4 passing through an amorphous silica membrane.

- To establish the efficiency of the microporous membrane amorphous silica, by collecting binary and single permeation data for gaseous flow through this membrane, supported by α-alumina.

- Analysis of the data collected from permeation tests performed on specially constructed laboratory apparatus will include calculations of the various separation factors and selectivities for the gases considered.

- To establish the role of ceramic-based membranes in recent separation technology, particularly gas separation, and the industrial application potential these specific membranes hold for the future.

1.4 SCOPE OF INVESTIGATION

This dissertation deals with the following aspects:

- A broad literature overview (Chapter 2) regarding relevant concepts necessary to understand the investigation at hand.

- The design and construction of high pressure (up to 20 bar) and moderate temperature (up to 100 °C) membrane separation apparatus with an appropriate membrane cell. This detail is reported in detail in chapter 3.

- Implementing an experimental procedure involving permeation with supported membranes by using NaA membrane as test membrane. The variables examined are, feed composition, temperature, pressure and membrane orientation.

- The results obtained from permeation tests, and interpretation of the pure component permeation data obtained for amorphous silica (Chapter 4).

- The processing of binary permeation data collected and the interpretation thereof (Chapter 5).

- Conclusions and remarks regarding the outcomes of the investigation (Chapter 6).

CHAPTER 2

Literature Overview

2.1 INTRODUCTION

In this chapter a broad overview is given of the various concepts that pertain to the research project at hand. Concepts and terminology used concerning separation technology, the latest developments in membrane gas separation concerning regarding amorphous silica membranes in particular, is also dealt with in this chapter.

2.2 MEMBRANE DESCRIPTION AND CLASSIFICATION

A membrane can be defined as a semi-permeable active or passive barrier, which permits preferential passage of one or more selected species or components of a gaseous and/or liquid mixture solution under a certain driving force [Hsieh, 1996]. The driving force for permeation can be a concentration, pressure, temperature or an electrical potential gradient [Mulder, 1998:15].

Membranes can be used for various applications, and in general, membranes are used for [Vroon, 1996:293]:

- Separation of mixtures,
- Manipulation of chemical reactions.

For these applications membranes can be classified according to the type of separation involved, e.g. microfiltration, ultrafiltration, reverse osmosis, gas separation and pervaporation or they can be classified in terms of the materials they are composed of, viz., polymer or inorganic membranes. A further division can be made on the basis of their structure, e.g. dense or porous, symmetric or asymmetric. A further division of symmetric and asymmetric membranes are summarised in Figure 2.1.

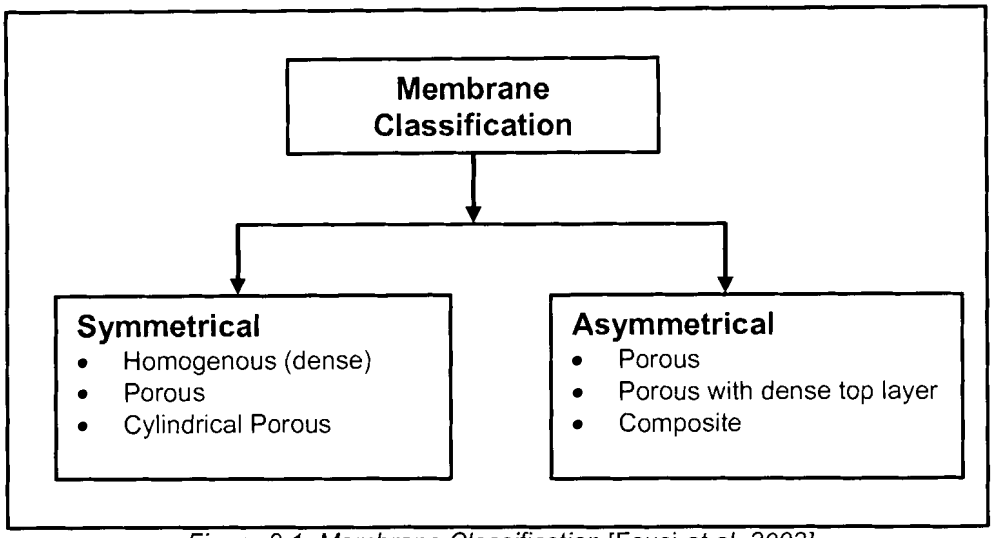

Figure 2.1: Membrane Classification [Fausi *et al*, *2003]*

The primary component that is rejected in membrane processes is referred to as the retentate (or solute) while the component passing through the membrane is termed permeate (or solvent). Figure 2.2. depicts this.

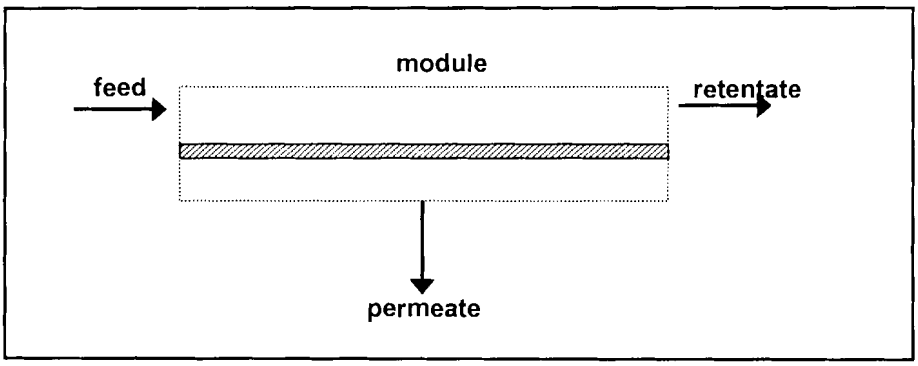

Figure 2.2: Membrane process with feed stream split. [Mulder, 1998]

There are primarily two modes of operation for membrane processes (see Figure 2.3), classified according to the direction of the feed stream relative to the orientation of the membrane surface: dead-end filtration and cross-flow filtration.

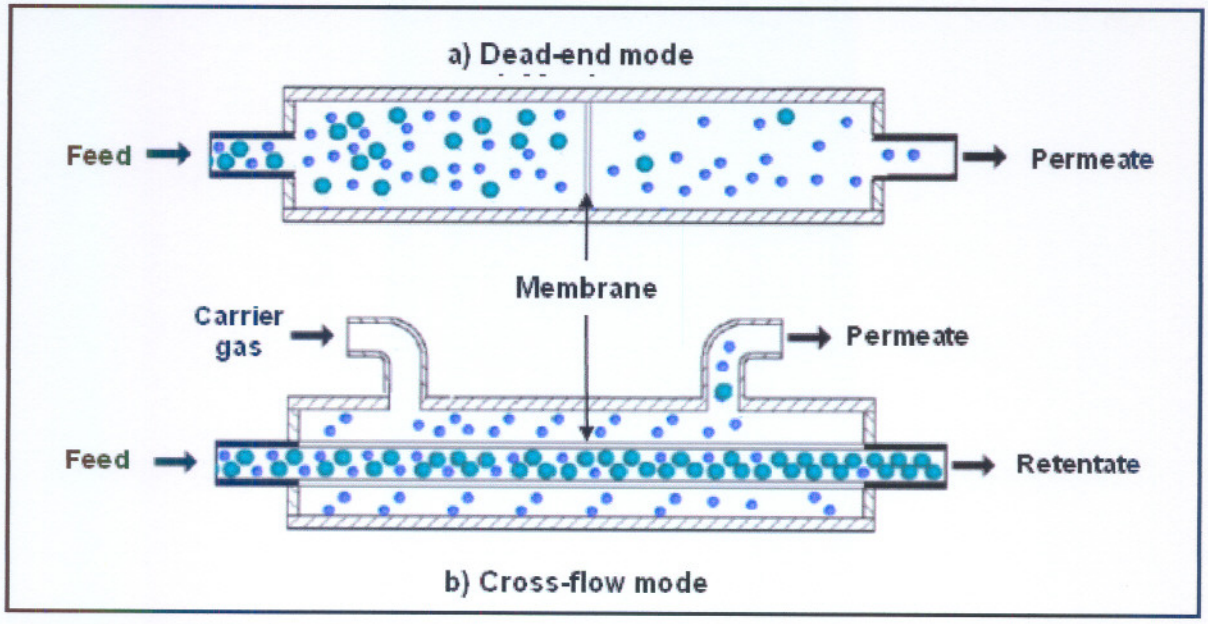

Figure 2.3: Modes of operation for a membrane process: a.) Cross-flow filtration mode and b.) Dead-end filtration mode [Hsieh, 1996]

In cross-flow mode, the membrane is usually tubular, and an optional sweep gas can be used which dilutes the permeate, and lowers the partial pressure of the components, thus enhancing the flux through the membrane. In dead-end mode however, the membrane is usually a disk, and no sweep gas is used [Seader *et al*, 1998].

The key to an efficient and economical membrane separation process is the manner in which the membrane is packaged and modularized.

Desirable attributes of a membrane are:

1. Good permeability,
2. High selectivity,
3. Chemical and mechanical compatibility with the processing environment,
4. Stability, freedom from fouling and reasonable useful life,
5. Amenability to fabrication and packaging, and
6. Ability to withstand large pressure differences across the membrane thickness.

2.3 MICRO-POROUS,CERAMIC-BASED MEMBRANES

2.3.1 Zeolites

Today, development in the field of membrane technology is driven by several factors. Established commercialized membrane technologies may suffer from some limitations such as low thermal or chemical stability, membrane fouling, low permeability and low selectivity. Due to their favourable separation applications, zeolites have rapidly gained attention in modern times.

Zeolites are **crystalline** microporous aluminasilicalites. They are composed of a network of SiO_4 and AlO_4 tetrahedra which are interconnected through oxygen atoms. In this way a one, - two or three-dimensional network is formed. The framework exhibits a negative charge when aluminum is incorporated in the aluminosilicates. The negative charge is compensated by a positive ion (e.g. Na^+, K^+, Ca^{2+}, or H^+). The Si/Al ratio determines the hydrophilic/hydrophobic nature, the ion-exchange capacity, the catalytic activity and the acid stability. Hydrophilic membranes are more water selective and hydrophobic membranes are more selective towards organic compounds (organophilic). The pore size of the zeolite channels is determined by the number of oxygen atoms that form the aperture ring (usually 6, 8, 10, 12 atoms) [Sommer & Melin, 2005].

Zeolites are also often referred to as molecular sieves, because of the exclusion of some molecules from the pores based on their molecular size. The framework of some zeolites is, however not a rigid structure and molecules that are larger than the zeolite pores are able to adsorb in the zeolite by deforming the pores.

Typical zeolite structures are depicted in Figure 2.4, where the pores in the zeolite structure are clearly visible.

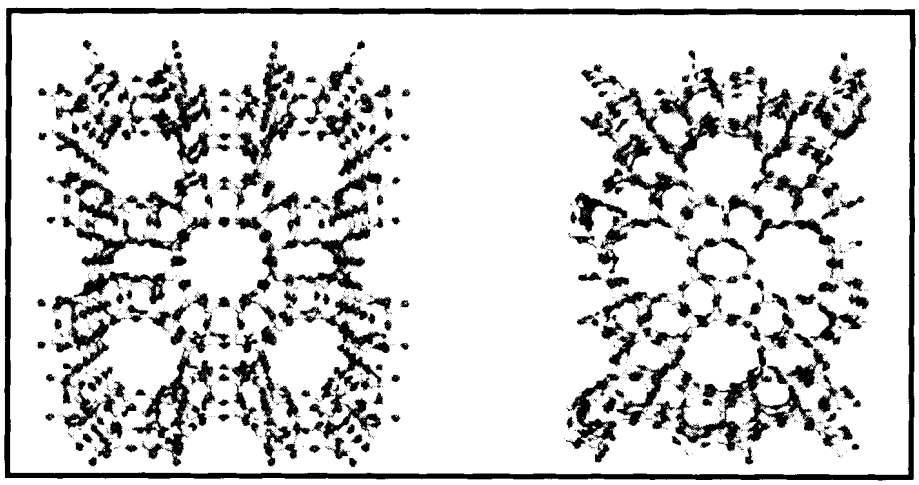

Figure 2.4: *The structures of zeolites mordenite (a) and silicalite (b). The pores in the zeolite* structure are clearly visible [Schuring, 2002].

Zeolite membranes do exhibit various advantages and disadvantages, when one considers them for industrial use.

The advantages are:

- Zeolites can potentially separate molecules in a continuous way.
- They are highly stable under thermal cycling, high temperatures, and harsh physical and chemical environments, which other membranes cannot withstand.
- The chemistry of the zeolites can be modified to provide catalytic properties, to change them between hydrophobic and hydrophilic surfaces, to change the pore size and structure (creating different types of zeolites), etc., which make them useful for many different applications.
- Tailored selectivities, low energy consumption, and potential for combined reaction-separation systems [Nair *et al*, 2001].
- Several Zeolites are known to separate organic molecules based on their properties of preferential adsorption, preferential diffusion, or pure molecular sieving (size exclusion) [Nair *et al*, 2001].
- High separation selectivities have been reported for a variety of mixtures using different types of zeolite membranes, with the most common being MFI zeolites such as silicalite and ZSM-5.
- A great advantage of using zeolites is that these catalysts, because of the specific structure of the pores and cages, not all products can be easily formed, and as a result can dramatically enhance the *selectivity* (i.e. the fraction of desired products of all products that are formed) of the reaction.

The disadvantages associated with these types of membranes are however:

- In general zeolites are relatively expensive to manufacture.
- They require some sort of support, normally stainless steel, but alumina supports are also used often as of late [Biesheuval *et al.* 1998).
- Zeolite membranes are always imperfect, meaning that defects always exist which retract form the quality of the separation obtained [Van Bekkum *et al*, 1991].

2.3.2 NaA Zeolite Membrane

NaA zeolite membrane belongs to the class of membrane where separation can take place by means of molecular sieving i.e. separation based on the molecule size of the specific component is of importance. It is important to note that this type of membrane is mainly used for pervaporation [Chen,2005].

NaA is built up of a three-dimensional network of SiO_4 and AlO_4 tetrahedra (see Figure 2.5), and in this way a cage-like pattern exists where a pore of 0.41 nm is formed. [Mulder, 1998] Since this pore size is similar to the kinetic diameter of the low hydrocarbon compounds as well as oxygen (O_2), nitrogen (N_2), and carbon dioxide (CO_2), it is possible to used A-type zeolite membranes to obtain high separation performance.

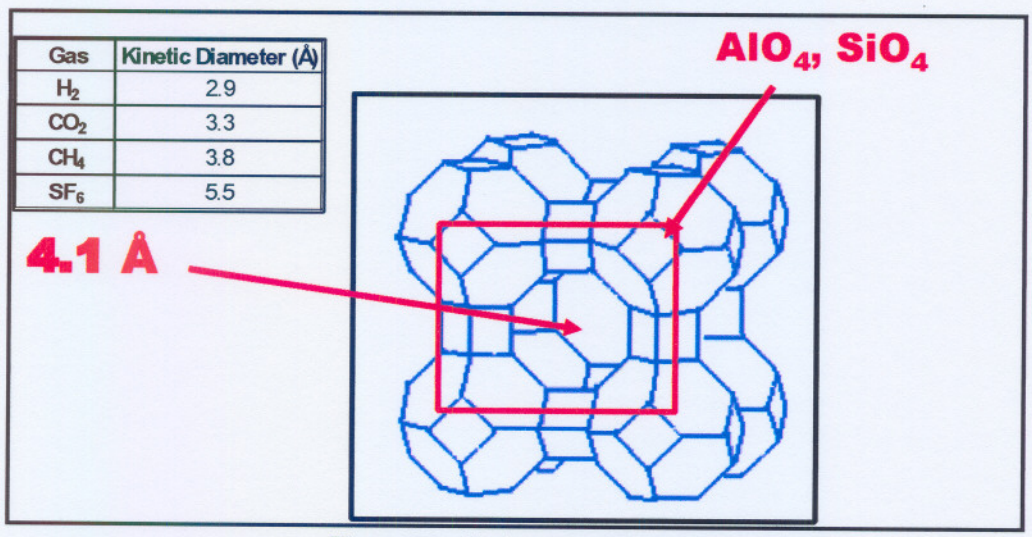

Figure 2.5: NaA zeolite Membrane Structure

Due to the fact that NaA contains a high amount of aluminium, this type of membrane is hydrophilic in nature.

A number of uses for NaA have been reported:

- Pervaporation dehydration of organic/water mixtures developed by Mitsui Engineering and Shipbuilding Co.Ltd [Xu, et al., 2004].
- Continuous separation of linear and branched alkanes.
- Removal of radioactive wastes.

2.3.3 Amorphous Silica

Inorganic micro-porous membranes can be further subdivided into amorphous or crystalline types. Zeolite membranes are important examples of the crystalline type. Amorphous silica is an inorganic material containing exceptionally small pores (microporous).

The pore diameters of this material is usually smaller than 4Å and shows high fluxes for small molecules (such as hydrogen) combined with high selectivities for these molecules with respect to larger ones.

Membranes based on this material have an asymmetric structure with the actual selective microporous silica positioned on a support structure comprising several

α and γ-alumina layers. Silica membranes were discovered more than a decade ago and are still subject of extensive study [Peters *et al.*, 2004].

The chemical and thermal stability of silica membranes are favourable compared to those of organic membranes. These properties make silica membranes interesting candidates for separation of permanent gases in chemically and thermally aggressive environments [Benes, 2000].

Two different types of micro-porous silica membranes can be distinguished; Chemical Vapour Infiltrated (CVI) membranes, which are commercially available, and sol-gel derived silica membranes, which are not yet commercially available.

In the past decade sol-gel derived micro-porous silica membranes have been studied extensively, starting with Uhlhorn *et al.* (1989) and De Lange (1995). Improvements in the synthesis of supported silica membranes have resulted in very thin defect free layers [De Vos and Verweij, 1998a]. Due to the small pore size these silica membranes show high fluxes for small molecules like hydrogen, helium, carbon dioxide and oxygen, and high selectivities for these molecules with respect to larger gas molecules, such as SF6 and various hydrocarbons.

The thin layers are dip-coated onto a multi-layered porous supporting structure, usually consisting of a γ-alumina layer on top of an α-alumina layer, see *Figure 2.6*.

The γ-layer provides a smooth surface with sufficiently small pores to enable formation of the silica layer from sol particles, while the α-layer provides mechanical strength. Details about the synthesis can be found in section 2.3.5.

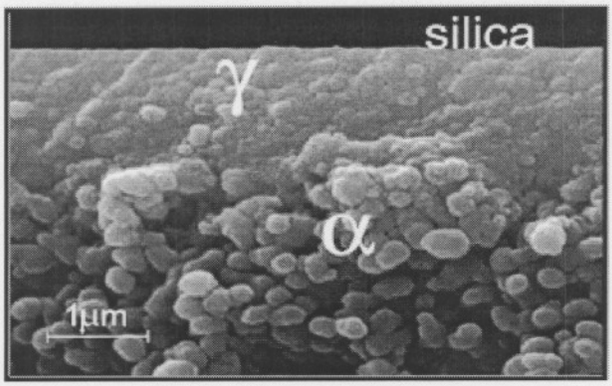

Figure 2.6: SEM-micrograph of supported silica membrane [Benes, 2000]

2.3.4 Membrane Supports

Membrane synthesis is still an empirical activity in which a lot of chemical knowledge and experience is needed, so that the synthesis of membranes is not quite obvious. Two counteracting requirements are asked for; a thin layer, to achieve sufficiently high fluxes and a defect free layer, to achieve high separation efficiencies. A membrane thus requires some sort of support structure to provide mechanical strength and to improve the performance of the membrane.

Membrane supports are usually micro-porous and can have a significant influence on the membrane performance [Van de Graaf, 1999]

Porous ceramic and stainless steel supports can be used for high temperature applications. Recent trends when working with membranes however, is to use an alumina support (α - Al_2O_3). This type of support is more economical in a laboratory-scale situation. [Van Bekkum *et al.*, 1991].

The supports may take the form of large flat disks, which is used currently on an industrial scale and prove to be advantageous from an academic point of view, but a current trend however, is to synthesize tubular supports that prove to be structurally stronger, more economical, easier to scale-up and practical for installation purposes. A disadvantage however, of this geometry is high costs associated with tubular ceramic membrane supports and a low surface area-to-volume ratio (typically < 500 $m^2.m^{-3}$) [Peters et al., 2004].

2.3.5 Membrane Manufacturing

A proper investigation into the performance of a membrane can only be undertaken if certain general concepts regarding the manufacturing of a membrane are clearly understood.

NaA Zeolite Synthesis

Recent literature on the synthesis of zeolites reveals that the synthesis process for well known zeolite composite structures are still carried out batch-wise, using a so called in-situ hydrothermal synthesis coating method onto porous (alumina, stainless steel) supports.
Successful membrane formation in one-process requires nucleation and growth of zeolite crystals on the support surface, a process that competes with solution events.

All zeolite synthesis entails that firstly a gel or clear solution is prepared containing the silicon and aluminum required for the final zeolite structure. After aging this precursor solution, both the ceramic support and the solution is added to a autoclave (stainless steel container), sealed and placed in an oven. The autoclave containing the solution is heated. At elevated temperature (and pressure - sealed autoclave), crystallization of the zeolite starts. This heated process is referred to as the hydrothermal treatment and is part of any zeolite synthesis - as it is the step where the zeolite structure is formed. After maintaining the autoclave at elevated temperatures the crystallization continues until the all the aluminum and silicon have been depleted in the solution. After cooling, the membrane is removed, washed and dried. It is now ready for use.

Amorphous Silica Synthesis

This type of membrane has been licensed to Sulzer Chemtech GmbH Membrane Technology, Neunkirchen, Germany and is now commercialized as Pervap® SMS. The tubular ceramic support made from α- and γ-alumina, usually has an outer diameter of 0.014 m, an inner diameter of 0.008 m and a length of 1m. The asymmetric support consists of four layers in total. The theoretical fundamentals of the manufacturing process are as follows [Sommer *et al.*, 2005]:

The base support provides mechanical strength, whereas the intermediate layers compensate for the surface roughness and reduce the pore size, in order to obtain a defect free support for

the final separation layer. Firstly, the macroporous α-alumina is extruded from a ceramic paste, which is followed by a sintering procedure. Secondly, two α-alumina layers are film-coated onto the base tube using a colloidal suspension, which involves a drying and sintering step. Thirdly, a γ-alumina layer is applied by slip-coating a boehmite sol, which is transformed during a heat treatment. Finally, the selective layer of amorphous silica is generated through a sol–gel process. A silicon alkoxide is hydrolyzed, resulting in the production of a polymeric inorganic silica sol. The sol is coated onto the support by dipping, followed by a drying step and calcination at 400 °C. The thickness of the silica separation layer as measured by scanning electron microscopy is usually in the range of 150–200 nm. From gas separation measurements with single compounds of different kinetic diameters, the pore size has been estimated to be about 0.4 nm. Due to its hydrophilic nature, this membrane can be used for dehydration [Sommer et al, 2005]. The amorphous silica can be modified by the incorporation of methyl- or ethyl-groups. That way the chemical and thermal stability of the membrane top layer can be increased and adapted to the separation of small polar organic compounds like methanol or ethanol from non-polar organics. Another type of microporous silica membranes has been supplied by Pervatech BV, Enter, The Netherlands which is now offering this technology in co-operation with Kuhni AG, Allschwil, Switzerland. These membranes are made following a similar preparation method. The separation layer is applied on the inside of a commercial asymmetric ceramic tube, which has an outer diameter of 0.01 m, an inner diameter of 0.007m and a length of 0.3 m. Thereby, the ethanol diluted sol flows vertically through the porous support for 4 s. By the extraction of ethanol, a gel is formed with chain-shaped silicon structures. After calcination, a thin top layer with small micropores is formed. All commercially available membranes are sealed with Viton or ethylene-propylene-diene monomer (EPDM) O-rings in a tubular three-end stainless steel module. The effective membrane areas were between 4×10^{-3} and 6×10^{-3} m^2, depending upon the diameter of the investigated membrane and its length, which ranges between 0.15 and 0.25 m.

2.4 TRANSPORT CONCEPTS IN GAS SEPARTION MEMBRANES

Gas Permeation

Gas permeation involves gases on a high pressure side of a membrane permeating though the membrane to a low-pressure side [Seader *et al.*, 1998].

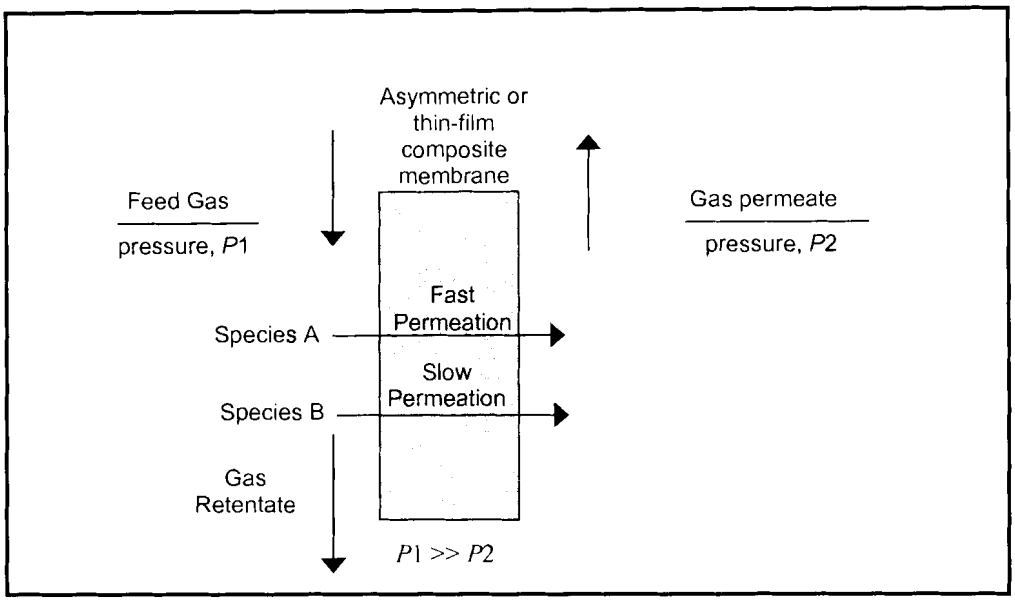

Figure 2.7: Gas Permeation

In Figure 2.7 above, the products are a permeate that is enriched in component A and a retentate that is enriched in B. A near perfect separation is generally not achievable. If the membrane is microporous, as for example in high temperature applications, pore size is extremely important because it is usually necessary to block the passage of species B [Seader *et al.*, 1998].

Gas permeation must compete with distillation at cryogenic conditions, absorption, and pressure-swing adsorption. The advantages of gas permeation are [Seader *et al*, 1998]:

- Low capital investment,
- Ease of installation,
- Ease of operation,
- Absence of rotating parts,

- High process flexibility,
- Low weight and space requirements,
- Low environmental impact, and
- If a feed gas is already at high pressure resulting in no compression of the gas, then no utilities are required.

Gas permeation also competes favourably with other separation processes for hydrogen recovery because of high separation factors that are achieved.
Many theories describing transport through microporous materials is available in literature. The fact that not all microporous media are uniform and that more than one mobile species may be present results in increasing complexity of the theories.

The single gas permeance can be explained as the result of three simultaneous permeation mechanisms (Van de Graaf *et al.*, 1998a): 1) permeation through defects, 2) activated gaseous diffusion (also called activated translation diffusion) and 3) surface diffusion of adsorbed species. The first of these mechanisms is the dominant one for molecules whose kinetic diameter is larger than the membrane pores. In this case, it is likely that Knudsen (meso-porous defects) or viscous (macro-porous defects) behaviour will be observed, although the balance between both types also depends on the operating pressure and temperature. Permeation through defects can also be important for molecules that are weakly (low in energy) or not at all adsorbed on the zeolite.

The permeance of a single gas as a function of temperature for a defect-free micro- porous membrane is in most general case, similar to the one shown in figure 2.8. The qualitative interpretation of this trend considers a combination of two transport mechanisms: the surface diffusion and the gas translational diffusion (activated transport).
At low temperatures, the amount of gas adsorbed in the membrane pores is high; in particular, in the first part of the reported curve (figure 2.8) (AB) the permeance increases with temperature because the mobility of the adsorbed molecules increases, even if the surface coverage decreases. In some cases it is possible to reach a maximum (B) after which the increase in mobility cannot compensate the decrease of the surface coverage (BC). Point (C) is representative of the temperature at which the amount of adsorbed gas is not relevant anymore. In the ABC part of the transport occurs mainly via adsorption followed by surface diffusion.

At higher temperature (CD) the transport is controlled by the activated transport through the micropores (gas translation diffusion) [Algieri *et al*, 2003].

In the case of a mixture, the selective adsorption is important in determining the membrane separation properties; more species can pass through the membrane pores more easily than the others.

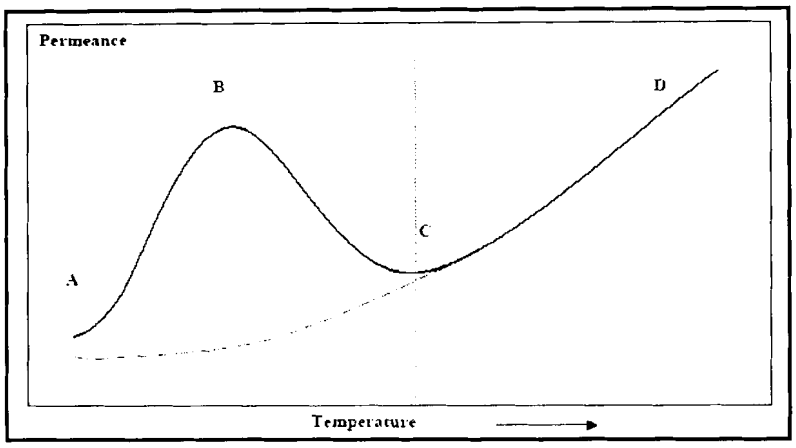

Figure 2.8: Qualitative diagram showing the dependence of single gas permeance with temperature

When only the membrane quality is assessed, a simple phenomenological approach is sufficient.

For single gas permeation of permanent gases through amorphous microporous silica membranes, at sufficiently high temperatures, and low pressures, transport is activated and permeance is independent of pressure [Peters *et al*, 2004].

Permeance is thus described by:

$$p \equiv \frac{N}{\Delta p} = (H_O D_O) \exp\left(\frac{(Q - E_D)}{RT}\right) \qquad (2.1)$$

where N is the molar flux, Δp is the partial pressure difference across the membrane, H_o and D_o are pre-exponential factors related to the Henry and diffusion coefficients, respectively, and R and T the universal gas constant and temperature respectively. The overall thermally activated nature of transport arises from the simultaneous occurrence of diffusion (E_D) and sorption (Q).

The ratio of the permeances of two pure gases measured at the same temperature is the ideal selectivity or permselectivity (α) [Algieri et al, 2003]:

$$\alpha\left(\frac{i}{j}\right):\frac{permeance_i}{permeance_j} \qquad (2.2)$$

As both the driving force and the permeability or permeance depend markedly on the mechanism of transport, it is important to understand the nature of transport in membranes. Since only microporous or dense membranes are permselective, the following mechanisms for the transport of liquid or gas molecules through a porous membrane are depicted in the figures below [Seader *et al.*, 1998]:

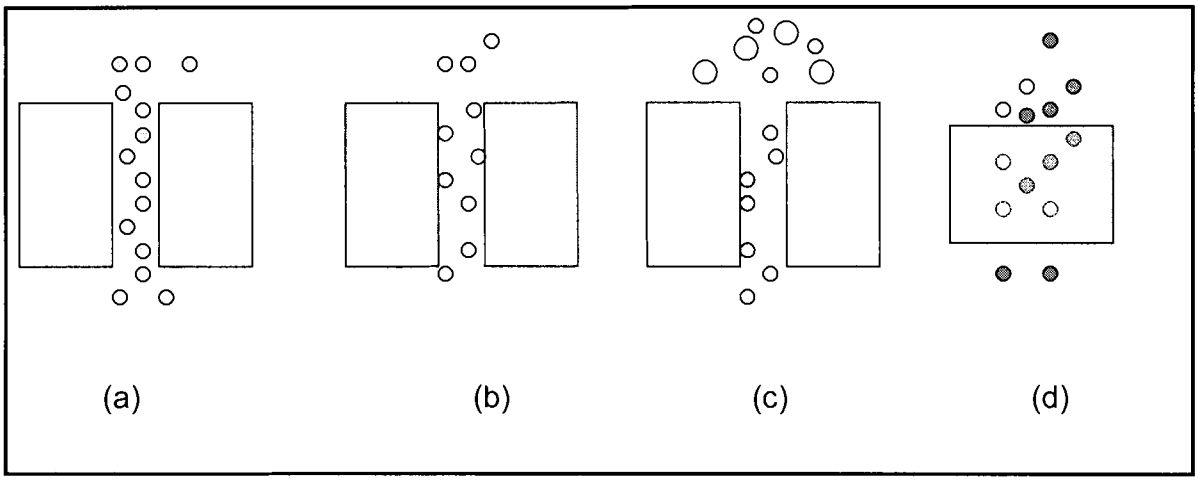

Fig 2.9: Mechanisms of transport in membranes. (Flow is downward.) (a) Bulk-flow through pores; (b) diffusion through pores; (c) restricted diffusion through pores; (d) solution diffusion through dense membranes.

If the pore diameter is large compared to the molecular diameter, and a pressure difference exists across the membrane, bulk or convective flow through the pores occurs, as shown in (a). Such a flow is generally undesirable because it is not permselective and, therefore, no separation between the components of the feed occurs. If fugacity, activity, chemical potential, concentration or partial pressure differences exist across the membrane for the various components, but the pressure is the same on both sides of the membrane, permselective diffusion of the components through the pores will take place, effecting a separation as shown in (b). If the pores are of the order of molecular size for at least some of the components in the feed mixture, the diffusion of these components will be restricted (hindered) as shown in (c),

resulting in enhanced separation. Molecules of size larger than the pores will be prevented altogether from diffusing through the pores. This special case is highly desirable and is referred to as sieving. Another special case exists for gas diffusion where the pore size and/or pressure (typically a vacuum) is such that the mean free path of the molecules is greater that the pore diameter, resulting in so-called Knudsen diffusion, which is dependent on molecular weight.

The equations used to represent the three permeation mechanisms are given by equations 2.3 to 2.5 [Choi *et al,* 2003].

$$J_{knudsen} = \frac{2\varepsilon_{sup} r_p}{3\tau}\sqrt{\frac{8}{\pi MRT}}\frac{\Delta P}{\delta_{sup}} \tag{2.3}$$

$$J_{viscous} = \frac{\varepsilon_{sup} r_p^2}{8\tau\eta RT}\overline{P}\frac{\Delta P}{\delta} \tag{2.4}$$

Where $\overline{\mathbf{P}}$ is the average pressure in the support.

$$\mathbf{J_{surface}} = \mathbf{D_{surface}}\frac{\Delta \mathbf{P}}{\delta} \tag{2.5}$$

The surface diffusion coefficient in the support can be calculated with the mean free path model (Kärger and Ruthven, 1992):

$$\mathbf{D_{surface}} = \frac{3}{8\sigma^2}\left(\frac{\mathbf{kT}}{\mathbf{P}}\right)\left(\frac{\mathbf{kT}}{\mathbf{M\pi}}\right)^{1/2} \tag{2.6}$$

Where

k = Boltsmann constant

M = Molecular mass

σ = Molecular diameter

P = pressure

The surface flux can then be calculated by equation (2.7):

$$\mathbf{J_{surface}} = \frac{3}{8\sigma^2}\left(\frac{\mathbf{kT}}{\mathbf{P}}\right)\left(\frac{\mathbf{kT}}{\mathbf{M\pi}}\right)^{1/2}\frac{\Delta \mathbf{P}}{\delta} \tag{2.7}$$

If al three types of flow were present, the total flux through the support would be the sum of each, thus:

$$\mathbf{J_{TOTAL}} = \mathbf{J_{Knudsen}} + \mathbf{J_{viscous}} + \mathbf{J_{surface}} \tag{2.8}$$

2.5 TRENDS IN MEMBRANE GAS SEPARATION

Membrane separators can be used as a single separation step, but are being more commonly used as part of an integrated separation system where compression, distillation, and other separation steps may be involved.

Gas membranes offer low capital cost, low energy consumption, ease of operation, cost effectiveness even at low gas volumes and good weight and space efficiency.

Even after a decade of commercial use, membrane-based gas separation (GS) technologies have not completely displaced other existing technologies. The new technology gradually gains market share from the competing technologies in those applications where it has a clear economic or technical advantage or it expands into market areas where the competing technologies have no position or application. Both market-pull and technology-push factors have contributed to the establishment of a distinct technology industry centered on membrane technology. Separation technologies can be competitive, but also complementary. Different separation processes may be combined in a given application to operate synergistically.

Today's largest uses of gas separation membranes in industry are in the production of nitrogen from air and the removal of condensable organic vapors from air. Other areas of application of gas separation membranes are depicted in Table 2.1. [Fausi *et al,* 2003]

Table 2.1: Gas separation membrane application [Fausi, et al, 2003]

Common Gas Separation	Application
O_{2l}/N_2	Oxygen enrichment, inert gas generation
H_2/Hydrocarbons	Refinery hydrogen recovery
H_2/N_2	Ammonia Purge gas
H_2/CO	Syngas ratio adjustment
CO_2/Hydrocarbons	Acid gas treatment, landfill gas upgrading
H_2O/Hydrocarbons	Natural gas dehydration
H_2S/Hydrocarbons	Sour gas treating
He/Hydrocarbons	Helium separation
He/N_2	Helium recovery
Hydrocarbons/Air	Hydrocarbons recovery, pollution control
H_2O/Air	Air dehumidification

The mechanism of gas separation by membranes depends on the structure of the membrane. Gas separation mechanisms can be divided into three classes, namely [van den Graaf, 1998]:

Knudsen diffusion – for pores between 2 and 50 nm. This kind of gas flow is dependent on the mean free path of the gas molecules relative to the pore diameter of the membrane. This kind of flow (flux) can be expressed by the equation [Mulder, 1998]:

$$J = \frac{\pi \cdot n \cdot r^2 \cdot D_k \cdot \Delta p}{R \cdot T \cdot \tau \cdot \ell} \tag{2.9}$$

where D_k, the Knudsen diffusion coefficient, is given by $D_k = 0.66 \cdot r \cdot \sqrt{\frac{8 \cdot R \cdot T}{\pi \cdot M_w}}$

Molecular sieving – for pores smaller than 2 nm. **Zeolite membranes fall into this category.**
Dense – no pores exist and permeation occurs by dissolution of a component in the dense matrix followed by diffusion through the matrix.
Gas separation is known as a developing process and most gas separation membranes are of the solution-diffusion mechanism type.
The key membrane performance variables are selectivity, permeability and durability. For solution-diffusion membranes, permeability is defined as the product of the solubility and diffusivity. Traditionally, there has been a tradeoff between selectivity and permeability; high selectivity membranes tend to exhibits less permeability and vice versa.

2.6 MEMBRANE RESEARCH

2.6.1 Gas separation membrane research

Studies to establish the efficiency of supported zeolite and silica membranes have been performed on various occasions. The following are extracts of articles found for gas permeation and separation membranes in general. The membranes of concern are NaA, silcalite-1 and amorphous silica. Articles related to these membranes are thus reviewed. Identifying various shortcomings and suggesting possible improvements is only possible if such a study is conducted.

Single Component Permeation

NaA

This membrane is known for its small pore size (0.41 nm), smaller than that of the MFI zeolite (~ 0.55 nm). For gas separations, zeolite membranes (in particular NaA) are still in the laboratory scale. Most investigations focus on MFI (ZSM-5 & silicalite-1) zeolite membranes, while few studies regarding type A zeolites have been undertaken.

A-type zeolite membrane has been proposed as a good candidate for the separation of several industrially important gases. The pore size of NaA zeolite is 0.41 nm, smaller than the molecular size of the short-chain alkanes (>0.43 nm). The small pore size of NaA zeolite makes the separation of small molecules by difference in size possible.

Not many articles pertaining to the gases considered for this study i.e. hydrogen, methane and carbon dioxide, separated by NaA are available, but the following is a summary of all important articles already done with this membrane for the purposes of gas permeation:

- Chen *et al.* (2005) reports that the permeance of H_2, O_2, N_2 and C_3H_8 decreases as the kinetic molecular diameter increases, which shows that the molecular sieving of the zeolite NaA membrane plays a main role in the separation of molecules. The NaA zeolite membrane also has a good quality of separation while maintaining a high hydrogen permeance of 2.64×10^{-6} mol.m^{-2}.s^{-1}.Pa^{-1}.
- From numerous gas permeation results, Xu *et al (2001).* reports that the quality of NaA zeolite membranes is generally poor.
- Xu *et al. (2001).* synthesized a high quality NaA zeolite membrane from a homogeneous clear solution, and gas permeance was measured to evaluate the quality of the as-synthesized NaA zeolite membrane.
- The support used for the NaA membrane synthesized by Xu *et al. (2001)* is an α-Al_2O_3 support.
- The permeances of H_2, O_2, N_2 and *n*-C_4H_{10} decreased as the molecular kinetic diameters of the gases increased, which showed the molecular sieving effect of the NaA zeolite membrane. This phenomenon can be seen in Figure 2.10 [Xu *et al., 2001].*

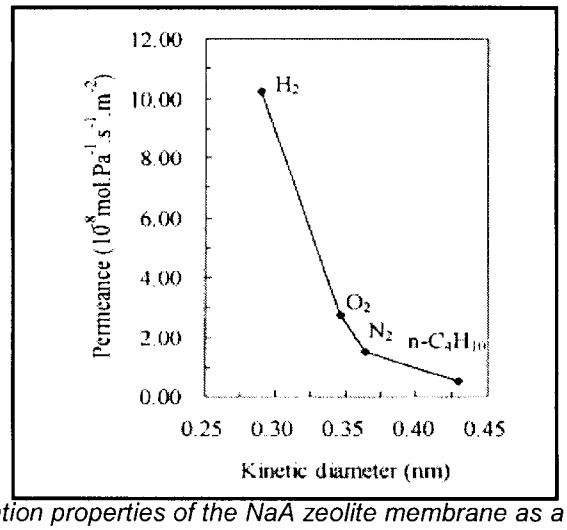

Figure 2.10: Gas permeation properties of the NaA zeolite membrane as a function of gas molecular kinetic diameters at 25 °C and 0.1 MPa pressure difference. [Xu et al., 2001]

- Attempts to prepare A-type zeolite membrane for gas separation started by Wang et al. in 1994. A NaA zeolite membrane was deposited on a porous support. The gas permeance decreased in the following order: $C_2H_4 > CO_2 > CH_4 > N_2 > O_2$. The gas permeance sequence did not follow the order of gas molecular kinetic diameters, which suggested that the permeation was controlled by surface diffusion through grain boundaries, rather than by molecular sieving through zeolite channels. [Xu *et al.*, 2004]
- Aoki *et al (1999).* reported that a NaA zeolite membrane was synthesised on a porous support tube. The gas permeance decreased in the following order: $H_2 > O_2 > CH_4 > CO_2 = N_2 = C_3H_8$, which at least in part, exhibited the molecular sieving effect of NaA zeolite membrane.
- Compared with literature data on gas permeation properties of NaA zeolite membranes (shown in table 2.3), the NaA zeolite membrane from the study of Xu *et al.* (2004) showed a better gas permeation performance.

Silicalite-1

Bakker et al. (1996) reports the contribution of the molecule size and shape influence on one-component permeation through a silicalite-1 membrane. One component permeation experiments were performed from 193 to 500 K, varying the partial feed pressure form 0.05 kPa to 500 kPa, by using helium as sweep gas.

The breakthrough curves for the various components were plotted and the time taken to reach 95% steady state permeation level was reported and discussed for various components. Figures 2.11 and 2.12 depict his findings:

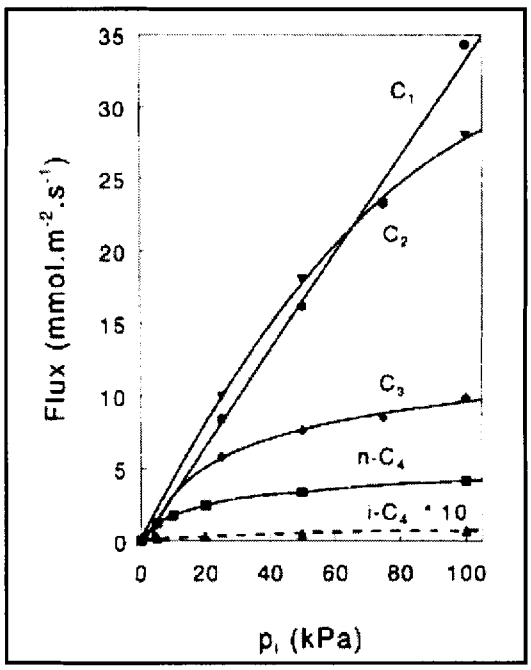

*Figure 2.11: Permeation flux of methane, ethane, propane, n-butane and /-butane as function of the partial feed pressure at 295 K. The total pressure was 100 kPa, obtained by adding helium to the feed. [*Bakker *et al., 1996]*

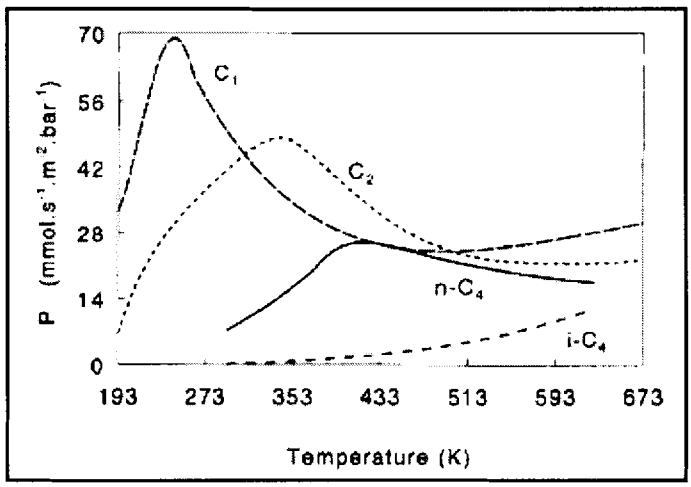

*Figure 2.12: Permeance of 100 kPa methane, ethane, butane, and /-butane as a function of the temperature. The applied sweep gas flow rate was 200 ml/min NPT. For the calculation of the /-butane permeance it is assumed that the helium counter-diffusion equals the helium counter-diffusion with n-butane as feed. Results for methane and ethane are obtained with membrane WTSS-1C. [*Bakker *et al., 1996]*

Burggraaf *et al.* (1998) studied the permeation of different individual gases between room temperature and 473K, using a silicalite membrane with a very few defects. They distinguished four different regimes: 1) the Henry sorption regime, 2) the Langmuir sorption regime, 3) the saturation regime and 4) the size exclusion regime. In the Henry adsorption regime the flux increases linearly with an increase in pressure of the permeating component at the feed side. In the Langmuir sorption regime the feed pressure dependence is non-linear and a maximum in the flux and temperature curves can be observed due to divergent effects of temperature in the adsorption and diffusion processes. In the saturation regime, the flux becomes independent on the feed side pressure and increases with temperature. The size exclusion regime applies to molecules whose kinetic diameter is slightly in excess of the zeolite pore diameter (e.g. 2, 2 dimethylbutane).

Algieri et al. (2003) conducted permeability tests at room temperature (ΔP = 200 kPa), which showed that the selectivity of small gas molecules (viz. Hydrogen and nitrogen) relative to sulphur hexafluoride (SF_6) is higher than the Knudsen limit, indicating molecular sieving. For all gases (hydrogen, carbon dioxide, nitrogen, oxygen and methane) and in the whole range of experimental conditions considered, the permeate was observed to increase linearly with Δ P.

Burggraaf (1999) performed an analysis and evaluation in theoretical terms for single gas permeation through silicalite membranes considering the following groups of phenomena and regimes:

- Permeation in the Henry adsorption regime.
- Linear increase of the permeation with feed pressure and an increase or decrease with temperature.
- Permeation in the Langmuir adsorption regime.
- Occurrence of maxima in the relation between permeation and temperature.
- Permeation in the saturation regime.
- The permeation is a no or weak function of the pressure.
- Occurrence of a minimum in the relation between permeation and temperature.
- Importance of the ratio of the molecular diameter and of the pore (channel, cavity, window) diameter for the interpretation of permeation models.
- Importance of synthesis conditions, microstructure and measuring conditions.

Amorphous Silica

Many publications report permeances and results obtained with amorphous silica membranes strictly for pervaporation application. Gas separation applications with these type membranes is thus still fairly recent.

Asaeda *et al.* (2001) fabricated porous silica membranes coated on cylindrical porous α-alumina tubes by hot coating methods. A large hydrogen permeance of 1.3×10^{-6} mol.m^{-2}.s^{-1}.Pa^{-1} was found. The permeance of hydrogen and helium were only slightly dependent on temperature while the carbon dioxide permenace showed a large temperature dependency.

A carbo dioxide permeance of 0.9×10^{-6} mol.m^{-2}.s^{-1}.Pa^{-1} was found at 35 °C, and a permeance ratio of CO_2/CH_4 was around 80-110 at 35 °C - 50°C decreasing with increasing temperature.

According to de Vos *et al. (1991)*, permeance through microporous amorphous silica membranes occurs by solid-state-type diffusion of molecules. The permeance flux can be derived form Fick's first law.

For single permeances for Si (400) ;(400 refers to the calcination temperature), at a pressure difference of 1 bar and mean pressure of 1.5 bar, the permeance is nearly independent on temperature. Figure 2.13 illustrates this dependence:

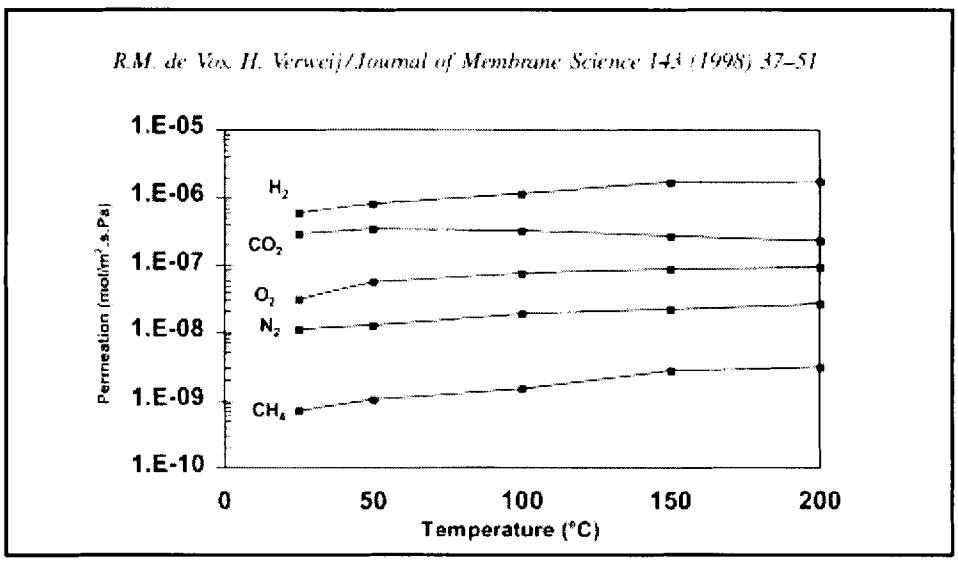

*Figure.2.13. Temperature dependence of the permeance for the Si(400) membranes at ΔP=1 bar and a mean pressure of 1.5 bar [*de Vos *et al, 1991.]*

For SI (600) is seems that the hydrogen permeance increases with temperature. Carbon dioxide however, seems to decrease with an increase in temperature (range 100 to 300 °C). Furthermore De Vos *et al.* (1999) reports permeances of 4.72×10^{-7} to 18.5×10^{-7} mol.m^{-2}.s^{-1}.Pa^{-1} for S_i (400) and 2.32×10^{-7} to 5.4×10^{-7} mol.m^{-2}.s^{-1}.Pa^{-1} for S_i(600) for Hydrogen gas in a temperature range of 25 to 300 °C and trans-membrane pressure of 0.5 to 3 bar. Carbon dioxide permeances are slightly lower (2.01×10^{-7} mol.m^{-2}.s^{-1}.Pa^{-1} to 3.19×10^{-7} mol.m^{-2}.s^{-1}.Pa^{-1}) for Si (400) and for methane the permeance is of the order 10^3 smaller than the permeance of Carbon dioxide.

Iwamoto *et al.* (2005), conducted studies on a microporous amorphous silica membrane synthesised by thermal conversion in air of polysilazane on a silicon nitride (Si_3N_4) porous substrate.

The polysilazane-derived (PSZ-derived) amorphous silica membrane exhibited an H_2 permeance of 1.3×10^{-8} mol.m^{-2}.Pa^{-1} at 573 K. Permeances of PSZ-derived amorphous silica membrane are plotted in Figure 2.14. The permeances of each gas increases with increasing permeation temperature, following Arrhenius low. According to mechanisms of Knudsen diffusion and viscous flow, permeation of a gas molecule in a porous medium leads to decreasing temperature with increasing temperature.

Based on the plot it is clear that the dominant mechanism of each gas is activated diffusion.

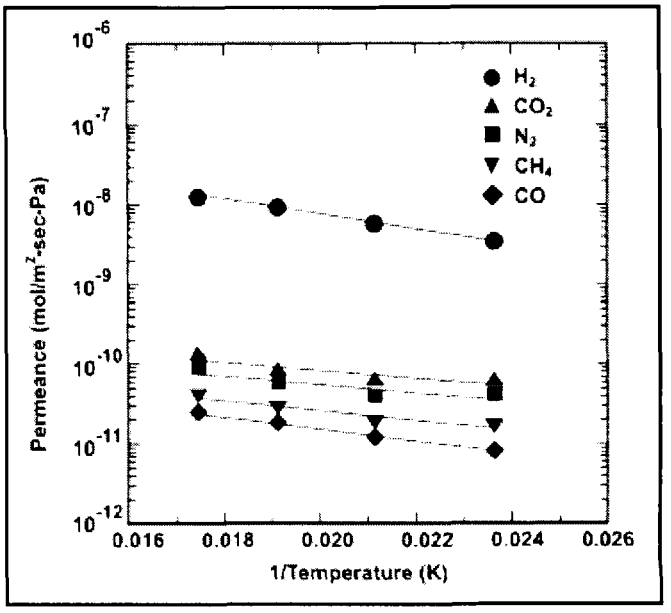

Figure 2.14: Arrhenius plots of permeances of PSZ-derived amorphous silica membrane. [Iwamoto et al., 2005]

So *et al.* (1998) did various pore modification steps in preparing a silica-alumina composite membrane. In Figure 2.15 gas permeance of the membrane prepared by the first step pore modification (i.e. in situ sol-gel method) are plotted as a function of trans-membrane pressure at the temperatures T=298.473 and 673 K.

It can be seen form the figure that the gas permeance of the membrane was nearly independent of trans-membrane pressure up to 280 kPa and decreased as temperature was increased.

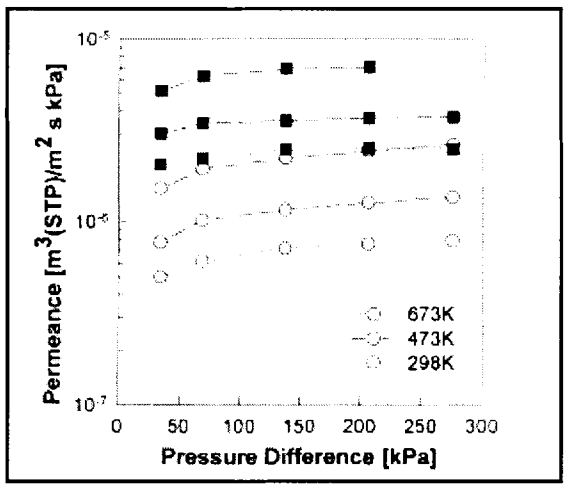

Figure 2.15: Hydrogen and Nitrogen permeances of membrane modified by in situ sol-gel method (filled- H_2, unfilled – CO_2) [So et al.,1998].

Permeation of silica membrane investigated by Kim *et al.* (2001) revealed that permeance decreased with increasing molecular size of the permeant.

Permeance of H_2, N_2 and CH_4 at a permeance temperature of 100 °C were 3.2×10^{-7},3.9×10^{-8} and 2.7×10^{-9} mol.m^{-2}.s^{-1}.Pa^{-1}, respectively for the case of a membrane which was prepared with x = 0.1 and calcinated at 600 °C.

Lee *et al.* (2004) investigated the gas permeation properties of a hydrogen permeable silica membrane supported on alumina. The membrane was highly permeable and showed a hydrogen permeance of the order of 10^{-7} mol.m^{-2}.s^{-1}.Pa^{-1} at 873 K. This membrane was however, used for pervaporation purposes.

Binary Permeances

NaA

Very little information regarding the gas separation properties of this membrane have been published. Most work published related to this membrane is based on single permeation characteristics and optimal membrane synthesis.

Silicalite-1

To explore the separation potential of a silicalite-1 membrane, *Bakker et al.*(1996) performed permeation measurements with several mixtures. It was observed that besides shape and size of the molecules, adsorption is important for the separation selectivity. Therefore, binary mixtures were studied with various combinations of weakly, moderately or strongly adsorbing components. Furthermore the permeation of various mixtures as separate functions of temperature (295-623K) and absolute feed pressure (100 to 500 kPa) were examined.

The transient permeation curves for the binary mixtures were plotted and contrasted with the one component data. There was a remarkable difference between the binary mixture and the one component systems. The separation selectivities for each system was determined in favour of the more selective component in the mixture. Steady state permeances and separation selectivities were plotted as functions of temperature for the different binary mixtures. Figure 2.16 shows the results of the effect of an incremental pressure in crease form 100 to 500 kPa on the permeation (separation selectivity) of a binary mixture at constant temperature:

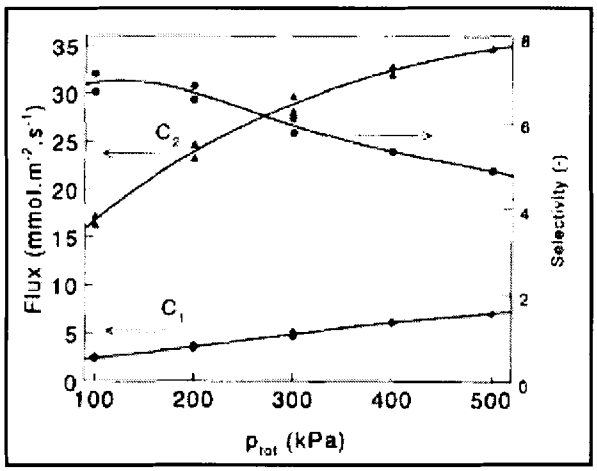

Figure 2.16: Permeation and separation selectivity towards ethane of a methane/ethane mixture (50/50) as a function of the absolute pressure at feed side at 295 K. The pressure at the permeate (helium) side was kept constant at 100 kPa.

Kapteijn et al. (1998) reported the permeation results for a 95:5 binary mixture of hydrogen and n-butane, as well as their pure component fluxes at 0.95 and 0.05 bar partial pressure, selectivity. In the unary experiments the steady state hydrogen permeation flux was about 20 times larger that that of n-butane at the applied conditions, whereas in the binary system it had dropped by a factor of more than a hundred while the n-butane flux remained unaltered. In the latter experiments the hydrogen permeated first and appeared at the same time as in the unary experiment, but then decreased quickly and reached its final, low value as the n-butane disappeared. An n-butane selectivity of more than 1000 over hydrogen was found. Similar trends have been found for methane/n-butane mixtures.

The temperature dependency of the permeation of binary mixtures (1:1) were presented for hydrogen/n-butane and hydrogen/carbon dioxide. At room temperature n-butane permeated preferentially while hydrogen hardly permeated. At increasing temperatures the n-butane flux increased, passed through a maximum at about 430 K then decreased and levelled off around 600 K. The hydrogen flux started to increase noticeably above 400 K when the n-butane flux had reached its highest value. At 480 K it equalled that of n-butane and at 600K it had become 2.5 times as high. In the case of hydrogen/carbon dioxide mixture a similar trend was observed, on the understanding that carbon dioxide reaches its maximum already at 330 K and hydrogen exhibits only a nearly linear increase as a function of temperature. Also in the case the perm-selectivity reverses as a function of temperature. At low temperature the stronger adsorbing component permeates preferentially, while at thigh temperature hydrogen does, so an inversion of the selectivity takes place. It can be noted that for n-butane the results, at 0.5 bar partial pressure were identical in the case of unary or in a binary mixture with methane.

Van den Broeke et al. (1998) studied the permeation characteristics of a binary mixture of CO_2 and CH_4 using silicailite-1 membranes. The results are depicted in Figures 2.3 (a) & (b). One can see that the flux for carbon dioxide is hardly affected by the presence of the weakly adsorbed methane in the mixture. On the other hand, the flux of methane is reduced considerably

Amorphous Silica

In the publication of Koukou *et al. (1999)*, experimental work was performed using gas mixture of H_2/CH_4 on ceramic high-selective microporous silica membranes for gas separation:

- The permeate appeared to be rich in H_2 and the following results of the permeation experiments are visible in Figure 2.17:

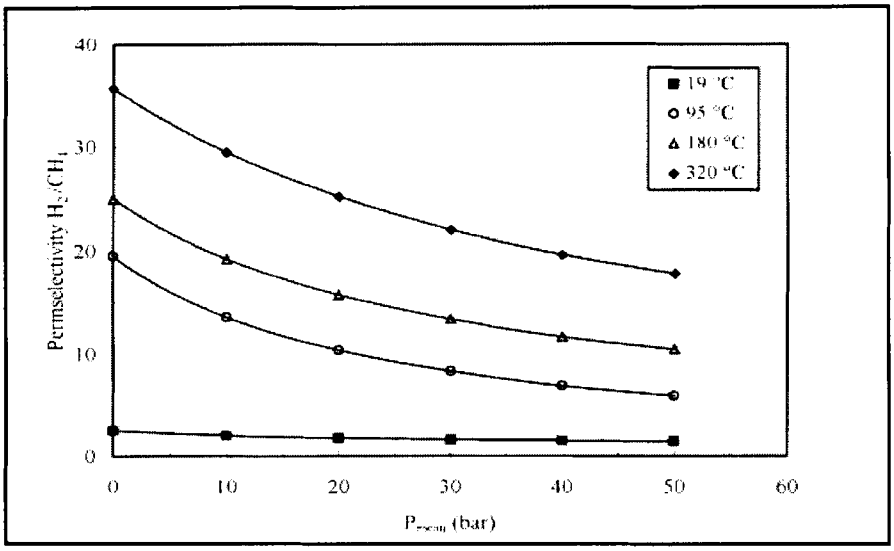

Figure. 2.17: Ratio of H2 and CH4 permeabilities at different temperatures. [Koukou et al., 1999]

De Vos *et al.* (1991) reports the following permselectivities and separation factors for Si (400) using 50/50 gas mixtures for trans-membrane pressures of 0.5 to 3 bar and a temperature range of 25 to 200 °C:

- H_2/CO_2 – permselectivities of 2.3 up to a maximum 7.5, and a separation factor of 6.8 maximum.
- H_2/CH_4 - permselectivities of 377 up to a maximum 844, and a separation factor of 334 maximum.
- CO_2/CH_4 - permselectivities of 123 up to a maximum 326, and a separation factor of 45 maximum.

The separation factors for the three gas mixtures on the trans-membrane pressure, for the Si (400) membrane were independent on the trans-membrane pressure at a temperature of 200 °C.

CHAPTER 3

Experimental

3.1 INTRODUCTION

All aspects with regard to experimental work done in this study are discussed in detail in this chapter. These include among others the apparatus used, the membrane properties and methodology used.

Membrane technology consists of many facets, which have been given much attention in the research field. Among these are membrane process installation designs as well as the design of suitable membrane modules used for housing the membrane [Nunes, 2003].

Many different apparatus configurations as well as different membrane modules are designed, depending on the type of membrane used.

Microporous inorganic membranes (r_{pore}< 1 nm) have great potential for gas separation, since they exhibit molecular sieve-like properties (separation of the gas molecules is based on the exclusion of some molecules from the pores based on their molecular size) and a good stability towards higher temperatures and corrosive atmospheres. Moreover, inorganic membranes can be used in membrane reactors for conversion enhancement in dehydrogenation reactions [De Vos *et al*, 1997].

Zeolite membranes (specifically NaA), are manufactured locally by the chemistry department at the North-west university (Potchefstroom). This type of membrane is a suitable separation membrane used mainly for pervaporation, but because it is a suitable molecular sieving material for molecules with a kinetic diameter smaller than 4.1 Å it can also be used for gas separation. Since this membrane is also readily available - this type of membrane would be the best option to use ideally as a test membrane, where trends with regard to the analysis of gas separation can be seen.

Amorphous silica membrane is also an ideal candidate used for gas separation since this type of membrane has extremely small pores, and molecular sieving can also take place in this membrane. This type of membrane is also selective towards hydrogen and one can obtain high selectivities with this membrane [Benes, 2000].

Because of the properties that silica and NaA membranes hold, these membranes serve the correct purpose to use as part of this study, which is to observe whether the separation of Fischer Tropsch gases is possible. There are however, many other options that one should consider when deciding upon a membrane for gas separation. These are given in section 3.2.

3.2 MEMBRANE SELECTION

The economic viability of any membrane separation process is selectivity, productivity and stability. It is thus important that great care is taken when choosing a membrane for a specific application.

Thus, two general criteria apply to all separation processes: (a) the separation must be feasible technically, and (b) the separation must be feasible economically [Mulder, 1998].

To achieve a feasible separation technically might mean that integrated systems, developed as economically as possible, can achieve this.

The performance or efficiency of a given membrane is determined by two parameters; its selectivity and the flux through the membrane.

Ideal gas separation membranes possess a high flux and a high selectivity [Mulder, 1998]. There is however, a trade-off between flux, and selectivity. Although a high flux is preferred to meet flow conditions in other parts of the plant in most applications, a minimum selectivity has to be maintained to make the process feasible.

The following criteria should also be considered when deciding upon choosing a membrane for separation purposes [Mulder, 1998]:

- Commercial availability,
- Hydrophobicity/hydrophilicity,
- Structure, and
- Supports.

Microporous silica membranes have thus been developed specifically to satisfy commercial needs, and gas separation on these membranes are studied extensively [De Vos *et al.*, 1997; Benes, 2000].

The membranes chosen for this study are selective to certain gases (H_2 for silica), commercially available, do exhibit hydrophobic/hydrophilic characteristics, and possess the correct structure for successful gas transport and separation.

Table 3.1 lists some of the characteristics these membranes have.

Table 3.1: Properties of the membranes used for this investigation

Membrane Material	Support Material	Hydrophobic / Hydrophilic	Configuration	Membrane Area (m^2)
NaA-zeolite	α - Alumina	Hydrophilic	Tubular	0.003
Amorphous Silica	α - Alumina γ – Alumina	Hydrophobic	Tubular	0.00656

3.3 MEMBRANE CHARACTERISTICS AND PROPERTIES

3.3.1 NaA

The composite tubular membrane, obtained from the chemistry department at the North-west University, Potchefstroom, (see Figures 3.1 and 3.2) used in this study consists of a thin NaA zeolite layer (optical thickness of 3.5 μm, as determined from Scanning electron microscopy(SEM))].

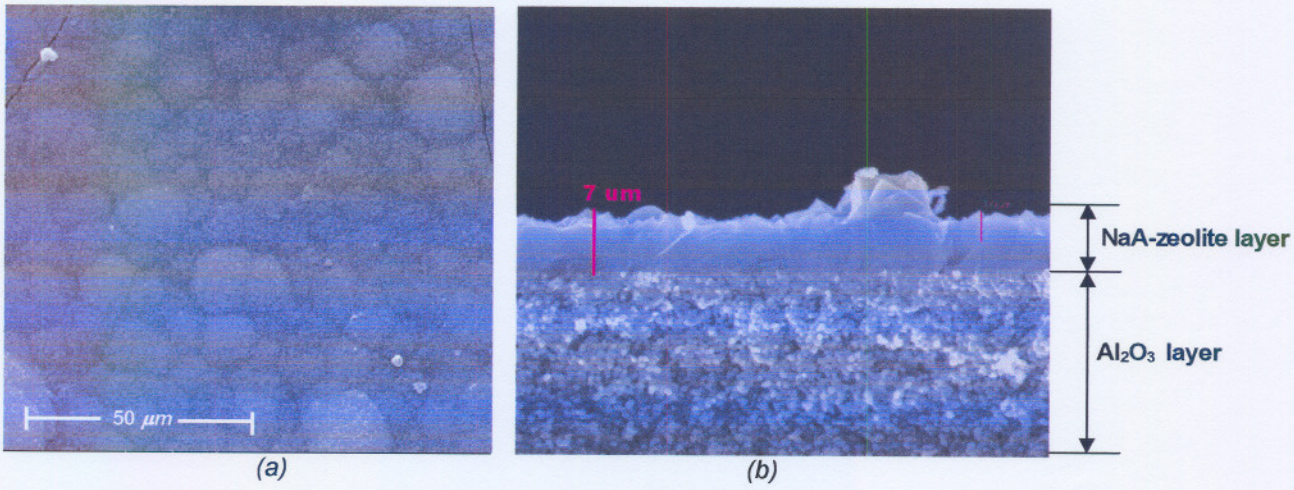

Fig 3.1: Scanning electron microscopy photos of NaA Zeolite membrane (a) Top view – typical crystal structure can be seen (b) Cross-sectional view from side – the alumina support is clearly visible and the NaA crystal structure on top of the support.

The membrane used in this study has a double coating (7 μm) on an α-alumina support.

The support thickness is approximately 1.3 mm with a porosity of 36.8 ± 5 % [Zah, J, 2005], and the surface area of the membrane used in this study was 0.00267 m^2.

The support has an average pore diameter of dp = 0.167 ± (0.003) μm and a Silicon/Aluminium ratio of 1.

This membrane is hydrophilic in nature due to the high amount of aluminium.

The temperature limit of this membrane is not yet known since this is an experimental membrane. To avoid risk or damage to the membrane no temperature permeation experiments were performed on this membrane. A pressure not exceeding 10 bar was placed on this membrane.

The tubular NaA-zeolite membrane used in this study is shown in Figure 3.2.

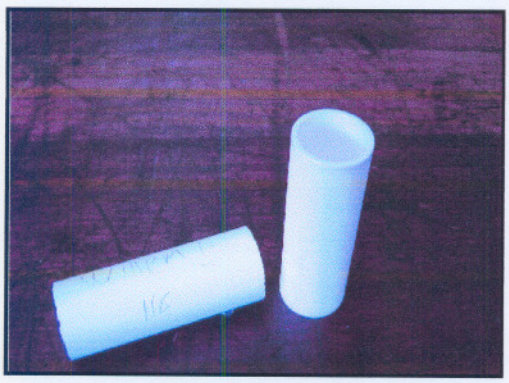

Figure 3.2: NaA Zeolite Membranes

3.3.2 Amorphous Silica Membrane

An Amorphous silica membrane (membrane code 1059, serial number 0079) was purchased from Pervatech, BV. ® in the Netherlands along with the membrane module (Module type PVM-250-10-1-250).

This membrane has an asymmetric structure, consisting of a selective angstrom size silica layer positioned on a support structure comprising α and γ-alumina layers (see Figures 3.3 and 3.4).

This membrane is known for its selectivity towards hydrogen gas in particular, and recently much research was done on this membrane's ability to perform efficiently as a gas separation membrane [Benes, 2000]. The membrane is 25 cm in length, with an outside diameter of 10 mm and an inside diameter of 7 mm.

This membrane can withstand a maximum temperature of 250 ºC (Producer specifications). The ceramic tube itself can withstand up to over 50 bar, however because of material stresses in the sealing area at the end of the tube in the module housing it is recommended not to exceed 25 bar (Producer recommendations).

The ceramic membrane is calcinated at 400 ºC; theoretically it must be possible to go up to 250 ºC. One has to be aware of the amorphous nature of the silica and the sensitivity in presence of water above 100 ºC. The silica material exhibits a kind of re-arranging behavior (comparable

with creep in polymers) in which the material becomes denser. This is enhanced by the presence of water.

With regards to the support structure, Table 3.12 lists the layers comprising the support along with the characteristics of each layer as determined from a scanning electron microscopy analysis (see Figure 3.4 a to e)

Table 3.2: Silica membrane characteristics

Characteristic	α-layer	γ-layer	Silica layer
Mean Pore Diameter	3 μm	3-4 nm	0.3-0.4 nm
Thickness	1.3 mm	39 μm	1.2 μm
Porosity	35 – 40%	30 – 35%	30 – 35%
Wall thickness	1.5 mm	-	-
Outside diameter	10 mm	-	-
Inside diameter	7 mm	-	-

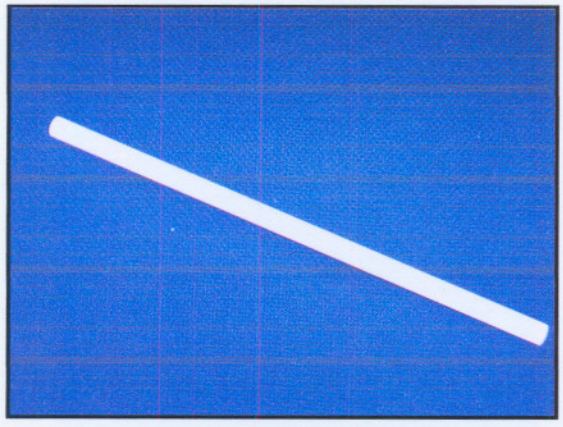

Fig 3.3: Amorphous silica membrane

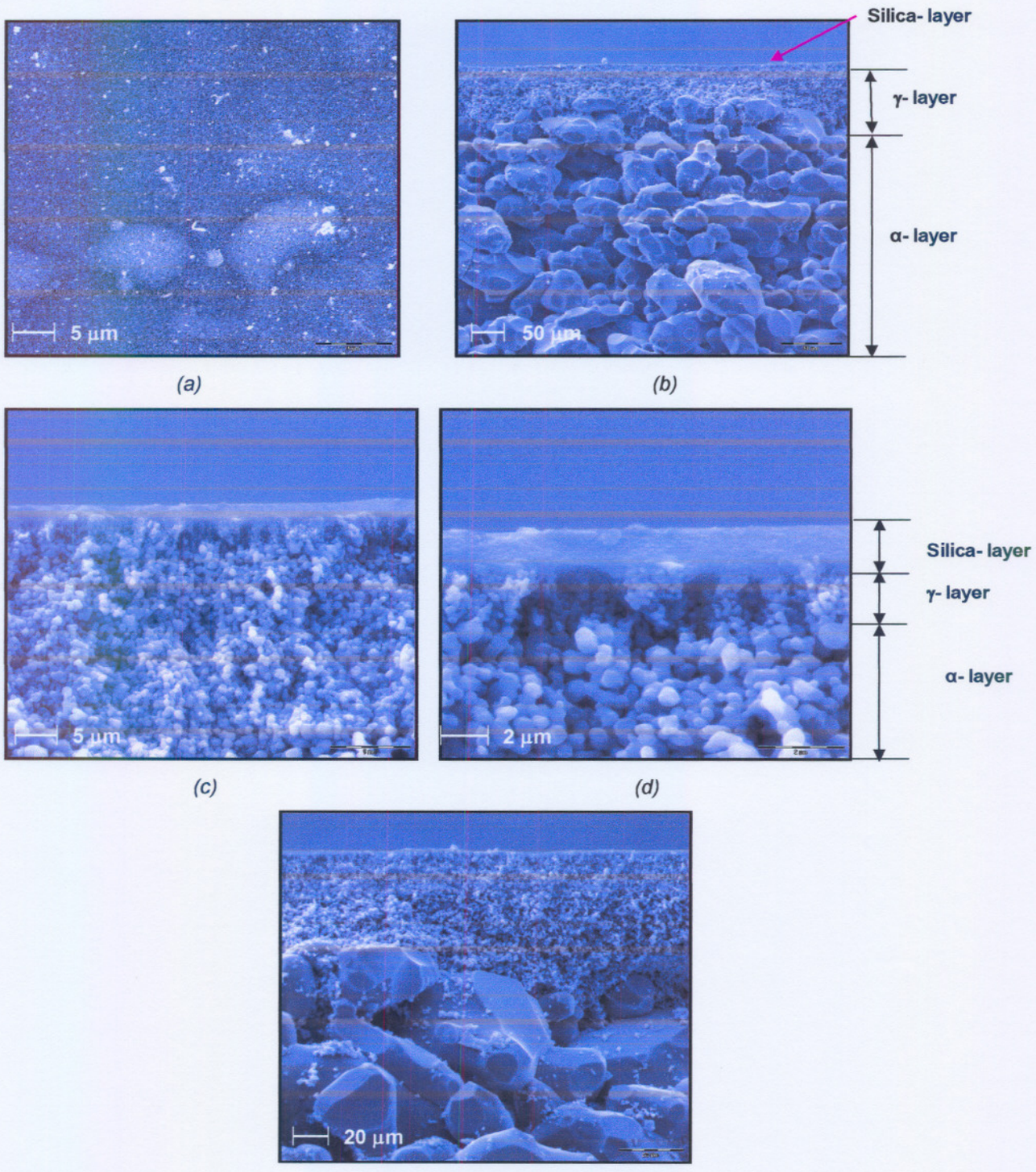

Fig 3.4: Scanning electron microscopy images of the silica membrane (a) top view at 5 um (b) Cross-sectional side-view at 50 um (c) Cross-sectional side view at 5 um (d) Cross-sectional side view at 2 um (e) Cross-sectional side view at 20 um

3.4 EXPERIMENTAL APPARATUS

All experimental runs were done on a standard gas separtion setup [Bai et al, 1995]. In this study no sweep was used. All pure component flow rates were measured with bubble flow meters with an accuracy of 95%. All binary gas analysis were performed on a gas chromatograph (Varian ® Star 3400) using a fused silica capillary column (Carboxen™ 1010 PLOT Supelco®) with an accuracy of 96%.

3.4.1 Gas Separation Setup

A schematic representation of the gas separtion set-up used in this study is shown in Figure 3.5:

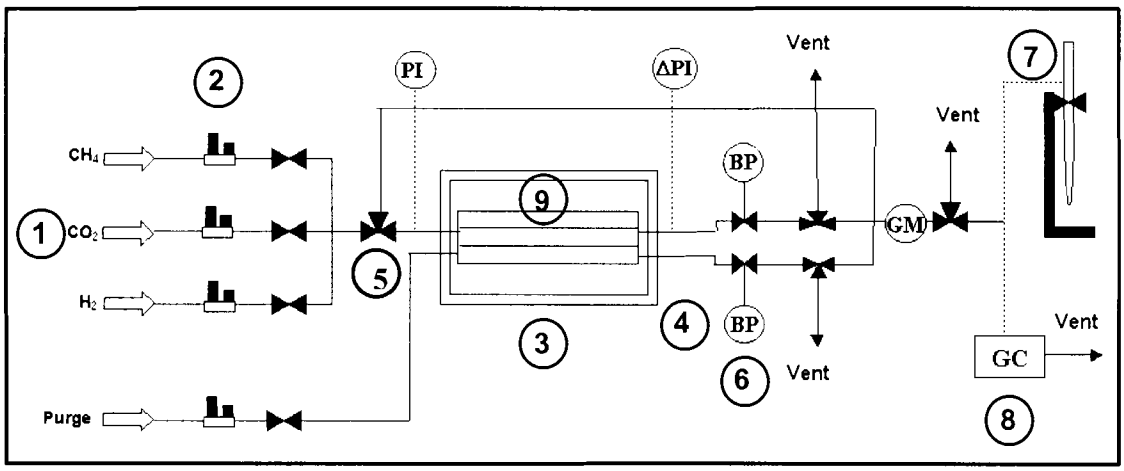

Figure 3.5: Drawing of experimental setup.

A laboratory-scale process was designed and developed specifically for gas separation applications, for temperatures up to 100 °C and differential pressures up to 3 bar. Special care was taken to ensure that a practical design was made in order to minimize operational difficulties. A complete equipment specification list is given in tables 3.5 and 3.6.

As is depicted in Figure 3.5, the process flows from left to right, starting with feeding of the different gases (1) through the mass flow controllers (2) to the membrane module (9), where the supported membrane is housed. The module is placed inside an oven (3) to enable accurate control of the operating temperature within the module. A one-way valve (non-return valve) (5) is placed before the module to prevent back-flow of any gases.

An accurate thermo-couple (± 2 °C) is placed inside the membrane module for accurate temperature recording inside the membrane.

The outlets of the module are the permeate on the shell-side, and the retentate on the tube-side. These are each fitted with a backpressure regulator (6), which is employed to break the

stream pressure form a maximum of 10 bar to atmospheric pressure. In this way the differential pressure across the membrane can be controlled, and the sweep gas flow rate can be controlled.

A sweep gas (nitrogen) line is fitted on the shell-side of the module, should permeation experiments require this optional element. A non-return valve is fitted in this line too.

Across the membrane a pressure difference may exist or be induced, thus a differential pressure meter is connected to the main feed line (high pressure line) and the sweep gas line (lower pressure line).

Analysis equipment is comprised of a gas chromatograph (8) (Varian ® Star 3400) for binary detection of gases, and a bubble meter (7) for single permeances. The apparatus is able to reach stable conditions in terms of pressure and temperature fairly quickly. (± 10 min.)

Various pieces of the experimental equipment used in this study are shown in Figures 3.6 to 3.9.

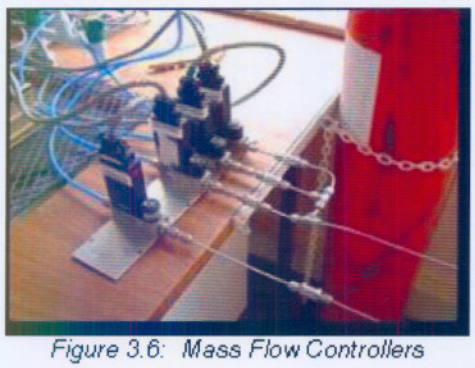

Figure 3.6: Mass Flow Controllers

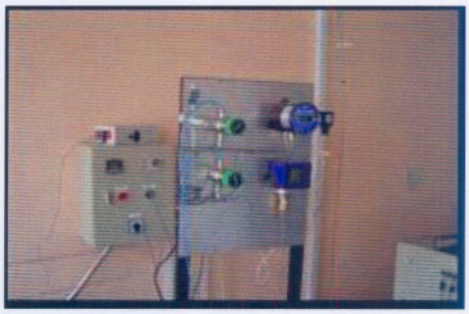

Figure 3.7: Back Pressure regulators and metres

Figure 3.8: Convection oven with module inside

Figure 3.9: Analyzing equipment

The membrane module used for the different membranes are shown in Figures 3.10 and 3.12. Both module designs are of such a nature that they are relatively easy to clean, and require little or no maintenance. They are compact designs that can easily be installed into the separation system.

The membrane module (see Figures 3.10 & 3.11) used for screening of the NaA membrane, consists of a tubular middle piece and two circular end pieces, which are fixed to either end of the middle piece with screws. The end pieces each have two concentric circular grooves into which high-temperature,

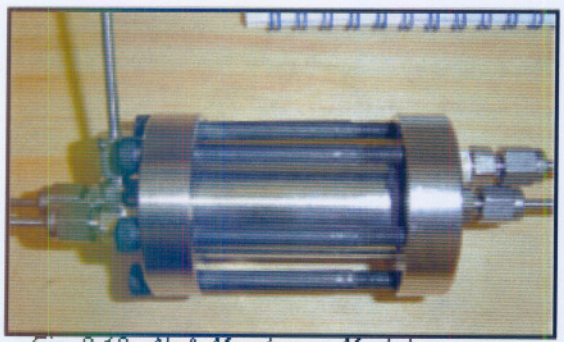

Fig. 3.10: NaA Membrane Module

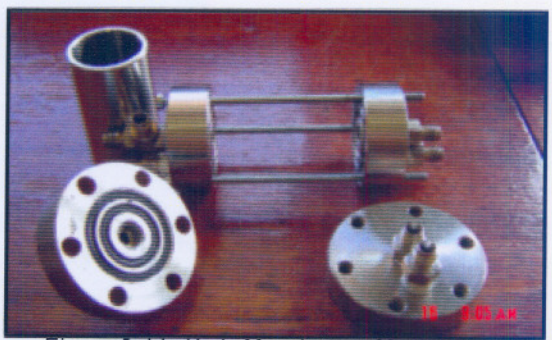

Figure 3.11: NaA Membrane Module in Detail

high pressure Viton O-rings are placed for proper sealing of the membrane. The Viton O-rings can however, only resist temperatures up to 473 K, and cannot be used at elevated temperatures. For this reason, and the fact that the temperature that the membrane can withstand is unknown, the operating temperature was limited to 473 K.

A schematic drawing of the module used for the screening of the silica membrane is based on drawing no. PVM.010D.00.00 and can be seen in Figure E.1 (See Appendix E). Figure 3.12 depicts the membrane module used to house the amorphous silica membrane.
The module housing is constructed of SS 316, developed for applications at high temperatures; therefore one can choose specific seals, depending on the thermal and chemical conditions present during the separation process.

The mechanical characteristics of the module type PVM-250-10-1-250 is summarized in Table 3.3:

Table 3.3: Mechanical characteristics of silica membrane module

Part Characteristic	Attribute
Material of housing	SS 316
Length of membrane tubes	250 mm
Length of SS housing	276 mm, Total length: 368 mm
Diameter of ceramic tube	10 mm outside and 7 mm inside
No. of tubes in module	1
Thermal resistance construction	250 ° C
Assembling of tubes into housing	Graphite Seals and Viton O-rings

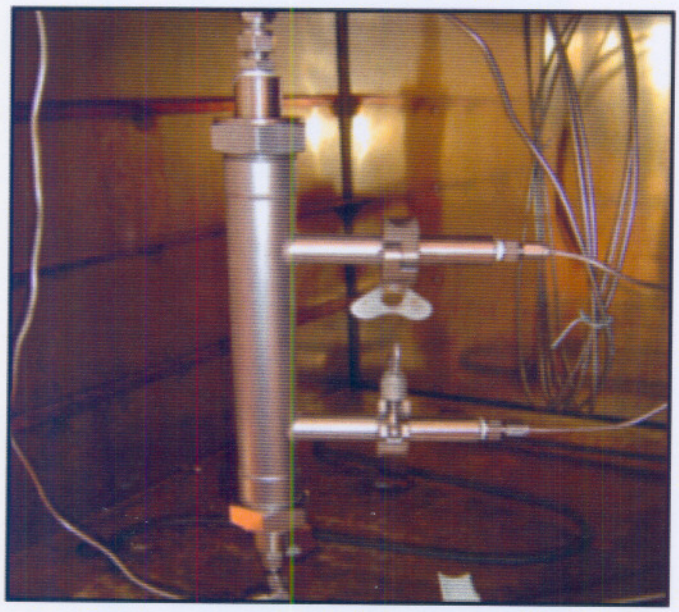

Fig 3.12: Amorphous silica membrane module fitted inside the oven

3.5 MODULE AND MEMBRANE SEALING

NaA

The ends of the tublular membrane were sealed specifically for the temperature application.

At room temperature, the sealing comprised Viton O-rings and polysulphone coating on the ends of the tube. This application can withstand a temperature of up to 473 K. For high temperature applications a Silicone sealant *LOCTITE®* was considered that is non-corrosive, non-slumping, and has a high performance. This sealant is however, not very user-friendly, since the membrane cannot be removed from the membrane housing without damaging it.

The integrity of both the membranes and the seals of the housing was tested by determining the flux of SF6 gas (kinetic diameter of 5.5 Å) through the membrane. SF6 is the largest gas molecule and should theoretically not pass through the membranes. A high flux of SF6 on the shell side would thus indicate a leak through the seals or major membrane failure; while a very low flux would indicate either a slow leak through the seals or a flux of SF6 through inter particle pores of the membrane.

For the NaA membrane no SF6 gas could be detected on the shell side of the membrane, indicating good sealing of the membrane, and good membrane integrity.

For the silica membrane, a very low flux of SF6 was observed. The very low SF6 flux can be seen in Figure 3.13 (See Appendix F for data):

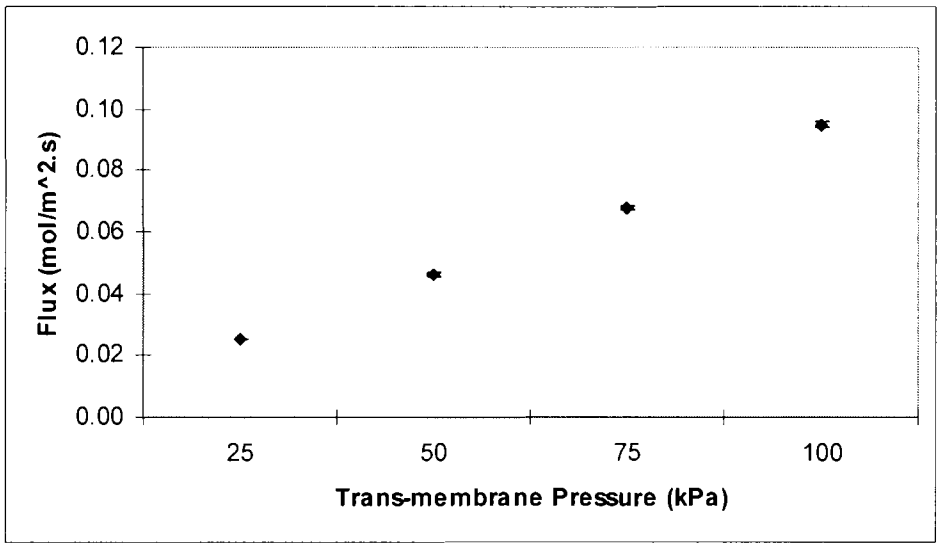

Figure 3.13: SF6 gas flux through the amorphous silica membrane

Silica

The ceramic membrane tubes are glazed with glass at both ends for about 10 mm. The sealing with O-rings or graphite seals is on the outer side of the glazed section. This glazed section of the membrane tube fits in the seals of the module.
The characteristics of the different kinds of seals available for the module are:

Table 3.4: Different types of seal:

Seal Type:	Inner Ø:	Thickness:	Height:
EPDM	9.12	3.53	-
Viton	9.12	3.53	-
Kalrez	9.12	3.53	-
Graphite (produced by Pervatech,BV)	10	3.45	5

3.6 MEMBRANE MANUFACTURING

NaA

This membrane was manufactured in-house by the membrane group within the separation science and technology membrane research group at the North West University.
Details of the synthesis method are discussed in detail by Zah. [Zah, J, 2005]
A typical in-house manufactured membrane support will have the following properties, and hence the properties of the support used for this study:

Table 3.5: Typical membrane support properties

Property	Value
Water Permeability	41 $L.m^{-2}.hr^{-1}.bar^{-1}$
Porosity	37%
Pore size	167 nm

Silica

Since this membrane is an industrial membrane obtained from Pervatech in the Netherlands, bought commerically for this project, the exact procedures used in making this membrane are not known. Chapter 2, however, does discuss the broad steps that are followed in making this type of membrane. (See Chapter 2, section 2.3.5)

3.7 EXPERIMENTAL METHODOLOGY

3.7.1 Screening of NaA membrane for pure Gases

To become familiar with gas permeation concepts and setup, permeation experiments were performed on the NaA membrane obtained from chemistry. This membrane can thus be seen as some sort of "test" membrane.

Single permeance experiments were performed according to the pressure drop method, where a differential pressure is maintained across the membrane. Since counter diffusion of gas normally occurs when one incorporates a sweep gas, and permeation does not necessitate this, no sweep gas was used to remove the permeate. Furthermore, a sweep gas was not used on the permeate side of the membrane cell for this study because of the fact that the permeate is diluted to such an extent, that analysis becomes intricate; it thus is not practical to use a sweep gas. An increase in energy consumption required for both pumping and downstream separation is also another deterrent when using this option [Chung,1999].

Single gas flow rates were analyzed with a bubble meter. The permeance magnitude of pure gases through an in-house manufactured NaA membrane were investigated with regard to varying feed flow rates (50 – 208 ml/min), trans-membrane pressure (1 – 3 bar) and membrane orientation (shell-and tube side). The influence of variable feed flow rate and trans-membrane pressure on the permeation flux can be seen in Figure 3.x.

On commencement of each experimental run, the membrane was fist purged with nitrogen, and a stable system was reached within 15 minutes before commencement of each run. The runs were repeated five times and led to reproducible results (within 10%). There was also no sign of remaining gas in the membrane, reducing the flux of other components.

The influence of variable feed flow rate and trans-membrane pressure on the permeation flux can be seen in figures 3.14 to 3.17 (all data for these figures is available in appendix G).

INFLUENCE OF FLOW RATE

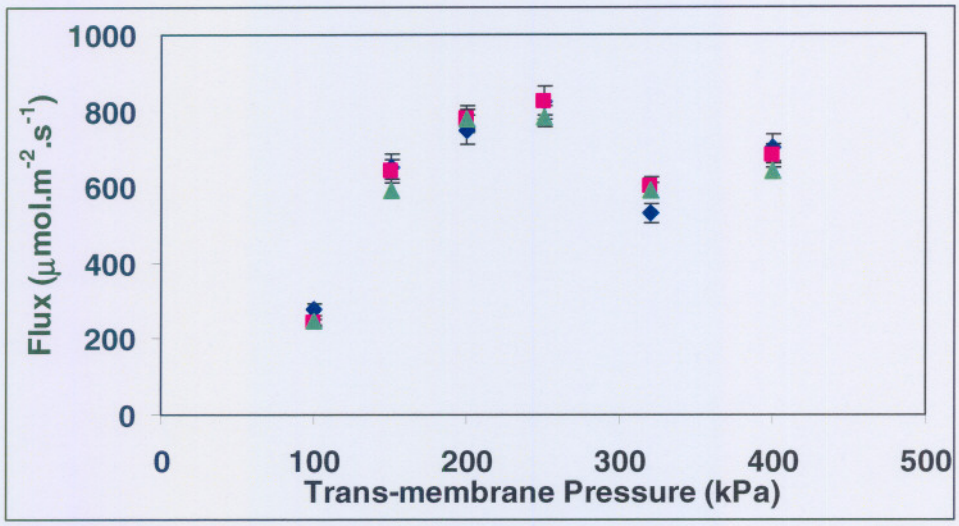

Figure 3.14: Hydrogen flux through NaA at different feed flow rates (◆ 208 ml/min ■ 100 ml/min ▲ 50 ml/min)

In Figure 3.14 the flux of the gases hydrogen and methane can be seen to be independent of flow rate. Only one flow rate will then be chosen for the single permeances of amorphous silica.

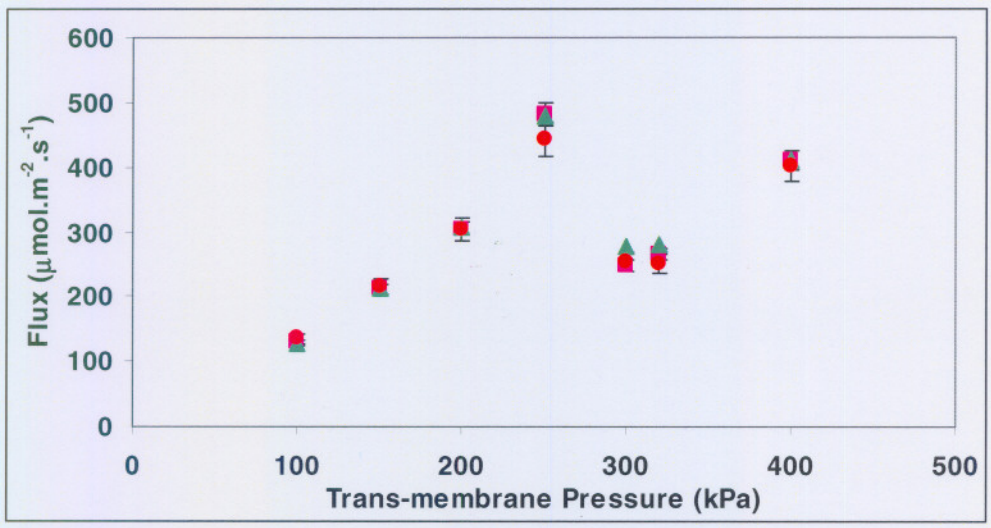

Figure 3.15: Methane flux through NaA at different feed flow rates (■ 208 ml/min ▲ 157.4 ml/min ● 100 ml/min)

For both Figures 3.14 and 3.15 there is an increase in flux as the trans- membrane pressure increases, up till a pressure of 250 kPa, upon which a minimum in flux is observed, and then a further increase is evident.

It is clear that hydrogen permeates preferentially through this membrane. This is also what is expected from literature findings.

It is not known what causes a max/min. trend in the permeation, but it is suspected that inter and intra-molecular water particles are still present in the membrane, blocking the passage of permeation. The membrane must thus be heated at 100 °C for not less than an hour, to rid of the excess water in the membrane pores.

INFLUENCE OF MEMBRANE ORIENTATION

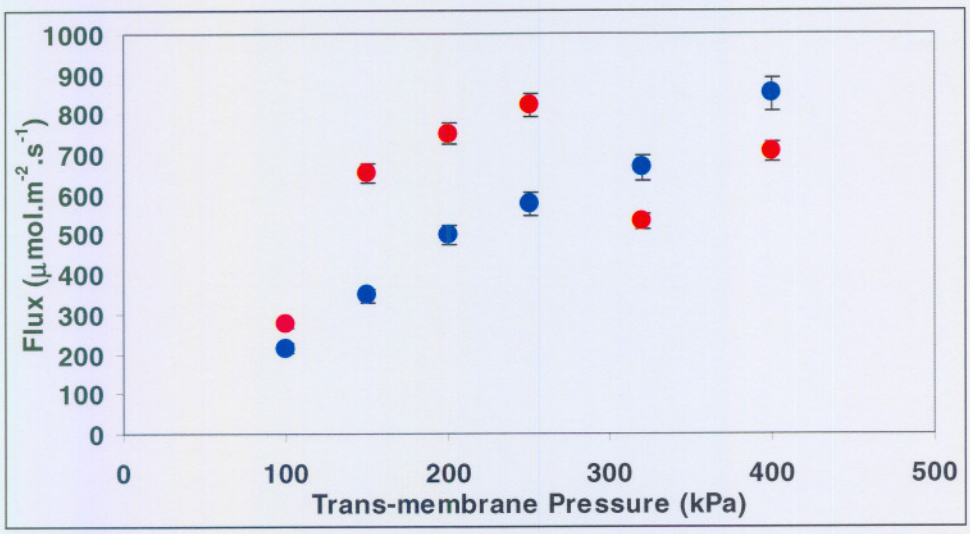

Figure 3.16: Influence of Membrane Orientation on Hydrogen flux (Hydrogen Shell side Tube side)

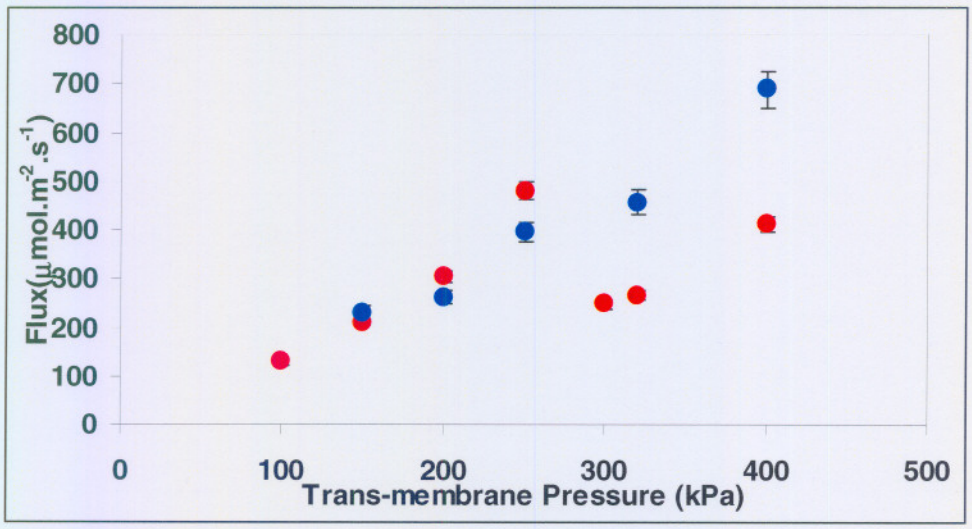

Figure 3.17: Influence of Membrane Orientation on Methane Flux (● Shell side ● Tube side)

In figures 3.16 and 3.17, it seems that the tube side flux is slightly higher than shell side flux for pressures below 250 kPa.

A reverse then takes place above 250 kPa where the shell side flux is higher than for tube side.

At 200 kPa, the ideal selectivities for tube and shell side are 2.5 and 2.2, respectively. At 400 kPa, the ideal selectivities for tube and shell side are 1.7 and 1.4, respectively. It would thus be better to feed gas on the tube side.

One can assess from the ideal selectivites (α_{id}) whether separation will be possible theoretically. Binary permeances will confirm if separation of the gases is possible. (not in the scope of this study)

INFLUENCE OF TRANS-MEMBRANE PRESSURE

The flux shows max./min. trends on tube side at a trans-membrane pressure of 250 kPa, and there is a linear trend in flux on the shell side. See Figures 3.18 and 3.19.

The order of permeance seems to be hydrogen > methane > carbon dioxide.

An ideal selectivity as high as 3.5 was obtained for this membrane.

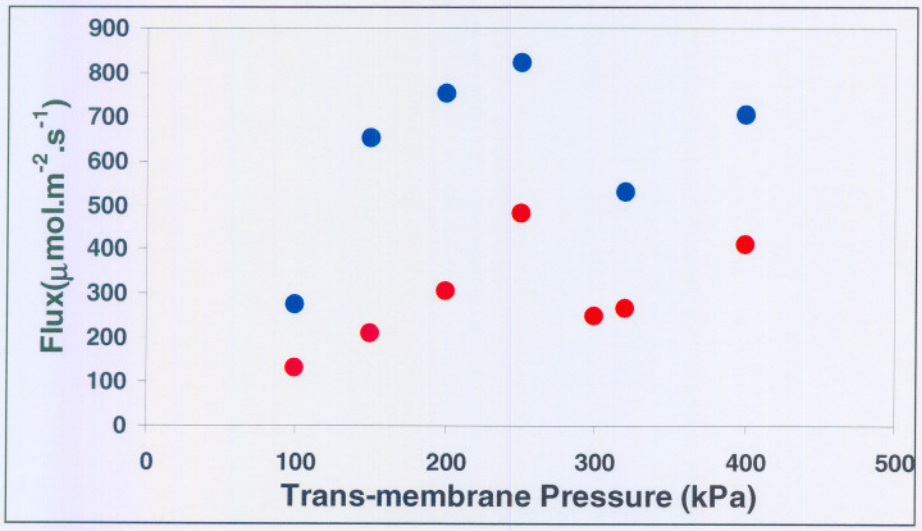

Figure 3.18: Influence of Trans-membrane pressure on flux (● Hydrogen at 208 ml/min ● Methane at 208 ml/min)

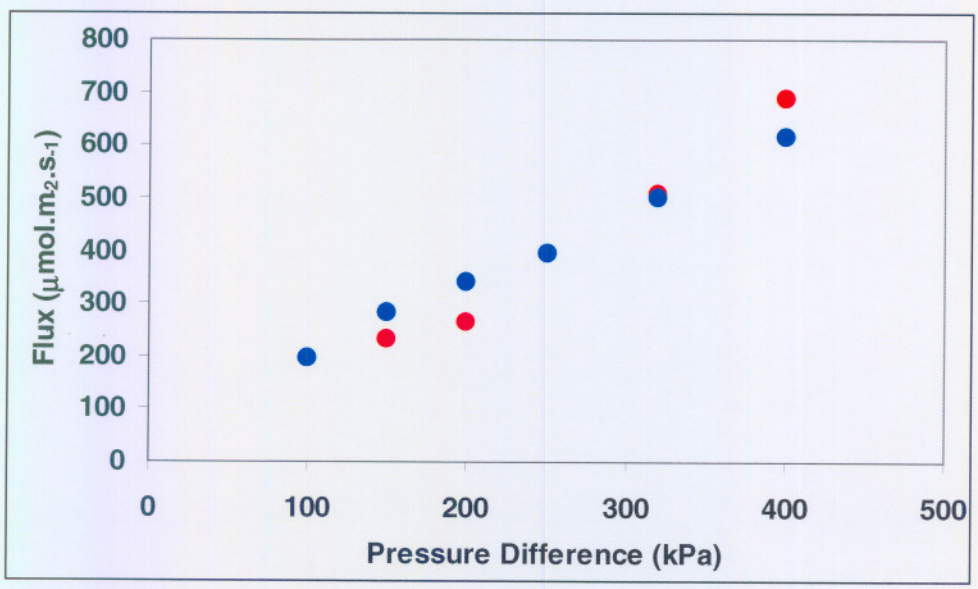

Figure 3.19: Influence of Trans-membrane pressure on shell side flux (● Hydrogen at 208 ml/min ● Methane at 208 ml/min)

3.7.2 Screening of Amorphous Silica Membrane for pure Gases

The single permeances for this membrane took place exactly as with NaA membrane experiments. However, only one flow rate was chosen, since for single permeances the flow rate is independent of pressure. The flow rate chosen for these experiments was higher (2.5 l/min) since a large enough pressure build-up is required due to the fact that the silica membrane has a larger permeation area. Ambient moisture can easily condense inside silica micropores, it is thus extremely important to evacuate pores via an outgoing procedure prior to startup of any permeation experiment. The outgoing procedure was thus conducted at 100 °C for at least 3 hours with dry nitrogen purging across the membrane.

Since this membrane is used industrially, temperature experiments could be performed on this membrane to asses the influence of this property on the flux of gas. Detail results and **interpretation based** on single permeance results is given in Chapter 4 of this dissertation. Processed data for all amorphous silica experiments are available in appendix C.

INFLUENCE OF MEMBRANE ORIENTATION

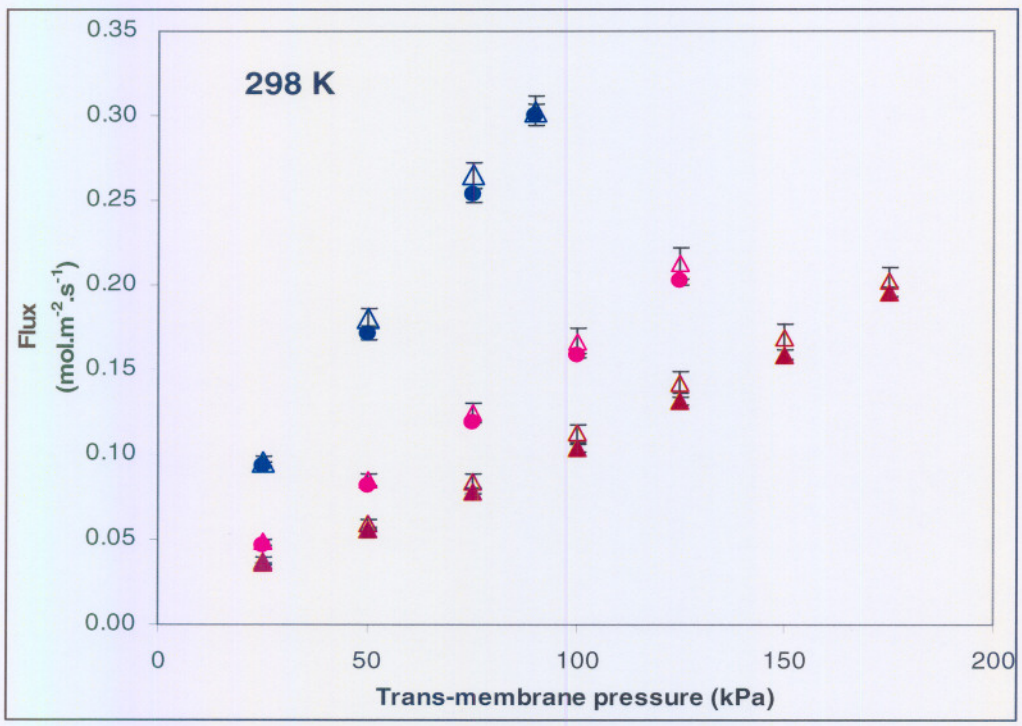

Figure 3.20: Influence of Membrane Orientation for silica membrane (● H2 – Tube side △ H2 – Shell side ● CH4 – Tube side △ CH4 – Shell side ▲ CO2 –Tube side △ CO2 – Shell side)

INFLUENCE OF TRANS-MEMBRANE PRESSURE

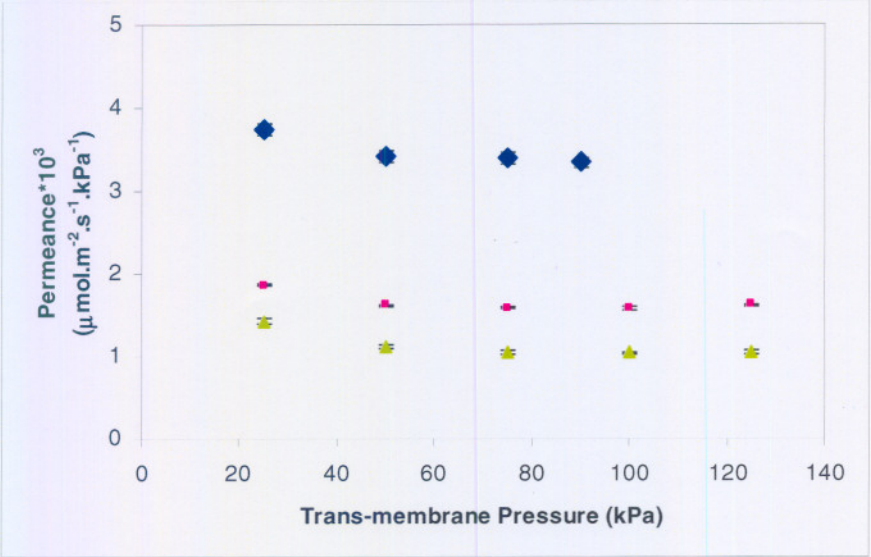

Figure 321: Permeance vs. ΔP for all three gases for silica membrane (◆ Hydrogen ▪ Methane ▲ Carbon dioxide)

BINARY PERMEANCES

Gas analysis took place by means of the GC. A direct gas line was also connected to the GC to enable the feed to be analyzed before entering the membrane. An auto-sampler ensured that gas was inserted into the GC at a constant rate, and thus retention times for each of the gases will always remain constant.

All aspects with regard to binary permeation experiments done on this membrane is dealt with in chapter 5.

Table 3.6: Equipment Utilized fro Gas permeation Experiments

Equipment Type	Qty.	Supplier	Specifications
NaA Membrane Module	1	University Workshop	Stainless steel design Max P = bar
Silica Membrane Module	1	Pervatech BV	See section 3.x
Non-return valve	3		7 kPa feed pressure to open
Electronic pressure transducer	1	Wika Instruments Ltd.	Transmitter range: 0-40 bar
Electronic differential pressure meter	1	Wika Instruments Ltd.	Range: 0 -2.5 bar
Convection Oven	1	Custom Furnaces C.C.	Convection heating. Accurate range: 200-400 °C. Max. Temperature: 600 °C Accuracy: ± 5°C
Thermocouple	1	Eurotherm	Type K. Accuracy: ± 2 °C
Back pressure regulator	2	Swagelok Ltd.	Stainless steel. Outside diameter: 3 mm Inside diameter: 1mm
Mass flow controller	3	Brooks Instruments B.V.	Max flow: 300 ml/min
Gas Chromatograph (Varian Star 3400®)	1	Varian	
1/8 " piping	15 m		Stainless Steel
Gas cylinder regulators	4	Vetgas, Potchefstroom	High pressure: 0-25 bar

Table 3.7: Gas Specifications

Gas	Qty	Supplier	Specification
Methane (cylinder)	1	Afrox Ltd.	Purity > 99.9%
Hydrogen (cylinder)	1	Afrox Ltd	Purity > 99.9%
Carbon dioxide (cylinder)	1	Afrox Ltd	Purity > 99.9%
Helium (cylinder)	1	Afrox Ltd	Purity > 99.9%
Synair (cylinder)	1	Afrox Ltd	Purity > 99.9%

CHAPTER 4 Single Permeation Results & Discussion

4.1 INTRODUCTION

In this chapter single gas permeation results are discussed, and the influence of various parameters and their effect on the permeance of a single gas through an amorphous silica membrane is investigated.

Single permeance of a gas through a particular type of membrane is dependent not only on the type of membrane and support structure used, but also process conditions such as temperature, pressure and various others (membrane orientation) also play a vital role.

4.2 MECHANISMS OF TRANSPORT

When considering permeation or flow through a microporous membrane, different flow regimes related to flux exist in each layer of the asymmetric membrane. The pore ranges where these type of flow mechanisms are said to dominate is given in Table 4.1 [Choi *et al.*, 2001]

Table 4.1: Regimes for different types of flow in microporous materials

Type of flow	Pore range
Viscous flow	> 20 nm
Molecular diffusion	> 10 nm
Knudsen diffusion	2 – 100 nm
Surface flow	< 1.5 nm

From Table 4.1 it can be seen that some of the regimes overlap and therefore, the contribution of each flow type to the overall flow in the membrane has to be determined.

The pore sizes of each layer in the silica membrane structure for this study are known, and the different flow regime in each layer can thus be determined.

According to Table 4.1, the following regimes are expected be present at each membrane layer:

Table 4.2: Regimes expected for the layers of the silica membrane

Layer	Pore size Range	Expected Flow regime
α-layer	3 μm	Viscous
γ-layer	3 - 4 nm	Knudsen
Silica layer	0.3 – 0.4 nm	Surface Flow

In a single gas experiment the ratio of the mean free path is not necessarily such that molecules can only "see" the wall or only "see" each other. As a result Knudsen diffusion and viscous flow can occur simultaneously. Many authors have observed that for porous media these two mechanisms can simply be assumed additive [Present & DeBethune, 1948].

It is thus recommended that the percentage contribution of each flow regime to the support layer be determined. To do this one needs to calculate the various pressure points that exist at each interface point of the layers in the membrane structure.
The composite membrane with the different inter-layer pressures is schematically represented in Figure 4.2:

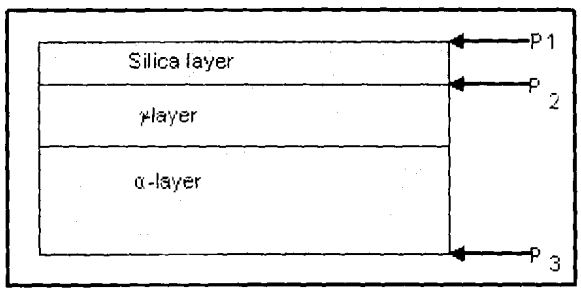

Figure 4.1: Different pressure points in the asymmetric membrane

The total flux of any gas flowing through the membrane at any given time is the sum of the different fluxes that exist due to the different flow regimes in the membrane i.e.

$$J_{total} = J_{viscous} + J_{knudsen} + J_{surface} \qquad (2.8)$$

The equations used to represent the three permeation mechanisms are given by equations 4.2 to 4.5 as in chapter 2.

$$J_{knudsen} = \frac{2\varepsilon_{sup} r_p}{3\tau}\sqrt{\frac{8RT}{\pi M}}\frac{\Delta P}{\delta_{sup} RT} \tag{2.3}$$

$$J_{viscous} = \frac{\varepsilon_{sup} r_p^2}{8\tau\eta RT}\overline{P}\frac{\Delta P}{\delta} \tag{2.4}$$

Where $\overline{P}$ is the average pressure in the support.

$$J_{surface} = D_{surface}\frac{\Delta P}{\delta} \tag{2.5}$$

The surface diffusion coefficient in the support can be calculated with the mean free path model (Kärger and Ruthven, 1992):

$$D_{surface} = \frac{3}{8\sigma^2}\left(\frac{kT}{P}\right)\left(\frac{kT}{M\pi}\right)^{1/2} \tag{2.6}$$

Where

k = Boltsmann constant

M = Molecular mass

σ = Molecular diameter

P = pressure

The surface flux can then be calculated by equation (4.4):

Sample Calculation:

For an applied trans-membrane gauge pressure (P_1-P_3) of 0.3 bar at a temperature of 298 K, a pure **hydrogen** flux (J_{total}) of 0.128 mol.m^{-2}.s^{-1} is obtained.

The permeate side pressure (P_3) is standard atmospheric pressure in Potchefstroom, which is 86.5 kPa at any given day. The feed side pressure (P_1) can then be determined as the sum of the trans-membrane gauge pressure and the permeate side pressure. Thus, $P_1 = (P_{atmospheric} + \Delta P) = 116.5$ kPa.

Flow contributions for each membrane layer can then be determined with the following values known: *(The attached CD-ROM contains the excel calculations used to determine the transport mechanism in the support of the membrane as well as the pressure drops across each layer in the membrane structure).*

Table 4.3: Properties used for sample flow contribution calculations

Property	Unit	Value
		Support Layer (Combined)
r_p	m	1.5×10^{-6}
ε_{sup}	-	0.35
τ	-	2.86
η for H_2 gas	$N.s.m^{-2}$	89.6×10^{-7}
δ	m	1.5×10^{-3}
R	$J.mol^{-1}.K^{-1}$	8.314
T	K	298
σ (Molecular Diameter)	m	2.89×10^{-10}
M (Molecular weight of H_2 gas)	$Kg.mol^{-1}$	2×10^{-3}

For the support-layer:

$$\Delta P = P_2 - P_3 \text{ and } \bar{P} = \frac{1}{2}(P_2 + P_3)$$

Based on the above equation, the only unknown is P_2.

From excel solver P_2 = *86 725.223 Pa* is obtained.

Thus this leads to the following percentage contributions for each layer. (Table 4.4)

Table 4.4: Percentage contribution of different flow regimes through the membrane layers

Flux type	% Contribution
	support-layer (combined)
$J_{viscous}$	15.8 %
$J_{knudsen}$	**84.2%**
$J_{surface}$	0%

From Table 4.4 it can be seen that Knudsen flow is the dominant mechanism of transport in the support.

4.3 CALCULATION OF TRANS-MEMBRANE PRESSURE

Permeance can be defined as the flow or flux through a membrane due to a differential pressure that exists across the **active membrane layer**.
Experimentally, the trans-membrane gauge pressure correlates with the pressure difference determined by subtracting the permeate side pressure from the feedside (retentate) pressure. The actual trans-membrane pressure therefore needs to be determined by incorporating the different types of flow through each layer of the composite membrane.

To calculate the permeance the trans-membrane pressure across the active silica layer should be determined. In section 4.2, all the pressures at the different interfaces (support and active layer) of the membrane layer was determined.
From Figure 4.2 it can be seen that the true trans-membrane pressure, $\Delta P = (P_1-P_2) + (P_2-P_3)$.
This pressure can thus be calculated as follows:

The pressure difference across the support-layer is now:
$\Delta P_{23} = P_2 - P_3 = 86\ 725.223 - 86\ 500 = 0.225$ kPa

The pressure difference across the active silica layer is now:

$\Delta P_{12} = P_1 - P_2 = 116\ 500 - 86\ 725.223 = 29.775$ kPa

The total pressure difference across the membrane structure $\Delta P_{total} = \Delta P_{23} + \Delta P_{12} = 30$ kPa, which coincides with the experimental trans-membrane pressure. The trans-membrane pressure values used to calculate the permeance (see Appendix A) is thus the pressure drop across the silica layer i.e. ΔP_{12} (This pressure drop was calculated for each point in the excel sheet). It is very important to note that the permeance was calculated with steady state flux i.e. the flux through the silica layer and support is the same.

The greatest pressure difference is thus across the silica-layer, which coincides with similar findings from Lee *et al.* (2004) and De Vos *et al.* (1999).

4.4 EXPERIMENTAL ERROR AND REPEATABILITY

All experiments were repeated three times, and the experimental deviation obtained from each run never exceeded 15%. An experimental error was calculated for each run, and can be seen in appendix (D).

The experimental error for each data point is represented as a y-error bar in each figure and shows that these results are reproducible and conclusive.

Based on the single permeance runs obtained for NaA membrane in chapter 3, it was found that the flow rate is independent of feed pressure for single permeances.

For this reason, only one flow rate was chosen to investigate the effect of pressure and temperature on single component permeances through the amorphous silica membrane.

4.5 INFLUENCE OF TRANS-MEMBRANE PRESSURE

In Figures 4.2, 4.3 and 4.4 the permeances of each gas is shown as a function of the trans-membrane pressure (this is the pressure across the active silica layer as well as the alumina layers) and in these figures it can be seen that permeance decreases slightly with an increase in trans-membrane pressure.

This implies that the flux has a linear dependence on the trans-membrane pressure, which is in agreement with literature findings reported by Algieri *et al.* (2003) and Van de Graaf (1999).

Gas molecules collide with each other when under the influence of an applied force. These molecules also collide with the walls of the membrane pores when permeating through a membrane [Mulder, 1998]. If the applied force or pressure difference is increased, the number of collisions would also increase resulting in a longer residence time of the gas molecules in the membrane. The highest permeance values at the lowest applied trans-membrane pressure of 25 kPa may be as a result of less gas molecule collisions against the pore walls. Another possibility is that the membrane be considered as similar to a small packed bed reactor, where the ΔP decreases for lower flow rates. At a trans-membrane pressure of 25 kPa, this effect thus plays a role resulting in higher fluxes.

Furthermore, higher permeances seem to be observed for trans-membrane pressures smaller than 55 kPa for all gases. This, as already mentioned, might be indicative of low gas coverage on pore walls at low pressure gradients [Chung, 1999].

De Vos et al. (1999) states that for Si (400) amorphous silica membrane (the 400 represents calcination temperature), Hydrogen and Carbon dioxide permeance are slightly dependent on pressure if the trans-membrane pressure (ΔP) is smaller that 0.5 bar.

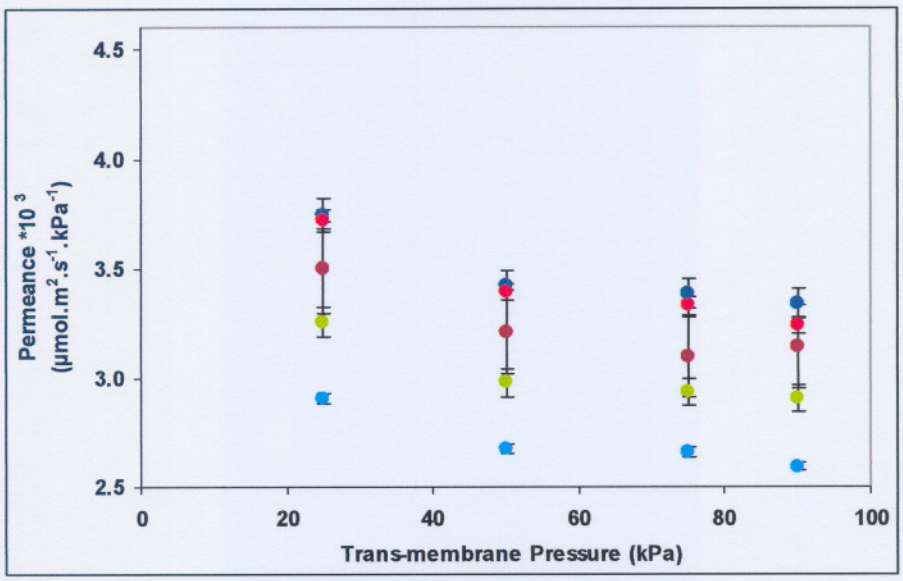

Figure 4.2: Influence of trans-membrane pressure on pure hydrogen (298.15 K 313.15 K 328.15 K 343.15 K 363.15 K)

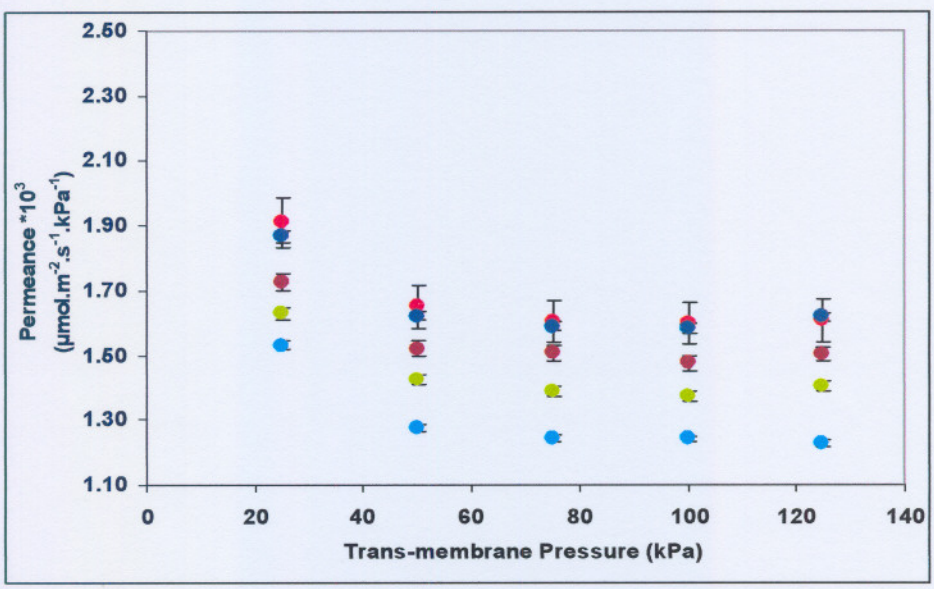

Figure 4.3: Influence of trans-membrane pressure on pure methane (298.15 K 313.15 K 328.15 K 343.15 K 363.15 K)

Carbon dioxide seems to experience a minimum in permeance at approximately 100 kPa, and an increase in permeance is observed for trans-membrane pressures at 100 kPa (see Figure 4.4).

The results of this deviation from the trend of the other two gases might be due to the fact that this gas contributes to adsorption on to the surface of the membrane, thus most likely contributing to surface diffusion on the silica layer [De Vos *et al.*, 1999] and [Benes, 2000].

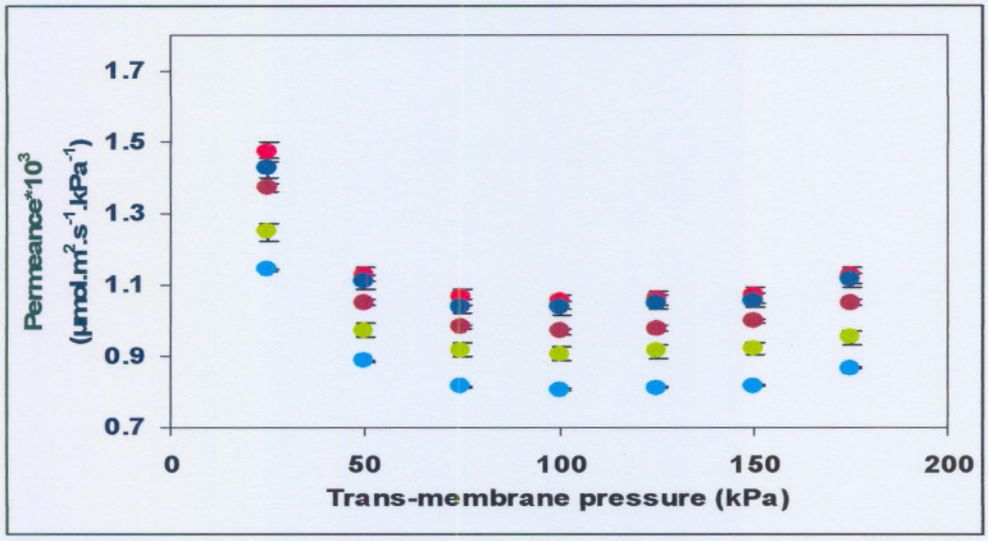

Figure 4.4: Influence of trans-membrane pressure on pure carbon dioxide (298.15 K 313.15 K 328.15 K 343.15 K 363.15 K)

The influence of the trans-membrane pressure on the flux (J) is shown in Figure 4.5. Both experimental data and the Knudsen flow model for flux as in chapter 2 (equation 2.3), are shown in this Figure. From the Figure it is evident that Knudsen flow is most definite the dominating flow mechanism through the membrane, since the model deviates minimally from the experimental data. All data for Figure 4.5 can be seen in Appendix L.

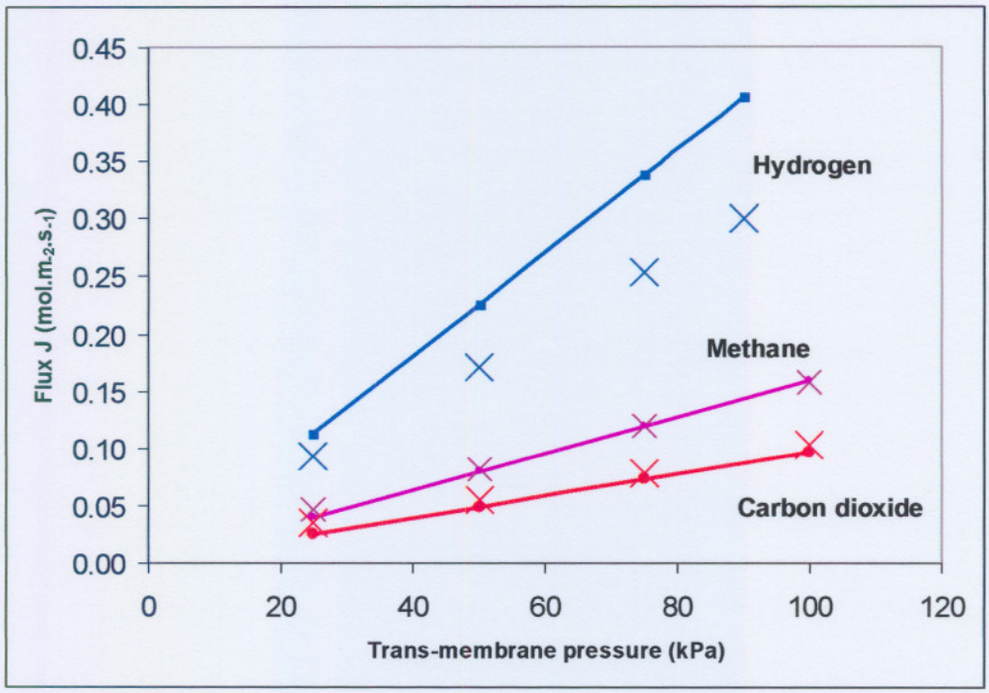

Figure 4.5: Influence of trans-membrane pressure on flux at 298 K (× Experimental Data — Fitted Knudsen flow Model)

Knudsen flow occurs when the mean free path of the diffusing molecules becomes comparable or larger than the pore size of the membrane. Collision between the gas molecules are now less frequent than collisions with the pore wall [Mulder, 1998].

The nearly independent nature of permeance towards an increase in trans-membrane pressure is indicative to Knudsen flow as seen in eq. 2.1 (see Chapter 2 – Literature Survey). Relevant studies by So et al. (1998:152) also revealed a nearly independent permeance response towards trans-membrane pressure. According to So *et al.* this result is in agreement to a predominant Knudsen flow mechanism present in the amorphous silica membrane.

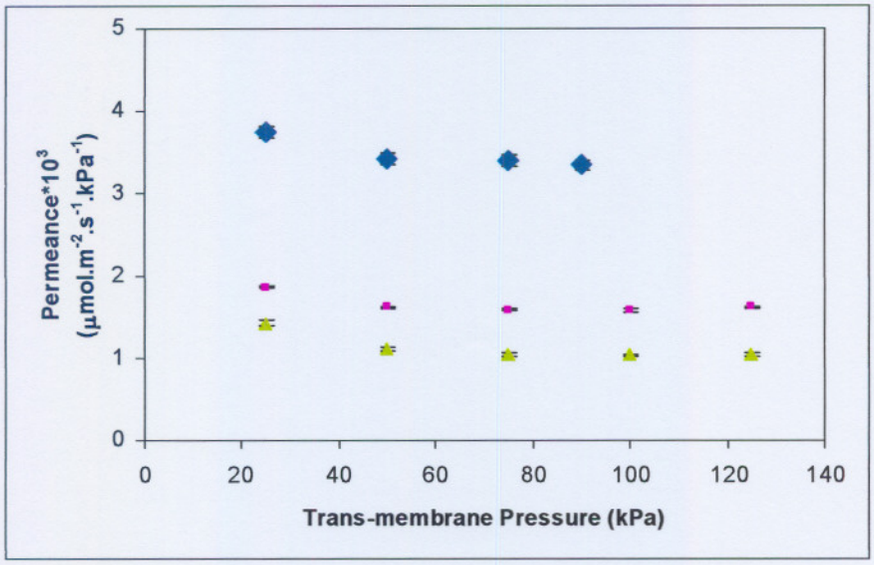

Figure 4.6: Permeance vs. ΔP for all three gases (◆ Hydrogen ▪ Methane ▲ Carbon dioxide)

Figure 4.6 shows the order of permeance for the three investigated gases. The amorphous silica membrane showed the strongest affinity towards hydrogen (N_{H2} = 3.7 x 10^{-3} mol.m^{-2}.s^{-1}.kPa^{-1}) followed by methane (N_{CH4} = 1.9 x 10^{-3} mol.m^{-2}.s^{-1}.kPa^{-1}) and then carbon dioxide (N_{CO2} = 1.4 x 10^{-3} mol.m^{-2}.s^{-1}.kPa^{-1}).

According to de Vos *et al.* (1999), the order of permeance that he found was hydrogen>carbon dioxide> methane. A hydrogen permeance as high as 2×10^{-6} mol.m^{-2}.Pa^{-1} was obtained with the Carbon dioxide values 10 times lower, and Methane the least permeating (50 times slower).

In contradiction to literature as stated above, it seems that hydrogen and then methane permeates preferentially through the membrane. Carbon dioxide is the least permeable gas molecule, and this could be due to the adsorption characteristics of this gas when it comes into contact with the membrane.

In the article of Lee *et al.* (2004), the order of permeance of the gases is in agreement with this study. Lee *et al.* (2004) attributes this permeance order to Knudsen flow dominating in the membrane since there is an inverse dependence on the molecular weight. Since Knudsen flow has proven to be the dominating flow mechanism, the same argument as Lee can be taken into consideration.

4.6 INFLUENCE OF TEMPERATURE

Temperature experiments were performed at various trans-membrane pressures, and results obtained are reproducible and accurate within 15%. The influence of feed temperature on the permenace is shown in Figures 4.7, 4.8 and 4.9 for hydrogen, methane and carbon dioxide, respectively.

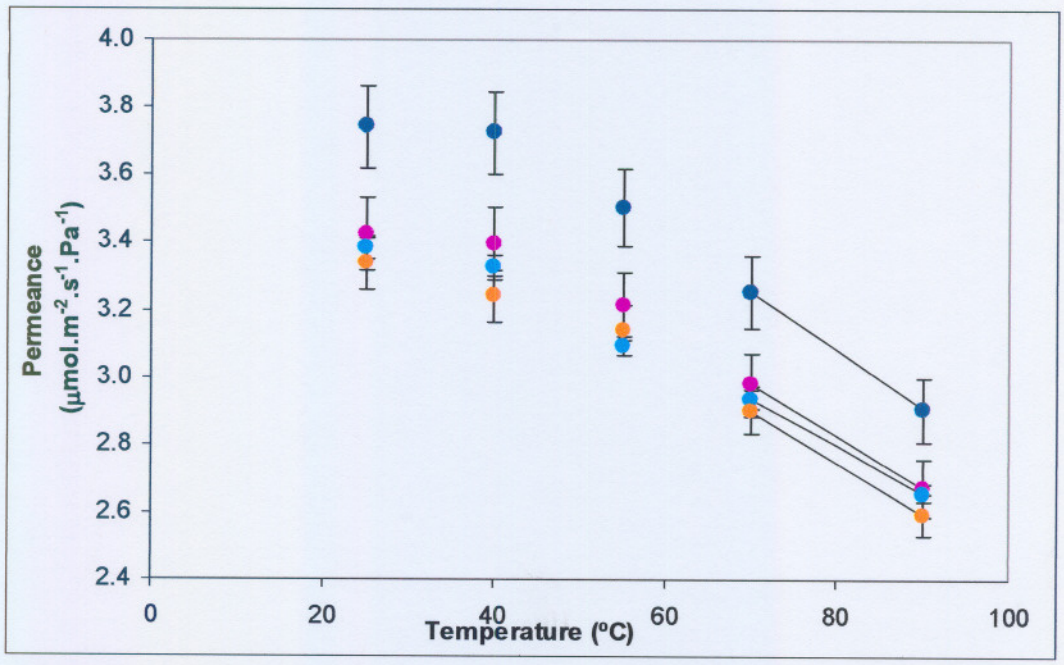

Figure 4.7: Permeance dependence on T for H_2. (0.25 bar 0.5 bar 0.75 bar 0.9 bar)

Figures 4.7, 4.8 and 4.9, show a permeation dependency on temperature for all the gases. With an increase in temperature, permeance exhibits a decreasing trend.

According to Algieri *et al.*, (2003), the maximum observed in the permeance (in Figures 4.7, 4.8 and 4.9, the maxima are at temperatures of 293 and 313 K) at a certain temperature is due to the fact that mobility of adsorbed molecules increased up to a point where the increase in mobility of the adsorbed molecules cannot compensate a decrease in surface coverage. The decrease in permeance can thus be attributed to surface diffusion in the active silica layer.

The decrease in permeance could also be attributed to Knudsen flow, since in Knudsen flow the permeance is inversely proportional to the square root of the temperature.

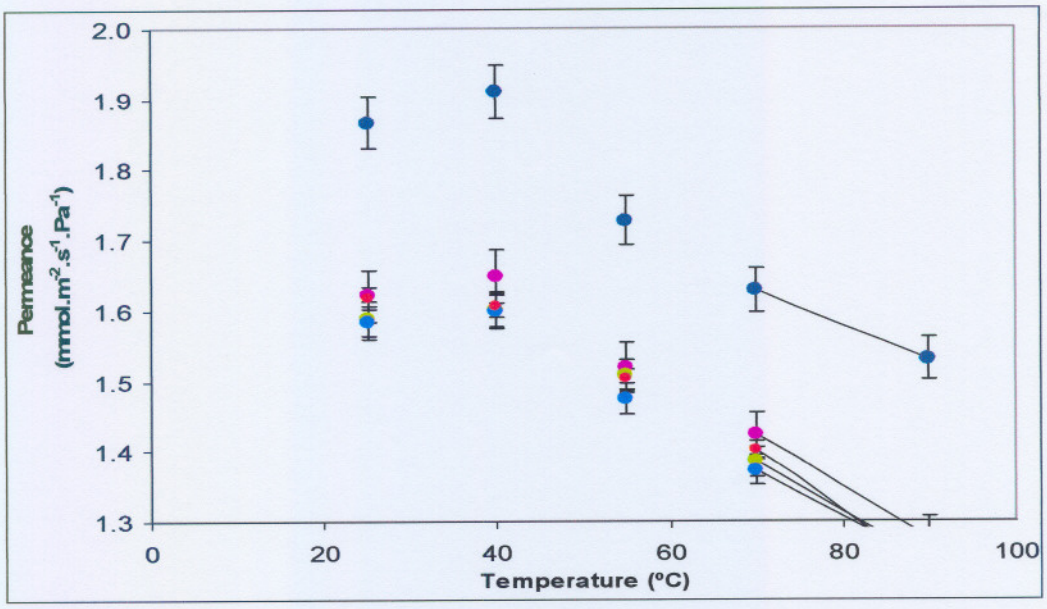

Figure 4.8: Permeance dependence on T for CH_4 (0.25 bar 0.5 bar 0.75 bar 1 bar 1.25 bar)

Asaeda (2001) found that CO_2 gas had the same decreasing temperature dependency for permeation, and explained this phenomenon due to larger adsorption of CO_2 at low temperatures.

De Vos *et al.* (1999) collected permeance data at different pressures and temperature, and found that for most gases a temperature dependence similar to Knudsen diffusion was evident i.e. a slight increase in permeance with a decreasing temperature. His results coincide with results found for this study.

Iwamoto *et al.* (2005) states that according to mechanisms of Knudsen diffusion and viscous flow, permeation of a gas molecule in a porous medium leads to decreasing permeance with increasing temperature.

Lee *et al.* (2004) attributes the decrease trend of permeance with an increase in temperature to Knudsen flow through the alumina support used in his studies. Based on this, one can also consider Knudsen flow as the dominant flow in the membrane.

As a consequence of Knudsen-like temperature dependence this is likely to be caused by the support which has a large influence on the permeation properties of the membrane.

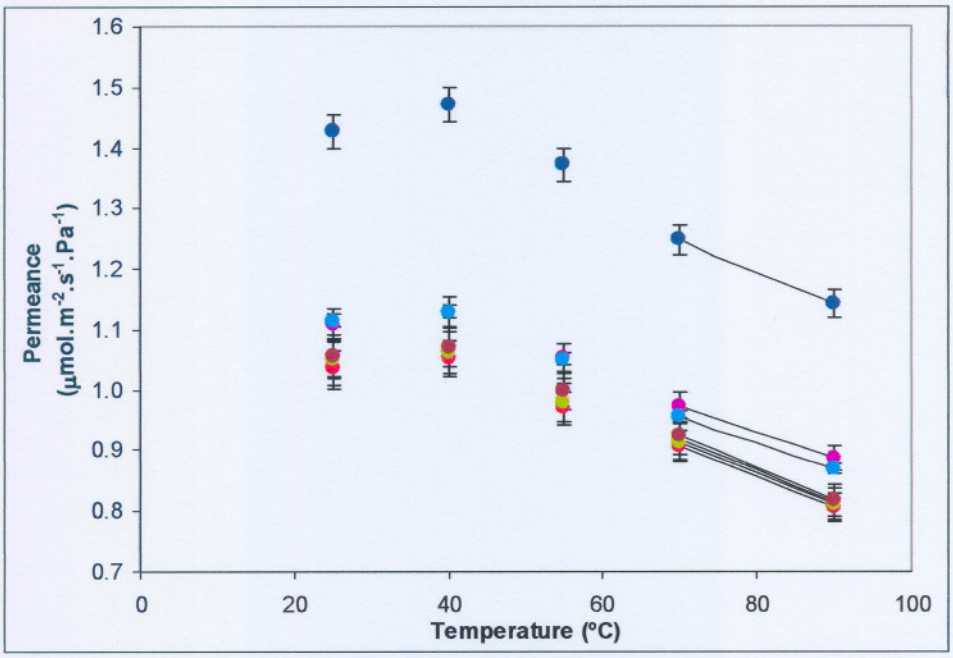

Figure 4.9: Permeance dependence on T for CO_2 (● 0.25 bar ● 0.5bar ● 0.75 bar ● 1 bar ● 1.25bar ● 1.5bar ● 1.75 bar)

Since the decreasing trend in permeance with increasing temperature can be ascribed to the adsorption properties of the gases, this can also be indicative of the fact that activation energy (E_a) for permeance is not always positive, as stated by de Vos *et al.* (1999).

To further explain why the activation energy E_a can be negative, consider the single permeance of a gas through an amorphous silica membrane. According to De Vos *et al.* (1999) the permeance flux can be derived from Fick's first law:

$$J = -D\frac{dC}{dx} \qquad 4.1$$

in which D is the chemical diffusion coefficient, C the local concentration of molecules and x the coordinate along the permeance direction. Gas-phase diffusion limitations can be neglected and thermodynamic equilibrium can be assumed at a membrane interface. The concentrations of molecules at both membrane surfaces can thus be derived from equilibrium gas-phase adsorption data. According to literature, the only quantitative adsorption data available for amorphous microporous silica in the literature is by de Lange et al. [1995]. In addition the complication is met that it is not exactly known what type of amorphous silica best represents

the silica layers used by de Vos *et al.* [1999]. Hence they had to rely on data available for silicalite that can be regarded as a model system for the microporous membrane silica. From the silicalite adsorption data one can conclude that under measurement conditions, gas adsorption is mostly in the low-coverage Henry's law regime:

$$c = kP \qquad 4.2$$

in which k is a proportionality constant that depends on temperature according to:

$$k = k_o \exp\left(\frac{Q_{st}}{RT}\right) \qquad 4.3$$

where K_0 is a temperature-independent proportionality constant, Q_{st} the isosteric heat of adsorption, R the gas constant and T the absolute temperature. The validity of Henry's law implies that the concentration of molecules absorbed in the microporous solid is small compared to the number of available sites (pores). In the Henry (and Langmuir) law adsorption regime, ~D is independent of the concentration. Its temperature dependence is given by:

$$D = D_o \exp\left(\frac{E_m}{RT}\right) \qquad 4.4$$

in which $\sim D_0$ is a temperature-independent proportionality constant and E_m is the positive mobility energy. E_m, represents the energy barrier between two adjacent sorption sites. Since ~D is independent of c, Eq. (4.1) can be written as:

$$J = -D\frac{\Delta C}{L} \qquad 4.5$$

in which ΔC is the concentration difference between both membrane surfaces and L is the membrane thickness. Combining Eqs. (4.2) to (4.5) yields:

$$J = -D_o K_o \exp\left(\frac{Q_{st} - E_m}{RT}\right)\frac{\Delta P}{L} = -J_o \exp\left(\frac{E_a}{RT}\right)\frac{\Delta P}{L} \qquad 4.6$$

in which we define a new temperature-independent proportionality constant J_0 , $\sim D_0K_0$ and effective activation energy for permeance:

$$E_a = E_m - Q_{st} \qquad 4.7$$

E_a can have any sign; we have used a sign convention such that J increases with temperature if E_a is positive.

4.7 INFLUENCE OF MEMBRANE ORIENTATION

The influence of membrane orientation on the permeation flux was investigated by feeding the gas either in the tube side (directly onto the silica layer) or through the shell side (directly onto the α-alumina layer) of the tubular membrane cell.

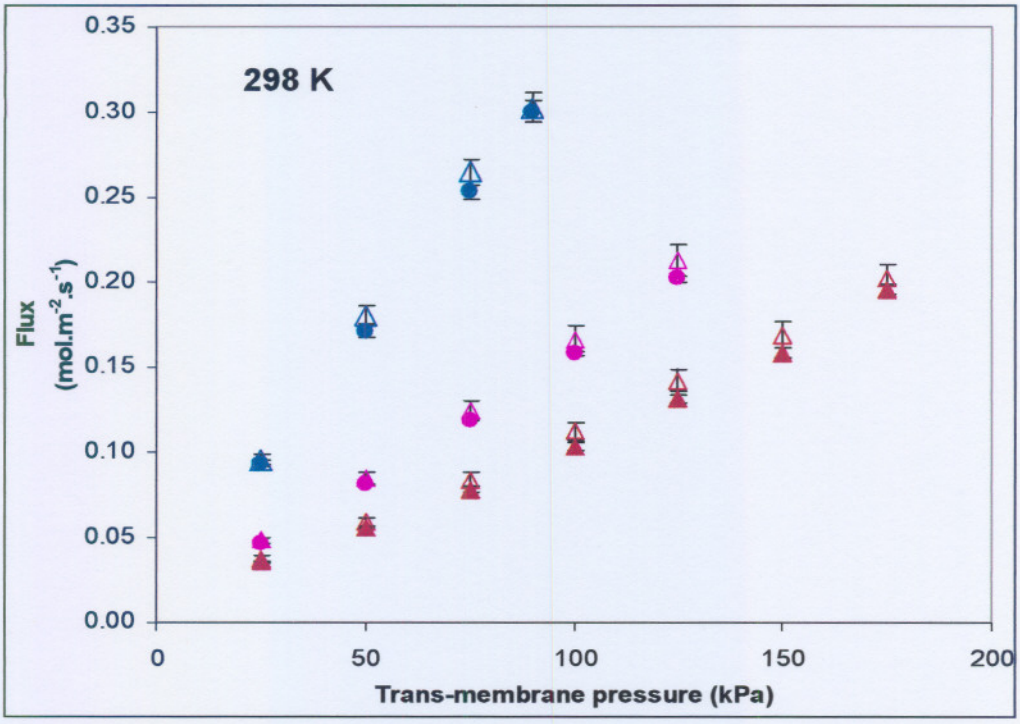

Figure 4.10: Influence of Membrane Orientation (● H2 – Tube side △H2 – Shell side ● CH4 – Tube side △ CH4 – Shell side ▲ CO2 –Tube side △ CO2 – Shell side)

Figure 4.10 depicts the linear relationship between flux and the trans-membrane pressure. An increase in the trans-membrane pressure would lead to an increase in the flux through the membrane.

It is clear from the findings that feeding directly onto the support results in a slightly higher permeance, as opposed to feeding directly on the silica layer. This finding is in agreement with a similar result obtained for a silicailte-1 membrane in the studies of van de Graaf (1999).

A possible explanation for slightly higher permeances on the shell side could be the fact that gas is not directly introduced on the active layer of the membrane where adsorption might occur more readily or as Van de Graaf (1999) found that the resistance of the active layer is higher than that of the support, and thus the passage of the gas molecules are slowed if it is introduced directly onto the active silica layer.

The support layer has a considerable effect on permeation. Although the transport in the support layer is faster than in the active silica layer, the support is still thicker and it has a low porosity. This makes the resistance of the support layer non-negligible and causes a substantial concentration gradient across this layer.

4.8 THEORETICAL SELECTIVITES

Permselectivites

The microporous nature of a membrane can be perceived from the permselectivity, F_α according to de Vos *et al.* (1999).

The permselectivity of a membrane is just the division of the permeation values of the two pure gases passing through the membrane.

Permselectivity values are compared with the Knudsen diffusion limit $\alpha_{Kn(i/j)}$; when this mechanism is predominant light gases permeate faster than heavier gases. The selectivity in the case of Knudsen diffusion is independent on the pressure and is proportional to the inverse square root of the molecular weight i.e. [Mulder, 1998]:

$$\alpha_{knij} = \sqrt{\frac{M_j}{M_i}} \qquad 4.8$$

An experimental selectivity higher than the Knudsen limit may indicate that the mean pore size of the membrane is comparable to the molecular dimensions of the largest species [Algieri *et al.*, 2003].

Resistance though the support must therefore, not be ignored since it might dominate the transport properties.

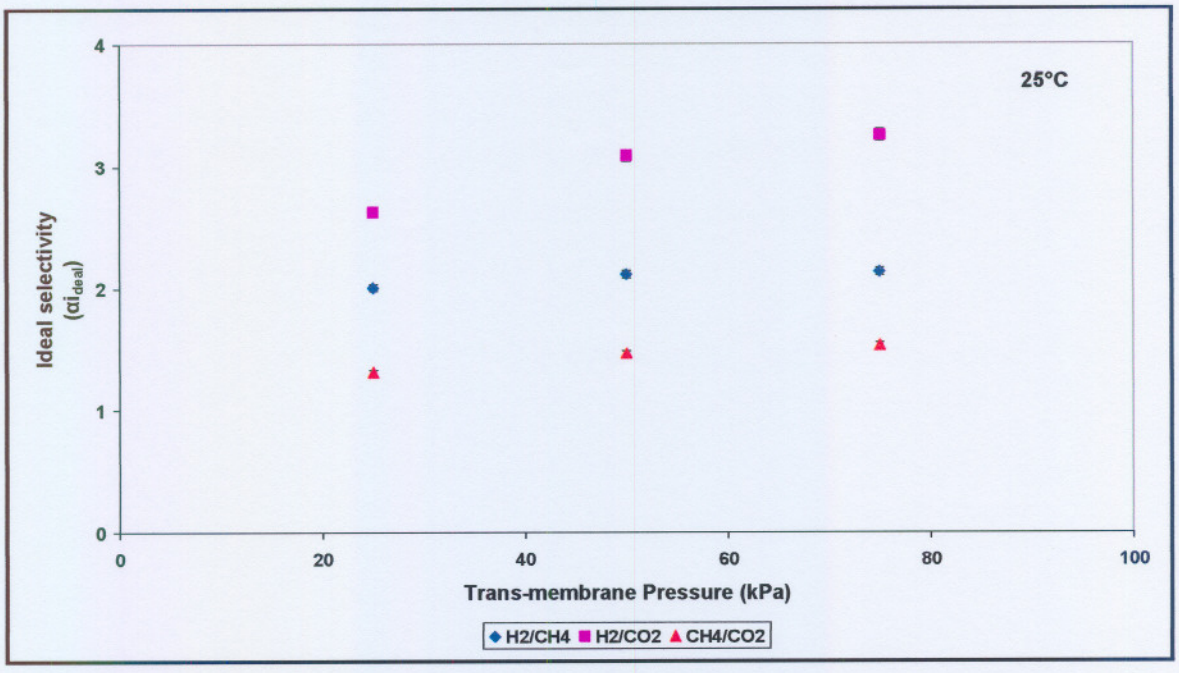

Figure 4.11: Ideal selectivity dependencies on trans-membrane pressure at 25°C.

The ideal selectivities for the amorphous silica membrane showed a slight increase to an increase in trans-membrane pressure. This response is mainly dependent on the slight decrease in permeance to trans-membrane pressure for the pure gasses as seen in Figure 4.1. The highest ideal selectivities for the different gas mixtures investigated are H_2/CH_4 (α_{Ideal} = 2.14, H_2/CO_2 (α_{Ideal} = 3.27) and CH_4/CO_2 (α_{Ideal} = 1.53). From Figure 4.10 it is clear that the amorphous silica membrane shows the largest affinity towards H_2, followed by CH_4 and CO_2.

The Knudsen selectivities for the gas mixtures of concern in this study are H_2/CH_4 (α_{Kudsen} = 2.83, H_2/CO_2 (α_{Kudsen} = 4.69) and CH_4/CO_2 (α_{Kudsen} = 1.66) as calculated using eq. 2.3 in Chapter 2 (Literature Survey).The ideal selectivities for H_2/CH_4 and CH_4/CO_2 closely resemble the Knudsen-like separation values. The lower ideal selectivity for the mixture H_2/CO_2 in comparison to the Knudsen selectivity value can be as a result of the possible surface diffusion characteristics of CO_2 as mentioned in section 4.3.1. A similar dependency on ideal selectivity to trans-membrane pressure was obtained by De Vos *et al.*, (1999).

The influence of temperature on ideal selectivities for H_2, CH_4 and CO_2 mixtures are shown in Figure 4.12.

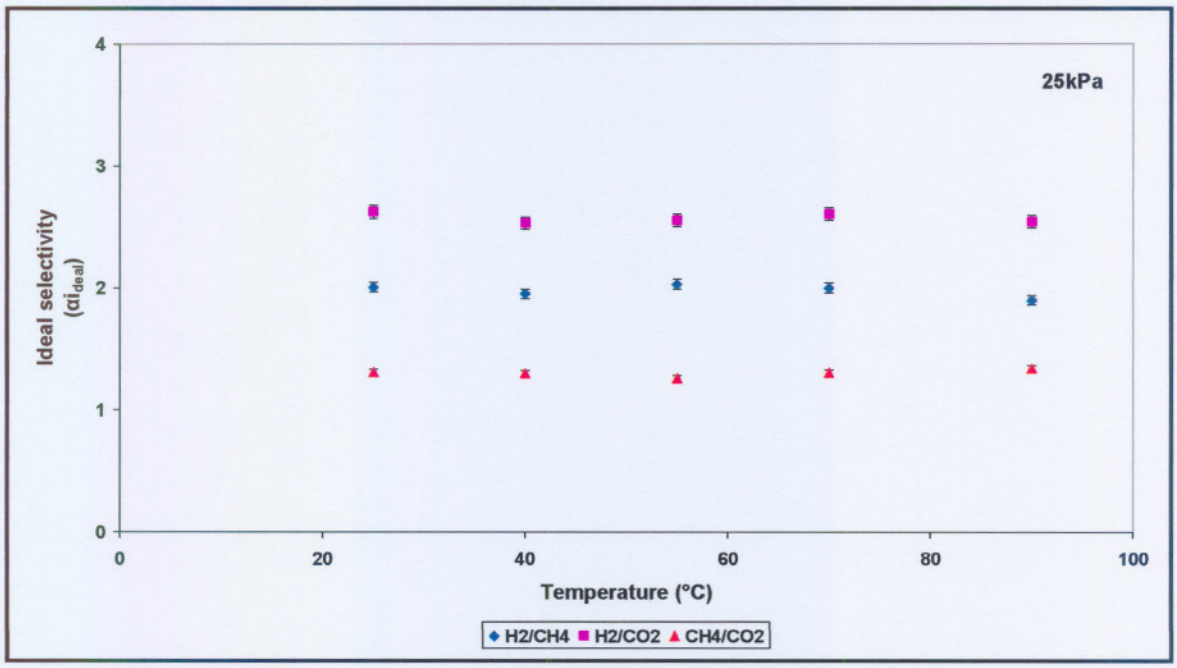

Figure 4.12: Ideal selectivity dependencies on temperature at 25kPa.

No significant dependence for the ideal selectivities was found with a change in temperature as seen in Figure 4.12.

The influence of membrane orientation on the ideal selectivities for H_2, CH_4 and CO_2 mixtures are shown in Figure 4.13.

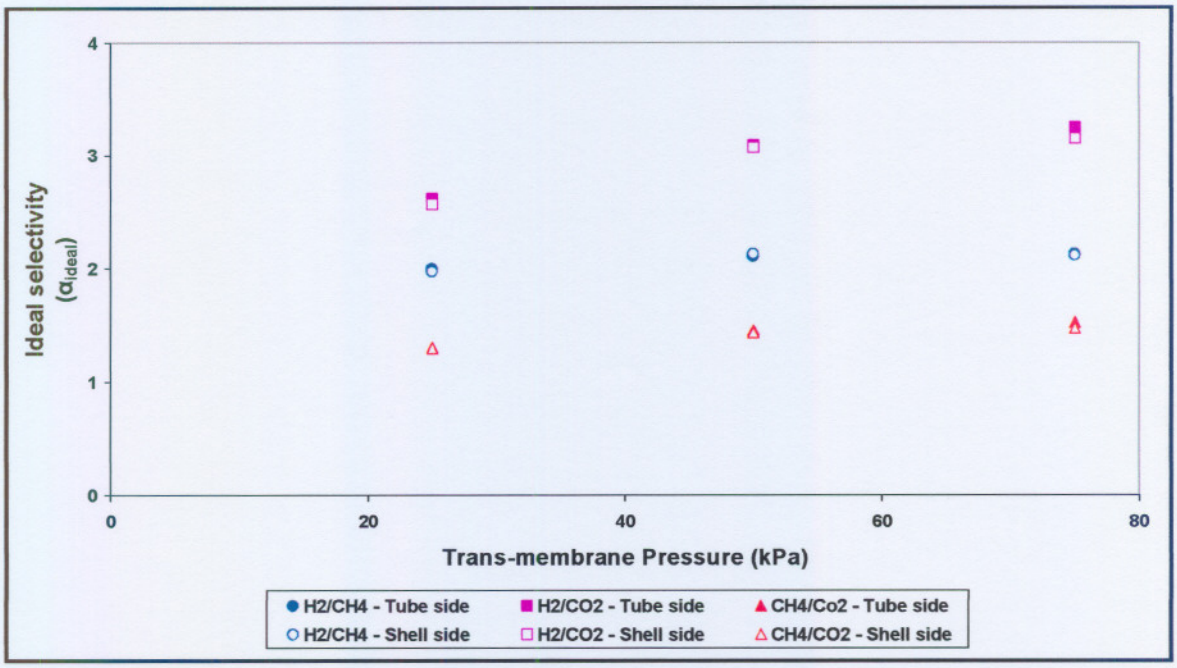

Figure 4.13: Ideal selectivity dependencies on membrane orientation at 25°C.

From Figure 4.13 it is clear that a change in membrane orientation has no significant effect on the ideal selectivities for the different gas mixtures.

Table 4.5: Permselectivities obtained from single gas permeations

		Permselectivities							
		H2/CH4	H2/CO2	CH4/CO2	H2/CH4	H2/CO2	CH4/CO2	H2/CO2	CH4/CO2
		Trans-membrane Pressure (kPa)							
		25			50			75	100
Temperature (°C)	25	2.005	2.624	1.309	2.112	3.089	1.463	3.255	1.527
	40	1.950	2.531	1.298	2.058	3.005	1.460	3.122	1.520
	55	2.028	2.553	1.259	2.113	3.052	1.444	3.149	1.521
	70	1.998	2.606	1.304	2.094	3.058	1.460	3.197	1.512
	90	1.896	2.542	1.341	2.095	3.011	1.438	3.266	1.540

Permselectivities for this membrane represent Knudsen-like separation values, since in most cases the permselectivity is of the order of unity [De Vos *et al.*, 1999].

As a consequence of these "Knudsen-like" values, De Vos *et al.* (1999) believes that these values can be attributed to the support having a large influence, especially for hydrogen, on the permeance through the composite membrane structure.

Based on the findings of De Vos *et al.*, it was also found that the permselectivites are pressure independent for all gases, which indicates that the transport through the γ-alumina membranes was mainly in the Knudsen regime. Their findings are confirmed by Figure 4.12, where permselectivity is independent of the temperature.
In Figure 4.12, it can be seen that the investigated membrane is selective towards hydrogen, followed by methane and then the least selective to carbon dioxide. The selectivity, however, is lower than expected, and it seems that separation for the resulting combination of three gas mixtures won't be achieved, since the permselectivity values are lower than the Knudsen separation values in this case. Binary permeation selectivity values obtained will confirm whether this is true.

4.9 CONCLUSION

It is clear from the results that the effectiveness of any separation process by means of a membrane strongly depends on the three factors investigated in this chapter, namely the operating temperature, the trans-membrane pressure used and the orientation of the membrane with respect to the feed gas. In this study however, any of the conditions leads to an insignificant change in the selectivity of the membrane as a whole.

There is also evidence of adsorption of the gases onto the membrane surface, especially in the case of carbon dioxide, and furthermore results are also indicative of the fact that an amorphous silica membrane is selective to hydrogen in general, but that gas separation is not expected to be achieved successfully in this study. Binary permeation results are thus expected to reveal that successful separation with this membrane is not likely to occur.

CHAPTER 5

Binary Permeation Results & Discussion

5.1 INTRODUCTION

This chapter entails the results obtained from binary gas mixture permeation experiments, and follows the same structure as chapter 4.
Parameters concerning the silica membrane performance as a function of temperature, pressure, composition and membrane configuration will be discussed.

5.2 METHODOLOGY

The effect of operating conditions on the separation of binary mixtures by the membrane takes a systematic structure:

- The *composition* of the binary mixtures was varied at constant temperature and feed pressure. Five mixtures of the binary gas mixtures H_2/CH_4, CH_4/CO_2 and H_2/CO_2 were used. The mixture compositions were 20/80, 50/50, 35/65, 80/20 and 65/35, based on volume percent.
- The *trans-membrane pressure* was increased (Max. 100 kPa trans-membrane pressure) at constant temperature and composition.
- The effect of *temperature* under constant feed pressure and composition was investigated. (Max. temperature of 373.15 K)
- The influence of *orientation* of the membrane on the separation performance was also investigated.

Analyses of the binary mixtures were done by means of a gas chromatograph (Varian Star 3400) as already discussed in chapter 3. Gas sampling of the GC was automated by means of an on-line gas sampler; causing the retention times of the gases to remain constant.
Calibration of the gas chromatograph for the analyses of the various gases were done using the proportionality constant method; [Vosloo, 2005]. A direct feed connection to the gas chromatograph was made, enabling the feed to be analyzed first; so as to obtain a proportionality constant, that could be used for the permeate.

Since analysis of the permeation consists of a binary gas separation system, the calculation is fairly simple:
When analyzing the feed (composition/concentration is known) for two-component permeation, this would be represented as two peaks on a chromatogram. A specific height (more accurate as opposed to an area) of the peak would correspond to a specific concentration of the gas concerned in the binary gas mixture. Simply represented, the gas concentration is directly proportional to the peak height:

$$\text{Concentration} \propto \text{Height}$$

which would imply:

$$\text{Concentration} = k \times \text{Height} \qquad 5.1$$

Once an average proportionality constant is obtained, calculation of the permeate is possible. Two chromatographic peaks can then be seen and the heights known. The permeate concentration can then be calculated from equation. 5.1.

All test runs were carried out three times so as to obtain a fairly accurate proportionality constant as well as to obtain a standard deviation. The statistical data for the chromatogram heights can be seen in appendix K.
At the start of each set of experiments, the membrane was heated up to 373 K for approximately two hours, in order to remove adsorbed components. This treatment gave reproducible separation results.

Definition

Throughout this chapter, reference will be made to the selectivity of the membrane (α). This membrane characteristic can be determined from the permeate and feed compositions during permeation. The selectivity of the membrane towards component i in a mixture containing i and j (α_{ij}) is determined by [Mulder, 1998]:

$$\alpha_{ij} = \frac{y_{i,perm} / y_{j,perm}}{y_{i,feed}} \qquad 5.2$$

5.3 EXPERIMENTAL ERROR AND REPEATIBILITY

During binary gas permeation experiments, three experimental readings were taken at each feed condition. In general, the maximum experimental error obtained (peak heights, permeance and selectivities) was **15%** with a 95% confidence interval. The binary gas permeation results were thus assumed to be repeatable and trustworthy.

All permeance and selectivity deviations are represented as y-error bars on the graphs in this chapter.

The experimental errors for each data point with regard to peak heights, permeances and selectivities are given in appendix K.

5.4 INFLUENCE OF COMPOSITION

In many membrane studies attention is primarily paid to the temperature and pressure dependence of the selectivity. Surprisingly, only a little is known about the concentration dependence of a silica membrane.

Separation processes are part of integrated processes, where in many cases, the outlet stream of one unit is the inlet stream to another unit in the process. Inconsistencies in an outlet stream could lead to varying parameters for an inlet stream entering a separate unit.

In a membrane separation unit temperature and pressure are usually constant and knowledge about the separation features of the silica membrane is required to choose the optimal conditions. The composition of a mixture changes throughout the separation unit until the desired purity is achieved. For the proper design of a separation unit, the composition dependence of the selectivity is thus, an important factor and must be take into account.

The influence of mixture composition on the selectivity and permeance can be seen in Figures 5.1 to 5.6.

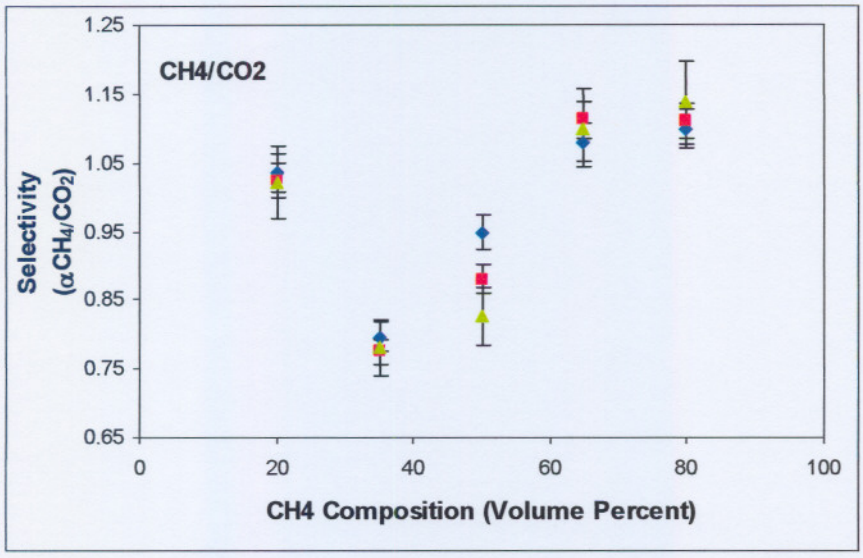

Figure 5.1: Selectivity dependence on composition for a CH_4/CO_2 gas mixture. (◆ 50 kPa ■ 80 kPa ▲ 100 kPa)

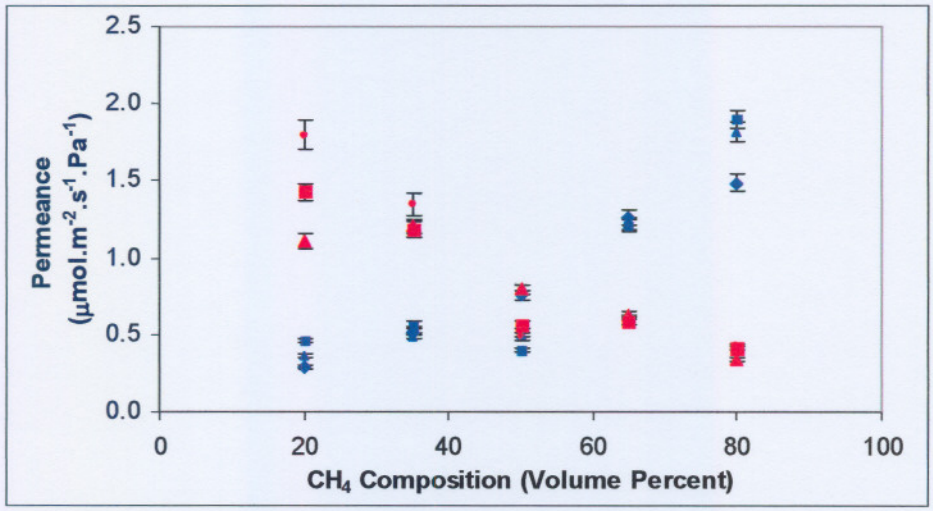

Figure 5.2: Permeance dependence on composition for a binary CH_4/CO_2 mixture. (◆ CH_4– 50 kPa, ▲ CH_4-80 kPa ■ CH_4 – 100 kPa ▲ CO_2-50kPa ■ CO_2– 80 kPa • CO_2 – 100 kPa)

In Figures 5.1 and 5.2 the dependence of the selectivity and permeance on the composition for a CH_4/CO_2 gas mixture is shown. In Figure 5.1 it is evident that the selectivity towards methane in the mixture increases when the composition of this component is increased in the gas mixture. At low composition of methane, it seems that the membrane is more selective towards carbon dioxide.

This composition dependence reflects that the blocking of the silica pores is more efficient when the concentration of the preferentially permeating component increases relative to that of the retained component. To explain this further:

Carbon dioxide is known to be a slow, strong adsorbing molecule, while methane is a fast, weakly adsorbing molecule [van de Graaf, 1999]. In a mixture, this could lead to an increase initially in permeance of the fast, weakly adsorbed molecule, but as time progresses, the fast, weakly adsorbed molecule is replaced by the slow, strongly adsorbing molecule, which is carbon dioxide in this case. This will thus have a blocking effect on the permeation of the methane.

These results are in agreement with results obtained from Van de Graaf. (1999:142)

Van de Graaf, (1999) investigated the separation performance of a silicalite-1 membrane, and found that the selectivity of an ethane/methane mixture increases when the content of the component preferentially separated from the mixture increases. There is thus, an increase in selectivity towards a certain component *i* in a mixture *i/j* when its composition increases in the mixture.

Figure 5.2 depicts the permeances of the two gas components. The permeance of carbon dioxide in this case is reduced as the methane content in the mixture is increased. This is typical for mixtures of fast, weakly adsorbing components (methane) and slow, strongly adsorbing components, (carbon dioxide), that both fit into the silica pores. For these types of mixtures, separation is dominated by differences in adsorption [Van de Graaf, 1999: 161].

The dependence on composition based on figures 5.3 to 5.6 indicates that there are mutual interactions between the two components relative to the figure concerned.

In Figures 5.3 and 5.5, the selectivity dependence on compositions is plotted.

The Figures indicate a minimum in selectivity at 40 volume percent hydrogen composition.

This trend could also once again be an indication of the blocking effect of the adsorbing component, leading to an overall decrease in selectivity of the membrane towards the faster less adsorbing molecule (hydrogen in this case).

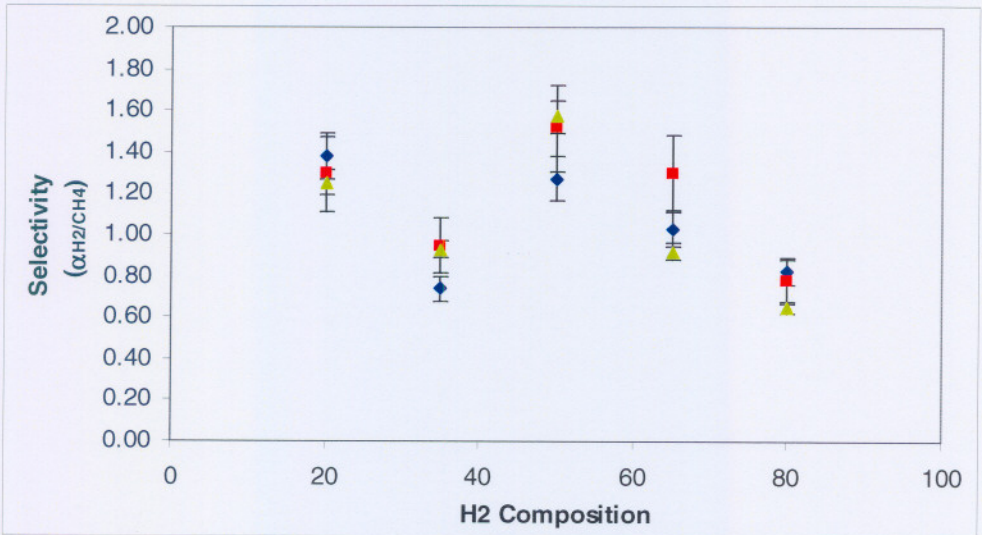

Figure 5.3: Selectivity dependence on composition for a H_2/CH_4 gas mixture. (◆ 50 kPa ■ 80 kPa ▲ 100 kPa)

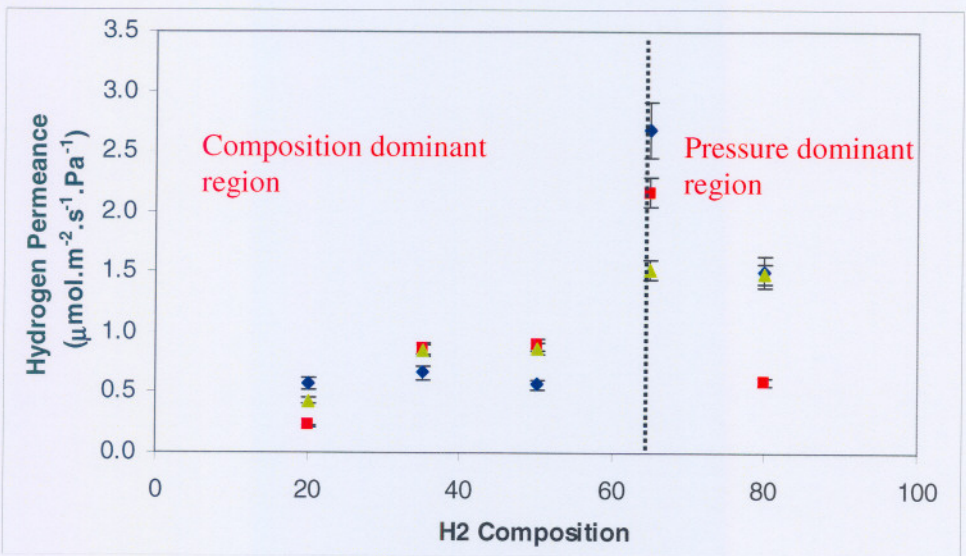

Figure 5.4: Hydrogen Permeance dependence on composition for a H_2/CH_4 gas mixture. (◆ 50 kPa ■ 80 kPa ▲ 100 kPa)

For the permeance results in Figures 5.4 and 5.6, one notices that the permeance of the faster, weaker adsorbing molecule increases up to a 65 volume percent composition, upon which a maximum is observed, and then a decreasing trend in permeance occurs.

The increase in permeance of the preferentially permeating molecule is what is expected. The decrease however, seems to be a possible result of another mechanism that has an opposing effect on permeation, namely the trans-membrane pressure. An indirect relation in permeance with pressure is observed in both figures for compositions exceeding 65 volume percent i.e. the permeance decreases as the pressure increases, which is in well agreement with the definition of permeance since $P = Flux/\Delta P$.

The effect of increasing permeance with increasing composition is the dominant effect up till 65 volume percent compositions. Once permeation exceeds 65 volume percent composition, the dominant effect of pressure seems to result in a decrease in permeance. The dominant parameter of the two mentioned (composition and pressure) determines the permeance path. (See Figure 5.4 for this effect)

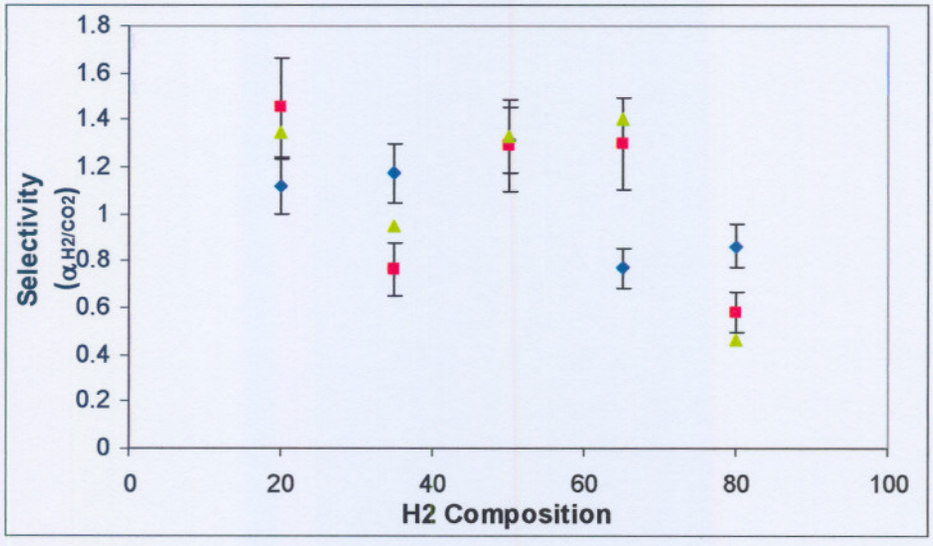

Figure 5.5: Selectivity dependence on composition for a H_2/CO_2 gas mixture. (◆ 50 kPa ■ 80 kPa ▲ 100 kPa)

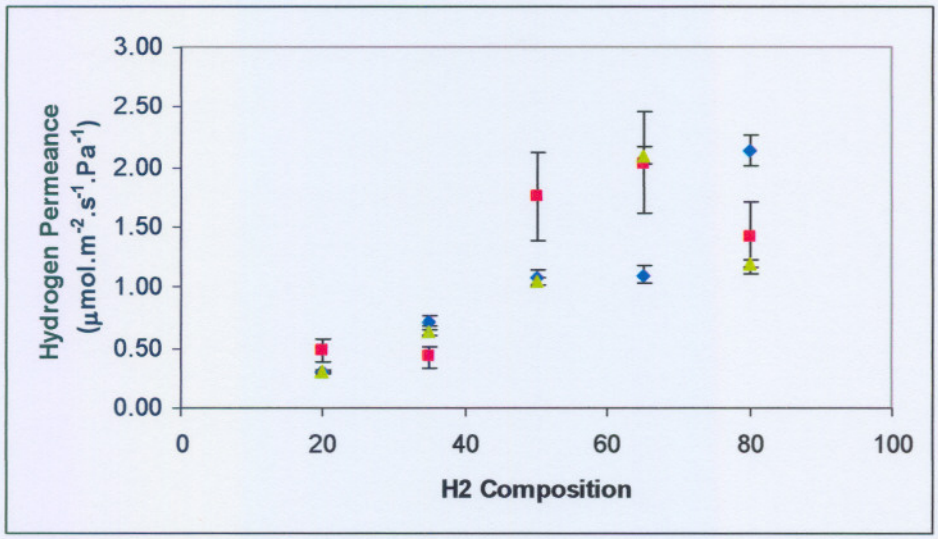

Figure 5.6: Hydrogen Permeance dependence on composition for a H_2/CO_2 gas mixture. (◆ 50 kPa ■ 80 kPa ▲ 100 kPa)

5.5 INFLUENCE OF TRANS-MEMBRANE PRESSURE

The permeance and selectivity dependencies on trans-membrane pressure for various gas mixtures of H_2/CH_4, H_2/CO_2 and CH_4/CO_2 are shown in Figure 5.7 to 5.10.

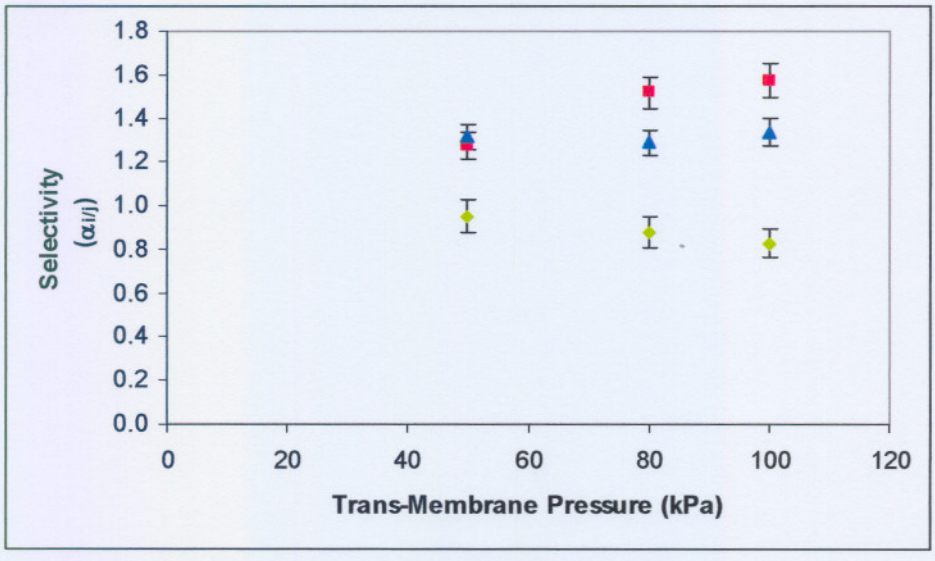

Figure 5.7: Selectivity dependence on trans-membrane pressure for 50/50 gas mixtures (◆ $\alpha CH_4/CO_2$ ■ $\alpha H_2/CH_4$ ▲ $\alpha H_2/CO_2$)

From Figures 5.7 to 5.10 it is visible that the selectivity dependency on trans-membrane pressure is insignificant. Selectivities obtained for all the binary mixtures are more or less the same with a slightly higher selectivity for H_2/CH_4 (α = 1.6) followed by H_2/CO_2 (α = 1.3) and CH_4/CO_2 (α = 0.95). De Vos *et al.* (1998) found a similar nearly pressure-independent response of selectivity for all the gas mixtures investigated.

De Vos states that these results can be expected if one assumes that under the separation conditions used, there is only a limited mutual influence of the gas flows, due to relatively low concentration in the membrane phase (Henry sorption theory!). Henry's law states that the concentration inside a membrane is proportional to the applied pressure [Mulder, 1998: 234]. If the concentration of gas is very low in the silica, the concentration is then nearly independent of pressure, resulting in a nearly independent response of selectivity with pressure.

This result is also supported by the fact that the separation factors are of the same order of magnitude as the permselectivities. These possible explanations could also explain results found for this study, since the same results are evident.

Similar studies conducted also motivate this result. [So *et al.*, 1998: Kapteijn *et al.*, 1998]

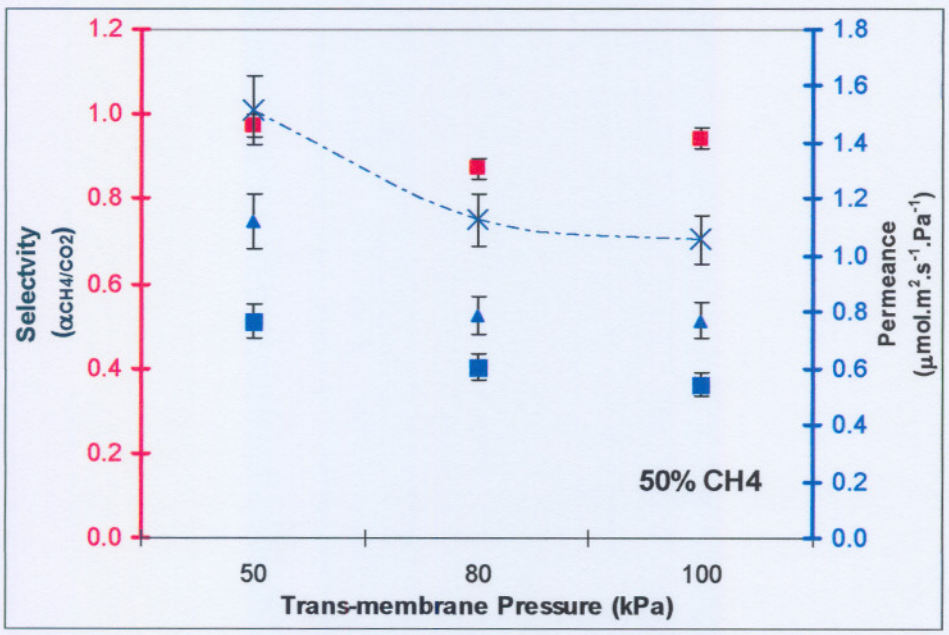

Figure 5.8: Selectivity and Permeance dependence on trans-membrane pressure for a 50:50 binary CH_4/CO_2 gas mixture. (■ $\alpha CH_4/CO_2$ ▲ CH_4 Permeance ■ CO_2 Permeance ⟋ Total Permeance)

It should be noted that the broken lines in Figures 5.8, 5.9 and 5.10 are not lines representing a fitted model, but are just a guide to the eye, to indicate the trend of the total permeance dependence on applied trans-membrane pressure.

The dependence of permeance on the trans-membrane pressure for a CH_4/CO_2 gas mixture is depicted in figure 5.8. One notices that there is a slight dependence on the trans-membrane pressure with regard to permeance for the two gases concerned. Both gas permeances in the mixture seem to decrease initially with an increase in trans-membrane pressure. This result indicates that the same permeances response to trans-membrane pressure for the binary mixtures was obtained, in comparison to the single gas permeation results. A slight decrease in permeance for an increase in trans-membrane pressure was found.

The nearly independent permeance response is in agreement with the Knudsen-like transport mechanism as mentioned in section 4.6.

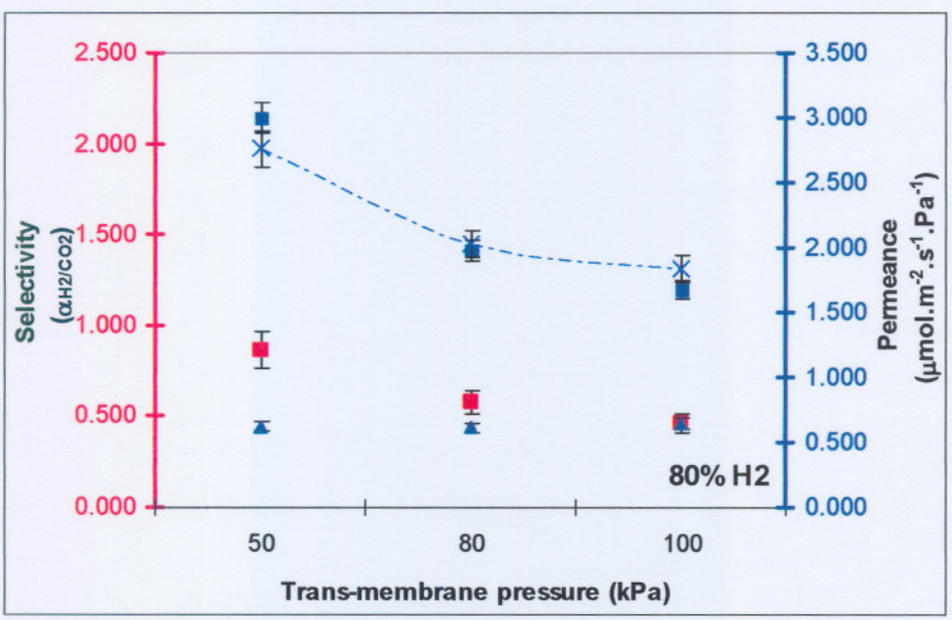

Figure 5.9: Selectivity and Permeance dependence on trans-membrane pressure for a 80:20 binary H2/CO2 gas mixture. (■ $\alpha H_2/CO_2$ ▲ CO_2 Permeance ■ H_2 Permeance ⊣×⊢ Total Permeance)

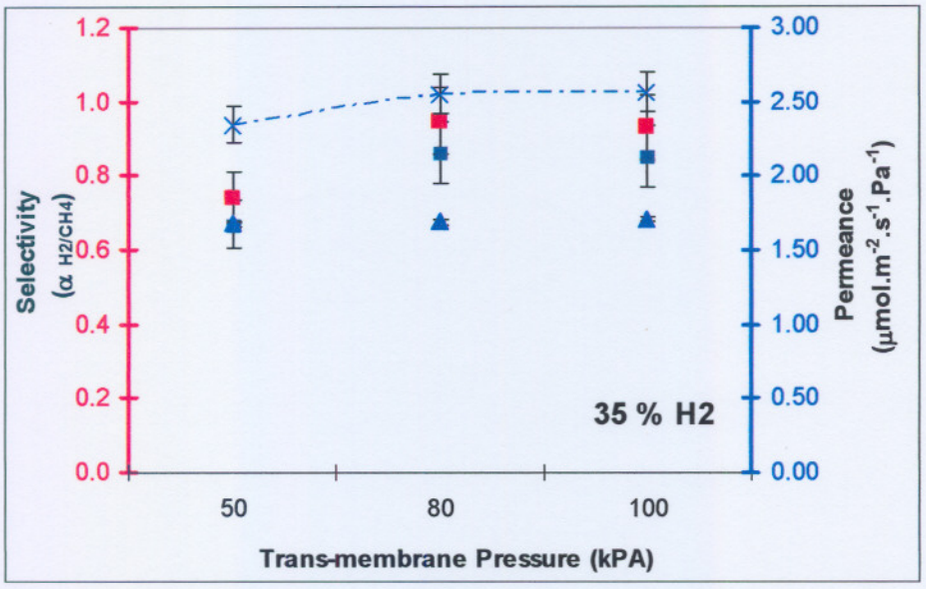

Figure 5.10: Selectivity and Permeance dependence on trans-membrane pressure for a 35:65 binary H2/CH4 gas mixture. (■ $\alpha H_2/CH_4$ ▲ CH_4 Permeance ■ H_2 Permeance ⟡ Total Permeance)

5.6 INFLUENCE OF TEMPERATURE

This membrane showed no noticeable trends with regard to temperature range experiments. Numerous experiments were conducted at different temperatures ranging from 25 to 100 ºC, but it seemed as if binary gas selectivities and permeances are independent of temperature within this range. The independence of selectivity on temperature is well in agreement with the findings obtained for ideal selectivity dependence on temperature. In certain instances there was however, evidence of a similar trend in permeance as with single gas permeances, where a very slight decreasing permeance resulted in an increase in temperature. This type of temperature dependence is once again indicative of Knudsen diffusion, which coincides with single gas permeation results. (De Vos *et al.*, 1999)

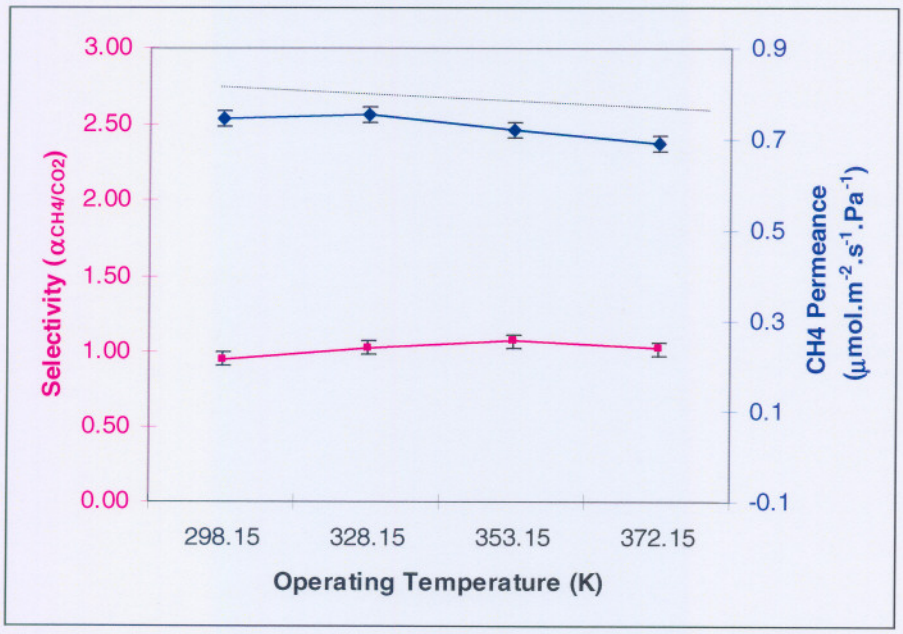

Figure 5.11: Selectivity and Permeance dependency on Temperature for a 50:50 mixture at 50 kPa

Figures 5.11 and 5.12 show that permeance tends towards a slight decrease with an increase in temperature, but it seems as if selectivity is not affected by temperature at all.

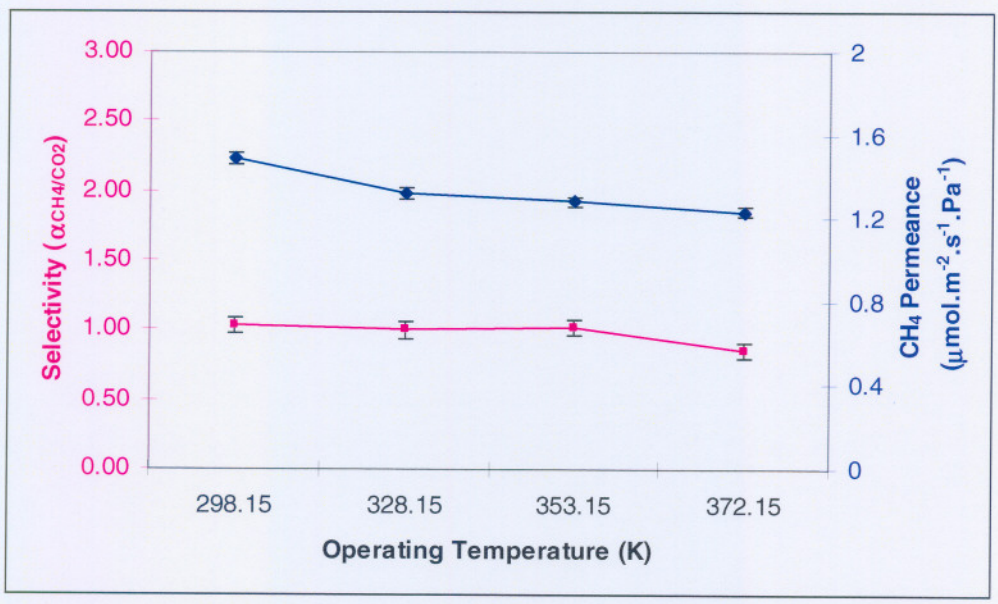

Figure 5.12: Selectivity and Permeance dependency on Temperature for a 80:20 mixture at 50 kPa

Due to the temperature limits of the viton seals, further temperature experiments beyond this range (> 373 K) on this membrane had to be abandoned.

5.7 INFLUENCE OF MEMBRANE ORIENTATION

The influence of membrane orientation on binary gas permeances is shown in Figure 5.13 (Tube side) and Figure 5.14 (Shell side).

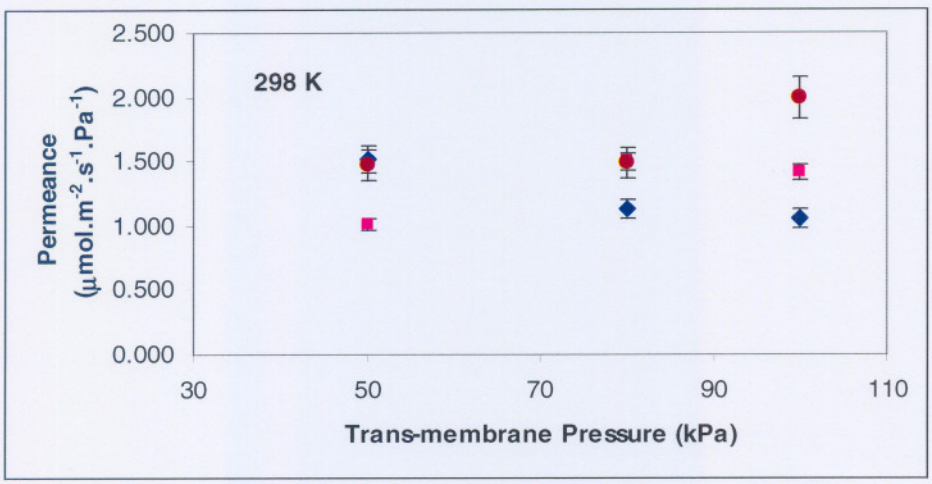

Figure 5.13: Tube side permeances versus trans-membrane pressure (◆ CH_4/CO_2 ■ H_2/CH_4 ● H_2/CO_2)

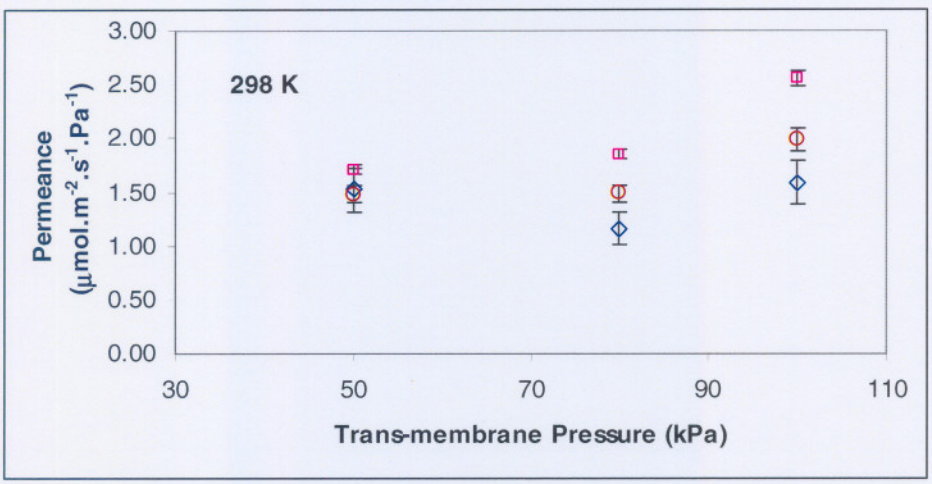

Figure 5.14: Shell side permeances versus trans-membrane pressure (◇ CH_4/CO_2 □ H_2/CH_4 ○ H_2/CO_2)

From Figure 5.13 and 5.14 it is evident that the change in membrane orientation from tube side to shell side reveals slightly higher permeances for all binary mixtures investigated. The higher permeance values for binary permeation on the shell side are in agreement with the single gas permeation results in section 4.8

Once again it can be stated that the resistance of the active silica layer is higher than that of the support, hindering passage of gas introduced directly onto the active layer. Based on binary results, the effect the support layer has on permeance can once again not be ignored.

The influence of membrane orientation on selectivities for the gas mixtures investigated is shown in Figure 5.15 (Tube side) and Figure 5.16 (Shell side).

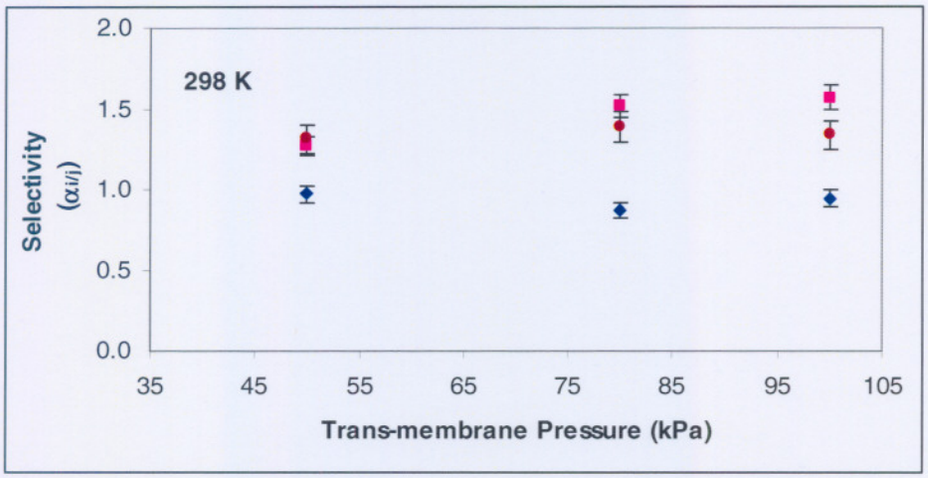

Figure 5.15: Tube side Selectivities versus trans-membrane pressure (◆ CH_4/CO_2 ■ H_2/CH_4 ● H_2/CO_2)

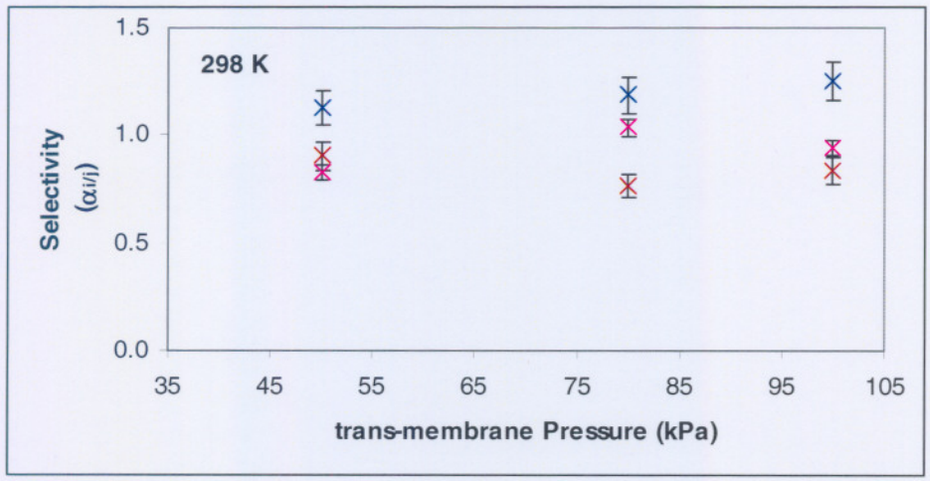

Figure 5.16: Shell side Selectivities versus trans-membrane pressure (× CH_4/CO_2 × H_2/CH_4 × H_2/CO_2)

From Figures 5.15 and 5.16 it is shown that the change in membrane orientation from tube side to shell side revealed only slightly higher selectivities for CH_4/CO_2 and lower selectivities for H_2/CH_4 and H_2/CO_2 mixtures. In the single permeance experiment, the ideal selectivities were independent of membrane orientation. In the presence of the silica layer, the resistance for exiting the support layer is higher for methane than for carbon dioxide, since carbon dioxide blocks the pores of the silica layer for methane. This results in higher apparent selectivity of the support towards methane, since methane is also a fast, weakly adsorbing component. The effect of the support layer on the separation performance of the composite membrane will thus strongly depend on the resistance of the support in a given configuration compared to that of the silica layer. The balance between the two is determined by the mobility of the components under study in the silica layer relative to the support layer.
The same trends with regard to permeance and selectivity can be seen in appendix L (L-1), with an operating temperature of 353 K.

5.8 SELECTIVITY VALUES AND GENERAL FINDINGS

The low selectivity values obtained for all three gas mixtures may be as a result of mutual interactions between the components as stated by De Vos *et al.* (1999). The selectivities for all three gas mixtures were found to be slightly lower than the theoretical or ideal selectivities as seen in section 4.8. The separation selectivities of this membrane coincide with the selectivities obtained for pure gases in that both selectivities display Knudsen selectivity characteristics.

Based on these findings the separation of the Fischer-Tropsch gases using an amorphous silica membrane was **not** achieved in this investigation, and any changes in operating conditions would not improve this result.

5.9 CONCLUSION

With regards to the specific operating conditions and selectivities one could see that there are slight dependencies, but not significant to qualify this membrane as a gas separation membrane. Personal consultation via email with Mr. Frans. M Velterop (Pervatech, BV) revealed that this membrane has been designed specifically for pervaporation and gas separation with this membrane still requires further investigation in terms of the design of this membrane.

CHAPTER 6

General Conclusions and Evaluation

6.1 INTRODUCTION

Silica membranes have been known for about a decade, and in general are known to exhibit good separation characteristics. They are also known for applications in the fields of gas separation, liquid separation and pervaporation. The high fluxes and selectivities found for micro-porous silica membranes offer numerous perspectives for applications, including natural gas purification, selective CO_2-removal and industrial H_2-purification. A specific application is their potential use in high temperature membrane reactors, for the selective removal of H_2 in order to increase conversion efficiency of thermodynamically limited reactions.

In this study, the permeation characteristics and possible gas separation capabilities of an amorphous silica membrane was investigated. Permeance and selectivity dependencies on trans-membrane pressure, temperature and membrane orientation were investigated for the Fischer-Tropsch gases, H_2, CO_2 and CH_4. Results are of no use if they are not interpreted and certain conclusions can be drawn. This chapter contains all conclusions that can be drawn based on this study in its entirety.

6.2 EXPERIMENTAL ASPECTS

Experimentally it is important to acquire knowledge regarding the experimental methodology, and to identify certain areas that may cause a problem with regards to experimental work. An example of this was the use of a sweep gas for permeance experiments. The use of a sweep gas was considered, but regarded as impractical due to dilution of the permeate to such an extent that analysis of gases became intricate.

It is also of vital importance prior to carrying out experiments that one has to become acquainted with the gas separation setup, and the concepts used in gas separation. For this, a NaA zeolite membrane (manufactured locally within the Science Separation group at the North-west University) was available, and various screen tests could be performed on this membrane. This is where various trends familiar to gas separation could be seen and various experimental methods employed could be reviewed.

All experiments were performed on a standard gas separation setup. This setup was both user-friendly and very seldom did problems arise with any breakages in apparatus. Any leaks in the system were also fairly easy to detect.
With regards to experimental errors and repeatability, one could conclude that in general these parameters were fairly low, and thus one could assume that the results are conclusive and reproducible. The graphs also display the experimental deviations for each data point, and thus this allowed the data to be interpreted more accurately.

6.3 SINGLE PERMEATION RESULTS

Due to the amount of research done regarding amorphous silica membrane used for gas separation in particular, much of the data relied on, and the possible explanations for various trends was based on literature available for silicalite membranes. This membrane can be regarded as a model system for the microporous membrane silica. Silicalite is a pure silica with elliptical straight channels (5.7 Å × 5.7 Å), and sinusoidal channels (5.4 Å pore diameter) almost comparable to amorphous silica.

Upon investigation, it was found that the main mechanism of transport in this membrane is Knudsen transport which is dominant in the active silica layer. This finding is in agreement with the findings of Lee *et al.* (2004) and De Vos *et al.* (1999).
High permeance values were observed for Hydrogen, Methane and Carbon dioxide with the amorphous silica membrane showing the largest affinity towards hydrogen followed by methane and carbon dioxide (N_{H2} = 3.7 x 10^{-3} mol.m^{-2}.s^{-1}.kPa, N_{CH4} = 1.9 x 10^{-3} mol.m^{-2}.s^{-1}.kPa and N_{CO2} = 1.4 x 10^{-3} mol.m^{-2}.s^{-1}.kPa). However, very low ideal selectivities ($\alpha_{i/j}$ < 4) for these Fischer-Tropsch gases were achieved. It was concluded that this may be as a result of the possible adsorption characteristics of the gases onto the membrane. Furthermore, the membrane did not exhibit molecular sieving properties, (where molecules are excluded based on particle size), but rather exhibited "possible" adsorption dominating transport.

Single gas permeance dependency on trans-membrane pressure indicated a near independent response while temperature changes revealed slightly lower permeance values at elevated temperatures. Both these responses are related to Knudsen-like transport through the membrane. The permeance for all three gases showed an inverse square root dependence on

temperature of the diffusing gas molecule. This characteristic feature of gas transport is in agreement with Knudsen flow. The majority of the single gas permeation results were in agreement with similar literature studies [So *et al.*, 1998:152, De Vos *et al.*, 1999, Iwamoto, 2005 and Lee *et al.*, 2002].

Feeding the pure gases directly onto the support (shell side) of the membrane resulted in a slightly higher permeance, as opposed to feeding directly on the silica layer (tube side). A possible explanation for slightly higher permeances on the shell side could be the fact that gas shows much greater adsorption behavior on the amorphous silica layer of the membrane. Another possible explanation for this is the role that the resistance across the active silica layer could play in blocking the passage of the gas molecules, resulting in a lower permeance if gas is introduced directly on to the silica layer. This finding is in agreement with similar results obtained for a silicailte-1 membrane in the studies of Van de Graaf (1999).

Theoretical or ideal selectivities obtained were in the order of Knudsen factors. From the permeance data the membrane revealed the highest theoretical separation capability towards H_2/CO_2 (α_{Ideal} = 3.08) followed by H_2/CH_4 (α_{Ideal} = 2.11) and then CH_4/CO_2 (α_{Ideal} = 1.5).

It was also found that the ideal selectivities were independent of all operating conditions. (temperature, trans-membrane pressure and orientation) Based on the single permeance data it could be concluded that successful separation was not likely to occur, but despite the separation one could still form a basic concept as to the influence that various operating conditions have on the membrane performance.

6.4 BINARY PERMEATION RESULTS

Actual selectivities obtained indicated similar separation factors for all gas mixtures e.g. the 50:50 mixtures where H_2/CO_2 (α = 1.3), H_2/CH_4 (α = 1.27) and CH_4/CO_2 (α = 0.97). These separation factors are however, much lower than the above mentioned theoretical membrane selectivities which implies that almost no separation occurred.
Selectivity dependencies on trans-membrane pressure revealed no significant response.
Tube side (amorphous silica layer) feed of the gas mixtures revealed separation factors in the order of H_2/CO_2 followed by CH_4/CO_2 and H_2/CH_4. Shell side feed showed a change in

separation order with CH_4/CO_2 separation being the highest followed by H_2/CH_4 and then H_2/CO_2. Based on the binary permeation results it could be concluded that in a binary mixture, both gases display mutual interaction, but in most cases one component displays stronger adsorption abilities than the other component in the binary mixture. This adsorbing ability results in available transport sites on the membrane to be blocked by the strongest adsorbing component, thus limiting the passage for the other component in the mixture and decreasing the permeance of that component.

6.5 GAS SEPARATION POTENTIAL AND APPLICATION

Inorganic membranes need greater advantages than low cost and abundance if they are to compete with other adsorbents in gas separation processes i.e. they must demonstrate superior performance in specific separations.

Successful gas separation on this specific amorphous silica membrane was not achieved. This membrane would essentially be classified as Knudsen-diffusion membrane because of the fact that it cannot compete with other membranes of its type, due to the low selectivities that one achieved with it. In the work of other researchers, high amorphous membrane selectivities have however been reported, and it seems that successful gas separation with this type of membrane is achievable. Industrially this type of membrane is already in use and it has great potential in its application as part of integrated separating systems.

A possible explanation for the low selectivity values could also be a result of defects that occurred during the manufacturing process of this membrane.

Upon further investigation as to why the low the separation selectivities were obtained for this silica membrane in particular, it became obvious that this membrane as well as the membrane module were specifically designed for pervaporation. Contact with the membrane manufacturing company (Pervatech, BV) led me to believe this.

.

6.6 FINAL REMARKS

The present work has given insight in the important factors involved in permeation through a silica membrane. It should be noted that it is difficult to compare various types of membranes under the same membrane operating conditions, since some of the reported membranes are made of different materials and those made with amorphous silica were structurally modified. Furthermore, it should also be noted that all operated under different conditions to achieve their respective best performance.

From an experimental approach, the selectivities and permeances of various Fischer-Tropsch gases could be investigated and the effect that different operating conditions have on these parameters. This allowed the comparison of literature data on permeations and selectivities, and can even lead to a critical look at membranes and the optimization of membranes.
In conclusion it can be stated that the objectives of this thesis were thus carried out successfully.

6.7 RECOMMENDATIONS

Recommendations regarding this study and future studies include:

The adsorption characteristics of each gas with regard to the silica membrane must be investigated prior to the permeation experiments in order to thoroughly explain the gas transport though the membrane and possible separation scenarios. An entire study devoted to this will enable a better understanding of the membrane performance and transport concepts as a whole.

Because membrane fabrication is a very delicate and intensive process, the chance of membrane defection is always a possibility. Therefore, in order to more accurately determine the separation characteristics of a membrane, permeation experiments should be done on different membranes of the same type.

From literature studies focusing on gas separation it clear that different membranes inhibit different separation characteristics. It is thus recommended that different type of gas separation membranes must be used e.g. zeolite membranes, to determine which are more effective for the separation of Fischer-Tropsch gases.

Appendix A

Sample Calculations

The following sample calculations hold for all experimental results:

Flux Calculation:

At 25 kPa, and a temperature of 298 K, the average time per 200 ml on the soap flow bubble metre for hydrogen gas fed on the tube side of the silica membrane was obtained as 11.62 seconds.

The flow rate in ml/min is thus:

$$\frac{200ml}{11.62s} \times \frac{60s}{1\min}$$

$$= 1032.7ml/\min$$

Conversion to l/s:

$$\frac{1032.7ml}{\min} \times \frac{l}{1000ml} \times \frac{1\min}{60s}$$

$$= 0.0172l/s$$

With the following properties known, the flowrate in mol/s can then be calculated:

Table A.1: Properties used for calculations

Property	Unit	Value
Temperature T: (variable)	K	298.15
Universal gas constant	L.atm/mol.K	0.082
Atmospheric pressure (variable):	atm	0.865
Membrane area (constant):	m^2	0.00656

The flow rate is thus calculated as:

$$\frac{0.0172l}{s} \times \frac{0.865atm}{(0.0821l.atm/mol.K) \times 298.15K}$$

$$= 6.085 \times 10^{-4} mol/s$$

With the membrane area known, the flux is then calculated as:

$$\frac{6.085 \times 10^{-4} mol/s}{0.00656m^2}$$

$$= 0.093 mol.m^{-2}.s^{-1}$$

With the flux known, the excel spreadsheet on the CD-ROM in the back of the dissertation, calculates the trans-membrane pressure across the active silica layer.

With a total trans-membrane pressure of 25 kPa, the permeance can then be calculated as:

$$\frac{Flux}{\Delta Psilica}$$

$$\frac{0.093 mol.m^{-2}.s^{-1}}{24836.352Pa}$$

$$= 3.7 \times 10^{-6} mol.m^{-2}.s^{-1}.Pa^{-1}$$

$$= 3.7 umol.m^{-1}.s^{-1}.Pa^{-1}$$

Appendix B

Amorphous silica Single Permeance Raw Data

Tube side Times

Table B.1: Hydrogen Gas Raw Data for Amorphous Silica

		Permeate flow rate (s/200ml)														
	ΔP	25 °C			40 °C			55 °C			70 °C			90 °C		
No.	(bar)	Run 1	Run 2	Run 3	Run 1	Run 2	Run 3	Run 1	Run 2	Run 3	Run 1	Run 2	Run 3	Run 1	Run 2	Run 3
1	0.25	11.77	11.5	11.72	11	11.09	11.22	10.68	11.03	11.88	11.12	11.72	11.62	12.03	12.16	12.3
2	0.25	11.81	11.59	11.12	10.87	11.41	11.09	10.75	10.93	11.74	11.34	11.72	11.44	12.31	12.22	12.21
3	0.25	11.47	11.31	11.69	10.78	11.18	11.04	10.78	11	11.82	11.41	11.56	11.51	12.15	12.13	12.18
4	0.25	11.44	11.31	11.6	10.81	11	11	10.88	10.98	11.85	11.5	11.82	11.56	12.22	12.19	12.17
5	0.25	11.61	11.39	11.65	10.99	11.1	10.88	10.81	11.06	11.92	11.19	11.69	11.61	12.18	12.28	12.25
AVG	**0.25**	**11.62**	**11.42**	**11.56**	**10.89**	**11.16**	**11.05**	**10.78**	**11.00**	**11.84**	**11.31**	**11.70**	**11.55**	**12.18**	**12.20**	**12.22**
1	0.5	6.29	6.43	6.35	6.04	5.97	6.15	6.31	5.97	6.08	6.25	6.28	6.31	6.56	6.58	6.54
2	0.5	6.18	6.43	6.31	6.15	6.09	6.08	6.22	5.97	6.12	6.32	6.12	6.45	6.53	6.71	6.58
3	0.5	6.19	6.25	6.28	5.94	6.06	6.02	6.19	6.01	6.18	6.31	6.12	6.4	6.66	6.67	6.7
4	0.5	6.19	6.31	6.44	6.16	6	6.02	6.21	5.92	6.08	6.28	6.22	6.29	6.62	6.62	6.65
5	0.5	6.23	6.45	6.19	6.1	6.03	5.97	6.25	5.94	6.13	6.44	6.28	6.33	6.65	6.66	6.65
AVG	**0.5**	**6.22**	**6.37**	**6.31**	**6.08**	**6.03**	**6.05**	**6.24**	**5.96**	**6.12**	**6.32**	**6.20**	**6.36**	**6.60**	**6.65**	**6.62**
1	0.75	4.29	4.28	4.12	4.07	4.19	4.06	4.22	4.28	4.19	4.34	4.22	4.21	4.5	4.48	4.4
2	0.75	4.21	4.35	4.22	4.09	4.16	4.13	4.25	4.19	4.15	4.38	4.22	4.15	4.41	4.42	4.38
3	0.75	4.2	4.47	4.13	4.1	4.15	4.18	4.19	4.15	4.23	4.28	4.35	4.28	4.22	4.49	4.44
4	0.75	4.17	4.25	4.31	4.07	4.13	4.02	4.28	4.21	4.22	4.22	4.13	4.3	4.44	4.54	4.5
5	0.75	4.22	4.31	4.22	4.1	4.09	4.16	4.26	4.26	4.24	4.28	4.22	4.26	4.47	4.48	4.46
AVG	**0.75**	**4.22**	**4.33**	**4.20**	**4.09**	**4.14**	**4.11**	**4.24**	**4.22**	**4.21**	**4.30**	**4.23**	**4.24**	**4.41**	**4.48**	**4.44**
1	0.9	3.55	3.69	3.59	3.54	3.5	3.6	3.44	3.41	3.38	3.59	3.5	3.65	3.59	3.69	3.78
2	0.9	3.65	3.69	3.5	3.5	3.47	3.47	3.56	3.37	3.45	3.63	3.63	3.54	3.85	3.78	3.84
3	0.9	3.6	3.54	3.66	3.47	3.5	3.5	3.57	3.37	3.51	3.66	3.56	3.58	3.84	3.85	3.76
4	0.9	3.63	3.56	3.56	3.55	3.63	3.52	3.56	3.43	3.48	3.57	3.53	3.61	3.79	3.78	3.88
5	0.9	3.59	3.53	3.52	3.5	3.52	3.56	3.61	3.38	3.5	3.65	3.6	3.5	3.8	3.88	3.76
AVG	**0.9**	**3.60**	**3.60**	**3.57**	**3.51**	**3.52**	**3.53**	**3.55**	**3.39**	**3.46**	**3.62**	**3.56**	**3.58**	**3.77**	**3.80**	**3.80**

Table B.2: Methane Gas Raw Data for Amorphous Silica

		Permeate flow rate (s/200ml)														
	ΔP	25 °C			40 °C			55 °C			70 °C			90 °C		
No.	(bar)	Run 1	Run 2	Run 3	Run 1	Run 2	Run 3	Run 1	Run 2	Run 3	Run 1	Run 2	Run 3	Run 1	Run 2	Run 3
1	0.25	22.92	23.21	23.18	21.82	21.87	20.69	22.9	22.57	22.68	23.09	23.38	22.78	23.16	23.21	23.15
2	0.25	23.43	23.03	22.97	21.62	22.16	20.72	22.63	22.56	22.72	22.94	23.47	22.98	23.16	23.28	23.22
3	0.25	23.19	23.07	22.78	21.67	21.73	21.12	22.75	22.53	22.84	22.71	23.35	23.09	23.03	23.19	23.28
4	0.25	22.95	22.92	23.5	21.71	21.81	21.06	22.78	22.6	22.75	22.53	23.31	23.1	22.75	23.31	23.18
5	0.25	23.1	23	23.44	21.85	21.69	21.17	22.71	22.47	22.8	22.31	23.41	22.88	22.63	23.25	23.2
AVG	**0.25**	**23.12**	**23.05**	**23.17**	**21.73**	**21.85**	**20.95**	**22.75**	**22.55**	**22.76**	**22.72**	**23.38**	**22.97**	**22.95**	**23.25**	**23.21**
1	0.5	13.14	13.34	13.37	12.41	12.75	12.18	12.94	13.13	12.89	13.19	13.06	13.11	13.94	14	13.9
2	0.5	13.14	13.28	13.28	12.37	12.84	12.37	12.63	13.16	12.76	13.28	13.09	13.16	13.75	13.95	13.78
3	0.5	13.66	13.13	13.13	12.35	12.69	12.06	12.62	13.16	12.95	13.28	13.19	13.08	13.94	13.94	13.63
4	0.5	13.67	13.16	13.15	12.4	12.75	12.25	12.57	13.16	12.82	13.25	13.09	13.21	13.98	13.9	13.75
5	0.5	13.73	13.44	12.97	12.45	12.73	12.31	12.66	13.12	12.9	13.27	13.15	13.24	13.94	13.94	13.81
AVG	**0.5**	**13.47**	**13.27**	**13.18**	**12.40**	**12.75**	**12.23**	**12.68**	**13.15**	**12.86**	**13.25**	**13.12**	**13.16**	**13.91**	**13.95**	**13.77**
1	0.75	9.08	9.06	9.1	8.57	8.75	8.37	8.72	8.6	8.63	9.06	8.94	9.05	9.46	9.47	9.49
2	0.75	9.09	9.12	9.1	8.62	8.69	8.38	8.72	8.59	8.69	8.91	9.04	8.99	9.5	9.52	9.5
3	0.75	9	9.15	9	8.56	8.78	8.31	8.72	8.63	8.74	9.07	9.16	9.1	9.5	9.43	9.5
4	0.75	8.99	9.1	9.03	8.59	8.75	8.33	8.8	8.52	8.66	8.97	9.13	8.97	9.35	9.55	9.56
5	0.75	8.92	8.97	9.07	8.63	8.7	8.28	8.69	8.67	8.66	9.03	9.06	8.89	9.51	9.52	9.48
AVG	**0.75**	**9.02**	**9.08**	**9.06**	**8.59**	**8.73**	**8.33**	**8.73**	**8.60**	**8.68**	**9.01**	**9.07**	**9.00**	**9.46**	**9.50**	**9.51**
1	1	7.02	6.9	6.81	6.37	6.5	6.28	6.6	6.63	6.78	6.84	6.81	6.78	7.13	7.15	7.13
2	1	6.83	6.75	6.87	6.44	6.5	6.31	6.62	6.69	6.62	6.82	6.88	6.85	7.12	7.11	7.13
3	1	6.74	6.88	6.78	6.5	6.44	6.25	6.71	6.65	6.58	6.75	6.78	6.79	7.21	7.11	7.09
4	1	6.73	6.75	6.82	6.5	6.61	6.28	6.59	6.59	6.62	6.9	6.83	6.91	7.15	7.13	7.15
5	1	6.78	6.72	6.83	6.47	6.52	6.33	6.65	6.62	6.71	6.85	6.88	6.75	7.12	7.18	7.13
AVG	**1**	**6.82**	**6.80**	**6.82**	**6.46**	**6.51**	**6.29**	**6.63**	**6.64**	**6.66**	**6.83**	**6.84**	**6.82**	**7.15**	**7.14**	**7.13**
1	1.25	5.27	5.34	5.32	5.12	5.22	5.06	5.25	5.13	5.21	5.37	5.31	5.36	5.82	5.75	5.85
2	1.25	5.33	5.34	5.41	5.09	5.13	5.13	5.25	5.15	5.19	5.5	5.37	5.28	5.62	5.79	5.89
3	1.25	5.32	5.35	5.35	5.13	5.28	5.06	5.19	5.19	5.23	5.4	5.2	5.33	5.72	5.81	5.79
4	1.25	5.35	5.25	5.41	5.05	5.1	5.04	5.27	5.17	5.23	5.38	5.35	5.36	5.78	5.75	5.72
5	1.25	5.29	5.35	5.34	5.1	5.09	5.11	5.33	5.21	5.27	5.46	5.29	5.3	5.69	5.78	5.81
AVG	**1.25**	**5.31**	**5.33**	**5.37**	**5.10**	**5.16**	**5.08**	**5.26**	**5.17**	**5.23**	**5.42**	**5.30**	**5.33**	**5.73**	**5.78**	**5.81**

Table B.3: Carbon Dioxide Gas Raw Data for Amorphous Silica

		Permeate flow rate (s/200ml)														
	ΔP	25 °C			40 °C			55 °C			70 °C			90 °C		
No.	(bar)	Run 1	Run 2	Run 3	Run 1	Run 2	Run 3	Run 1	Run 2	Run 3	Run 1	Run 2	Run 3	Run 1	Run 2	Run 3
1	0.25	29.85	30.56	30.06	27.44	27.75	27.84	28.41	28.22	28.71	29.5	30.34	29.75	31.22	31.07	31.02
2	0.25	29.3	30.87	30.32	27.68	28.22	28.01	28.81	28.34	28.63	30.15	30.81	29.66	31.1	30.83	30.92
3	0.25	29.1	31.18	30.78	27.38	28.37	28.12	28.75	28.44	28.59	30	30.06	29.71	31.1	30.95	30.97
4	0.25	29.95	30.78	30.65	27.66	28.41	27.96	28.96	28.38	28.51	29.97	30.55	29.82	30.88	31.11	31.09
5	0.25	29.54	30.44	30.56	27.51	28.33	28.12	28.85	28.37	28.53	29.75	30.38	29.84	30.78	30.98	31.12
AVG	**0.25**	**29.55**	**30.77**	**30.47**	**27.53**	**28.22**	**28.01**	**28.76**	**28.35**	**28.59**	**29.87**	**30.43**	**29.76**	**31.02**	**30.99**	**31.02**
1	0.5	19.58	19.78	19.22	18.09	18.22	17.84	18.69	18.53	18.72	19.96	19.09	19.03	20.15	19.88	20.1
2	0.5	19.38	19.72	19.56	18.28	18.34	18	18.57	18.63	18.72	19.34	19.13	19.16	19.91	19.92	20
3	0.5	19.6	19.43	19.41	18.25	18.29	18.1	18.57	18.63	18.63	19.53	19.19	19.1	19.72	20.01	19.84
4	0.5	19.48	19.41	19.38	18.25	18.25	18.13	18.61	18.59	18.65	19.38	19.03	19.15	19.94	19.95	19.89
5	0.5	19.35	19.34	19.28	18.19	18.3	18.24	18.66	18.64	18.54	19.38	19.06	19.09	20.06	19.91	19.97
AVG	**0.5**	**19.48**	**19.54**	**19.37**	**18.21**	**18.28**	**18.06**	**18.62**	**18.60**	**18.65**	**19.52**	**19.10**	**19.11**	**19.96**	**19.93**	**19.96**
1	0.75	14.04	13.56	13.63	12.75	12.94	12.88	13.28	13.35	13.25	13.75	13.47	13.28	14.56	14.41	14.5
2	0.75	14.04	13.72	13.69	12.69	12.85	12.78	13.28	13.22	13.28	13.68	13.38	13.81	14.69	14.56	14.41
3	0.75	14.13	13.78	13.91	12.59	13	12.75	13.21	13.27	13.36	13.81	13.41	13.75	14.4	14.39	14.47
4	0.75	13.95	13.78	13.9	12.71	13.06	12.93	13.25	13.37	13.33	13.72	13.41	13.69	14.53	14.5	14.5
5	0.75	13.91	13.66	13.75	12.74	12.94	12.99	13.3	13.41	13.21	13.75	13.38	13.78	14.61	14.5	14.53
AVG	**0.75**	**14.01**	**13.70**	**13.78**	**12.70**	**12.96**	**12.87**	**13.26**	**13.32**	**13.29**	**13.74**	**13.41**	**13.66**	**14.56**	**14.47**	**14.48**
1	1	10.49	10.28	10.44	9.88	9.72	9.65	9.94	10.07	10.09	10.38	10.22	10.31	11.03	11.07	11.01
2	1	10.49	10.41	10.47	9.84	9.94	9.59	10.09	10.13	10.15	10.4	10.32	10.25	11	10.98	10.95
3	1	10.47	10.38	10.41	9.78	9.85	9.53	10.13	10.03	10.19	10.47	10.31	10.25	11	11	10.94
4	1	10.42	10.41	10.34	9.78	9.78	9.71	10	10.1	10.06	10.41	10.29	10.31	11	11.02	10.98
5	1	10.4	10.31	10.38	9.81	9.78	9.68	10.03	10.5	10.12	10.31	10.3	10.29	11	11	10.91
AVG	**1**	**10.45**	**10.36**	**10.41**	**9.82**	**9.81**	**9.63**	**10.04**	**10.17**	**10.12**	**10.39**	**10.29**	**10.28**	**11.01**	**11.01**	**10.96**
1	1.25	8.39	8.06	8.16	7.85	7.72	7.68	8	7.97	8.03	8.28	8.22	8.18	8.63	8.76	8.77
2	1.25	8.29	8.16	8.18	7.85	7.68	7.62	8.03	8	7.87	8.25	8.15	8.15	8.75	8.73	8.69
3	1.25	8.2	8.12	8.19	7.81	7.66	7.62	8.06	7.94	7.95	8.28	8.19	8.16	8.68	8.68	8.85
4	1.25	8.25	8.32	8.25	7.83	7.72	7.7	8.11	8.01	8.06	8.25	8.19	8.1	8.78	8.7	8.68
5	1.25	8.32	8	8.19	7.79	7.72	7.74	7.98	7.98	8.01	8.33	8.22	8.09	8.75	8.69	8.74

AVG	1.25	8.29	8.13	8.19	7.83	7.70	7.67	8.04	7.98	7.98	8.28	8.19	8.14	8.72	8.71	8.75
1	1.5	6.88	6.72	6.81	6.37	6.53	6.31	6.53	6.56	6.44	6.9	6.78	6.68	7.19	7.23	7.22
2	1.5	6.8	6.78	6.75	6.38	6.4	6.32	6.54	6.65	6.48	6.75	6.56	6.78	7.25	7.23	7.21
3	1.5	6.83	6.72	6.88	6.34	6.44	6.34	6.47	6.57	6.52	6.91	6.78	6.81	7.22	7.19	7.22
4	1.5	6.86	6.75	6.82	6.37	6.37	6.44	6.57	6.56	6.56	6.91	6.69	6.78	7.22	7.25	7.18
5	1.5	6.85	6.73	6.84	6.36	6.42	6.39	6.5	6.55	6.53	6.88	6.6	6.72	7.2	7.19	7.22
AVG	**1.5**	**6.84**	**6.74**	**6.82**	**6.36**	**6.43**	**6.36**	**6.52**	**6.58**	**6.51**	**6.87**	**6.68**	**6.75**	**7.22**	**7.22**	**7.21**
1	1.75	5.62	5.44	5.47	5.19	5.09	5.22	5.31	5.41	5.31	5.59	5.6	5.71	5.84	5.78	5.85
2	1.75	5.61	5.53	5.6	5.22	5.19	5.19	5.28	5.31	5.32	5.63	5.53	5.72	5.81	5.86	5.75
3	1.75	5.69	5.44	5.46	5.28	5.16	5.09	5.41	5.34	5.37	5.56	5.57	5.62	5.85	5.83	5.78
4	1.75	5.53	5.6	5.47	5.28	5.16	5.2	5.33	5.28	5.28	5.63	5.59	5.5	5.88	5.78	5.81
5	1.75	5.58	5.47	5.47	5.25	5.21	5.25	5.29	5.35	5.3	5.62	5.61	5.66	5.91	5.84	5.79
AVG	**1.75**	**5.61**	**5.50**	**5.49**	**5.24**	**5.16**	**5.19**	**5.32**	**5.34**	**5.32**	**5.61**	**5.58**	**5.64**	**5.86**	**5.82**	**5.80**

Shell Side Times

Table B.4: Hydrogen Gas Raw Data (shell side) for Amorphous Silica

		Permeate flow rate (s/200ml)														
	ΔP	25 °C			40 °C			55 °C			70 °C			90 °C		
No.	(bar)	Run 1	Run 2	Run 3	Run 1	Run 2	Run 3	Run 1	Run 2	Run 3	Run 1	Run 2	Run 3	Run 1	Run 2	Run 3
1	0.25	11.53	11.34	11.47	11.5	11.64	11.51	10.85	11.06	11.02	10.53	11.06	11.25	11.84	11.65	11.95
2	0.25	11.44	11.25	11.19	11.41	11.69	11.43	10.94	10.94	10.95	10.67	11.13	11.06	11.68	11.93	11.67
3	0.25	11.44	11.09	11.16	11.5	11.58	11.54	11.03	11	10.99	10.53	10.93	10.97	11.63	11.75	11.72
4	0.25	11.51	11.12	10.81	11.47	11.47	11.5	11.1	11.11	11.06	10.57	11.15	11.12	11.71	11.87	11.75
5	0.25	11.39	11.31	10.82	11.52	11.53	11.5	11.06	11.05	11	10.44	11.07	10.87	11.68	11.81	11.81
AVG	**0.25**	**11.46**	**11.22**	**11.09**	**11.48**	**11.58**	**11.50**	**11.00**	**11.03**	**11.00**	**10.55**	**11.07**	**11.05**	**11.71**	**11.80**	**11.78**
1	0.5	6	6.04	5.91	6.06	6.09	5.98	6.12	6.1	5.98	6.35	6.21	6.28	6.59	6.65	6.62
2	0.5	5.87	6.16	6	5.97	6.12	6.03	6.09	6.06	5.94	6.25	6.22	6.18	6.59	6.53	6.61
3	0.5	6.06	5.84	5.97	6.03	6.09	6	6.03	6	6.08	6.32	6.13	6.28	6.53	6.57	6.54
4	0.5	5.96	6.1	5.75	5.95	6.13	6	5.91	6.01	6.03	6.34	6.13	6.21	6.47	6.52	6.58
5	0.5	6.01	6.03	5.88	6.01	6	5.95	5.93	6.09	6.04	6.25	6.18	6.26	6.55	6.58	6.59
AVG	**0.5**	**5.98**	**6.03**	**5.90**	**6.00**	**6.09**	**5.99**	**6.02**	**6.05**	**6.01**	**6.30**	**6.17**	**6.24**	**6.55**	**6.57**	**6.59**
1	0.75	3.87	4.09	4.12	4	4.12	4.08	4.03	4.15	4.09	4.22	4.13	4.21	4.25	4.22	4.35
2	0.75	4.03	3.9	4.22	4.03	4.07	4	4.03	4.1	4.1	4.15	4.11	4.16	4.35	4.28	4.39
3	0.75	4.06	4	4.13	4.09	4.02	4.02	4.03	4.09	3.97	4.29	4.09	4.14	4.35	4.36	4.35
4	0.75	4.07	4.06	4.31	3.99	4.08	4.05	4.09	4.05	4.03	4.22	4.19	4.23	4.34	4.35	4.3
5	0.75	3.96	4.03	4.22	4	4.1	4	4.05	4	4.08	4.16	4.25	4.13	4.25	4.3	4.28
AVG	**0.75**	**4.00**	**4.02**	**4.20**	**4.02**	**4.08**	**4.03**	**4.05**	**4.08**	**4.05**	**4.21**	**4.15**	**4.17**	**4.31**	**4.30**	**4.33**
1	0.9	3.65	3.56	3.5	3.35	3.48	3.45	3.4	3.42	3.45	3.47	3.4	3.52	3.66	3.71	3.62
2	0.9	3.5	3.69	3.62	3.44	3.5	3.39	3.37	3.38	3.49	3.47	3.44	3.43	3.53	3.63	3.58
3	0.9	3.55	3.56	3.47	3.46	3.52	3.37	3.44	3.44	3.44	3.34	3.41	3.47	3.6	3.58	3.62
4	0.9	3.47	3.56	3.56	3.4	3.41	3.44	3.46	3.42	3.4	3.4	3.4	3.49	3.6	3.62	3.6
5	0.9	3.61	3.61	3.59	3.39	3.4	3.46	3.39	3.45	3.36	3.41	3.37	3.44	3.62	3.64	3.6
AVG	**0.9**	**3.56**	**3.60**	**3.55**	**3.41**	**3.46**	**3.42**	**3.41**	**3.42**	**3.43**	**3.42**	**3.40**	**3.47**	**3.60**	**3.64**	**3.60**

Table B.5: Methane Gas Raw Data (shell side) for Amorphous Silica

		Permeate flow rate (s/200ml)														
	ΔP	25 °C			40 °C			55 °C			70 °C			90 °C		
No.	(bar)	Run 1	Run 2	Run 3	Run 1	Run 2	Run 3	Run 1	Run 2	Run 3	Run 1	Run 2	Run 3	Run 1	Run 2	Run 3
1	0.25	22.1	21.38	23.1	20.97	20.88	20.91	20.78	20.76	20.74	22.65	22.61	22.63	23.16	23.18	23.2
2	0.25	22.03	22.19	23.15	20.97	20.98	20.57	20.94	20.84	20.79	22.63	22.65	22.6	23.06	23.13	23.11
3	0.25	21.69	21.31	22.91	21.18	21.12	20.69	20.84	20.86	20.72	22.59	22.58	22.55	23.15	23.15	23.15
4	0.25	22.31	22.22	23.06	21.09	21.04	20.72	21.03	20.79	20.83	22.59	22.52	22.58	23.18	23.22	23.16
5	0.25	22.15	21.51	23.14	21.03	21.1	20.66	20.88	20.83	20.69	22.57	22.6	22.54	23.1	23.18	23.16
AVG	**0.25**	**22.06**	**21.72**	**23.07**	**21.05**	**21.02**	**20.71**	**20.89**	**20.82**	**20.75**	**22.61**	**22.59**	**22.58**	**23.13**	**23.17**	**23.16**
1	0.5	12.47	13.37	12.38	12.09	12.22	12.25	12.72	12.49	12.54	12.66	12.84	12.81	14.07	13.5	13.47
2	0.5	12.91	13	12.44	11.94	12.63	12.31	12.66	12.56	12.61	12.73	12.85	12.85	13.65	13.44	13.37
3	0.5	12.66	12.81	12.41	12.03	12.63	12.28	12.79	12.5	12.53	12.74	12.75	12.77	13.5	13.38	13.41
4	0.5	12.84	12.87	12.52	11.94	12.59	12.34	12.61	12.53	12.46	13	12.69	12.8	13.66	13.48	13.38
5	0.5	12.79	12.6	12.41	12	12.53	12.25	12.62	12.48	12.5	12.81	12.76	12.88	13.62	13.51	13.45
AVG	**0.5**	**12.73**	**12.93**	**12.43**	**12.00**	**12.52**	**12.29**	**12.68**	**12.51**	**12.53**	**12.79**	**12.78**	**12.82**	**13.70**	**13.46**	**13.42**
1	0.75	8.37	8.81	8.72	8.41	8.37	8.34	8.69	8.7	8.75	9	8.97	9.06	9.03	9.15	9.15
2	0.75	8.44	8.81	8.72	8.34	8.25	8.38	8.84	8.7	8.68	8.97	8.72	9.12	9.06	9.07	9.12
3	0.75	8.47	8.87	8.66	8.34	8.25	8.43	8.76	8.61	8.63	8.97	8.82	8.96	9.18	9.12	9.07
4	0.75	8.45	8.75	8.71	8.45	8.31	8.38	8.72	8.65	8.62	8.91	8.88	8.93	9	9.21	9.11
5	0.75	8.34	8.84	8.69	8.29	8.34	8.34	8.85	8.68	8.58	8.94	8.93	9	9.09	9.1	9.15
AVG	**0.75**	**8.41**	**8.82**	**8.70**	**8.37**	**8.30**	**8.37**	**8.77**	**8.67**	**8.65**	**8.96**	**8.86**	**9.01**	**9.07**	**9.13**	**9.12**
1	1	6.19	6.47	6.54	6.25	6.29	6.16	6.6	6.48	6.61	6.47	6.66	6.5	6.93	7.11	6.98
2	1	6.37	6.57	6.61	6.19	6.12	6.25	6.56	6.42	6.59	6.63	6.53	6.58	6.94	6.95	7.12
3	1	6.34	6.59	6.55	6.16	6.09	6.18	6.6	6.45	6.66	6.66	6.59	6.61	6.93	7.06	7.08
4	1	6.35	6.47	6.51	6.18	6.15	6.28	6.44	6.43	6.53	6.56	6.69	6.52	7.09	6.93	7.1
5	1	6.37	6.54	6.63	6.21	6.25	6.16	6.63	6.48	6.71	6.56	6.65	6.56	6.97	6.97	7.02
AVG	**1**	**6.32**	**6.53**	**6.57**	**6.20**	**6.18**	**6.21**	**6.57**	**6.45**	**6.62**	**6.58**	**6.62**	**6.55**	**6.97**	**7.00**	**7.06**
1	1.25	5	5.15	5.06	4.97	4.97	4.84	5.09	4.99	5.06	5.19	5.32	5.2	5.44	5.39	5.52
2	1.25	5.15	5.12	5.06	4.95	4.97	4.97	5	5	5	5.19	5.09	5.19	5.38	5.46	5.5
3	1.25	4.9	5.13	5.07	5	4.65	4.82	5.03	5.02	5.02	5.25	5.22	5.2	5.34	5.53	5.49
4	1.25	5	5.17	5.1	4.91	4.72	4.85	5.09	5.02	5.05	5.19	5.25	5.13	5.5	5.47	5.54
5	1.25	5.03	5.12	5.05	4.96	4.88	4.79	5.11	5.04	5.09	5.25	5.22	5.23	5.41	5.4	5.56
AVG	**1.25**	**5.02**	**5.14**	**5.07**	**4.96**	**4.84**	**4.85**	**5.06**	**5.01**	**5.04**	**5.21**	**5.22**	**5.19**	**5.41**	**5.45**	**5.52**

Table B.6: Carbon Dioxide Gas Raw Data (shell side) for Amorphous Silica

		Permeate flow rate (s/200ml)														
	ΔP	25 °C			40 °C			55 °C			70 °C			90 °C		
No.	(bar)	Run 1	Run 2	Run 3	Run 1	Run 2	Run 3	Run 1	Run 2	Run 3	Run 1	Run 2	Run 3	Run 1	Run 2	Run 3
1	0.25	28.1	27.9	30.12	27.97	27.94	27.84	28.91	29.1	28.94	28.81	30.13	30.11	31.31	31.34	31.35
2	0.25	28.06	28.56	30.44	27.84	27.88	27.94	28.97	28.94	28.94	29.06	30.13	30.08	31.38	31.37	31.39
3	0.25	28.03	28.85	30.56	27.63	27.9	27.72	29.04	28.99	28.98	30.34	30.06	30.18	31.38	31.34	31.34
4	0.25	27.81	28.44	30.21	28.04	27.94	27.69	29.08	29.07	29.03	30.25	30.13	29.98	31.36	31.38	31.34
5	0.25	28.11	28.51	30.33	28.12	28.02	27.99	28.95	28.98	29	30.25	29.87	30.1	31.38	31.35	31.31
AVG	**0.25**	**28.02**	**28.45**	**30.33**	**27.92**	**27.94**	**27.84**	**28.99**	**29.02**	**28.98**	**29.74**	**30.06**	**30.09**	**31.36**	**31.36**	**31.35**
1	0.5	18.28	17.78	19.37	18.03	18.15	17.87	18.28	18.47	18.48	18.88	18.9	18.75	19.69	19.94	19.44
2	0.5	17.94	18.47	18.56	17.65	18.07	17.72	18.53	18.61	18.48	18.9	18.91	18.72	19.56	19.9	19.56
3	0.5	17.81	17.81	18.91	17.56	17.93	17.53	18.47	18.51	18.46	18.69	18.87	18.71	19.47	19.69	19.51
4	0.5	17.94	17.69	19.11	18	18.06	17.72	18.38	18.49	18.53	19.09	18.96	18.82	19.22	19.58	19.54
5	0.5	18.09	18.59	18.78	18.28	18.11	17.8	18.47	18.5	18.41	18.95	19.02	18.68	19.62	19.81	19.48
AVG	**0.5**	**18.01**	**18.07**	**18.95**	**17.90**	**18.06**	**17.73**	**18.43**	**18.52**	**18.47**	**18.90**	**18.93**	**18.74**	**19.51**	**19.78**	**19.51**
1	0.75	12.81	12.6	13.09	12.47	12.43	12.4	13.25	13.23	13.16	13.32	13.31	13.42	13.84	13.88	13.79
2	0.75	12.75	12.69	12.93	12.37	12.46	12.37	13.18	13.28	13.18	13.32	13.47	13.35	13.87	13.79	13.83
3	0.75	12.68	12.69	13	12.47	12.37	12.34	13.25	13.31	13.24	13.28	13.37	13.39	13.84	13.83	13.83
4	0.75	12.72	12.62	12.94	12.4	12.33	12.44	13.22	13.3	13.28	13.25	13.34	13.46	13.75	13.78	13.81
5	0.75	12.74	12.7	13.12	12.45	12.51	12.36	13.28	13.24	13.25	13.35	13.41	13.34	13.82	13.85	13.87
AVG	**0.75**	**12.74**	**12.66**	**13.02**	**12.43**	**12.42**	**12.38**	**13.24**	**13.27**	**13.22**	**13.30**	**13.38**	**13.39**	**13.82**	**13.83**	**13.83**
1	1	9.66	9.53	9.78	9.63	9.54	9.59	9.91	9.69	9.57	9.97	9.87	9.82	10.56	10.41	10.47
2	1	9.65	9.47	9.66	9.69	9.56	9.59	9.84	9.72	9.65	9.9	10	9.78	10.38	10.48	10.49
3	1	9.71	9.47	9.69	9.63	9.69	9.54	9.73	9.74	9.69	9.93	10	9.88	10.56	10.37	10.42
4	1	9.65	9.51	9.59	9.72	9.72	9.61	9.78	9.63	9.67	9.94	9.97	9.92	10.37	10.45	10.51
5	1	9.63	9.42	9.64	9.75	9.65	9.52	9.84	9.71	9.75	9.88	9.94	9.8	10.48	10.37	10.47
AVG	**1**	**9.66**	**9.48**	**9.67**	**9.68**	**9.63**	**9.57**	**9.82**	**9.70**	**9.67**	**9.92**	**9.96**	**9.84**	**10.47**	**10.42**	**10.47**
1	1.25	7.69	7.56	7.6	7.34	7.25	7.32	7.56	7.68	7.72	7.91	7.88	8	8.34	8.37	8.38
2	1.25	7.5	7.53	7.69	7.34	7.31	7.47	7.72	7.71	7.75	7.88	7.9	8.03	8.25	8.28	8.37
3	1.25	7.54	7.61	7.75	7.38	7.35	7.36	7.66	7.63	7.64	7.94	8.13	7.97	8.25	8.38	8.38
4	1.25	7.41	7.47	7.71	7.29	7.45	7.45	7.65	7.59	7.68	7.87	8	7.95	8.31	8.35	8.3

5	1.25	7.55	7.49	7.68	7.41	7.34	7.38	7.7	7.69	7.61	7.96	8	8.01	8.38	8.32	8.32
AVG	**1.25**	**7.54**	**7.53**	**7.69**	**7.35**	**7.34**	**7.40**	**7.66**	**7.66**	**7.68**	**7.91**	**7.98**	**7.99**	**8.31**	**8.34**	**8.35**
1	1.5	6.28	6.32	6.53	6.16	6.16	5.97	6.32	6.29	6.28	6.53	6.57	6.52	6.87	6.84	6.87
2	1.5	6.25	6.31	6.59	6.31	5.94	6.16	6.28	6.32	6.28	6.62	6.5	6.53	6.88	6.8	6.81
3	1.5	6.38	6.34	6.47	6.22	6.25	6.25	6.28	6.32	6.29	6.53	6.44	6.5	6.87	6.81	6.81
4	1.5	6.38	6.29	6.55	6.22	6.16	6.19	6.35	6.37	6.25	6.5	6.61	6.55	6.78	6.79	6.78
5	1.5	6.31	6.36	6.49	6.18	6.11	6.16	6.3	6.41	6.31	6.58	6.56	6.55	6.78	6.83	6.77
AVG	**1.5**	**6.32**	**6.32**	**6.53**	**6.22**	**6.12**	**6.15**	**6.31**	**6.34**	**6.28**	**6.55**	**6.54**	**6.53**	**6.84**	**6.81**	**6.81**
1	1.75	5.29	5.32	5.28	4.88	4.93	4.91	5.35	5.25	5.31	5.38	5.47	5.47	5.78	5.62	5.75
2	1.75	5.38	5.16	5.47	4.91	5.04	4.87	5.28	5.35	5.32	5.5	5.51	5.52	5.66	5.71	5.71
3	1.75	5.28	5.31	5.47	4.93	5.06	4.88	5.44	5.37	5.27	5.4	5.55	5.47	5.75	5.78	5.67
4	1.75	5.35	5.34	5.35	4.85	4.99	4.77	5.25	5.32	5.34	5.47	5.4	5.41	5.78	5.72	5.68
5	1.75	5.36	5.3	5.41	4.93	5.06	4.93	5.28	5.28	5.27	5.37	5.44	5.45	5.77	5.69	5.78
AVG	**1.75**	**5.33**	**5.29**	**5.40**	**4.90**	**5.02**	**4.87**	**5.32**	**5.31**	**5.30**	**5.42**	**5.47**	**5.46**	**5.75**	**5.70**	**5.72**

Appendix C

Amorphous silica Single Permeance Processed Data

SINGLE PERMEANCE DATA:

Table C.1: Hydrogen Single Permeance Data (Tube Side)

	H_2 - 25 °C			H_2 - 40 °C			H_2 - 55 °C			H_2 - 70 °C			H_2 - 90 °C		
Δ P	µmol/m².s.Pa			µmol/m².s.Pa			µmol/m².s.Pa			µmol/m².s.Pa			µmol/m².s.Pa		
(kPa)	Run 1	Run 2	Run 3	Run 1	Run 2	Run 3	Run 1	Run 2	Run 3	Run 1	Run 2	Run 3	Run 1	Run 2	Run 3
25	3.713	3.778	3.734	3.772	3.682	3.719	3.637	3.564	3.310	3.314	3.204	3.246	2.909	2.905	2.898
50	3.471	3.385	3.417	3.379	3.406	3.396	3.143	3.288	3.204	2.966	3.021	2.949	2.682	2.664	2.674
75	3.410	3.320	3.424	3.351	3.304	3.332	3.082	3.098	3.107	2.906	2.956	2.947	2.679	2.635	2.662
90	3.326	3.327	3.361	3.249	3.238	3.233	3.069	3.210	3.144	2.877	2.922	2.912	2.607	2.592	2.587

Table C.2: Hydrogen Single Permeance Data (Shell Side)

	H_2 - 25 °C			H_2 - 40 °C			H_2 - 55 °C			H_2 - 70 °C			H_2 - 90 °C		
Δ P	(µmol/m².s.Pa)			(µmol/m².s.Pa)			(µmol/m².s.Pa)			(µmol/m².s.Pa)			(µmol/m².s.Pa)		
(kPa)	Run 1	Run 2	Run 3	Run 1	Run 2	Run 3	Run 1	Run 2	Run 3	Run 1	Run 2	Run 3	Run 1	Run 2	Run 3
25	3.764	3.845	3.891	3.578	3.547	3.573	3.565	3.554	3.563	3.554	3.387	3.391	3.026	3.002	3.007
50	3.608	3.575	3.655	3.421	3.375	3.428	3.258	3.239	3.259	2.974	3.036	3.003	2.706	2.696	2.689
75	3.597	3.581	3.424	3.405	3.358	3.398	3.230	3.204	3.223	2.970	3.008	2.994	2.741	2.745	2.725
90	3.370	3.333	3.378	3.348	3.296	3.335	3.192	3.182	3.177	3.047	3.059	3.001	2.732	2.706	2.730

Table C.3: Methane Single Permeance Data (Tube Side)

	CH4 - 25 °C			CH_4 - 40 °C			CH_4 - 55 °C			CH_4 - 70 °C			CH_4 - 90 °C		
Δ P	µmol/m².s.Pa			µmol/m².s.Pa			µmol/m².s.Pa			µmol/m².s.Pa			µmol/m².s.Pa		
(kPa)	Run 1	Run 2	Run 3	Run 1	Run 2	Run 3	Run 1	Run 2	Run 3	Run 1	Run 2	Run 3	Run 1	Run 2	Run 3
25	1.866	1.872	1.862	1.890	1.880	1.961	1.723	1.739	1.723	1.650	1.603	1.632	1.544	1.524	1.527
50	1.602	1.626	1.637	1.657	1.611	1.679	1.545	1.491	1.524	1.414	1.429	1.424	1.273	1.270	1.286
75	1.595	1.584	1.587	1.593	1.568	1.643	1.497	1.519	1.506	1.387	1.378	1.388	1.248	1.243	1.242
100	1.582	1.586	1.581	1.591	1.577	1.633	1.477	1.477	1.471	1.372	1.371	1.375	1.239	1.241	1.243
125	1.625	1.620	1.608	1.612	1.591	1.617	1.491	1.517	1.500	1.383	1.414	1.408	1.237	1.227	1.219

Table C.4: Methane Single Permeance Data (Shell Side)

	CH4 - 25 °C			CH_4 - 40 °C			CH_4 - 55 °C			CH_4 - 70 °C			CH_4 - 90 °C		
Δ P	(μmol/m².s.Pa)			(μmol/m².s.Pa)			(μmol/m².s.Pa)			(μmol/m².s.Pa)			(μmol/m².s.Pa)		
(kPa)	Run 1	Run 2	Run 3	Run 1	Run 2	Run 3	Run 1	Run 2	Run 3	Run 1	Run 2	Run 3	Run 1	Run 2	Run 3
25	1.956	1.986	1.870	1.952	1.954	1.984	1.876	1.883	1.889	1.658	1.659	1.660	1.532	1.529	1.530
50	1.694	1.668	1.735	1.712	1.641	1.672	1.546	1.567	1.565	1.466	1.467	1.462	1.293	1.316	1.320
75	1.709	1.631	1.653	1.637	1.649	1.635	1.490	1.508	1.510	1.395	1.410	1.386	1.302	1.293	1.295
100	1.706	1.652	1.642	1.657	1.662	1.655	1.493	1.519	1.480	1.425	1.415	1.430	1.270	1.264	1.254
125	1.720	1.680	1.703	1.657	1.698	1.693	1.548	1.564	1.554	1.438	1.436	1.445	1.309	1.300	1.283

Table C.5: Carbon Dioxide Permeance Data (Tube Side)

	CO_2 - 25 °C			CO_2 - 40 °C			CO_2 - 55 °C			CO_2 - 70 °C			CO_2 - 90 °C		
Δ P	μmol/m².s.Pa			μmol/m².s.Pa			μmol/m².s.Pa			μmol/m².s.Pa			μmol/m².s.Pa		
(kPa)	Run 1	Run 2	Run 3	Run 1	Run 2	Run 3	Run 1	Run 2	Run 3	Run 1	Run 2	Run 3	Run 1	Run 2	Run 3
25	1.460	1.402	1.416	1.492	1.456	1.467	1.363	1.383	1.371	1.255	1.232	1.260	1.142	1.143	1.142
50	1.108	1.104	1.114	1.128	1.124	1.137	1.053	1.054	1.051	0.960	0.981	0.981	0.888	0.889	0.887
75	1.026	1.050	1.044	1.079	1.057	1.064	0.985	0.981	0.984	0.909	0.932	0.915	0.811	0.816	0.815
100	1.032	1.041	1.036	1.046	1.046	1.066	0.976	0.964	0.968	0.902	0.911	0.912	0.805	0.804	0.808
125	1.041	1.061	1.053	1.050	1.067	1.071	0.976	0.983	0.982	0.906	0.915	0.922	0.813	0.813	0.810
150	1.051	1.067	1.054	1.076	1.064	1.077	1.002	0.993	1.004	0.909	0.935	0.925	0.818	0.818	0.819
175	1.100	1.122	1.122	1.119	1.137	1.131	1.052	1.049	1.053	0.955	0.960	0.949	0.864	0.870	0.873

Table C.6: Carbon Dioxide Permeance Data (Shell Side)

	CO_2 - 25 °C			CO_2 - 40 °C			CO_2 - 55 °C			CO_2 - 70 °C			CO_2 - 90 °C		
Δ P	(μmol/m².s.Pa)			(μmol/m².s.Pa)			(μmol/m².s.Pa)			(μmol/m².s.Pa)			(μmol/m².s.Pa)		
(kPa)	Run 1	Run 2	Run 3	Run 1	Run 2	Run 3	Run 1	Run 2	Run 3	Run 1	Run 2	Run 3	Run 1	Run 2	Run 3
25	1.540	1.516	1.423	1.471	1.471	1.476	1.352	1.351	1.353	1.260	1.247	1.246	1.130	1.130	1.130
50	1.198	1.194	1.139	1.147	1.137	1.159	1.064	1.059	1.061	0.992	0.990	1.000	0.908	0.895	0.908
75	1.129	1.136	1.105	1.101	1.103	1.106	0.987	0.985	0.988	0.939	0.934	0.933	0.854	0.854	0.854
100	1.117	1.138	1.115	1.061	1.066	1.073	0.998	1.011	1.014	0.944	0.941	0.952	0.846	0.850	0.846
125	1.145	1.146	1.123	1.118	1.119	1.111	1.024	1.024	1.021	0.948	0.939	0.938	0.853	0.850	0.848
150	1.138	1.137	1.102	1.101	1.118	1.114	1.036	1.030	1.040	0.954	0.956	0.957	0.864	0.866	0.867
175	1.156	1.166	1.142	1.198	1.170	1.205	1.053	1.054	1.056	0.987	0.978	0.980	0.880	0.887	0.885

SINGLE FLUX DATA

Table C.7: Hydrogen Flux Data (Tube Side)

	H_2 - 25 °C			H_2 - 40 °C			H_2 - 55 °C			H_2 - 70 °C			H_2 - 90 °C		
Δ P	(mol/m^2.s)			(mol/m^2.s)			(mol/m^2.s)			(mol/m^2.s)			(mol/m^2.s)		
(kPa)	Run 1	Run 2	Run 3	Run 1	Run 2	Run 3	Run 1	Run 2	Run 3	Run 1	Run 2	Run 3	Run 1	Run 2	Run 3
25	0.093	0.094	0.093	0.094	0.092	0.093	0.091	0.089	0.083	0.083	0.080	0.081	0.073	0.073	0.072
50	0.174	0.169	0.171	0.169	0.170	0.170	0.157	0.164	0.160	0.148	0.151	0.147	0.134	0.133	0.134
75	0.256	0.249	0.257	0.251	0.248	0.250	0.231	0.232	0.233	0.218	0.222	0.221	0.201	0.198	0.200
90	0.299	0.299	0.302	0.292	0.291	0.291	0.276	0.289	0.283	0.259	0.263	0.262	0.235	0.233	0.233

Table C.8: Hydrogen Flux Data (Shell Side)

	H_2 - 25 °C			H_2 - 40 °C			H_2 - 55 °C			H_2 - 70 °C			H_2 - 90 °C		
Δ P	(mol/m^2.s)			(mol/m^2.s)			(mol/m^2.s)			(mol/m^2.s)			(mol/m^2.s)		
(kPa)	Run 1	Run 2	Run 3	Run 1	Run 2	Run 3	Run 1	Run 2	Run 3	Run 1	Run 2	Run 3	Run 1	Run 2	Run 3
25	0.094	0.096	0.097	0.089	0.089	0.089	0.089	0.089	0.089	0.089	0.085	0.085	0.076	0.075	0.075
50	0.180	0.179	0.183	0.171	0.169	0.171	0.163	0.162	0.163	0.149	0.152	0.150	0.135	0.135	0.134
75	0.270	0.269	0.257	0.255	0.252	0.255	0.242	0.240	0.242	0.223	0.226	0.225	0.206	0.206	0.204
90	0.303	0.300	0.304	0.301	0.297	0.300	0.287	0.286	0.286	0.274	0.275	0.270	0.246	0.244	0.246

Table C.9: Methane Flux Data (Tube Side)

	CH4 - 25 °C			CH_4 - 40 °C			CH_4 - 55 °C			CH_4 - 70 °C			CH_4 - 90 °C		
Δ P	(mol/m^2.s)			(mol/m^2.s)			(mol/m^2.s)			(mol/m^2.s)			(mol/m^2.s)		
(kPa)	Run 1	Run 2	Run 3	Run 1	Run 2	Run 3	Run 1	Run 2	Run 3	Run 1	Run 2	Run 3	Run 1	Run 2	Run 3
25	0.047	0.047	0.047	0.047	0.047	0.049	0.043	0.043	0.043	0.041	0.040	0.041	0.039	0.038	0.038
50	0.080	0.081	0.082	0.083	0.081	0.084	0.077	0.075	0.076	0.071	0.071	0.071	0.064	0.064	0.064
75	0.120	0.119	0.119	0.120	0.118	0.123	0.112	0.114	0.113	0.104	0.103	0.104	0.094	0.093	0.093
100	0.158	0.159	0.158	0.159	0.158	0.163	0.148	0.148	0.147	0.137	0.137	0.138	0.124	0.124	0.124
125	0.203	0.203	0.201	0.201	0.199	0.202	0.186	0.190	0.188	0.173	0.177	0.176	0.155	0.153	0.152

Table C.10: Methane Flux Data (Shell Side)

	CH4 - 25 °C			CH_4 - 40 °C			CH_4 - 55 °C			CH_4 - 70 °C			CH_4 - 90 °C		
Δ P	(mol/m^2.s)			(mol/m^2.s)			(mol/m^2.s)			(mol/m^2.s)			(mol/m^2.s)		
(kPa)	Run 1	Run 2	Run 3	Run 1	Run 2	Run 3	Run 1	Run 2	Run 3	Run 1	Run 2	Run 3	Run 1	Run 2	Run 3
25	0.049	0.050	0.047	0.049	0.049	0.050	0.047	0.047	0.047	0.041	0.041	0.042	0.038	0.038	0.038
50	0.085	0.083	0.087	0.086	0.082	0.084	0.077	0.078	0.078	0.073	0.073	0.073	0.065	0.066	0.066
75	0.128	0.122	0.124	0.123	0.124	0.123	0.112	0.113	0.113	0.105	0.106	0.104	0.098	0.097	0.097
100	0.171	0.165	0.164	0.166	0.166	0.165	0.149	0.152	0.148	0.143	0.141	0.143	0.127	0.126	0.125
125	0.215	0.210	0.213	0.207	0.212	0.212	0.194	0.195	0.194	0.180	0.180	0.181	0.164	0.162	0.160

Table C.11: Carbon Dioxide Flux Data (Tube Side)

	CO_2 - 25 °C			CO_2 - 40 °C			CO_2 - 55 °C			CO_2 - 70 °C			CO_2 - 90 °C		
Δ P	(mol/m^2.s)			(mol/m^2.s)			(mol/m^2.s)			(mol/m^2.s)			(mol/m^2.s)		
(kPa)	Run 1	Run 2	Run 3	Run 1	Run 2	Run 3	Run 1	Run 2	Run 3	Run 1	Run 2	Run 3	Run 1	Run 2	Run 3
25	0.037	0.035	0.035	0.037	0.036	0.037	0.034	0.035	0.034	0.031	0.031	0.031	0.029	0.029	0.029
50	0.055	0.055	0.056	0.056	0.056	0.057	0.053	0.053	0.053	0.048	0.049	0.049	0.044	0.044	0.044
75	0.077	0.079	0.078	0.081	0.079	0.080	0.074	0.074	0.074	0.068	0.070	0.069	0.061	0.061	0.061
100	0.103	0.104	0.104	0.105	0.105	0.107	0.098	0.096	0.097	0.090	0.091	0.091	0.080	0.080	0.081
125	0.130	0.133	0.132	0.131	0.133	0.134	0.122	0.123	0.123	0.113	0.114	0.115	0.102	0.102	0.101
150	0.158	0.160	0.158	0.161	0.160	0.161	0.150	0.149	0.151	0.136	0.140	0.139	0.123	0.123	0.123
175	0.192	0.196	0.196	0.196	0.199	0.198	0.184	0.184	0.184	0.167	0.168	0.166	0.151	0.152	0.153

Table C.12: Carbon Dioxide Flux Data (Shell Side)

	CO_2 - 25 °C			CO_2 - 40 °C			CO_2 - 55 °C			CO_2 - 70 °C			CO_2 - 90 °C		
Δ P	(mol/m^2.s)			(mol/m^2.s)			(mol/m^2.s)			(mol/m^2.s)			(mol/m^2.s)		
(kPa)	Run 1	Run 2	Run 3	Run 1	Run 2	Run 3	Run 1	Run 2	Run 3	Run 1	Run 2	Run 3	Run 1	Run 2	Run 3
25	0.038	0.038	0.036	0.037	0.037	0.037	0.034	0.034	0.034	0.032	0.031	0.031	0.028	0.028	0.028
50	0.060	0.060	0.057	0.057	0.057	0.058	0.053	0.053	0.053	0.050	0.050	0.050	0.045	0.045	0.045
75	0.085	0.085	0.083	0.083	0.083	0.083	0.074	0.074	0.074	0.070	0.070	0.070	0.064	0.064	0.064
100	0.112	0.114	0.112	0.106	0.107	0.107	0.100	0.101	0.101	0.094	0.094	0.095	0.085	0.085	0.085
125	0.143	0.143	0.140	0.140	0.140	0.139	0.128	0.128	0.128	0.118	0.117	0.117	0.107	0.106	0.106
150	0.171	0.171	0.165	0.165	0.168	0.167	0.155	0.155	0.156	0.143	0.143	0.144	0.130	0.130	0.130
175	0.202	0.204	0.200	0.210	0.205	0.211	0.184	0.184	0.185	0.173	0.171	0.172	0.154	0.155	0.155

Appendix D

Amorphous Silica
Single Permeance
Statistical Data

SINGLE PERMEANCE DATA ERROR STATISTICS:

Calculation of the standard deviations and percentage errors are as follows:

Assume one has three data points (n = 3) from experimental results, x_1, x_2 and x_3.

The mean of these data points ($\bar{x}$) is calculated as:

$$\bar{x} = \left(\frac{x_1 + x_2 + x_3}{n} \right)$$

in which case n = 3.

The standard deviation (σ) from the average is then defined as:

$$\sigma = \sqrt{\frac{n\sum x^2 - \left(\sum x\right)^2}{n(n-1)}}$$

Alpha is the significance level used to compute the confidence level. The confidence level equals 100*(1 - alpha) %, or in other words, an alpha of 0.05 indicates a 95 percent confidence level.

If one assumes alpha equals 0.05, the area under the standard normal curve that equals (1 - alpha), or 95 percent needs to be calculated. This value is ± 1.96. The confidence interval (c.i.) is therefore:

$$\bar{x} \pm 1.96 \cdot \left(\frac{\sigma}{\sqrt{n}} \right)$$

The average error (ε) is then calculated using the following formula:

$$error\% = 2 \cdot \frac{1.96 \cdot \frac{\sigma}{\sqrt{n}}}{\bar{x}} \times 100$$ for a confidence interval of 95

Tube Side Permeance Deviations:

Table D.1: Hydrogen Tube side Permeance Deviations

	25°C				40°C				55 °C				70 °C				90 °C				Average error across single P:
P (kPa)	$\bar{x}$	σ	c.i.	%ε	$\bar{x}$	σ	c.i.	%ε	$\bar{x}$	σ	c.i.	%ε	$\bar{x}$	σ	c.i.	%ε	$\bar{x}$	σ	c.i.	%ε	
25	3.742	0.027	0.031	1.642	3.725	0.037	0.042	2.244	3.504	0.140	0.158	9.030	3.255	0.045	0.051	3.162	2.904	0.004	0.005	0.335	3.282
50	3.424	0.035	0.040	2.346	3.394	0.011	0.013	0.740	3.212	0.140	0.158	9.851	2.979	0.031	0.035	2.346	2.673	0.007	0.008	0.614	3.179
75	3.385	0.046	0.052	3.085	3.329	0.019	0.022	1.308	3.096	0.059	0.067	4.330	2.936	0.022	0.024	1.667	2.658	0.018	0.021	1.551	2.388
90	3.338	0.016	0.018	1.104	3.240	0.007	0.008	0.481	3.141	0.010	0.012	0.743	2.904	0.019	0.022	1.513	2.595	0.009	0.010	0.758	0.920
Average Error across single T:				2.044				1.193				5.988				2.172				0.815	

Table D.2: Methane Tube side Permeance Deviations

	25°C				40°C				55 °C				70 °C				90 °C				Average error across single P:
P (kPa)	$\bar{x}$	σ	c.i.	%ε	$\bar{x}$	σ	c.i.	%ε	$\bar{x}$	σ	c.i.	%ε	$\bar{x}$	σ	c.i.	%ε	$\bar{x}$	σ	c.i.	%ε	
25	1.867	0.004	0.005	0.513	1.910	0.036	0.041	4.254	1.728	0.008	0.009	0.991	1.629	0.019	0.022	2.700	1.531	0.009	0.010	1.312	1.954
50	1.621	0.015	0.017	2.038	1.649	0.028	0.032	3.902	1.520	0.022	0.025	3.324	1.423	0.006	0.007	0.987	1.276	0.007	0.008	1.212	2.293
75	1.589	0.005	0.005	0.669	1.601	0.031	0.035	4.416	1.507	0.009	0.010	1.371	1.385	0.005	0.005	0.736	1.244	0.002	0.003	0.435	1.525
100	1.583	0.002	0.003	0.330	1.600	0.024	0.027	3.372	1.475	0.003	0.003	0.434	1.373	0.002	0.002	0.287	1.241	0.001	0.002	0.259	0.936
125	1.618	0.007	0.008	0.969	1.607	0.011	0.013	1.592	1.503	0.010	0.012	1.581	1.401	0.013	0.015	2.155	1.228	0.008	0.008	1.385	
Average Error across single T:				0.888				3.986				1.530				1.177				0.804	

Table D.3: Carbon Dioxide Tube side Permeance Deviations

	25°C				40°C				55 °C				70 °C				90 °C				Average error across single P:
P (kPa)	$\bar{x}$	σ	c.i.	%ε	$\bar{x}$	σ	c.i.	%ε	$\bar{x}$	σ	c.i.	%ε	$\bar{x}$	σ	c.i.	%ε	$\bar{x}$	σ	c.i.	%ε	
25	1.426	0.025	0.028	3.920	1.472	0.015	0.017	2.326	1.372	0.008	0.009	1.324	1.249	0.012	0.014	2.195	1.142	0.001	0.001	0.113	1.976
50	1.109	0.004	0.004	0.801	1.130	0.006	0.006	1.136	1.052	0.001	0.001	0.242	0.974	0.010	0.011	2.285	0.888	0.001	0.001	0.130	0.919
75	1.040	0.010	0.011	2.178	1.067	0.009	0.010	1.919	0.983	0.002	0.002	0.422	0.919	0.010	0.011	2.367	0.814	0.002	0.002	0.598	1.497
100	1.037	0.004	0.004	0.853	1.053	0.009	0.011	2.026	0.970	0.005	0.006	1.191	0.908	0.005	0.005	1.124	0.806	0.002	0.002	0.510	1.141
125	1.052	0.008	0.009	1.789	1.063	0.009	0.010	1.950	0.980	0.003	0.004	0.720	0.914	0.006	0.007	1.606	0.812	0.001	0.002	0.384	
150	1.057	0.007	0.008	1.485	1.072	0.006	0.006	1.167	1.000	0.005	0.005	1.066	0.923	0.011	0.012	2.582	0.818	0.000	0.000	0.107	
175	1.114	0.010	0.012	2.127	1.129	0.007	0.008	1.478	1.052	0.002	0.002	0.386	0.955	0.004	0.005	1.025	0.869	0.004	0.004	0.996	
Average Error across single T:				1.938				1.851				0.795				1.993				0.338	

Shell Side Permeance Deviations

Table D.4: Hydrogen Shell side Permeance Deviations

	25°C				40°C				55 °C				70 °C				90 °C				Average error across single P:
P (kPa)	$\bar{x}$	σ	c.i.	%ε	$\bar{x}$	σ	c.i.	%ε	$\bar{x}$	σ	c.i.	%ε	$\bar{x}$	σ	c.i.	%ε	$\bar{x}$	σ	c.i.	%ε	
25	3.833	0.052	0.059	3.082	3.566	0.014	0.016	0.878	3.560	0.005	0.006	0.317	3.444	0.078	0.088	5.107	3.011	0.010	0.012	0.774	2.032
50	3.613	0.033	0.037	2.058	3.408	0.024	0.027	1.561	3.252	0.009	0.011	0.654	3.004	0.025	0.029	1.898	2.697	0.007	0.008	0.593	1.353
75	3.534	0.078	0.088	4.997	3.387	0.021	0.023	1.379	3.219	0.011	0.012	0.757	2.991	0.016	0.018	1.205	2.737	0.009	0.010	0.727	1.813
100	3.360	0.020	0.022	1.327	3.326	0.022	0.025	1.504	3.183	0.006	0.007	0.437	3.036	0.025	0.028	1.864	2.723	0.012	0.013	0.973	1.221
Average Error across single T:				2.866				1.331				0.541				2.519				0.767	

Table D.5: Methane Shell side Permeance Deviations

	25°C				40°C				55 °C				70 °C				90 °C				Average error across single P:
P (kPa)	$\bar{x}$	σ	c.i.	%ε	$\bar{x}$	σ	c.i.	%ε	$\bar{x}$	σ	c.i.	%ε	$\bar{x}$	σ	c.i.	%ε	$\bar{x}$	σ	c.i.	%ε	
25	1.938	0.049	0.056	5.753	1.963	0.015	0.016	1.674	1.883	0.005	0.006	0.622	1.659	0.001	0.001	0.106	1.530	0.001	0.001	0.169	1.665
50	1.699	0.028	0.031	3.666	1.675	0.029	0.033	3.932	1.559	0.009	0.011	1.357	1.465	0.002	0.002	0.333	1.310	0.012	0.014	2.070	2.272
75	1.665	0.033	0.037	4.465	1.640	0.006	0.007	0.850	1.503	0.009	0.010	1.379	1.397	0.010	0.011	1.569	1.297	0.004	0.004	0.630	1.779
100	1.667	0.028	0.031	3.775	1.658	0.003	0.003	0.398	1.497	0.016	0.018	2.432	1.423	0.006	0.007	1.003	1.263	0.007	0.007	1.172	1.756
125	1.701	0.017	0.019	2.226	1.683	0.018	0.021	2.448	1.555	0.006	0.007	0.923	1.440	0.004	0.004	0.564	1.297	0.011	0.012	1.855	
Average Error across single T:				4.415				1.713				1.448				0.753				1.010	

Table D.6: Carbon Dioxide Shell side Permeance Deviations

	25°C				40°C				55 °C				70 °C				90 °C				Average error across single P:
P (kPa)	$\bar{x}$	σ	c.i.	%ε	$\bar{x}$	σ	c.i.	%ε	$\bar{x}$	σ	c.i.	%ε	$\bar{x}$	σ	c.i.	%ε	$\bar{x}$	σ	c.i.	%ε	
25	1.493	0.051	0.057	7.685	1.473	0.002	0.003	0.356	1.352	0.001	0.001	0.124	1.251	0.007	0.008	1.200	1.130	0.000	0.000	0.048	1.882
50	1.177	0.027	0.031	5.193	1.148	0.009	0.010	1.736	1.061	0.002	0.002	0.450	0.994	0.005	0.005	1.038	0.904	0.006	0.007	1.490	1.981
75	1.123	0.013	0.015	2.677	1.103	0.002	0.002	0.389	0.987	0.002	0.002	0.360	0.935	0.003	0.003	0.661	0.854	0.000	0.000	0.015	0.821
100	1.123	0.010	0.012	2.083	1.067	0.005	0.006	1.096	1.008	0.007	0.008	1.538	0.946	0.005	0.005	1.120	0.847	0.002	0.002	0.563	1.280
125	1.138	0.011	0.012	2.111	1.116	0.004	0.004	0.739	1.023	0.001	0.001	0.293	0.942	0.004	0.005	1.015	0.850	0.002	0.002	0.512	
150	1.126	0.017	0.019	3.371	1.111	0.007	0.008	1.469	1.035	0.004	0.005	0.884	0.955	0.001	0.002	0.321	0.866	0.002	0.002	0.399	
175	1.155	0.010	0.011	1.909	1.191	0.015	0.017	2.841	1.054	0.001	0.002	0.319	0.982	0.004	0.004	0.899	0.884	0.003	0.003	0.725	
Average Error across single T:				4.409				0.894				0.618				1.005				0.529	

Tube Side Flux Deviations:

Table D.7: Hydrogen Tube side Flux Deviations

	25°C				40°C				55 °C				70 °C				90 °C				Average error across single P:
P (kPa)	$\bar{x}$	σ	c.i.	%ε	$\bar{x}$	σ	c.i.	%ε	$\bar{x}$	σ	c.i.	%ε	$\bar{x}$	σ	c.i.	%ε	$\bar{x}$	σ	c.i.	%ε	
25	0.094	0.001	0.001	1.642	0.093	0.001	0.001	2.244	0.088	0.003	0.004	9.030	0.081	0.001	0.001	3.162	0.073	0.000	0.000	0.335	3.282
50	0.171	0.002	0.002	2.346	0.170	0.001	0.001	0.740	0.161	0.003	0.003	4.174	0.149	0.002	0.002	2.346	0.134	0.000	0.000	0.614	2.044
75	0.254	0.003	0.004	3.085	0.250	0.001	0.002	1.308	0.232	0.001	0.001	0.754	0.220	0.002	0.002	1.667	0.199	0.001	0.002	1.551	1.673
90	0.300	0.001	0.002	1.104	0.292	0.001	0.001	0.481	0.283	0.005	0.006	4.154	0.261	0.002	0.002	1.513	0.234	0.001	0.001	0.758	1.602
Average Error across single T:				2.044				1.193				4.528				2.172				0.815	

Table D.8: Methane Tube side Flux Deviations

	25°C				40°C				55 °C				70 °C				90 °C				Average error across
P (kPa)	$\bar{x}$	σ	c.i.	%ε	$\bar{x}$	σ	c.i.	%ε	$\bar{x}$	σ	c.i.	%ε	$\bar{x}$	σ	c.i.	%ε	$\bar{x}$	σ	c.i.	%ε	
25	0.047	0.000	0.000	0.513	0.048	0.001	0.001	4.254	0.043	0.000	0.000	0.991	0.041	0.000	0.001	2.700	0.038	0.000	0.000	1.312	1.954
50	0.081	0.001	0.001	2.038	0.082	0.001	0.002	3.902	0.076	0.001	0.001	3.324	0.071	0.000	0.000	0.987	0.064	0.000	0.000	1.212	2.293
75	0.119	0.000	0.000	0.669	0.120	0.002	0.003	4.416	0.113	0.001	0.001	1.371	0.104	0.000	0.000	0.736	0.093	0.000	0.000	0.435	1.525
100	0.158	0.000	0.000	0.330	0.160	0.002	0.003	3.372	0.148	0.000	0.000	0.434	0.137	0.000	0.000	0.287	0.124	0.000	0.000	0.259	0.936
125	0.202	0.001	0.001	0.969	0.201	0.001	0.002	1.592	0.188	0.001	0.001	1.581	0.175	0.002	0.002	2.155	0.153	0.001	0.001	1.385	
Average Error across single T:				0.888				3.986				1.530				1.177				0.804	

Table D.9: Carbon Dioxide Tube side Flux Deviations

	25°C				40°C				55 °C				70 °C				90 °C				Average error across single P:
P (kPa)	$\bar{x}$	σ	c.i.	%ε	$\bar{x}$	σ	c.i.	%ε	$\bar{x}$	σ	c.i.	%ε	$\bar{x}$	σ	c.i.	%ε	$\bar{x}$	σ	c.i.	%ε	
25	0.036	0.001	0.001	3.920	0.037	0.000	0.000	2.326	0.034	0.000	0.000	1.324	0.031	0.000	0.000	2.195	0.029	0.000	0.000	0.113	1.976
50	0.055	0.000	0.000	0.801	0.056	0.000	0.000	1.136	0.053	0.000	0.000	0.242	0.049	0.000	0.001	2.285	0.044	0.000	0.000	0.130	0.919
75	0.078	0.001	0.001	2.178	0.080	0.001	0.001	1.919	0.074	0.000	0.000	0.422	0.069	0.001	0.001	2.367	0.061	0.000	0.000	0.598	1.497
100	0.104	0.000	0.000	0.853	0.105	0.001	0.001	2.026	0.097	0.001	0.001	1.191	0.091	0.000	0.001	1.124	0.081	0.000	0.000	0.510	1.141
125	0.131	0.001	0.001	1.789	0.133	0.001	0.001	1.950	0.123	0.000	0.000	0.720	0.114	0.001	0.001	1.606	0.101	0.000	0.000	0.384	
150	0.159	0.001	0.001	1.485	0.161	0.001	0.001	1.167	0.150	0.001	0.001	1.066	0.138	0.002	0.002	2.582	0.123	0.000	0.000	0.107	
175	0.195	0.002	0.002	2.127	0.198	0.001	0.001	1.478	0.184	0.000	0.000	0.386	0.167	0.001	0.001	1.025	0.152	0.001	0.001	0.996	
Average Error across single T:				1.938				1.851				0.795				1.993				0.338	

Shell Side Flux Deviations:

Table D.10: Hydrogen Shell side Flux Deviations

	25°C				40°C				55 °C				70 °C				90 °C				Average error across single P:
P (kPa)	$\bar{x}$	σ	c.i.	%ε	$\bar{x}$	σ	c.i.	%ε	$\bar{x}$	σ	c.i.	%ε	$\bar{x}$	σ	c.i.	%ε	$\bar{x}$	σ	c.i.	%ε	
25	0.096	0.001	0.001	3.082	0.089	0.000	0.000	0.878	0.089	0.000	0.000	0.317	0.086	0.002	0.002	5.107	0.075	0.000	0.000	0.774	2.032
50	0.181	0.002	0.002	2.058	0.170	0.001	0.001	1.561	0.163	0.000	0.001	0.654	0.150	0.001	0.001	1.898	0.135	0.000	0.000	0.593	1.353
75	0.265	0.006	0.007	4.997	0.254	0.002	0.002	1.379	0.241	0.001	0.001	0.757	0.224	0.001	0.001	1.205	0.205	0.001	0.001	0.727	1.813
90	0.302	0.002	0.002	1.327	0.299	0.002	0.002	1.504	0.287	0.001	0.001	0.437	0.273	0.002	0.003	1.864	0.245	0.001	0.001	0.973	1.221
Average Error across single T:				2.866				1.331				0.541				2.519				0.767	

Table D.11: Methane Shell side Flux Deviations

	25°C				40°C				55 °C				70 °C				90 °C				Average error across single P:
P (kPa)	$\bar{x}$	σ	c.i.	%ε	$\bar{x}$	σ	c.i.	%ε	$\bar{x}$	σ	c.i.	%ε	$\bar{x}$	σ	c.i.	%ε	$\bar{x}$	σ	c.i.	%ε	
25	0.048	0.001	0.001	5.753	0.049	0.000	0.000	1.674	0.047	0.000	0.000	0.622	0.041	0.000	0.000	0.106	0.038	0.000	0.000	0.169	1.665
50	0.085	0.001	0.002	3.666	0.084	0.001	0.002	3.932	0.078	0.000	0.001	1.357	0.073	0.000	0.000	0.333	0.065	0.001	0.001	2.070	2.272
75	0.125	0.002	0.003	4.465	0.123	0.000	0.001	0.850	0.113	0.001	0.001	1.379	0.105	0.001	0.001	1.569	0.097	0.000	0.000	0.630	1.779
100	0.167	0.003	0.003	3.775	0.166	0.000	0.000	0.398	0.150	0.002	0.002	2.432	0.142	0.001	0.001	1.003	0.126	0.001	0.001	1.172	1.756
125	0.213	0.002	0.002	2.226	0.210	0.002	0.003	2.448	0.194	0.001	0.001	0.923	0.180	0.000	0.001	0.564	0.162	0.001	0.002	1.855	
Average Error across single T:				4.415				1.713				1.448				0.753				1.010	

Table D.12: Carbon Dioxide Shell side Flux Deviations

	25°C				40°C				55 °C				70 °C				90 °C				Average error across single P:
P (kPa)	$\bar{x}$	σ	c.i.	%ε	$\bar{x}$	σ	c.i.	%ε	$\bar{x}$	σ	c.i.	%ε	$\bar{x}$	σ	c.i.	%ε	$\bar{x}$	σ	c.i.	%ε	
25	0.037	0.001	0.001	7.685	0.037	0.000	0.000	0.356	0.034	0.000	0.000	0.124	0.031	0.000	0.000	1.200	0.028	0.000	0.000	0.048	1.882
50	0.059	0.001	0.002	5.193	0.057	0.000	0.000	1.736	0.053	0.000	0.000	0.450	0.050	0.000	0.000	1.038	0.045	0.000	0.000	1.490	1.981
75	0.084	0.001	0.001	2.677	0.083	0.000	0.000	0.389	0.074	0.000	0.000	0.360	0.070	0.000	0.000	0.661	0.064	0.000	0.000	0.015	0.821
100	0.112	0.001	0.001	2.083	0.107	0.001	0.001	1.096	0.101	0.001	0.001	1.538	0.095	0.000	0.001	1.120	0.085	0.000	0.000	0.563	1.280
125	0.142	0.001	0.002	2.111	0.139	0.000	0.001	0.739	0.128	0.000	0.000	0.293	0.118	0.001	0.001	1.015	0.106	0.000	0.000	0.512	
150	0.169	0.003	0.003	3.371	0.167	0.001	0.001	1.469	0.155	0.001	0.001	0.884	0.143	0.000	0.000	0.321	0.130	0.000	0.000	0.399	
175	0.202	0.002	0.002	1.909	0.208	0.003	0.003	2.841	0.185	0.000	0.000	0.319	0.172	0.001	0.001	0.899	0.155	0.000	0.001	0.725	
Average Error across single T:				4.409				0.894				0.618				1.005				0.529	

Appendix E

Amorphous Silica Membrane Mechanical Design Drawing

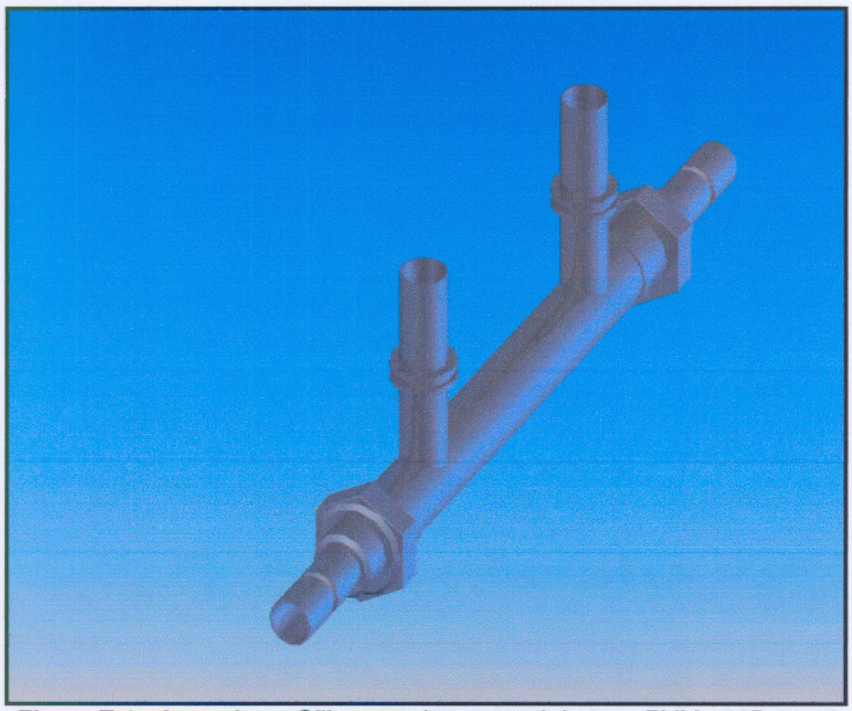

Figure E.1: Amorphous Silica membrane module type PVM.010D.00.00

Appendix F

SF6 Gas Permeation Data

Table F.1 lists certain permeation properties:

Table F.1: Constant Properties

Property	Unit	Value
Membrane Area	m^2	6.56E-03
Universal Gas constant (R)	$L.atm.mol^{-1}.K^{-1}$	0.082
Operating Temperature	K	298
Operating Pressure	atm	1

The flux and permeance obtained is listed in table F.2:

Table F.2: SF6 Permeance Data

ΔP (kPa)	Time (s)	flow rate (ml/s)	flow rate (ml/min)	flow rate (L/s)	flow rate (mol/s)	Flux ($mol/m^2.s$)	Permeance ($mol/m^2.s.kPa$)
25	50.780	3.939	236.314	0.004	1.612E-04	2.457E-02	9.826E-04
25	49.620	4.031	241.838	0.004	1.649E-04	2.514E-02	1.006E-03
25	47.860	4.179	250.731	0.004	1.710E-04	2.606E-02	1.043E-03
50	27.020	7.402	444.115	0.007	3.029E-04	4.617E-02	9.234E-04
50	26.980	7.413	444.774	0.007	3.034E-04	4.624E-02	9.247E-04
50	27.050	7.394	443.623	0.007	3.026E-04	4.612E-02	9.223E-04
75	18.290	10.935	656.096	0.011	4.475E-04	6.820E-02	9.094E-04
75	18.510	10.805	648.298	0.011	4.422E-04	6.739E-02	8.986E-04
75	18.580	10.764	645.856	0.011	4.405E-04	6.714E-02	8.952E-04
100	13.150	15.209	912.548	0.015	6.224E-04	9.486E-02	9.486E-04
100	13.050	15.326	919.540	0.015	6.272E-04	9.559E-02	9.559E-04
100	13.200	15.152	909.091	0.015	6.200E-04	9.451E-02	9.451E-04

Table F.3: SF6 Statistical Data

ΔP (kPa)	Average Flux - (mol/m2.s)	Standard Deviation (σ)	confidence interval	Percentage error (ε)
25	2.526E-02	6.174E-04	6.987E-04	2.766E+00
50	4.617E-02	4.902E-05	5.547E-05	1.201E-01
75	6.758E-02	4.540E-04	5.137E-04	7.602E-01
100	9.499E-02	4.519E-04	5.113E-04	5.383E-01

Appendix G

NaA Membrane Single Permeance Data

Table G.1: Hydrogen Gas Permeance data for NaA

Feed Flow rate	Permeate flow rate				Flux	Permeance	delta P
ml/min	ml/min	L/s	mol/s	umol/s	(umol/m^2.s)	(umol/m^2.s.Pa)	bar
208.478	1.244	2.073E-05	7.338E-07	0.734	282.231	0.931	1.01
208.478	1.224	2.041E-05	7.224E-07	0.722	277.854	0.917	1.01
208.478	1.210	2.017E-05	7.140E-07	0.714	274.604	0.906	1.01
208.478	1.178	1.963E-05	6.949E-07	0.695	267.272	0.882	1.01
208.478	1.244	2.073E-05	7.338E-07	0.734	282.231	0.931	1.01
					276.838	**0.914**	
208.478	2.814	4.690E-05	1.660E-06	1.660	638.595	1.419	1.5
208.478	2.876	4.794E-05	1.697E-06	1.697	652.677	1.450	1.5
208.478	2.899	4.831E-05	1.710E-06	1.710	657.722	1.462	1.5
208.478	2.899	4.831E-05	1.710E-06	1.710	657.722	1.462	1.5
208.478	2.876	4.794E-05	1.697E-06	1.697	652.677	1.450	1.5
					651.879	**1.449**	
208.478	3.492	5.821E-05	2.060E-06	2.060	792.482	1.321	2
208.478	3.417	5.695E-05	2.016E-06	2.016	775.333	1.292	2
208.478	3.275	5.459E-05	1.932E-06	1.932	743.168	1.239	2
208.478	3.222	5.371E-05	1.901E-06	1.901	731.195	1.219	2
208.478	3.119	5.198E-05	1.840E-06	1.840	707.632	1.179	2
					749.962	**1.250**	
208.478	3.106	5.176E-05	1.832E-06	1.832	704.702	0.940	2.5
208.478	3.619	6.031E-05	2.135E-06	2.135	821.161	1.095	2.5
208.478	3.968	6.614E-05	2.341E-06	2.341	900.453	1.201	2.5
208.478	3.722	6.203E-05	2.196E-06	2.196	844.593	1.126	2.5
208.478	3.676	6.127E-05	2.169E-06	2.169	834.243	1.112	2.5
					821.030	**1.095**	
208.478	2.340	3.900E-05	1.381E-06	1.381	531.000	0.553	3.2
208.478	2.232	3.720E-05	1.317E-06	1.317	506.505	0.528	3.2
208.478	2.122	3.536E-05	1.252E-06	1.252	481.430	0.501	3.2
208.478	2.232	3.720E-05	1.317E-06	1.317	506.505	0.528	3.2
208.478	2.762	4.604E-05	1.630E-06	1.630	626.834	0.653	3.2
					530.455	**0.553**	
208.478	2.773	4.621E-05	1.636E-06	1.636	629.152	0.524	4
208.478	3.119	5.198E-05	1.840E-06	1.840	707.632	0.590	4
208.478	3.505	5.841E-05	2.068E-06	2.068	795.260	0.663	4
208.478	3.240	5.400E-05	1.911E-06	1.911	735.143	0.613	4
208.478	2.874	4.789E-05	1.695E-06	1.695	652.052	0.543	4
					703.848	**0.587**	
100	1.063	1.772E-05	6.272E-07	0.627	241.227	0.781	1.03
100	1.064	1.774E-05	6.279E-07	0.628	241.484	0.782	1.03
100	1.121	1.869E-05	6.617E-07	0.662	254.483	0.824	1.03
100	1.058	1.764E-05	6.243E-07	0.624	240.121	0.777	1.03
100	1.063	1.772E-05	6.272E-07	0.627	241.227	0.781	1.03

					243.708	**0.789**	
100	2.833	4.721E-05	1.671E-06	1.671	642.816	1.428	1.5
100	2.519	4.198E-05	1.486E-06	1.486	571.572	1.270	1.5
100	2.657	4.429E-05	1.568E-06	1.568	602.960	1.340	1.5
100	3.322	5.537E-05	1.960E-06	1.960	753.867	1.675	1.5
100	2.833	4.721E-05	1.671E-06	1.671	642.816	1.428	1.5
					642.806	**1.428**	
100	3.178	5.297E-05	1.875E-06	1.875	721.125	1.202	2
100	3.555	5.924E-05	2.097E-06	2.097	806.567	1.344	2
100	3.559	5.931E-05	2.100E-06	2.100	807.523	1.346	2
100	3.382	5.637E-05	1.995E-06	1.995	767.466	1.279	2
100	3.429	5.714E-05	2.023E-06	2.023	777.991	1.297	2
					776.134	**1.294**	
100	3.505	5.841E-05	2.068E-06	2.068	795.260	1.060	2.5
100	3.597	5.995E-05	2.122E-06	2.122	816.238	1.088	2.5
100	3.382	5.637E-05	1.995E-06	1.995	767.466	1.023	2.5
100	3.886	6.477E-05	2.293E-06	2.293	881.790	1.176	2.5
100	3.807	6.345E-05	2.246E-06	2.246	863.886	1.152	2.5
					824.928	**1.100**	
100	2.674	4.456E-05	1.577E-06	1.577	606.722	0.632	3.2
100	2.703	4.505E-05	1.595E-06	1.595	613.281	0.639	3.2
100	2.646	4.409E-05	1.561E-06	1.561	600.302	0.625	3.2
100	2.560	4.266E-05	1.510E-06	1.510	580.838	0.605	3.2
100	2.625	4.374E-05	1.548E-06	1.548	595.575	0.620	3.2
					599.344	**0.624**	
100	3.055	5.092E-05	1.802E-06	1.802	693.220	0.578	4
100	2.982	4.970E-05	1.759E-06	1.759	676.682	0.564	4
100	2.555	4.259E-05	1.508E-06	1.508	579.849	0.483	4
100	3.333	5.556E-05	1.967E-06	1.967	756.380	0.630	4
100	3.119	5.198E-05	1.840E-06	1.840	707.632	0.590	4
					682.753	**0.569**	
50	1.048	1.746E-05	6.182E-07	0.618	237.772	0.793	1
50	1.106	1.843E-05	6.524E-07	0.652	250.919	0.836	1
50	1.076	1.793E-05	6.348E-07	0.635	244.169	0.814	1
50	1.094	1.824E-05	6.457E-07	0.646	248.355	0.828	1
50	1.106	1.843E-05	6.524E-07	0.652	250.919	0.836	1
					246.427	**0.821**	
50	2.513	4.188E-05	1.482E-06	1.482	570.136	1.267	1.5
50	2.705	4.509E-05	1.596E-06	1.596	613.834	1.364	1.5
50	2.417	4.029E-05	1.426E-06	1.426	548.543	1.219	1.5
50	2.540	4.234E-05	1.499E-06	1.499	576.412	1.281	1.5
50	2.806	4.677E-05	1.656E-06	1.656	636.803	1.415	1.5
					589.146	**1.309**	
50	3.322	5.537E-05	1.960E-06	1.960	753.867	1.256	2
50	3.286	5.476E-05	1.939E-06	1.939	745.610	1.243	2
50	3.663	6.105E-05	2.161E-06	2.161	831.187	1.385	2
50	3.517	5.862E-05	2.075E-06	2.075	798.056	1.330	2

50	3.322	5.537E-05	1.960E-06	1.960	753.867	1.256	2
					776.518	**1.294**	
50	3.555	5.924E-05	2.097E-06	2.097	806.567	1.075	2.5
50	3.440	5.734E-05	2.030E-06	2.030	780.668	1.041	2.5
50	3.468	5.780E-05	2.046E-06	2.046	786.985	1.049	2.5
50	3.311	5.519E-05	1.954E-06	1.954	751.371	1.002	2.5
50	3.517	5.862E-05	2.075E-06	2.075	798.056	1.064	2.5
					784.729	**1.046**	
50	2.667	4.444E-05	1.573E-06	1.573	605.104	0.630	3.2
50	2.632	4.386E-05	1.553E-06	1.553	597.142	0.622	3.2
50	2.625	4.374E-05	1.548E-06	1.548	595.575	0.620	3.2
50	2.560	4.266E-05	1.510E-06	1.510	580.838	0.605	3.2
50	2.521	4.202E-05	1.487E-06	1.487	572.052	0.596	3.2
					590.142	**0.615**	
50	2.879	4.798E-05	1.699E-06	1.699	653.303	0.544	4
50	2.773	4.621E-05	1.636E-06	1.636	629.152	0.524	4
50	2.825	4.708E-05	1.667E-06	1.667	641.000	0.534	4
50	3.119	5.198E-05	1.840E-06	1.840	707.632	0.590	4
50	2.542	4.237E-05	1.500E-06	1.500	576.900	0.481	4
					641.598	**0.535**	

Table G.2: Methane Gas Permeance data for NaA

Feed Flow rate	**Permeate Flow rate**				**Flux**	**Permeance**	**delta P**
ml/min	**ml/min**	**L/s**	**mol/s**	**umol/s**	**(umol/m^2.s)**	**J (umol/m^2.s.Pa)**	**bar**
208	0.692	1.153E-05	4.080E-07	0.408	136.002	0.449	1.01
208	0.689	1.148E-05	4.063E-07	0.406	135.440	0.447	1.01
208	0.619	1.031E-05	3.649E-07	0.365	121.645	0.401	1.01
208	0.650	1.083E-05	3.833E-07	0.383	127.756	0.422	1.01
208	0.643	1.071E-05	3.792E-07	0.379	126.387	0.417	1.01
					129.446	**0.427**	
208	1.065	1.774E-05	6.281E-07	0.628	209.360	0.465	1.5
208	1.008	1.680E-05	5.947E-07	0.595	198.245	0.441	1.5
208	1.021	1.702E-05	6.024E-07	0.602	200.809	0.446	1.5
208	1.142	1.904E-05	6.740E-07	0.674	224.667	0.499	1.5
208	1.150	1.917E-05	6.787E-07	0.679	226.218	0.503	1.5
					211.860	**0.471**	
208	1.558	2.596E-05	9.190E-07	0.919	306.322	0.505	2.02
208	1.594	2.657E-05	9.405E-07	0.940	313.484	0.517	2.02
208	1.543	2.572E-05	9.105E-07	0.910	303.486	0.501	2.02
208	1.554	2.591E-05	9.171E-07	0.917	305.687	0.504	2.02
208	1.520	2.533E-05	8.966E-07	0.897	298.874	0.493	2.02
					305.571	**0.504**	
208	2.582	4.303E-05	1.523E-06	1.523	507.725	0.677	2.5
208	2.366	3.943E-05	1.396E-06	1.396	465.281	0.620	2.5
208	2.340	3.900E-05	1.381E-06	1.381	460.200	0.614	2.5

208	2.463	4.105E-05	1.453E-06	1.453	484.381	0.646	2.5
208	2.475	4.125E-05	1.460E-06	1.460	486.779	0.649	2.5
					480.873	**0.641**	
208	1.349	2.248E-05	7.958E-07	0.796	265.277	0.295	3
208	1.291	2.151E-05	7.616E-07	0.762	253.863	0.282	3
208	1.293	2.155E-05	7.629E-07	0.763	254.300	0.283	3
208	1.241	2.068E-05	7.320E-07	0.732	243.994	0.271	3
208	1.149	1.914E-05	6.776E-07	0.678	225.872	0.251	3
					248.661	**0.276**	
208	1.319	2.199E-05	7.783E-07	0.778	259.444	0.270	3.2
208	1.326	2.210E-05	7.825E-07	0.782	260.821	0.272	3.2
208	1.280	2.133E-05	7.551E-07	0.755	251.696	0.262	3.2
208	1.379	2.298E-05	8.134E-07	0.813	271.129	0.282	3.2
208	1.468	2.446E-05	8.659E-07	0.866	288.638	0.301	3.2
					266.346	**0.277**	
208	2.222	3.704E-05	1.311E-06	1.311	437.020	0.364	4
208	1.984	3.307E-05	1.171E-06	1.171	390.196	0.325	4
208	1.992	3.320E-05	1.175E-06	1.175	391.751	0.326	4
208	2.078	3.463E-05	1.226E-06	1.226	408.571	0.340	4
208	2.165	3.608E-05	1.277E-06	1.277	425.668	0.355	4
					410.641	**0.342**	
157.4	0.664	1.106E-05	3.916E-07	0.392	130.526	0.422	1.03
157.4	0.628	1.047E-05	3.707E-07	0.371	123.581	0.400	1.03
157.4	0.671	1.119E-05	3.960E-07	0.396	131.986	0.427	1.03
157.4	0.680	1.133E-05	4.010E-07	0.401	133.660	0.433	1.03
157.4	0.617	1.028E-05	3.640E-07	0.364	121.344	0.393	1.03
					128.219	**0.415**	
157.4	1.093	1.822E-05	6.450E-07	0.645	215.006	0.475	1.51
157.4	1.168	1.947E-05	6.892E-07	0.689	229.742	0.507	1.51
157.4	1.030	1.717E-05	6.078E-07	0.608	202.602	0.447	1.51
157.4	1.078	1.797E-05	6.362E-07	0.636	212.069	0.468	1.51
157.4	1.004	1.673E-05	5.923E-07	0.592	197.449	0.436	1.51
					211.373	**0.467**	
157.4	1.639	2.732E-05	9.672E-07	0.967	322.392	0.537	2
157.4	1.645	2.741E-05	9.704E-07	0.970	323.452	0.539	2
157.4	1.399	2.332E-05	8.255E-07	0.826	275.176	0.459	2
157.4	1.601	2.668E-05	9.445E-07	0.944	314.822	0.525	2
157.4	1.529	2.548E-05	9.021E-07	0.902	300.702	0.501	2
					307.309	**0.512**	
157.4	2.362	3.937E-05	1.394E-06	1.394	464.548	0.619	2.5
157.4	2.622	4.371E-05	1.547E-06	1.547	515.714	0.688	2.5
157.4	2.283	3.805E-05	1.347E-06	1.347	448.993	0.599	2.5
157.4	2.683	4.472E-05	1.583E-06	1.583	527.707	0.704	2.5
157.4	2.256	3.759E-05	1.331E-06	1.331	443.591	0.591	2.5
					480.111	**0.640**	
157.4	1.375	2.291E-05	8.112E-07	0.811	270.383	0.300	3
157.4	1.391	2.319E-05	8.209E-07	0.821	273.644	0.304	3

157.4	1.283	2.139E-05	7.570E-07	0.757	252.342	0.280	3
157.4	1.453	2.422E-05	8.575E-07	0.858	285.841	0.318	3
157.4	1.572	2.621E-05	9.276E-07	0.928	309.212	0.344	3
					278.285	**0.309**	
157.4	1.375	2.291E-05	8.112E-07	0.811	270.383	0.282	3.2
157.4	1.520	2.533E-05	8.966E-07	0.897	298.874	0.311	3.2
157.4	1.388	2.313E-05	8.187E-07	0.819	272.885	0.284	3.2
157.4	1.459	2.432E-05	8.609E-07	0.861	286.954	0.299	3.2
157.4	1.403	2.339E-05	8.278E-07	0.828	275.948	0.287	3.2
					281.009	**0.293**	
157.4	2.116	3.526E-05	1.248E-06	1.248	416.062	0.347	4
157.4	1.926	3.209E-05	1.136E-06	1.136	378.676	0.316	4
157.4	2.143	3.571E-05	1.264E-06	1.264	421.412	0.351	4
157.4	2.024	3.374E-05	1.194E-06	1.194	398.095	0.332	4
157.4	2.256	3.759E-05	1.331E-06	1.331	443.591	0.370	4
					411.567	**0.343**	
100	0.651	1.086E-05	3.843E-07	0.384	128.089	0.415	1.03
100	0.627	1.046E-05	3.701E-07	0.370	123.374	0.399	1.03
100	0.780	1.301E-05	4.604E-07	0.460	153.480	0.497	1.03
100	0.752	1.254E-05	4.438E-07	0.444	147.938	0.479	1.03
100	0.610	1.017E-05	3.599E-07	0.360	119.963	0.388	1.03
					134.569	**0.435**	
100	1.312	2.187E-05	7.742E-07	0.774	258.082	0.574	1.5
100	1.017	1.695E-05	6.000E-07	0.600	199.992	0.444	1.5
100	1.041	1.735E-05	6.141E-07	0.614	204.711	0.455	1.5
100	1.094	1.823E-05	6.455E-07	0.645	215.163	0.478	1.5
100	1.012	1.687E-05	5.971E-07	0.597	199.047	0.442	1.5
					215.399	**0.479**	
100	1.355	2.258E-05	7.994E-07	0.799	266.475	0.444	2
100	1.703	2.838E-05	1.005E-06	1.005	334.833	0.558	2
100	1.538	2.564E-05	9.077E-07	0.908	302.552	0.504	2
100	1.574	2.623E-05	9.286E-07	0.929	309.536	0.516	2
100	1.559	2.599E-05	9.199E-07	0.920	306.641	0.511	2
					304.008	**0.507**	
100	2.318	3.864E-05	1.368E-06	1.368	455.932	0.608	2.5
100	2.308	3.846E-05	1.361E-06	1.361	453.828	0.605	2.5
100	2.222	3.704E-05	1.311E-06	1.311	437.020	0.583	2.5
100	2.333	3.888E-05	1.376E-06	1.376	458.769	0.612	2.5
100	2.098	3.497E-05	1.238E-06	1.238	412.571	0.550	2.5
					443.624	**0.591**	
100	1.291	2.151E-05	7.616E-07	0.762	253.863	0.282	3
100	1.290	2.150E-05	7.609E-07	0.761	253.644	0.282	3
100	1.298	2.163E-05	7.655E-07	0.766	255.180	0.284	3
100	1.293	2.155E-05	7.629E-07	0.763	254.300	0.283	3
100	1.293	2.155E-05	7.629E-07	0.763	254.300	0.283	3
					254.257	**0.283**	
100	1.116	1.860E-05	6.585E-07	0.658	219.485	0.229	3.2

100	1.376	2.294E-05	8.119E-07	0.812	270.631	0.282	3.2
100	1.344	2.240E-05	7.930E-07	0.793	264.326	0.275	3.2
100	1.364	2.273E-05	8.045E-07	0.805	268.171	0.279	3.2
100	1.174	1.956E-05	6.925E-07	0.692	230.820	0.240	3.2
					250.687	**0.261**	
100	2.078	3.463E-05	1.226E-06	1.226	408.571	0.340	4
100	1.921	3.201E-05	1.133E-06	1.133	377.706	0.315	4
100	2.161	3.602E-05	1.275E-06	1.275	425.055	0.354	4
100	2.212	3.687E-05	1.305E-06	1.305	435.086	0.363	4
100	1.854	3.090E-05	1.094E-06	1.094	364.633	0.304	4
					402.210	**0.335**	
50	0.190	3.165E-06	1.120E-07	0.112	37.340	0.124	1
50	0.150	2.500E-06	8.850E-08	0.088	29.499	0.098	1
50	0.197	3.277E-06	1.160E-07	0.116	38.662	0.129	1
50	0.136	2.273E-06	8.045E-08	0.080	26.817	0.089	1
50	0.133	2.212E-06	7.832E-08	0.078	26.105	0.087	1
					31.685	**0.106**	
50	0.168	2.800E-06	9.912E-08	0.099	33.041	0.073	1.5
50	0.163	2.709E-06	9.590E-08	0.096	31.967	0.071	1.5
50	0.152	2.529E-06	8.951E-08	0.090	29.836	0.066	1.5
					31.614	0.070	
50	0.925	1.541E-05	5.456E-07	0.546	181.867	0.303	2
50	0.997	1.662E-05	5.884E-07	0.588	196.136	0.327	2
50	0.918	1.530E-05	5.416E-07	0.542	180.531	0.301	2
50	0.964	1.607E-05	5.687E-07	0.569	189.581	0.316	2
50	0.970	1.616E-05	5.721E-07	0.572	190.684	0.318	2
					187.760	**0.313**	
50	0.341	5.678E-06	2.010E-07	0.201	66.997	0.089	2.5
50	0.289	4.810E-06	1.703E-07	0.170	56.761	0.076	2.5
50	0.290	4.834E-06	1.711E-07	0.171	57.036	0.076	2.5
50	0.281	4.676E-06	1.655E-07	0.166	55.169	0.074	2.5
50	0.287	4.790E-06	1.696E-07	0.170	56.522	0.075	2.5
					58.497	**0.078**	
50	0.400	6.661E-06	2.358E-07	0.236	78.601	0.087	3
50	0.367	6.117E-06	2.165E-07	0.217	72.177	0.080	3
50	0.429	7.155E-06	2.533E-07	0.253	84.427	0.094	3
50	0.382	6.365E-06	2.253E-07	0.225	75.099	0.083	3
					77.576	0.086	3.000
50	0.394	6.567E-06	2.325E-07	0.232	77.486	0.081	3.2
50	0.379	6.320E-06	2.237E-07	0.224	74.567	0.078	3.2
50	0.416	6.939E-06	2.456E-07	0.246	81.873	0.085	3.2
50	0.380	6.334E-06	2.242E-07	0.224	74.737	0.078	3.2
					77.166	**0.080**	
50	0.555	9.249E-06	3.274E-07	0.327	109.134	0.091	4
50	0.548	9.131E-06	3.232E-07	0.323	107.739	0.090	4
50	0.527	8.781E-06	3.108E-07	0.311	103.614	0.086	4
					106.829	0.089	

Table G.3: Hydrogen Gas Permeance data for NaA (Shell Side)

Feed Flow rate	Permeate Flow rate				Flux	Permeance	delta P
ml/min	ml/min	L/s	mol/s	umol/s	(umol/m^2.s)	(umol/m^2.s.kPa)	bar
208.478	1.149	1.914E-05	6.776E-07	0.678	225.872	0.745	1.01
208.478	1.122	1.870E-05	6.619E-07	0.662	220.634	2.866	1.01
208.478	1.053	1.754E-05	6.210E-07	0.621	207.009	2.690	1.01
208.478	0.986	1.643E-05	5.814E-07	0.581	193.816	2.519	1.01
208.478	1.143	1.905E-05	6.745E-07	0.675	224.839	2.920	1.01
					214.434	**2.348**	
208.478	1.714	2.857E-05	1.011E-06	1.011	337.129	0.749	1.50
208.478	1.847	3.079E-05	1.090E-06	1.090	363.286	2.866	1.50
208.478	1.594	2.657E-05	9.405E-07	0.940	313.484	2.690	1.50
208.478	1.825	3.041E-05	1.077E-06	1.077	358.867	2.519	1.50
208.478	1.812	3.019E-05	1.069E-06	1.069	356.266	2.920	1.50
					345.806	**2.349**	
208.478	2.500	4.167E-05	1.475E-06	1.475	491.647	0.819	2.00
208.478	2.538	4.230E-05	1.497E-06	1.497	499.134	2.866	2.00
208.478	2.538	4.230E-05	1.497E-06	1.497	499.134	2.690	2.00
208.478	2.463	4.105E-05	1.453E-06	1.453	484.381	2.519	2.00
208.478	2.636	4.394E-05	1.555E-06	1.555	518.433	2.920	2.00
					498.546	**2.363**	
208.478	3.119	5.198E-05	1.840E-06	1.840	613.281	0.818	2.50
208.478	2.857	4.762E-05	1.686E-06	1.686	561.882	2.866	2.50
208.478	2.874	4.789E-05	1.695E-06	1.695	565.112	2.690	2.50
208.478	2.727	4.545E-05	1.609E-06	1.609	536.342	2.519	2.50
208.478	3.000	5.000E-05	1.770E-06	1.770	589.977	2.920	2.50
					573.319	**2.363**	
208.478	3.456	5.760E-05	2.039E-06	2.039	679.696	0.708	3.20
208.478	3.282	5.470E-05	1.936E-06	1.936	645.489	2.866	3.20
208.478	3.304	5.507E-05	1.949E-06	1.949	649.754	2.690	3.20
208.478	3.456	5.760E-05	2.039E-06	2.039	679.696	2.519	3.20
208.478	3.401	5.669E-05	2.007E-06	2.007	668.908	2.920	3.20
					664.709	**2.341**	
208.478	4.399	7.331E-05	2.595E-06	2.595	865.068	0.721	4.00
208.478	4.132	6.887E-05	2.438E-06	2.438	812.640	2.866	4.00
208.478	4.178	6.964E-05	2.465E-06	2.465	821.694	2.690	4.00
208.478	4.573	7.622E-05	2.698E-06	2.698	899.354	2.519	4.00
208.478	4.286	7.143E-05	2.528E-06	2.528	842.824	2.920	4.00
					848.316	**2.343**	
100	1.004	1.673E-05	5.923E-07	0.592	197.449	0.639	1.03
100	0.864	1.439E-05	5.095E-07	0.509	169.826	2.866	1.03
100	0.949	1.581E-05	5.598E-07	0.560	186.583	2.690	1.03
100	0.935	1.559E-05	5.517E-07	0.552	183.908	2.519	1.03
100	0.954	1.590E-05	5.630E-07	0.563	187.652	2.920	1.03
					185.084	**2.327**	
100	1.463	2.439E-05	8.634E-07	0.863	287.793	0.640	1.50

100	1.326	2.210E-05	7.825E-07	0.782	260.821	2.866	1.50
100	1.420	2.367E-05	8.380E-07	0.838	279.345	2.690	1.50
100	1.429	2.381E-05	8.428E-07	0.843	280.941	2.519	1.50
100	1.451	2.418E-05	8.559E-07	0.856	285.288	2.920	1.50
					278.838	**2.327**	
100	2.000	3.333E-05	1.180E-06	1.180	393.318	0.656	2.00
100	2.308	3.846E-05	1.361E-06	1.361	453.828	2.866	2.00
100	1.913	3.189E-05	1.129E-06	1.129	376.261	2.690	2.00
100	1.884	3.141E-05	1.112E-06	1.112	370.588	2.519	2.00
100	2.152	3.587E-05	1.270E-06	1.270	423.226	2.920	2.00
					403.444	**2.330**	
100	2.152	3.587E-05	1.270E-06	1.270	423.226	0.564	2.50
100	2.389	3.981E-05	1.409E-06	1.409	469.727	2.866	2.50
100	2.471	4.119E-05	1.458E-06	1.458	485.977	2.690	2.50
100	2.742	4.570E-05	1.618E-06	1.618	539.284	2.519	2.50
100	2.683	4.472E-05	1.583E-06	1.583	527.707	2.920	2.50
					489.184	**2.312**	
100	3.093	5.155E-05	1.825E-06	1.825	608.223	0.634	3.20
100	2.669	4.448E-05	1.575E-06	1.575	524.890	2.866	3.20
100	3.722	6.203E-05	2.196E-06	2.196	731.981	2.690	3.20
100	3.695	6.158E-05	2.180E-06	2.180	726.572	2.519	3.20
100	3.906	6.510E-05	2.305E-06	2.305	768.199	2.920	3.20
					671.973	**2.326**	
100	4.178	6.964E-05	2.465E-06	2.465	821.694	0.685	4.00
100	4.360	7.267E-05	2.573E-06	2.573	857.524	2.866	4.00
100	4.373	7.289E-05	2.580E-06	2.580	860.024	2.690	4.00
100	3.695	6.158E-05	2.180E-06	2.180	726.572	2.519	4.00
100	4.412	7.353E-05	2.603E-06	2.603	867.613	2.920	4.00
					826.685	**2.336**	
50	0.949	1.581E-05	5.598E-07	0.560	186.583	0.622	1.00
50	1.048	1.747E-05	6.184E-07	0.618	206.141	2.866	1.00
50	1.039	1.731E-05	6.129E-07	0.613	204.286	2.690	1.00
50	0.952	1.587E-05	5.619E-07	0.562	187.294	2.519	1.00
50	1.002	1.670E-05	5.912E-07	0.591	197.053	2.920	1.00
					196.271	**2.323**	
50	1.429	2.381E-05	8.428E-07	0.843	280.941	0.624	1.50
50	1.416	2.361E-05	8.357E-07	0.836	278.554	2.866	1.50
50	1.423	2.372E-05	8.396E-07	0.840	279.875	2.690	1.50
50	1.419	2.365E-05	8.372E-07	0.837	279.081	2.519	1.50
50	1.482	2.470E-05	8.745E-07	0.874	291.490	2.920	1.50
					281.988	**2.324**	
50	1.622	2.703E-05	9.567E-07	0.957	318.906	0.532	2.00
50	1.816	3.027E-05	1.071E-06	1.071	357.129	2.866	2.00
50	1.734	2.890E-05	1.023E-06	1.023	341.027	2.690	2.00
50	1.601	2.668E-05	9.445E-07	0.944	314.822	2.519	2.00
50	1.834	3.056E-05	1.082E-06	1.082	360.621	2.920	2.00
					338.501	**2.305**	

50	2.125	3.541E-05	1.253E-06	1.253	417.830	0.557	2.50
50	2.069	3.448E-05	1.221E-06	1.221	406.880	2.866	2.50
50	1.913	3.189E-05	1.129E-06	1.129	376.261	2.690	2.50
50	1.685	2.809E-05	9.943E-07	0.994	331.447	2.519	2.50
50	2.222	3.704E-05	1.311E-06	1.311	437.020	2.920	2.50
					393.888	**2.310**	
50	2.841	4.735E-05	1.676E-06	1.676	558.690	0.582	3.20
50	2.591	4.318E-05	1.528E-06	1.528	509.479	2.866	3.20
50	2.669	4.448E-05	1.575E-06	1.575	524.890	2.690	3.20
50	2.475	4.125E-05	1.460E-06	1.460	486.779	2.519	3.20
50	2.152	3.587E-05	1.270E-06	1.270	423.226	2.920	3.20
					500.613	**2.315**	
50	2.982	4.970E-05	1.759E-06	1.759	586.458	0.489	4.00
50	2.841	4.735E-05	1.676E-06	1.676	558.690	2.866	4.00
50	3.198	5.330E-05	1.887E-06	1.887	628.973	2.690	4.00
50	3.356	5.593E-05	1.980E-06	1.980	659.929	2.519	4.00
50	3.311	5.519E-05	1.954E-06	1.954	651.188	2.920	4.00
					617.048	**2.297**	

Table G.4: Methane Gas Permeance data for NaA (Shell Side)

Feed flow rate	**Permeate**				**Flux**	**Permeance**	**delta P**
ml/min	**ml/min**	**L/s**	**mol/s**	**umol/s**	**(umol/m^2.s)**	**(umol/m^2.s.kPa)**	**bar**
208	1.048	1.747E-05	6.184E-07	0.618	206.141	0.458	1.5
208	1.044	1.740E-05	6.158E-07	0.616	205.281	0.456	1.5
208	0.921	1.536E-05	5.436E-07	0.544	181.197	0.403	1.5
208	1.059	1.766E-05	6.250E-07	0.625	208.325	0.463	1.5
208	1.012	1.687E-05	5.971E-07	0.597	199.047	0.442	1.5
					199.998	**0.444**	
208	1.127	1.878E-05	6.649E-07	0.665	221.629	0.369	2
208	1.171	1.952E-05	6.908E-07	0.691	230.280	0.384	2
208	1.151	1.919E-05	6.792E-07	0.679	226.392	0.377	2
208	1.261	2.101E-05	7.437E-07	0.744	247.889	0.413	2
208	1.071	1.786E-05	6.321E-07	0.632	210.706	0.351	2
					227.379	**0.379**	
208	1.543	2.572E-05	9.105E-07	0.910	303.486	0.405	2.5
208	1.913	3.189E-05	1.129E-06	1.129	376.261	0.502	2.5
208	1.601	2.668E-05	9.445E-07	0.944	314.822	0.420	2.5
208	1.868	3.113E-05	1.102E-06	1.102	367.358	0.490	2.5
208	1.773	2.955E-05	1.046E-06	1.046	348.686	0.465	2.5
					342.122	**0.456**	
208	2.308	3.846E-05	1.361E-06	1.361	453.828	0.473	3.2
208	2.366	3.943E-05	1.396E-06	1.396	465.281	0.485	3.2
208	2.344	3.906E-05	1.383E-06	1.383	460.919	0.480	3.2
208	2.069	3.448E-05	1.221E-06	1.221	406.880	0.424	3.2
208	2.080	3.467E-05	1.227E-06	1.227	409.138	0.426	3.2
					439.209	**0.458**	

208	2.964	4.941E-05	1.749E-06	1.749	582.981	0.486	4
208	2.841	4.735E-05	1.676E-06	1.676	558.690	0.466	4
208	2.982	4.970E-05	1.759E-06	1.759	586.458	0.489	4
208	3.378	5.631E-05	1.993E-06	1.993	664.388	0.554	4
208	2.947	4.912E-05	1.739E-06	1.739	579.545	0.483	4
					594.412	**0.495**	
100	0.923	1.538E-05	5.446E-07	0.545	181.531	0.403	1.5
100	0.900	1.501E-05	5.312E-07	0.531	177.064	0.393	1.5
100	0.943	1.571E-05	5.562E-07	0.556	185.411	0.412	1.5
100	0.941	1.568E-05	5.552E-07	0.555	185.062	0.411	1.5
100	0.975	1.625E-05	5.754E-07	0.575	191.800	0.426	1.5
					184.173	**0.409**	
100	1.293	2.155E-05	7.629E-07	0.763	254.300	0.424	2
100	1.286	2.144E-05	7.590E-07	0.759	252.992	0.422	2
100	1.263	2.104E-05	7.449E-07	0.745	248.307	0.414	2
100	1.351	2.252E-05	7.973E-07	0.797	265.755	0.443	2
100	1.395	2.326E-05	8.232E-07	0.823	274.408	0.457	2
					259.152	**0.432**	
100	1.629	2.714E-05	9.609E-07	0.961	320.291	0.427	2.5
100	1.818	3.030E-05	1.073E-06	1.073	357.562	0.477	2.5
100	1.697	2.828E-05	1.001E-06	1.001	333.697	0.445	2.5
100	1.799	2.998E-05	1.061E-06	1.061	353.703	0.472	2.5
100	1.706	2.844E-05	1.007E-06	1.007	335.595	0.447	2.5
					340.170	**0.454**	
100	2.107	3.511E-05	1.243E-06	1.243	414.309	0.432	3.2
100	1.899	3.165E-05	1.120E-06	1.120	373.403	0.389	3.2
100	2.287	3.811E-05	1.349E-06	1.349	449.677	0.468	3.2
100	2.180	3.634E-05	1.286E-06	1.286	428.762	0.447	3.2
100	2.297	3.828E-05	1.355E-06	1.355	451.743	0.471	3.2
					423.579	**0.441**	
100	2.841	4.735E-05	1.676E-06	1.676	558.690	0.466	4
100	2.793	4.655E-05	1.648E-06	1.648	549.326	0.458	4
100	3.178	5.297E-05	1.875E-06	1.875	624.975	0.521	4
100	2.698	4.496E-05	1.592E-06	1.592	530.554	0.442	4
100	2.641	4.401E-05	1.558E-06	1.558	519.346	0.433	4
					556.578	**0.464**	
50	1.078	1.797E-05	6.362E-07	0.636	212.069	0.471	1.5
50	1.021	1.702E-05	6.024E-07	0.602	200.809	0.446	1.5
50	1.091	1.818E-05	6.436E-07	0.644	214.537	0.477	1.5
50	1.010	1.684E-05	5.959E-07	0.596	198.645	0.441	1.5
50	1.050	1.751E-05	6.197E-07	0.620	206.574	0.459	1.5
					206.527	**0.459**	
50	1.277	2.128E-05	7.532E-07	0.753	251.054	0.418	2
50	1.273	2.122E-05	7.512E-07	0.751	250.414	0.417	2
50	1.323	2.205E-05	7.804E-07	0.780	260.131	0.434	2
50	1.323	2.205E-05	7.804E-07	0.780	260.131	0.434	2
50	1.463	2.439E-05	8.634E-07	0.863	287.793	0.480	2

					261.905	**0.437**	
50	1.672	2.787E-05	9.866E-07	0.987	328.861	0.438	2.5
50	1.758	2.931E-05	1.037E-06	1.037	345.824	0.461	2.5
50	1.771	2.952E-05	1.045E-06	1.045	348.274	0.464	2.5
50	1.667	2.778E-05	9.833E-07	0.983	327.765	0.437	2.5
50	1.786	2.976E-05	1.054E-06	1.054	351.177	0.468	2.5
					340.380	**0.454**	
50	2.262	3.771E-05	1.335E-06	1.335	444.930	0.463	3.2
50	2.190	3.650E-05	1.292E-06	1.292	430.640	0.449	3.2
50	1.992	3.320E-05	1.175E-06	1.175	391.751	0.408	3.2
50	2.095	3.492E-05	1.236E-06	1.236	411.995	0.429	3.2
50	2.069	3.448E-05	1.221E-06	1.221	406.880	0.424	3.2
					417.239	**0.435**	
50	2.825	4.708E-05	1.667E-06	1.667	555.533	0.463	4
50	2.809	4.682E-05	1.657E-06	1.657	552.412	0.460	4
50	2.650	4.417E-05	1.564E-06	1.564	521.181	0.434	4
50	2.627	4.378E-05	1.550E-06	1.550	516.617	0.431	4
50	2.804	4.673E-05	1.654E-06	1.654	551.380	0.459	4
					539.425	**0.450**	

Appendix H

NaA Membrane Single Permeance Statistical Data

All statistical results are calculated using the same statistical formulae as in appendix C.

Table H.1: Hydrogen Single permeance Statistical data for NaA

Feed flow rate	Differential Pressure	Mean Flux	Deviation	Confidence interval	Percentage error
ml/min	kPa	(umol/m^2.s)	σ	c.i.	% ε
208.478	100	276.838	5.580	4.891	3.53
100.000	100	243.708	5.408	4.740	3.89
50.000	100	246.427	4.981	4.366	3.54
208.478	150	651.879	7.015	6.149	1.89
100.000	150	642.806	61.639	54.029	16.81
50.000	150	589.146	31.789	27.865	9.46
208.478	200	749.962	30.469	26.707	7.12
100.000	200	776.134	31.673	27.763	7.15
50.000	200	776.518	32.967	28.897	7.44
208.478	250	821.030	64.140	56.222	13.70
100.000	250	824.928	42.447	37.206	9.02
50.000	250	784.729	18.915	16.580	4.23
208.478	320	530.455	50.675	44.419	16.75
100.000	320	599.344	11.012	9.652	3.22
50.000	320	590.142	11.968	10.491	3.56
208.478	400	703.848	59.350	52.023	14.78
100.000	400	682.753	57.924	50.772	14.87
50.000	400	641.598	42.044	36.853	11.49

Table H.2: Methane Single permeance Statistical data for NaA

Feed flow rate	Differential Pressure	Mean Flux	Deviation	Confidence interval	Percentage error
ml/min	kPa	(umol/m^2.s)	σ	c.i.	%ε
208.000	100	129.446	5.513	4.833	7.467
157.400	100	128.219	4.856	4.256	6.639
100.000	100	134.569	13.543	11.871	17.643
50.000	100	31.685	5.297	4.643	29.308
208.000	150	211.860	11.696	10.252	9.678
157.400	150	211.373	11.153	9.776	9.250
100.000	150	215.399	22.095	19.367	17.982
50.000	150	31.614	1.332	1.507	9.534
208.000	200	305.571	4.741	4.156	2.720
157.400	200	307.309	18.004	15.781	10.270
100.000	200	304.008	21.902	19.198	12.630
50.000	200	187.760	5.814	5.096	5.428
208.000	250	480.873	16.963	14.869	6.184
157.400	250	480.111	34.863	30.559	12.730
100.000	250	443.624	17.279	15.146	6.828
50.000	250	58.497	4.298	3.768	12.883
208.000	300	287.469	13.237	11.603	8.073
157.400	300	321.716	18.818	16.495	10.254
100.000	300	293.939	0.527	0.462	0.314
50.000	300	89.683	4.563	3.999	8.918
208.000	320	266.346	12.748	11.174	8.391
157.400	320	250.687	10.574	9.268	7.394
100.000	320	250.687	21.250	18.626	14.860
50.000	320	77.166	2.954	2.589	6.710
208.000	400	410.641	18.443	16.166	7.874
157.400	400	411.567	21.936	19.228	9.344
100.000	400	402.210	27.039	23.701	11.785
50.000	400	106.829	2.344	2.054	3.845

Table H.3: Hydrogen Single permeance Statistical data for NaA (Shell Side)

Feed flow rate	Differential Pressure	Mean Flux	Deviation	Confidence interval	Percentage error
ml/min	kPa	(umol/m^2.s)	σ	c.i.	%ε
208.000	100	247.901	12.310	10.791	8.706
100.000	100	213.969	8.898	7.800	7.291
50.000	100	226.903	8.206	7.193	6.340
208.000	150	399.776	18.469	16.189	8.099
100.000	150	322.356	9.499	8.326	5.166
50.000	150	325.998	4.819	4.224	2.591
208.000	200	576.654	11.353	9.951	3.451
100.000	200	466.409	31.148	27.302	11.707
50.000	200	391.331	18.907	16.573	8.470
208.000	250	662.796	26.230	22.991	6.938
100.000	250	565.531	41.793	36.633	12.955
50.000	250	455.361	36.911	32.353	14.210
208.000	320	768.449	14.560	12.762	3.321
100.000	320	776.847	91.147	79.894	20.569
50.000	320	578.743	45.213	39.631	13.696
208.000	400	980.712	31.296	27.432	5.594
100.000	400	955.706	52.207	16.025	3.354
50.000	400	713.350	38.699	33.921	9.510

Table H.4: Methane Single permeance Statistical data for NaA (Shell Side)

Feed flow rate	Differential Pressure	Mean Flux	Deviation	Confidence interval	Percentage error
ml/min	kPa	(umol/m^2.s)	σ	c.i.	%ε
208.000	150	231.212	9.893	8.672	7.501
100.000	150	212.917	4.858	4.258	4.000
50.000	150	238.759	6.159	5.399	4.523
208.000	200	262.866	12.175	10.672	8.120
100.000	200	299.598	9.544	8.366	5.585
50.000	200	302.780	13.611	11.931	7.881
208.000	250	395.517	28.578	25.050	12.667
100.000	250	393.260	13.738	12.041	6.124
50.000	250	393.503	10.004	8.679	4.411
208.000	320	507.756	25.746	22.567	8.889
100.000	320	489.684	28.652	25.114	10.257
50.000	320	482.357	18.605	16.308	6.762
208.000	400	687.182	36.298	31.817	9.260
100.000	400	643.443	36.875	32.322	10.047
50.000	400	623.612	16.877	14.793	4.744

Appendix I

Amorphous Silica
Binary Permeance
Raw Data

298 K:

Table I.1: CH_4/CO_2 Permeance Mixture Raw Data (298 K)

	Feed		Permeate		Permeate	Retentate	Permeate				Compo-	ΔP
	Height		Height		flow rate	Flow rate	CH4 Flow rate	CO2 Flow rate	CH4 Flow rate	CH4 Flow rate	sition	
	CH4	CO2	CH4	CO2	(ml/min)	(ml/min)	(ml/min)	(ml/min)	umol/s	μmol.m^{-2}.s^{-1}.Pa^{-1}	Fraction CH4	(kPa)
	2431	2117	2500	2200	727.3	1447.5	362.3	372.6	247.1	0.753	0.5	50
	2554	2129	2505	2245	707.1	1442.3	353.0	369.7	240.8	0.734	0.5	50
	2546	2197	2600	2250	700.0	1426.9	362.7	366.8	247.4	0.754	0.5	50
K1	2.057E-04	2.362E-04	2750	2800	735.4	1426.9	403.0	479.5	274.9	0.524	0.5	80
K2	1.958E-04	2.349E-04	2802	2742	720.1	1426.9	402.1	459.8	274.2	0.523	0.5	80
K3	1.964E-04	2.276E-04	2800	2650	730.6	1426.9	407.7	450.9	278.0	0.530	0.5	80
			2900	2700	800.0	1426.9	462.3	503.0	315.3	0.481	0.5	100
			3100	2750	850.0	1426.9	525.1	544.3	358.1	0.546	0.5	100
average K	1.993E-04	2.329E-04										
stdevp K	4.531E-06	3.780E-06										
C.D.	5.128E-06	4.277E-06										
Error %	**5.146**	**3.673**										

	Feed		Permeate		Permeate	Retentate	Permeate				Compo-	ΔP
	Height		Height		flow rate	Flow rate	CH4 Flow rate	CO2 Flow rate	CH4 Flow rate	CH4 Flow rate	sition	
	CH4	CO2	CH4	CO2	(ml/min)	(ml/min)	(ml/min)	(ml/min)	umol/s	μmol.m^{-2}.s^{-1}.Pa^{-1}	Fraction CH4	(kPa)
	1496	2882	1576	2930	662.7	1818.2	137.747	535.5	94.0	0.286	0.2	50
	1531	2921	1578	2887	662.7	1818.2	137.922	527.6	94.1	0.287	0.2	50
	1523	2900	1575	2927	662.7	1818.2	137.659	535.0	93.9	0.286	0.2	50
K1	1.337E-04	2.776E-04	1575	2927	1348.3	1226.6	280.062	1088.4	191.0	0.364	0.2	80
K2	1.306E-04	2.739E-04	1557	2904	1369.9	1226.6	281.286	1097.1	191.9	0.366	0.2	80
K3	1.313E-04	2.759E-04	1558	2930	1369.9	1226.6	281.467	1106.9	192.0	0.366	0.2	80
			1526	2858	2251.4	251.2	453.097	1774.5	309.0	0.471	0.2	100
			1442	2706	2251.4	251.2	428.156	1680.1	292.0	0.445	0.2	100
average K	1.319E-04	2.758E-04										
stdevp K	1.309E-06	1.514E-06										
C.D.	1.482E-06	1.71359E-06										
Error %	**1.123**	**0.621**										

	Feed		Permeate		Permeate	Retentate	Permeate				Compo-	ΔP
	Height		Height		flow rate	Flow rate	CH4 Flow rate	CO2 Flow rate	CH4 Flow rate	CH4 Flow rate	sition	
	CH4	CO2	CH4	CO2	(ml/min)	(ml/min)	(ml/min)	(ml/min)	umol/s	μmol.m^{-2}.s^{-1}.Pa^{-1}	Fraction CH4	(kPa)
	3485	1223	3659	1113	883.9	1523.5	724.243	160.787	494.0	1.506	0.8	50
	3448	1226	3679	1147	883.9	1523.5	728.202	165.699	496.7	1.514	0.8	50
	3805	1222	3478	1109	883.9	1523.5	688.417	160.209	469.5	1.432	0.8	50
K1	2.296E-04	1.635E-04	3686	1135	1707.0	748.0	1409.014	316.657	961.0	1.831	0.8	80
K2	2.320E-04	1.631E-04	3650	1095	1707.0	748.0	1395.252	305.498	951.6	1.813	0.8	80
K3	2.102E-04	1.637E-04	3656	1161	1707.0	748.0	1397.546	323.911	953.2	1.816	0.8	80
			3552	1013	2306.2	219.4	1834.453	381.836	1251.2	1.907	0.8	100
			3519	1117	2306.2	219.4	1817.409	421.037	1239.6	1.890	0.8	100
average K	2.239E-04	1.634E-04										
stdevp K	9.733E-06	2.269E-07										
C.D.	1.101E-05	2.567E-07										
Error %	**4.918**	**0.157**										

	Feed		Permeate		Permeate flow rate	Retentate Flow rate	Permeate				Compo-sition	ΔP
	Height		Height				CH4 Flow rate	CO2 Flow rate	CH4 Flow rate	CH4 Flow rate		
	CH4	CO2	CH4	CO2	(ml/min)	(ml/min)	(ml/min)	(ml/min)	umol/s	μmol.m^{-2}.s^{-1}.Pa^{-1}	Fraction CH4	(kPa)
	5484	3500	5869	3666	859.2	1572.1	609.696	306.2	415.8	1.268	0.65	50
	5338	3567	5824	3649	859.2	1572.1	605.021	304.8	412.7	1.258	0.65	50
	5309	3743	5799	3542	859.2	1572.1	602.424	295.8	410.9	1.253	0.65	50
K1	1.185E-04	1.000E-04	5827	3542	1323.5	1094.2	932.479	455.7	636.0	1.212	0.65	80
K2	1.218E-04	9.812E-05	5884	3512	1323.5	1094.2	941.601	451.9	642.2	1.224	0.65	80
K3	1.224E-04	9.351E-05	5849	3545	1650.6	783.6	1167.318	568.8	796.2	1.214	0.65	100
			5783	3540	1650.6	783.6	1154.146	568.0	787.2	1.200	0.65	100
average K	1.209E-04	9.721E-05										
stdevp K	1.707E-06	2.728E-06										
C.D.	1.931E-06	3.087E-06										
Error %	1.597	3.175										

	Feed		Permeate		Permeate flow rate	Retentate Flow rate	Permeate				Compo-sition	ΔP
	Height		Height				CH4 Flow rate	CO2 Flow rate	CH4 Flow rate	CH4 Flow rate		
	CH4	CO2	CH4	CO2	(ml/min)	(ml/min)	(ml/min)	(ml/min)	umol/s	μmol.m^{-2}.s^{-1}.Pa^{-1}	Fraction CH4	(kPa)
	4523	4485	3987	5044	776.7	1648.4	245.879	584.5	167.7	0.511	0.35	50
	4412	4248	4040	4956	776.7	1648.4	249.148	574.3	169.9	0.518	0.35	50
	4295	4344	4016	4960	776.7	1648.4	247.668	574.7	168.9	0.515	0.35	50
K1	7.738E-05	1.449E-04	3857	4951	1223.7	1291.7	374.742	903.8	255.6	0.487	0.35	80
K2	7.933E-05	1.530E-04	3926	4973	1223.7	1291.7	381.446	907.9	260.2	0.496	0.35	80
K3	8.149E-05	1.496E-04	3934	4914	1743.3	888.2	544.553	1278.1	371.4	0.566	0.35	100
			3910	5023	1743.3	888.2	541.231	1306.4	369.1	0.563	0.35	100
average K	7.940E-05	1.492E-04										
stdevp K	1.678E-06	3.316E-06										
C.D.	1.899E-06	3.752E-06										
Error %	2.391	2.515										

Table I.2: H_2/CH_4 Permeance Mixture Raw Data (298 K)

	Feed		Permeate		Permeate flow rate	Retentate Flow rate	Permeate				Compo-sition	ΔP
	Height		Height				H2 Flow rate	CH4 Flow rate	H2 Flow rate	H2 Flow rate		
	H2	CH4	H2	CH4	(ml/min)	(ml/min)	(ml/min)	(ml/min)	umol/s	μmol.m^{-2}.s^{-1}.Pa^{-1}	Fraction H2	(kPa)
	320	6408	170	2616	1079.8	1305.8	284.8	220.5	194.3	0.592	0.5	50
	329	6535	165	2480	1079.8	1305.8	276.4	209.1	188.5	0.575	0.5	50
	318	6276	152	2510	1079.8	1305.8	254.6	211.6	173.7	0.530	0.5	50
K1	1.563E-03	7.803E-05	197	2617	2298.9	115.8	702.6	469.7	479.2	0.913	0.5	80
K2	1.520E-03	7.651E-05	197	2500	2298.9	115.8	702.6	448.7	479.2	0.913	0.5	80
K3	1.572E-03	7.967E-05	190	2538	2298.9	115.8	677.7	455.5	462.2	0.881	0.5	80
			255	3227	2109.0	113.2	834.4	531.3	569.1	0.868	0.5	100
			252	3191	2109.0	113.2	824.6	525.4	562.4	0.857	0.5	100
average K	1.552E-03	7.807E-05										
stdevp K	2.282E-05	1.289E-06										
C.D.	2.582E-05	1.459E-06										
Error %	1.664	1.869										

	Feed		Permeate		Permeate flow rate	Retentate Flow rate	Permeate				Compo-sition	ΔP
	Height		Height				H2 Flow rate	CH4 Flow rate	H2 Flow rate	H2 Flow rate		
	H2	CH4	H2	CH4	(ml/min)	(ml/min)	(ml/min)	(ml/min)	umol/s	μmol.m^{-2}.s^{-1}.Pa^{-1}	Fraction H2	(kPa)
	281	1305	257	1428	962.6	877.2	723.1	211.8	493.2	1.504	0.8	50
	261	1253	260	1459	962.6	877.2	731.6	216.4	499.0	1.521	0.8	50
	280	1338	254	1555	962.6	877.2	714.7	230.7	487.4	1.486	0.8	50
K1	2.847E-03	1.533E-04	263	1557	592.2	1408.5	455.3	142.1	310.5	0.592	0.8	80
K2	3.065E-03	1.596E-04	265	1550	592.2	1408.5	458.7	141.5	312.9	0.596	0.8	80
K3	2.857E-03	1.495E-04	250	1659	592.2	1408.5	432.8	151.4	295.2	0.562	0.8	80
			314	2271	1576.9	909.1	1447.3	551.9	987.2	1.505	0.8	100
			306	2271	1576.9	909.1	1410.5	551.9	962.0	1.466	0.8	100
average K	2.923E-03	1.541E-04										
stdevp K	1.005E-04	4.184E-06										
C.D.	1.138E-04	4.735E-06										
Error %	**3.892**	**3.072**										

	Feed		Permeate		Permeate flow rate	Retentate Flow rate	Permeate				Compo-sition	ΔP
	Height		Height				H2 Flow rate	CH4 Flow rate	H2 Flow rate	H2 Flow rate		
	H2	CH4	H2	CH4	(ml/min)	(ml/min)	(ml/min)	(ml/min)	umol/s	μmol.m^{-2}.s^{-1}.Pa^{-1}	Fraction H2	(kPa)
	95	3615	129	3474	946.1	1390.0	256.1	737.9	174.6	0.532	0.2	50
	96	3573	143	3957	946.1	1390.0	283.8	840.5	193.6	0.590	0.2	50
	95	3504	150	4028	946.1	1390.0	297.7	855.6	203.1	0.619	0.2	50
K1	2.105E-03	2.213E-04	113	3674	638.4	1808.1	151.3	526.6	103.2	0.197	0.2	80
K2	2.083E-03	2.239E-04	120	3714	638.4	1808.1	160.7	532.3	109.6	0.209	0.2	80
K3	2.105E-03	2.283E-04	129	3686	638.4	1808.1	172.8	528.3	117.8	0.225	0.2	80
			118	3527	1671.3	823.0	413.7	1323.4	282.2	0.430	0.2	100
			119	3541	1671.3	823.0	417.3	1328.6	284.6	0.434	0.2	100
average K	2.098E-03	2.245E-04										
stdevp K	1.034E-05	2.894E-06										
C.D.	1.170E-05	3.274E-06										
Error %	**0.558**	**1.458**										

	Feed		Permeate		Permeate flow rate	Retentate Flow rate	Permeate				Compo-sition	ΔP
	Height		Height				H2 Flow rate	CH4 Flow rate	H2 Flow rate	H2 Flow rate		
	H2	CH4	H2	CH4	(ml/min)	(ml/min)	(ml/min)	(ml/min)	umol/s	μmol.m^{-2}.s^{-1}.Pa^{-1}	Fraction H2	(kPa)
	398	3860	520	4800	1498.1	980.9	1291.9	654.5	881.2	2.686	0.65	50
	390	3815	510	4905	1498.1	980.9	1267.1	668.8	864.2	2.635	0.65	50
	388	3862	527	5204	1498.1	980.9	1309.3	709.6	893.0	2.723	0.65	50
K1	1.633E-03	9.067E-05	518	4008	2337.7	164.2	2008.1	852.7	1369.7	2.610	0.65	80
K2	1.667E-03	9.174E-05	520	3840	2337.7	164.2	2015.9	817.0	1374.9	2.620	0.65	80
K3	1.675E-03	9.063E-05	360	3969	2365.3	134.8	1412.1	854.4	963.1	1.468	0.65	100
			385	3965	2365.3	134.8	1510.2	853.6	1030.0	1.570	0.65	100
average K	1.658E-03	9.101E-05										
stdevp K	1.816E-05	5.156E-07										
C.D.	2.055E-05	5.83E-07										
Error %	**1.239**	**0.641**										

	Feed		Permeate		Permeate flow rate	Retentate Flow rate	Permeate				Compo-sition	ΔP
	Height		Height				H2 Flow rate	CH4 Flow rate	H2 Flow rate	H2 Flow rate		
	H2	CH4	H2	CH4	(ml/min)	(ml/min)	(ml/min)	(ml/min)	umol/s	μmol.m^{-2}.s^{-1}.Pa^{-1}	Fraction H2	(kPa)
	480	5546	400	5657	1190.1	1246.5	345.679	803.9	235.8	0.719	0.35	50
	486	5442	350	5630	1190.1	1246.5	302.469	800.1	206.3	0.629	0.35	50
	480	5346	365	5735	1190.1	1246.5	315.432	815.0	215.1	0.656	0.35	50
K1	7.292E-04	1.172E-04	480	5825	1868.2	526.9	651.175	1299.4	444.1	0.846	0.35	80
K2	7.202E-04	1.194E-04	499	5834	1868.2	526.9	676.951	1301.4	461.7	0.880	0.35	80
K3	7.292E-04	1.216E-04	489	5732	2408.0	92.0	855.079	1648.2	583.2	0.889	0.35	100
			452	5705	2408.0	92.0	790.379	1640.4	539.1	0.822	0.35	100
average K	7.262E-04	1.194E-04										
stdevp K	4.244E-06	1.790E-06										
C.D.	4.802E-06	2.03E-06										
Error %	**0.661**	**1.696**										

Table I.3: H_2/CO_2 Permeance Mixture Raw Data (298 K)

	Feed Height		Permeate Height		Permeate flow rate	Retentate Flow rate	Permeate				Compo-sition	ΔP
							H2 Flow rate	CO2 Flow rate	H2 Flow rate	H2 Flow rate		
	H2	CO2	H2	CO2	(ml/min)	(ml/min)	(ml/min)	(ml/min)	umol/s	μmol.m^{-2}.s^{-1}.Pa^{-1}	Fraction H2	(kPa)
	265	2359	300	2250	851.1	1691.7	500.3	398.4	341.2	1.040	0.5	50
	251	2384	320	2216	851.1	1691.7	533.7	392.4	364.0	1.110	0.5	50
	250	2469	314	2231	851.1	1691.7	523.7	395.1	357.2	1.089	0.5	50
K1	1.887E-03	2.120E-04	315	2120	1300.0	883.7	802.5	573.4	547.3	0.834	0.5	100
K2	1.992E-03	2.097E-04	300	2150	1280.0	883.7	752.5	572.6	513.2	0.782	0.5	100
K3	2.000E-03	2.025E-04	310	2255	1280.0	883.7	777.6	600.6	530.3	0.808	0.5	100
			300	2000	1000.0	116.5	587.9	416.1	401.0	0.764	0.5	80
			305	2100	1120.0	116.5	669.4	489.4	456.6	0.870	0.5	80
average K	1.960E-03	2.081E-04										
stdevp K	5.159E-05	4.031E-06										
C.D.	5.838E-05	4.562E-06										
Error %	**2.979**	**2.192**										

	Feed Height		Permeate Height		Permeate flow rate	Retentate Flow rate	Permeate				Compo-sition	ΔP
							H2 Flow rate	CO2 Flow rate	H2 Flow rate	H2 Flow rate		
	H2	CO2	H2	CO2	(ml/min)	(ml/min)	(ml/min)	(ml/min)	umol/s	μmol.m^{-2}.s^{-1}.Pa^{-1}	Fraction H2	(kPa)
	327	1034	369	1509	1142.9	1165.6	996.8	322.4	679.9	2.073	0.8	50
	344	1146	380	1323	1142.9	1165.6	1026.5	282.6	700.1	2.135	0.8	50
	345	1037	395	1360	1142.9	1165.6	1067.0	290.6	727.8	2.219	0.8	50
K1	2.446E-03	1.934E-04	255	1387	1817.3	556.6	1095.3	471.2	747.1	1.424	0.8	80
K2	2.326E-03	1.745E-04	253	1388	1817.3	556.6	1086.7	471.5	741.2	1.412	0.8	80
K3	2.319E-03	1.929E-04	200	1372	2363.8	180.0	1117.4	606.2	762.1	1.162	0.8	100
			208	1438	2363.8	180.0	1162.1	635.4	792.6	1.208	0.8	100
			210	1427	2363.8	180.0	1173.3	630.5	800.2	1.220	0.8	100
average K	2.364E-03	1.869E-04										
stdevp K	5.865E-05	8.782E-06										
C.D.	6.637E-05	9.938E-06										
Error %	**2.808**	**5.316**										

	Feed Height		Permeate Height		Permeate flow rate	Retentate Flow rate	Permeate				Compo-sition	ΔP
							H2 Flow rate	CO2 Flow rate	H2 Flow rate	H2 Flow rate		
	H2	CO2	H2	CO2	(ml/min)	(ml/min)	(ml/min)	(ml/min)	umol/s	μmol.m^{-2}.s^{-1}.Pa^{-1}	Fraction H2	(kPa)
	104	2845	120	2720	671.9	1590.1	154.2	514.3	105.1	0.321	0.2	50
	108	2750	104	2769	671.9	1590.1	133.6	523.5	91.1	0.278	0.2	50
	102	2940	115	2721	671.9	1590.1	147.7	514.5	100.8	0.307	0.2	50
K1	1.923E-03	2.812E-04	146	2769	1003.3	1186.2	280.1	781.8	191.0	0.291	0.2	100
K2	1.852E-03	2.909E-04	130	2727	1003.3	1186.2	249.4	770.0	170.1	0.259	0.2	100
K3	1.961E-03	2.721E-04	135	2790	1281.1	853.1	330.7	1005.8	225.5	0.344	0.2	100
			148	2809	1281.1	853.1	362.5	1012.7	247.3	0.471	0.2	80
			150	2783	1281.1	853.1	367.4	1003.3	250.6	0.478	0.2	80
average K	1.912E-03	2.814E-04										
stdevp K	4.517E-05	7.677E-06										
C.D.	5.111E-05	8.687E-06										
Error %	**2.673**	**3.087**										

	Feed		Permeate		Permeate flow rate	Retentate Flow rate	Permeate				Compo-sition	ΔP
	Height		Height				H2 Flow rate	CO2 Flow rate	H2 Flow rate	H2 Flow rate		
	H2	CO2	H2	CO2	(ml/min)	(ml/min)	(ml/min)	(ml/min)	umol/s	μmol.m^{-2}.s^{-1}.Pa^{-1}	Fraction H2	(kPa)
	350	3615	259	3486	1100.6	1369.3	539.822	379.6	368.2	1.123	0.65	50
	322	3536	251	3461	1100.6	1369.3	523.148	376.9	356.8	1.088	0.65	50
	360	3464	258	3364	1100.6	1369.3	537.738	366.3	366.8	1.118	0.65	50
K1	1.857E-03	9.682E-05	495	3541	1694.1	555.6	1588.099	593.6	1083.2	2.064	0.65	80
K2	2.019E-03	9.898E-05	480	3497	1694.1	555.6	1539.975	586.2	1050.3	2.001	0.65	80
K3	1.806E-03	1.010E-04	486	3753	2162.2	166.2	1990.002	802.9	1357.3	2.069	0.65	100
			499	3482	2162.2	166.2	2043.232	744.9	1393.6	2.124	0.65	100
average K	1.894E-03	9.895E-05										
stdevp K	9.076E-05	1.723E-06										
C.D.	1.027E-04	1.95E-06										
Error %	5.423	1.971										

	Feed		Permeate		Permeate flow rate	Retentate Flow rate	Permeate				Compo-sition	ΔP
	Height		Height				H2 Flow rate	CO2 Flow rate	H2 Flow rate	H2 Flow rate		
	H2	CO2	H2	CO2	(ml/min)	(ml/min)	(ml/min)	(ml/min)	umol/s	μmol.m^{-2}.s^{-1}.Pa^{-1}	Fraction H2	(kPa)
	500	5051	601	5346	820.4	1554.4	347.7	573.2	237.1	0.723	0.35	50
	480	5070	605	4971	820.4	1554.4	350.0	533.0	238.7	0.728	0.35	50
	510	4809	600	5093	820.4	1554.4	347.1	546.1	236.7	0.722	0.35	50
K1	7.000E-04	1.287E-04	285	5007	1225.1	1125.7	246.2	801.6	167.9	0.320	0.35	80
K2	7.292E-04	1.282E-04	480	5055	1225.1	1125.7	414.7	809.3	282.8	0.539	0.35	80
K3	6.863E-04	1.352E-04	485	5110	1790.2	701.3	612.2	1195.5	417.6	0.637	0.35	100
			480	5095	1790.2	701.3	605.9	1192.0	413.3	0.630	0.35	100
average K	7.051E-04	1.307E-04										
stdevp K	1.788E-05	3.173E-06										
C.D.	2.024E-05	3.590E-06										
Error %	2.870	2.747										

328 K:

Table I.4: CH_4/CO_2 Permeance Mixture Raw Data (328 K)

	Feed		Permeate		Permeate flow rate	Retentate Flow rate	Permeate				Compo-sition	ΔP
	Height		Height				CH4 Flow rate	CO2 Flow rate	CH4 Flow rate	CH4 Flow rate		
	CH4	CO2	CH4	CO2	(ml/min)	(ml/min)	(ml/min)	(ml/min)	umol/s	μmol.m^{-2}.s^{-1}.Pa^{-1}	Fraction CH4	(kPa)
	2634	2135	2691	2110	482.5	2094.2	248.9	237.0	169.8	0.863	0.5	30
	2675	2172	2626	2127	482.5	2094.2	242.9	238.9	165.7	0.842	0.5	30
	2521	2138	2612	2121	482.5	2094.2	241.6	238.2	164.8	0.837	0.5	30
K1	1.898E-04	2.342E-04	2713	2173	696.3	1795.5	362.1	352.2	247.0	0.753	0.5	50
K2	1.869E-04	2.302E-04	2771	2239	696.3	1795.5	369.9	362.9	252.3	0.769	0.5	50
K3	1.983E-04	2.339E-04	2669	2134	696.3	1795.5	356.3	345.9	243.0	0.741	0.5	50
			2595	2110	1291.2	1123.2	642.3	634.1	438.1	0.835	0.5	80
			2595	2107	1291.2	1123.2	642.3	633.2	438.1	0.835	0.5	80
average K	1.917E-04	2.328E-04										
stdevp K	4.845E-06	1.808E-06										
C.D.	5.482E-06	2.046E-06										
	2.860	0.879										

	Feed		Permeate		Permeate flow rate	Retentate Flow rate	Permeate				Compo-sition	ΔP
	Height		Height				CH4 Flow rate	CO2 Flow rate	CH4 Flow rate	CH4 Flow rate		
	CH4	CO2	CH4	CO2	(ml/min)	(ml/min)	(ml/min)	(ml/min)	umol/s	$\mu mol.m^{-2}.s^{-1}.Pa^{-1}$	Fraction CH4	(kPa)
	1209	2999	1577	2864	427.6	2002.2	113.174	326.3	77.2	0.392	0.2	30
	1100	3001	1515	2851	427.6	2002.2	108.725	324.8	74.2	0.377	0.2	30
	1280	3008	1563	2856	427.6	2002.2	112.169	325.4	76.5	0.389	0.2	30
K1	1.654E-04	2.668E-04	1613	2873	609.1	1876.0	164.901	466.3	112.5	0.343	0.2	50
K2	1.818E-04	2.666E-04	1538	2877	609.1	1876.0	157.233	466.9	107.2	0.327	0.2	50
K3	1.563E-04	2.660E-04	1564	2946	609.1	1876.0	159.891	478.1	109.1	0.332	0.2	50
			1570	2895	1060.4	2172.6	279.406	817.9	190.6	0.363	0.2	80
			1610	2899	1060.4	2172.6	286.525	819.0	195.4	0.372	0.2	80
average K	1.678E-04	2.664E-04										
stdevp K	1.058E-05	3.421E-07										
C.D.	1.197E-05	3.872E-07										
	7.131	**0.145**										

	Feed		Permeate		Permeate flow rate	Retentate Flow rate	Permeate				Compo-sition	ΔP
	Height		Height				CH4 Flow rate	CO2 Flow rate	CH4 Flow rate	CH4 Flow rate		
	CH4	CO2	CH4	CO2	(ml/min)	(ml/min)	(ml/min)	(ml/min)	umol/s	$\mu mol.m^{-2}.s^{-1}.Pa^{-1}$	Fraction CH4	(kPa)
	3599	1011	3616	1045	500.6	1845.2	406.5	107.6	277.3	1.409	0.8	30
	3687	973	3629	993	500.6	1845.2	408.0	102.2	278.3	1.414	0.8	30
	3412	937	3619	984	500.6	1845.2	406.9	101.3	277.5	1.410	0.8	30
K1	2.223E-04	1.978E-04	3633	956	787.6	1659.8	642.6	154.8	438.3	1.336	0.8	50
K2	2.170E-04	2.055E-04	3584	991	787.6	1659.8	633.9	160.5	432.4	1.318	0.8	50
K3	2.345E-04	2.134E-04	3555	995	787.6	1659.8	628.8	161.1	428.9	1.307	0.8	50
			3558	997	1358.0	1132.8	1085.1	278.4	740.1	1.410	0.8	80
			3562	975	1358.0	1132.8	1086.3	272.2	740.9	1.412	0.8	80
average K	2.246E-04	2.056E-04										
stdevp K	7.321E-06	6.378E-06										
C.D.	8.285E-06	7.218E-06										
	3.689	**3.510**										

Table I.5: H_2/CH_4 Permeance Mixture Raw Data (328 K)

	Feed		Permeate		Permeate flow rate	Retentate Flow rate	Permeate				Compo-sition	ΔP
	Height		Height				H2 Flow rate	CH4 Flow rate	H2 Flow rate	H2 Flow rate		
	H2	CH4	H2	CH4	(ml/min)	(ml/min)	(ml/min)	(ml/min)	umol/s	$\mu mol.m^{-2}.s^{-1}.Pa^{-1}$	Fraction CH4	(kPa)
	220	2680	177	2566	751.7	1811.8	313.2	375.7	213.6	1.085	0.5	30
	203	2499	160	2545	751.7	1811.8	283.1	372.6	193.1	0.981	0.5	30
	215	2530	170	2676	751.7	1811.8	300.8	391.8	205.2	1.042	0.5	30
K1	2.273E-03	1.866E-04	177	2630	833.7	1334.8	347.3	427.0	236.9	0.722	0.5	50
K2	2.463E-03	2.001E-04	195	2610	833.7	1334.8	382.7	423.8	261.0	0.796	0.5	50
K3	2.326E-03	1.976E-04	175	2678	833.7	1334.8	343.4	434.8	234.2	0.714	0.5	50
			211	2613	1763.0	688.5	875.6	897.2	597.2	1.138	0.5	80
			207	2745	1763.0	688.5	859.0	942.5	585.9	1.116	0.5	80
average K	2.354E-03	1.948E-04										
stdevp K	8.022E-05	5.878E-06										
C.D.	9.078E-05	6.652E-06										

	Feed		Permeate				Permeate					
	Height		Height		Permeate flow rate	Retentate Flow rate	H2 Flow rate	CH4 Flow rate	H2 Flow rate	H2 Flow rate	Compo-sition	ΔP
	H2	CH4	H2	CH4	(ml/min)	(ml/min)	(ml/min)	(ml/min)	umol/s	$\mu mol.m^{-2}.s^{-1}.Pa^{-1}$	Fraction CH4	(kPa)
	255	1503	250	1497	855.9	1433.1	724.5	170.3	494.1	2.511	0.8	30
	217	1481	240	1407	855.9	1433.1	695.5	160.1	474.4	2.410	0.8	30
	240	1531	235	1462	855.9	1433.1	681.0	166.3	464.5	2.360	0.8	30
K1	3.137E-03	1.331E-04	232	1502	1470.0	897.1	1154.7	293.5	787.5	2.401	0.8	50
K2	3.687E-03	1.350E-04	235	1474	1470.0	897.1	1169.6	288.0	797.7	2.432	0.8	50
K3	3.333E-03	1.306E-04	229	1550	1470.0	897.1	1139.7	302.8	777.4	2.370	0.8	50
			240	1438	2175.2	308.4	1767.5	415.8	1205.6	2.297	0.8	80
			238	1496	2175.2	308.4	1752.8	432.5	1195.5	2.278	0.8	80
average K	3.386E-03	1.329E-04										
stdevp K	2.273E-04	1.804E-06										
C.D.	2.572E-04	2.041E-06										

	Feed		Permeate				Permeate					
	Height		Height		Permeate flow rate	Retentate Flow rate	H2 Flow rate	CH4 Flow rate	H2 Flow rate	H2 Flow rate	Compo-sition	ΔP
	H2	CH4	H2	CH4	(ml/min)	(ml/min)	(ml/min)	(ml/min)	umol/s	$\mu mol.m^{-2}.s^{-1}.Pa^{-1}$	Fraction CH4	(kPa)
	427	3334	220	3806	572.3	1896.7	58.477	512.1	39.9	0.203	0.2	30
	430	3478	240	3803	572.3	1896.7	63.794	511.7	43.5	0.221	0.2	30
	435	3400	215	3667	572.3	1896.7	57.148	493.4	39.0	0.198	0.2	30
K1	4.684E-04	2.400E-04	230	3881	865.6	1504.4	92.460	789.7	63.1	0.192	0.2	50
K2	4.651E-04	2.300E-04	222	3372	865.6	1504.4	89.244	686.2	60.9	0.186	0.2	50
K3	4.598E-04	2.353E-04	231	3684	865.6	1504.4	92.862	749.7	63.3	0.193	0.2	50
			242	3780	1374.6	926.9	154.489	1221.5	105.4	0.201	0.2	80
			214	3573	1374.6	926.9	136.614	1154.6	93.2	0.178	0.2	80
average K	4.644E-04	2.351E-04										
stdevp K	3.551E-06	4.058E-06										
C.D.	4.018E-06	4.593E-06										
	0.865	**1.954**										

Table I.6: H_2/CO_2 Permeance Mixture Raw Data (328 K)

	Feed		Permeate				Permeate					
	Height		Height		Permeate flow rate	Retentate Flow rate	H2 Flow rate	CO2 Flow rate	H2 Flow rate	H2 Flow rate	Compo-sition	ΔP
	H2	CO2	H2	CO2	(ml/min)	(ml/min)	(ml/min)	(ml/min)	umol/s	$\mu mol.m^{-2}.s^{-1}.Pa^{-1}$	Fraction CH4	(kPa)
	241	2378	280	2204	517.2	1858.5	284.5	242.6	194.0	0.986	0.5	30
	250	2293	269	2400	517.2	1858.5	273.3	264.2	186.4	0.947	0.5	30
	275	2379	250	2220	517.2	1858.5	254.0	244.4	173.2	0.880	0.5	30
K1	2.075E-03	2.103E-04	267	2336	773.4	1667.4	405.6	384.5	276.6	0.843	0.5	50
K2	2.000E-03	2.181E-04	285	2473	773.4	1667.4	432.9	407.0	295.3	0.900	0.5	50
K3	1.818E-03	2.102E-04	306	2523	773.4	1667.4	464.8	415.3	317.1	0.967	0.5	50
			252	2322	1165.4	1206.0	576.9	575.9	393.5	0.750	0.5	80
			260	2390	1165.4	1206.0	595.2	592.8	406.0	0.774	0.5	80
			250	2427	1165.4	1206.0	572.3	602.0	390.3	0.744	0.5	80
average K	1.964E-03	2.128E-04										
stdevp K	1.077E-04	3.695E-06										
C.D.	1.219E-04	4.182E-06										

	Feed		Permeate		Permeate	Retentate	Permeate				Compo-	ΔP
	Height		Height		flow rate	Flow rate	H2 Flow rate	CO2 Flow rate	H2 Flow rate	H2 Flow rate	sition	
	H2	CO2	H2	CO2	(ml/min)	(ml/min)	(ml/min)	(ml/min)	umol/s	µmol.m^{-2}.s^{-1}.Pa^{-1}	Fraction CH4	(kPa)
	235	1403	260	1220	730.5	1524.1	1292.8	256.0	881.8	4.481	0.8	30
	237	1432	230	1319	730.5	1524.1	1143.6	276.8	780.0	3.964	0.8	30
	266	1529	251	1274	730.5	1524.1	1248.1	267.3	851.2	4.325	0.8	30
K1	3.404E-03	1.426E-04	244	1307	1039.9	1112.1	885.3	200.1	603.8	1.841	0.8	50
K2	3.376E-03	1.397E-04	250	1301	1039.9	1112.1	907.1	199.2	618.7	1.886	0.8	50
K3	3.008E-03	1.308E-04	279	1392	1039.9	1112.1	1012.3	213.1	690.4	2.105	0.8	50
			238	1309	1791.9	557.7	433.0	100.5	295.4	0.563	0.8	80
			235	1330	1791.9	557.7	427.6	102.1	291.6	0.556	0.8	80
			245	1379	1791.9	557.7	445.8	105.9	304.0	0.579	0.8	80
average K	3.262E-03	1.377E-04										
stdevp K	1.806E-04	4.998E-06										
C.D.	2.044E-04	5.656E-06										
	6.265	**4.108**										

	Feed		Permeate		Permeate	Retentate	Permeate				Compo-	ΔP
	Height		Height		flow rate	Flow rate	H2 Flow rate	CO2 Flow rate	H2 Flow rate	H2 Flow rate	sition	
	H2	CO2	H2	CO2	(ml/min)	(ml/min)	(ml/min)	(ml/min)	umol/s	µmol.m^{-2}.s^{-1}.Pa^{-1}	Fraction CH4	(kPa)
	260	3323	190	3225	419.5	1740.4	58.7	332.7	40.1	0.204	0.2	30
	289	3088	187	3137	419.5	1740.4	57.8	323.7	39.4	0.200	0.2	30
	267	3362	180	3247	419.5	1740.4	55.6	335.0	37.9	0.193	0.2	30
K1	7.692E-04	2.407E-04	135	3027	653.8	1519.0	65.0	486.7	44.4	0.135	0.2	50
K2	6.920E-04	2.591E-04	147	3231	653.8	1519.0	70.8	519.5	48.3	0.147	0.2	50
K3	7.491E-04	2.380E-04	130	3142	653.8	1519.0	62.6	505.2	42.7	0.130	0.2	50
			115	3251	1006.1	1204.4	85.3	804.4	58.1	0.111	0.2	80
			113	3149	1006.1	1204.4	83.8	779.2	57.1	0.109	0.2	80
average K	7.368E-04	2.459E-04										
stdevp K	3.269E-05	9.365E-06										
C.D.	3.699E-05	1.060E-05										
	5.020	**4.309**										

353 K:

Table I.7: CH_4/CO_2 Permeance Mixture Raw Data (353 K)

	Feed		Permeate		Permeate	Retentate	Permeate				Compo-	ΔP
	Height		Height		flow rate	Flow rate	CH4 Flow rate	CO2 Flow rate	CH4 Flow rate	CH4 Flow rate	sition	
	CH4	CO2	CH4	CO2	(ml/min)	(ml/min)	(ml/min)	(ml/min)	umol/s	µmol.m^{-2}.s^{-1}.Pa^{-1}	Fraction CH4	(kPa)
	2485	2111	2679	2132	418.9	2036.2	227.2	218.5	155.0	0.788	0.5	30
	2499	1948	2669	2161	418.9	2036.2	226.4	221.4	154.4	0.785	0.5	30
	2426	2081	2749	2053	418.9	2036.2	233.2	210.4	159.0	0.808	0.5	30
K1	2.012E-04	2.369E-04	2652	2024	637.1	1791.9	342.1	315.4	233.3	0.711	0.5	50
K2	2.001E-04	2.567E-04	2690	2112	637.1	1791.9	347.0	329.1	236.6	0.721	0.5	50
K3	2.061E-04	2.403E-04	2713	2106	637.1	1791.9	349.9	328.2	238.7	0.728	0.5	50
			2661	2083	958.0	1403.5	516.1	488.1	352.0	0.671	0.5	80
			2632	2066	958.0	1403.5	510.5	484.1	348.2	0.663	0.5	80
			2634	2060	958.0	1403.5	510.9	482.7	348.4	0.664	0.5	80
average K	2.025E-04	2.446E-04										
stdevp K	2.613E-06	8.651E-06										
C.D.	2.957E-06	9.789E-06										

	Feed		Permeate		Permeate flow rate	Retentate Flow rate	Permeate				Compo-sition	ΔP
	Height		Height				CH4 Flow rate	CO2 Flow rate	CH4 Flow rate	CH4 Flow rate		
	CH4	CO2	CH4	CO2	(ml/min)	(ml/min)	(ml/min)	(ml/min)	umol/s	μmol.m^{-2}.s^{-1}.Pa^{-1}	Fraction CH4	(kPa)
	3591	743	3754	780	498.5	1691.7	415.621	103.0	283.5	1.440	0.8	30
	3572	784	3781	821	498.5	1691.7	418.610	108.4	285.5	1.451	0.8	30
	3645	740	3762	787	498.5	1691.7	416.506	103.9	284.1	1.443	0.8	30
K1	2.228E-04	2.692E-04	3741	803	739.4	1482.1	614.254	157.2	419.0	1.277	0.8	50
K2	2.240E-04	2.551E-04	3773	777	739.4	1482.1	619.509	152.2	422.5	1.288	0.8	50
K3	2.195E-04	2.703E-04	3762	740	739.4	1482.1	617.702	144.9	421.3	1.284	0.8	50
			3783	886	1234.1	1061.9	1036.812	289.6	707.2	1.347	0.8	80
			3807	823	1234.1	1061.9	1043.390	269.0	711.6	1.356	0.8	80
			3865	798	1234.1	1061.9	1059.286	260.8	722.5	1.377	0.8	80
average K	2.221E-04	2.649E-04										
stdevp K	1.898E-06	6.908E-06										
C.D.	2.148E-06	7.82E-06										
	0.967	**2.951**										

	Feed		Permeate		Permeate flow rate	Retentate Flow rate	Permeate				Compo-sition	ΔP
	Height		Height				CH4 Flow rate	CO2 Flow rate	CH4 Flow rate	CH4 Flow rate		
	CH4	CO2	CH4	CO2	(ml/min)	(ml/min)	(ml/min)	(ml/min)	umol/s	μmol.m^{-2}.s^{-1}.Pa^{-1}	Fraction CH4	(kPa)
	717	3299	750	2959	390.5	1940.7	79.860	281.2	54.5	0.277	0.2	30
	744	3303	768	2994	390.5	1940.7	81.776	284.5	55.8	0.283	0.2	30
	740	3260	770	2976	390.5	1940.7	81.989	282.8	55.9	0.284	0.2	30
K1	2.789E-04	2.425E-04	810	2952	622.4	1775.1	137.469	447.1	93.8	0.286	0.2	50
K2	2.688E-04	2.422E-04	900	2912	622.4	1775.1	152.744	441.1	104.2	0.318	0.2	50
K3	2.703E-04	2.454E-04	910	2913	622.4	1775.1	154.441	441.2	105.3	0.321	0.2	50
			900	2894	991.2	1426.3	243.246	698.1	165.9	0.316	0.2	80
			950	2874	991.2	1426.3	256.760	693.3	175.1	0.334	0.2	80
			860	2850	991.2	1426.3	232.435	687.5	158.5	0.302	0.2	80
average K	2.727E-04	2.434E-04										
stdevp K	4.469E-06	1.442E-06										
C.D.	5.057E-06	1.632E-06										
	1.855	**0.670**										

	Feed		Permeate		Permeate flow rate	Retentate Flow rate	Permeate				Compo-sition	ΔP
	Height		Height				CH4 Flow rate	CO2 Flow rate	CH4 Flow rate	CH4 Flow rate		
	CH4	CO2	CH4	CO2	(ml/min)	(ml/min)	(ml/min)	(ml/min)	umol/s	μmol.m^{-2}.s^{-1}.Pa^{-1}	Fraction CH4	(kPa)
	5104	3462	6108	3622	524.5	1828.3	396.4	192.6	270.3	1.374	0.65	30
	5132	3642	5963	3463	524.5	1828.3	387.0	184.1	263.9	1.341	0.65	30
	5547	3273	6026	3541	524.5	1828.3	391.0	188.3	266.7	1.355	0.65	30
K1	1.274E-04	1.011E-04	5923	3677	768.0	1618.0	562.8	286.3	383.9	1.170	0.65	50
K2	1.267E-04	9.610E-05	5995	3585	768.0	1618.0	569.7	279.1	388.5	1.185	0.65	50
K3	1.172E-04	1.069E-04	6062	3636	768.0	1618.0	576.0	283.1	392.9	1.198	0.65	50
			5982	3603	1159.4	1226.2	858.1	423.5	585.3	1.115	0.65	80
			5915	3628	1159.4	1226.2	848.5	426.4	578.7	1.103	0.65	80
			5974	3646	1159.4	1226.2	857.0	428.6	584.5	1.114	0.65	80
average K	1.237E-04	1.014E-04										
stdevp K	4.639E-06	4.428E-06										
C.D.	5.250E-06	5.010E-06										
	4.243	**4.942**										

	Feed		Permeate		Permeate flow rate	Retentate Flow rate	Permeate				Compo-sition	ΔP
	Height		Height				CH4 Flow rate	CO2 Flow rate	CH4 Flow rate	CH4 Flow rate		
	CH4	CO2	CH4	CO2	(ml/min)	(ml/min)	(ml/min)	(ml/min)	umol/s	µmol.m^{-2}.s^{-1}.Pa^{-1}	Fraction CH4	(kPa)
	4500	5932	4185	5195	333.7	1929.3	119.3	193.5	81.4	0.414	0.35	30
	4019	5789	4258	5147	333.7	1929.3	121.4	191.7	82.8	0.421	0.35	30
	3826	5752	4168	5132	333.7	1929.3	118.8	191.1	81.1	0.412	0.35	30
K1	7.778E-05	1.096E-04	4023	5151	695.5	1718.4	239.1	399.9	163.1	0.497	0.35	50
K2	8.709E-05	1.123E-04	4252	5198	695.5	1718.4	252.7	403.5	172.4	0.525	0.35	50
K3	9.148E-05	1.130E-04	4285	5261	695.5	1718.4	254.7	408.4	173.7	0.530	0.35	50
			4111	5113	1050.8	1042.6	369.1	599.7	251.8	0.480	0.35	80
			4075	5135	1050.8	1042.6	365.9	602.3	249.6	0.476	0.35	80
			4137	5171	1050.8	1042.6	371.5	606.5	253.3	0.483	0.35	80
average K	8.545E-05	1.116E-04										
stdevp K	5.712E-06	1.476E-06										
C.D.	6.464E-06	1.670E-06										
	7.565	**1.496**										

Table I.8: H_2/CH_4 Permeance Mixture Raw Data (353 K)

	Feed		Permeate		Permeate flow rate	Retentate Flow rate	Permeate				Compo-sition	ΔP
	Height		Height				H2 Flow rate	CH4 Flow rate	H2 Flow rate	H2 Flow rate		
	H2	CH4	H2	CH4	(ml/min)	(ml/min)	(ml/min)	(ml/min)	umol/s	µmol.m^{-2}.s^{-1}.Pa^{-1}	Fraction CH4	(kPa)
	158	2672	210	2616	670.8	1702.9	436.2	336.0	297.5	1.512	0.5	30
	153	2593	190	2623	670.8	1702.9	394.6	336.9	269.2	1.368	0.5	30
	175	2570	179	2619	670.8	1702.9	371.8	336.4	253.6	1.289	0.5	30
K1	3.165E-03	1.871E-04	180	2592	997.0	1378.3	555.7	494.9	379.0	1.156	0.5	50
K2	3.268E-03	1.928E-04	186	2587	997.0	1378.3	574.2	493.9	391.6	1.194	0.5	50
K3	2.857E-03	1.946E-04	181	2628	997.0	1378.3	558.8	501.7	381.1	1.162	0.5	50
			182	2601	1053.6	743.0	593.8	524.8	405.0	0.772	0.5	80
			191	2595	1053.6	743.0	623.1	523.6	425.0	0.810	0.5	80
			167	2608	1053.6	743.0	544.8	526.2	371.6	0.708	0.5	80
average K	3.097E-03	1.915E-04										
stdevp K	1.745E-04	3.173E-06										
C.D.	1.974E-04	3.591E-06										
	6.376	**1.875**										

	Feed		Permeate		Permeate flow rate	Retentate Flow rate	Permeate				Compo-sition	ΔP
	Height		Height				H2 Flow rate	CH4 Flow rate	H2 Flow rate	H2 Flow rate		
	H2	CH4	H2	CH4	(ml/min)	(ml/min)	(ml/min)	(ml/min)	umol/s	µmol.m^{-2}.s^{-1}.Pa^{-1}	Fraction CH4	(kPa)
	200	1512	213	1502	819.7	1415.1	660.5	161.9	450.5	2.289	0.8	30
	226	1530	204	1487	819.7	1415.1	632.6	160.3	431.5	2.192	0.8	30
	210	1520	215	1489	819.7	1415.1	666.7	160.5	454.7	2.311	0.8	30
K1	4.000E-03	1.323E-04	208	1516	1360.0	915.1	1070.2	271.2	729.9	2.225	0.8	50
K2	3.540E-03	1.307E-04	192	1480	1360.0	915.1	987.9	264.7	673.8	2.054	0.8	50
K3	3.810E-03	1.316E-04	196	1479	1360.0	915.1	1008.4	264.6	687.8	2.097	0.8	50
			206	1487	1940.7	88.7	1512.4	379.6	1031.6	1.966	0.8	80
			215	1484	1940.7	88.7	1578.5	378.8	1076.6	2.051	0.8	80
			234	1497	1940.7	88.7	1718.0	382.1	1171.8	2.233	0.8	80
average K	3.783E-03	1.315E-04										
stdevp K	1.888E-04	6.365E-07										
C.D.	2.136E-04	7.202E-07										
	5.647	**0.548**										

	Feed		Permeate		Permeate flow rate	Retentate Flow rate	Permeate				Compo-sition	ΔP
	Height		Height				H2 Flow rate	CH4 Flow rate	H2 Flow rate	H2 Flow rate		
	H2	CH4	H2	CH4	(ml/min)	(ml/min)	(ml/min)	(ml/min)	umol/s	µmol.m^{-2}.s^{-1}.Pa^{-1}	Fraction CH4	(kPa)
	69	3676	53	3839	522.5	1669.0	85.497	436.0	58.3	0.296	0.2	30
	60	3619	55	3819	522.5	1669.0	88.723	433.8	60.5	0.307	0.2	30
	66	3748	58	3806	522.5	1669.0	93.563	432.3	63.8	0.324	0.2	30
K1	2.899E-03	2.176E-04	55	3860	886.7	1370.9	150.568	744.0	102.7	0.313	0.2	50
K2	3.333E-03	2.211E-04	56	3813	886.7	1370.9	153.305	734.9	104.6	0.319	0.2	50
K3	3.030E-03	2.134E-04	58	3865	886.7	1370.9	158.780	745.0	108.3	0.330	0.2	50
			51	3822	852.0	910.5	134.149	707.8	91.5	0.174	0.2	80
			55	3832	852.0	910.5	144.670	709.7	98.7	0.188	0.2	80
			51	3852	852.0	910.5	134.149	713.4	91.5	0.174	0.2	80
average K	3.087E-03	2.174E-04										
stdevp K	1.820E-04	3.111E-06										
C.D.	2.060E-04	3.521E-06										
	6.672	**1.620**										

	Feed		Permeate		Permeate flow rate	Retentate Flow rate	Permeate				Compo-sition	ΔP
	Height		Height				H2 Flow rate	CH4 Flow rate	H2 Flow rate	H2 Flow rate		
	H2	CH4	H2	CH4	(ml/min)	(ml/min)	(ml/min)	(ml/min)	umol/s	µmol.m^{-2}.s^{-1}.Pa^{-1}	Fraction CH4	(kPa)
	424	3607	422	3774	824.7	1625.3	561.9	287.8	383.2	1.947	0.65	30
	420	3807	378	3770	824.7	1625.3	503.3	287.5	343.3	1.744	0.65	30
	382	3810	440	3739	824.7	1625.3	585.9	285.2	399.6	2.030	0.65	30
K1	1.533E-03	9.703E-05	454	3793	828.4	1194.4	607.2	290.6	414.1	1.263	0.65	50
K2	1.548E-03	9.194E-05	460	3713	828.4	1194.4	615.2	284.4	419.6	1.279	0.65	50
K3	1.702E-03	9.186E-05	465	3848	828.4	1194.4	621.9	294.8	424.2	1.293	0.65	50
			360	3950	1964.0	471.3	1141.5	717.4	778.5	1.483	0.65	80
			377	3842	1964.0	471.3	1195.4	697.7	815.3	1.554	0.65	80
			371	3878	1964.0	471.3	1176.3	704.3	802.3	1.529	0.65	80
average K	1.594E-03	9.361E-05										
stdevp K	7.625E-05	2.420E-06										
C.D.	8.628E-05	2.739E-06										
	5.413	**2.926**										

	Feed		Permeate		Permeate flow rate	Retentate Flow rate	Permeate				Compo-sition	ΔP
	Height		Height				H2 Flow rate	CH4 Flow rate	H2 Flow rate	H2 Flow rate		
	H2	CH4	H2	CH4	(ml/min)	(ml/min)	(ml/min)	(ml/min)	umol/s	µmol.m^{-2}.s^{-1}.Pa^{-1}	Fraction CH4	(kPa)
	372	5643	310	5762	682.2	1740.8	211.7	466.4	144.4	0.734	0.35	30
	350	5534	360	5877	682.2	1740.8	245.9	475.7	167.7	0.852	0.35	30
	344	5386	355	5829	682.2	1740.8	242.5	471.8	165.4	0.840	0.35	30
K1	9.409E-04	1.152E-04	360	5878	1065.1	1355.9	383.9	742.7	261.8	0.798	0.35	50
K2	1.000E-03	1.175E-04	389	5853	1065.1	1355.9	414.8	739.6	282.9	0.863	0.35	50
K3	1.017E-03	1.207E-04	360	5831	1065.1	1355.9	383.9	736.8	261.8	0.798	0.35	50
			385	5871	1643.8	792.4	633.6	1145.0	432.2	0.823	0.35	80
			350	5853	1643.8	792.4	576.0	1141.5	392.9	0.749	0.35	80
			360	5837	1643.8	792.4	592.5	1138.3	404.1	0.770	0.35	80
average K	9.861E-04	1.178E-04										
stdevp K	3.277E-05	2.255E-06										
C.D.	3.709E-05	2.55E-06										
	3.761	**2.167**										

Table I.9: H_2/CO_2 Permeance Mixture Raw Data (353 K)

	Feed		Permeate		Permeate flow rate	Retentate Flow rate	Permeate				Compo-sition	ΔP
	Height		Height				H2 Flow rate	CO2 Flow rate	H2 Flow rate	H2 Flow rate		
	H2	CO2	H2	CO2	(ml/min)	(ml/min)	(ml/min)	(ml/min)	umol/s	µmol.m^{-2}.s^{-1}.Pa^{-1}	Fraction H2	(kPa)
	228	1316	219	1346	686.1	1559.8	551.438	140.0	376.1	1.911	0.8	30
	220	1229	198	1350	686.1	1559.8	498.560	140.4	340.0	1.728	0.8	30
	207	1428	211	1316	686.1	1559.8	531.294	136.9	362.4	1.841	0.8	30
K1	3.509E-03	1.520E-04	260	1343	1023.9	1178.8	976.985	208.4	666.4	2.032	0.8	50
K2	3.636E-03	1.627E-04	261	1310	1023.9	1178.8	980.743	203.3	668.9	2.039	0.8	50
K3	3.865E-03	1.401E-04	250	1353	1023.9	1178.8	939.409	210.0	640.7	1.953	0.8	50
			294	1360	1704.5	600.2	1839.149	351.4	1254.4	2.390	0.8	80
			289	1283	1704.5	600.2	1807.871	331.5	1233.1	2.350	0.8	80
			280	1335	1704.5	600.2	1751.570	345.0	1194.7	2.276	0.8	80
average K	3.670E-03	1.516E-04										
stdevp K	1.472E-04	9.262E-06										
C.D.	1.666E-04	1.048E-05										
	4.540	**6.914**										

	Feed		Permeate		Permeate flow rate	Retentate Flow rate	Permeate				Compo-sition	ΔP
	Height		Height				H2 Flow rate	CO2 Flow rate	H2 Flow rate	H2 Flow rate		
	H2	CO2	H2	CO2	(ml/min)	(ml/min)	(ml/min)	(ml/min)	umol/s	µmol.m^{-2}.s^{-1}.Pa^{-1}	Fraction H2	(kPa)
	61	3241	74	3111	380.5	1690.1	86.5	291.6	59.0	0.300	0.2	30
	65	3248	66	3345	380.5	1690.1	77.1	313.5	52.6	0.267	0.2	30
	70	3253	70	3257	380.5	1690.1	81.8	305.3	55.8	0.283	0.2	30
K1	3.279E-03	2.468E-04	65	3304	546.3	1539.1	109.0	444.7	74.4	0.227	0.2	50
K2	3.077E-03	2.463E-04	60	3182	546.3	1539.1	100.7	428.2	68.7	0.209	0.2	50
K3	2.857E-03	2.459E-04	58	3188	546.3	1539.1	97.3	429.0	66.4	0.202	0.2	50
			72	3222	851.9	1214.2	188.4	676.2	128.5	0.245	0.2	80
			79	3197	851.9	1214.2	206.7	670.9	141.0	0.269	0.2	80
			72	3214	851.9	1214.2	188.4	674.5	128.5	0.245	0.2	80
average K	3.071E-03	2.464E-04										
stdevp K	1.721E-04	3.735E-07										
C.D.	1.948E-04	4.226E-07										
	6.343	**0.172**										

	Feed		Permeate		Permeate flow rate	Retentate Flow rate	Permeate				Compo-sition	ΔP
	Height		Height				H2 Flow rate	CO2 Flow rate	H2 Flow rate	H2 Flow rate		
	H2	CO2	H2	CO2	(ml/min)	(ml/min)	(ml/min)	(ml/min)	umol/s	µmol.m^{-2}.s^{-1}.Pa^{-1}	Fraction H2	(kPa)
	239	3309	297	3294	1847.1	625.8	1493.6	637.8	1018.7	5.176	0.65	30
	254	3400	290	3300	1847.1	625.8	1458.4	639.0	994.7	5.054	0.65	30
	225	3309	285	3225	1847.1	625.8	1433.2	624.5	977.5	4.967	0.65	30
K1	2.720E-03	1.058E-04	281	3250	622.2	1544.4	476.0	212.0	324.7	0.990	0.65	50
K2	2.559E-03	1.029E-04	283	3383	622.2	1544.4	479.4	220.7	327.0	0.997	0.65	50
K3	2.889E-03	1.058E-04	265	3380	622.2	1544.4	448.9	220.5	306.2	0.934	0.65	50
			261	3523	1439.4	1567.3	1022.8	531.6	697.6	1.329	0.65	80
			265	3520	1439.4	1567.3	1038.5	531.1	708.3	1.350	0.65	80
			280	3523	1439.4	1567.3	1097.3	531.6	748.4	1.426	0.65	80
average K	2.723E-03	1.048E-04										
stdevp K	1.347E-04	1.335E-06										
C.D.	0.0001524	1.51E-06										
	5.597	**1.441**										

372 K:

Table I.10: CH_4/CO_2 Permeance Mixture Raw Data (372 K)

	Feed		Permeate		Permeate flow rate	Retentate Flow rate	Permeate				Compo-sition	ΔP
	Height		Height				CH4 Flow rate	CO2 Flow rate	CH4 Flow rate	CH4 Flow rate		
	CH4	CO2	CH4	CO2	(ml/min)	(ml/min)	(ml/min)	(ml/min)	umol/s	μmol.m^{-2}.s^{-1}.Pa^{-1}	Fraction CH4	(kPa)
	2637	2020	2775	2165	447.4	1984.6	242.4	240.2	165.4	0.840	0.5	30
	2556	2179	2755	2145	447.4	1984.6	240.7	238.0	164.2	0.834	0.5	30
	2492	1872	2765	2109	447.4	1984.6	241.6	234.0	164.8	0.837	0.5	30
K1	1.896E-04	2.475E-04	2756	2128	619.5	1792.8	333.4	327.0	227.4	0.693	0.5	50
K2	1.956E-04	2.295E-04	2713	2119	619.5	1792.8	328.2	325.6	223.9	0.683	0.5	50
K3	2.006E-04	2.671E-04	2788	2141	619.5	1792.8	337.3	329.0	230.1	0.701	0.5	50
			2750	2107	941.2	1437.1	505.5	491.9	344.7	0.657	0.5	80
			2742	2152	941.2	1437.1	504.0	502.4	343.7	0.655	0.5	80
			2699	2096	941.2	1437.1	496.1	489.3	338.4	0.645	0.5	80
average K	1.953E-04	2.480E-04										
stdevp K	4.510E-06	1.537E-05										
C.D.	5.104E-06	1.739E-05										
	2.613	**7.011**										

	Feed		Permeate		Permeate flow rate	Retentate Flow rate	Permeate				Compo-sition	ΔP
	Height		Height				CH4 Flow rate	CO2 Flow rate	CH4 Flow rate	CH4 Flow rate		
	CH4	CO2	CH4	CO2	(ml/min)	(ml/min)	(ml/min)	(ml/min)	umol/s	μmol.m^{-2}.s^{-1}.Pa^{-1}	Fraction CH4	(kPa)
	3925	671	3751	784	94.9	1740.8	74.318	22.4	50.7	0.258	0.8	30
	3811	629	3787	720	94.9	1740.8	75.031	20.6	51.2	0.260	0.8	30
	3768	696	3779	761	94.9	1740.8	74.873	21.8	51.1	0.259	0.8	30
K1	2.038E-04	2.981E-04	3714	779	757.9	1529.3	587.410	177.8	400.6	1.221	0.8	50
K2	2.099E-04	3.180E-04	3763	754	757.9	1529.3	595.160	172.1	405.9	1.238	0.8	50
K3	2.123E-04	2.874E-04	3761	743	757.9	1529.3	594.844	169.6	405.7	1.237	0.8	50
			3776	895	1150.2	1088.9	906.319	310.0	618.2	1.178	0.8	80
			3789	820	1150.2	1088.9	909.439	284.0	620.3	1.182	0.8	80
			3862	802	1150.2	1088.9	926.961	277.8	632.2	1.205	0.8	80
average K	2.087E-04	3.011E-04										
stdevp K	3.575E-06	1.268E-05										
C.D.	4.046E-06	1.435E-05										
	1.939	**4.766**										

	Feed		Permeate		Permeate flow rate	Retentate Flow rate	Permeate				Compo-sition	ΔP
	Height		Height				CH4 Flow rate	CO2 Flow rate	CH4 Flow rate	CH4 Flow rate		
	CH4	CO2	CH4	CO2	(ml/min)	(ml/min)	(ml/min)	(ml/min)	umol/s	μmol.m^{-2}.s^{-1}.Pa^{-1}	Fraction CH4	(kPa)
	730	3280	1677	2853	417.6	1967.2	195.888	290.6	133.6	0.679	0.2	30
	754	3341	1682	2972	417.6	1967.2	196.472	302.7	134.0	0.681	0.2	30
	667	3221	1668	3035	417.6	1967.2	194.837	309.2	132.9	0.675	0.2	30
K1	2.740E-04	2.439E-04	1672	3041	565.1	1791.0	264.247	419.1	180.2	0.549	0.2	50
K2	2.653E-04	2.394E-04	1781	3091	565.1	1791.0	281.474	426.0	192.0	0.585	0.2	50
K3	2.999E-04	2.484E-04	1645	2997	565.1	1791.0	259.980	413.1	177.3	0.541	0.2	50
			1633	2933	842.3	1506.3	384.710	602.6	262.4	0.500	0.2	80
			1642	2694	842.3	1506.3	386.830	553.5	263.8	0.503	0.2	80
			1613	2902	842.3	1506.3	379.998	596.2	259.2	0.494	0.2	80
average K	2.797E-04	2.439E-04										
stdevp K	1.469E-05	3.642E-06										
C.D.	1.663E-05	4.121E-06										
	5.944	**1.690**										

Table I.11: H_2/CH_4 Permeance Mixture Raw Data (372 K)

	Feed		Permeate				Permeate					
	Height		Height		Permeate flow rate	Retentate Flow rate	H2 Flow rate	CH4 Flow rate	H2 Flow rate	H2 Flow rate	Compo-sition	ΔP
	H2	CH4	H2	CH4	(ml/min)	(ml/min)	(ml/min)	(ml/min)	umol/s	µmol.m^{-2}.s^{-1}.Pa^{-1}	Fraction H2	(kPa)
	167	2327	120	2618	634.8	1712.7	236.0	340.7	160.9	0.818	0.5	30
	165	2502	115	2678	634.8	1712.7	226.1	348.5	154.2	0.784	0.5	30
	153	2497	118	2672	634.8	1712.7	232.0	347.7	158.3	0.804	0.5	30
K1	2.994E-03	2.149E-04	116	2648	959.7	1332.8	344.8	520.9	235.2	0.717	0.5	50
K2	3.030E-03	1.998E-04	123	2649	959.7	1332.8	365.6	521.1	249.4	0.760	0.5	50
K3	3.268E-03	2.002E-04	123	2641	959.7	1332.8	365.6	519.6	249.4	0.760	0.5	50
			127	2658	1133.1	780.6	445.7	617.4	304.0	0.579	0.5	80
			129	2629	1133.1	780.6	452.8	610.7	308.8	0.588	0.5	80
			128	2641	1133.1	780.6	449.3	613.4	306.4	0.584	0.5	80
average K	3.097E-03	2.050E-04										
stdevp K	1.215E-04	6.992E-06										
C.D.	1.375E-04	7.912E-06										
	4.439	**3.860**										

	Feed		Permeate				Permeate					
	Height		Height		Permeate flow rate	Retentate Flow rate	H2 Flow rate	CH4 Flow rate	H2 Flow rate	H2 Flow rate	Compo-sition	ΔP
	H2	CH4	H2	CH4	(ml/min)	(ml/min)	(ml/min)	(ml/min)	umol/s	µmol.m^{-2}.s^{-1}.Pa^{-1}	Fraction H2	(kPa)
	198	1488	179	1526	767.3	1455.7	530.5	154.6	361.8	1.839	0.8	30
	202	1510	173	1518	767.3	1455.7	512.7	153.8	349.7	1.777	0.8	30
	223	1547	180	1519	767.3	1455.7	533.5	153.9	363.9	1.849	0.8	30
K1	4.040E-03	1.344E-04	234	1603	1218.3	925.2	1101.2	257.9	751.1	2.290	0.8	50
K2	3.960E-03	1.325E-04	255	1547	1218.3	925.2	1200.0	248.9	818.5	2.495	0.8	50
K3	3.587E-03	1.293E-04	222	1564	1218.3	925.2	1044.7	251.6	712.5	2.172	0.8	50
			263	1575	2003.3	148.8	2035.2	416.6	1388.1	2.645	0.8	80
			264	1532	2003.3	148.8	2042.9	405.3	1393.4	2.655	0.8	80
			243	1625	2003.3	148.8	1880.4	429.9	1282.6	2.444	0.8	80
average K	3.863E-03	1.320E-04										
stdevp K	1.974E-04	2.112E-06										
C.D.	2.234E-04	2.390E-06										
	5.783	**1.810**										

	Feed		Permeate				Permeate					
	Height		Height		Permeate flow rate	Retentate Flow rate	H2 Flow rate	CH4 Flow rate	H2 Flow rate	H2 Flow rate	Compo-sition	ΔP
	H2	CH4	H2	CH4	(ml/min)	(ml/min)	(ml/min)	(ml/min)	umol/s	µmol.m^{-2}.s^{-1}.Pa^{-1}	Fraction H2	(kPa)
	52	3921	48	3989	546.9	1673.6	98.481	438.9	67.2	0.341	0.2	30
	54	3994	50	3989	546.9	1673.6	102.585	438.9	70.0	0.356	0.2	30
	54	4017	45	4008	546.9	1673.6	92.326	441.0	63.0	0.320	0.2	30
K1	3.846E-03	2.040E-04	51	3992	796.6	1398.1	152.405	639.7	103.9	0.317	0.2	50
K2	3.704E-03	2.003E-04	52	3956	796.6	1398.1	155.393	634.0	106.0	0.323	0.2	50
K3	3.704E-03	1.992E-04	46	4025	796.6	1398.1	137.463	645.0	93.8	0.286	0.2	50
			55	4011	1286.9	925.2	265.500	1038.3	181.1	0.345	0.2	80
			58	3912	1286.9	925.2	279.981	1012.7	191.0	0.364	0.2	80
			52	3939	1286.9	925.2	251.018	1019.7	171.2	0.326	0.2	80
average K	3.751E-03	2.012E-04										
stdevp K	6.715E-05	2.082E-06										
C.D.	7.599E-05	2.356E-06										
	2.026	**1.171**										

Table I.12: H_2/CO_2 Permeance Mixture Raw Data (372 K)

	Feed		Permeate		Permeate flow rate	Retentate Flow rate	Permeate				Compo-sition	ΔP
	Height		Height				H2 Flow rate	CO2 Flow rate	H2 Flow rate	H2 Flow rate		
	H2	CO2	H2	CO2	(ml/min)	(ml/min)	(ml/min)	(ml/min)	umol/s	µmol.m^{-2}.s^{-1}.Pa^{-1}	Fraction H2	(kPa)
	146	2709	182	2247	501.3	1904.8	305.8	208.5	208.6	1.060	0.5	30
	162	2746	190	2297	501.3	1904.8	319.3	213.1	217.8	1.107	0.5	30
	141	2651	198	2245	501.3	1904.8	332.7	208.3	226.9	1.153	0.5	30
K1	3.425E-03	1.846E-04	246	2282	586.5	1652.9	483.7	247.7	329.9	1.006	0.5	50
K2	3.086E-03	1.821E-04	245	2283	586.5	1652.9	481.7	247.8	328.6	1.002	0.5	50
K3	3.546E-03	1.886E-04	241	2258	586.5	1652.9	473.9	245.1	323.2	0.985	0.5	50
			171	2236	1103.3	1269.8	632.5	456.6	431.4	0.822	0.5	80
			186	2301	1103.3	1269.8	687.9	469.9	469.2	0.894	0.5	80
			161	2311	1103.3	1269.8	595.5	471.9	406.1	0.774	0.5	80
average K	3.352E-03	1.851E-04										
stdevp K	1.945E-04	2.689E-06										
C.D.	2.201E-04	3.043E-06										
	6.565	**1.644**										

	Feed		Permeate		Permeate flow rate	Retentate Flow rate	Permeate				Compo-sition	ΔP
	Height		Height				H2 Flow rate	CO2 Flow rate	H2 Flow rate	H2 Flow rate		
	H2	CO2	H2	CO2	(ml/min)	(ml/min)	(ml/min)	(ml/min)	umol/s	µmol.m^{-2}.s^{-1}.Pa^{-1}	Fraction H2	(kPa)
	210	1371	246	1382	657.5	1505.0	630.5	135.1	430.0	2.185	0.8	30
	200	1334	250	1360	657.5	1505.0	640.7	133.0	437.0	2.221	0.8	30
	206	1331	269	1361	657.5	1505.0	689.4	133.1	470.2	2.389	0.8	30
K1	3.810E-03	1.459E-04	270	1357	1063.4	1185.0	1119.0	214.6	763.3	2.327	0.8	50
K2	4.000E-03	1.499E-04	261	1381	1063.4	1185.0	1081.7	218.3	737.8	2.249	0.8	50
K3	3.883E-03	1.503E-04	291	1355	1063.4	1185.0	1206.1	214.2	822.6	2.508	0.8	50
			275	1439	1505.0	618.6	1613.2	322.0	1100.3	2.097	0.8	80
			278	1406	1505.0	618.6	1630.8	314.6	1112.3	2.119	0.8	80
			287	1448	1505.0	618.6	1683.6	324.0	1148.3	2.188	0.8	80
average K	3.898E-03	1.487E-04										
stdevp K	7.841E-05	1.992E-06										
C.D.	8.872E-05	2.254E-06										
	2.276	**1.516**										

	Feed		Permeate		Permeate flow rate	Retentate Flow rate	Permeate				Compo-sition	ΔP
	Height		Height				H2 Flow rate	CO2 Flow rate	H2 Flow rate	H2 Flow rate		
	H2	CO2	H2	CO2	(ml/min)	(ml/min)	(ml/min)	(ml/min)	umol/s	µmol.m^{-2}.s^{-1}.Pa^{-1}	Fraction H2	(kPa)
	71	3037	70	3314	355.3	1173.6	67.9	284.8	46.3	0.235	0.2	30
	73	3454	70	3326	355.3	1173.6	67.9	285.9	46.3	0.235	0.2	30
	76	3469	80	3335	355.3	1173.6	77.6	286.6	52.9	0.269	0.2	30
K1	2.817E-03	2.634E-04	80	3371	548.5	1549.7	119.8	447.3	81.7	0.249	0.2	50
K2	2.740E-03	2.316E-04	78	3347	548.5	1549.7	116.8	444.1	79.6	0.243	0.2	50
K3	2.632E-03	2.306E-04	74	3312	548.5	1549.7	110.8	439.4	75.6	0.230	0.2	50
			79	3402	857.6	1236.7	184.9	705.7	126.1	0.240	0.2	80
			83	3361	857.6	1236.7	194.3	697.2	132.5	0.252	0.2	80
			76	3282	857.6	1236.7	177.9	680.8	121.3	0.231	0.2	80
average K	2.729E-03	2.419E-04										
stdevp K	7.601E-05	1.523E-05										
C.D.	8.601E-05	1.724E-05										
	3.151	**7.127**										

SHELL SIDE BINARY DATA

298 K

Table I.13: CH_4/CO_2 Shell Side Permeance Mixture Raw Data (298 K)

	Feed Height		Permeate Height		Permeate flow rate	Permeate CH4 Flow rate	Permeate CO2 Flow rate	Permeate CH4 Flow rate	Permeate CH4 Flow rate	Compo-sition	ΔP
	CH4	CO2	CH4	CO2	(ml/min)	(ml/min)	(ml/min)	umol/s	µmol.m^{-2}.s^{-1}.Pa^{-1}	Fraction CH4	(kPa)
	3767	4020	4516	4300	638.90	382.70	338.97	261.02	0.95	0.5	50
	3777	4103	4610	4293	648.20	396.35	343.35	270.33	0.98	0.5	50
	3765	4035	4500	4400	640.50	382.30	347.72	260.75	0.95	0.5	50
K1	1.327E-04	1.244E-04	4530	3933	820.23	492.84	398.04	336.14	0.76	0.5	80
K2	1.324E-04	1.219E-04	4500	4202	813.56	485.59	421.80	331.20	0.75	0.5	80
K3	1.328E-04	1.239E-04	4347	3986	819.11	472.28	402.85	322.12	0.73	0.5	80
			4325	3934	1200.00	688.39	582.48	469.52	0.85	0.5	100
			4300	3600	1500.00	855.51	666.28	583.51	1.06	0.5	100
			4582	3885	1650.00	1002.78	790.93	683.95	1.24	0.5	100
average K	1.326E-04	1.234E-04									
stdevp K	1.845E-07	1.094E-06									
C.D.	6.781E-07	4.018E-06									
Error %	**0.511**	**3.257**									

Table I.14: H_2/CH_4 Shell Side Permeance Mixture Raw Data (298 K)

	Feed Height		Permeate Height		Permeate flow rate	Permeate H2	Permeate CH4	Permeate H2	Permeate H2 Flow	Compo-sition	ΔP
	H2	CH4	H2	CH4	(ml/min)	(ml/min)	(ml/min)	umol/s	µmol.m^{-2}.s^{-1}.Pa^{-1}	Fraction H2	(kPa)
	345	4031	299	4453	830.5	361.6	453.9	246.6	1.50	0.5	30
	356	4022	318	4348	827.0	383.0	441.3	261.2	1.58	0.5	30
	330	4172	310	4497	828.7	374.1	457.4	255.2	1.55	0.5	30
K1	1.449E-03	1.240E-04	395	4578	1271.2	731.2	714.3	498.7	1.81	0.5	50
K2	1.404E-03	1.243E-04	387	4423	1279.3	721.0	694.5	491.8	1.79	0.5	50
K3	1.515E-03	1.198E-04	388	4394	1284.8	726.0	692.9	495.2	1.80	0.5	50
			340	4293	2414.5	1195.5	1272.2	815.4	1.65	0.5	90
			345	4371	2352.9	1182.2	1262.3	806.3	1.63	0.5	90
			350	4361	2371.5	1208.8	1269.3	824.5	1.67	0.5	90
average K	1.456E-03	1.227E-04									
stdevp K	4.545E-05	2.045E-06									
C.D.	1.670E-04	7.514E-06									
Error %	**11.468**	**6.122**									

Table I.15: H_2/CO_2 Shell Side Permeance Mixture Raw Data (298 K)

	Feed Height		Permeate Height		Permeate flow rate	Permeate H2	Permeate CO2	Permeate H2	Permeate H2 Flow rate	Compo-sition	ΔP
	H2	CO2	H2	CO2	(ml/min)	(ml/min)	(ml/min)	umol/s	μmol.m^{-2}.s^{-1}.Pa^{-1}	Fraction H2	(kPa)
	343	3393	355	3737	660.07	338.12	359.08	230.62	0.84	0.5	50
	357	3455	326	3963	662.25	311.53	382.05	212.48	0.77	0.5	50
	340	3457	381	3958	658.62	362.09	379.48	246.96	0.90	0.5	50
K1	1.458E-03	1.474E-04	310	4017	1100.00	492.05	643.24	335.60	0.76	0.5	80
K2	1.401E-03	1.447E-04	290	3851	1150.00	481.23	644.68	328.22	0.75	0.5	80
K3	1.471E-03	1.446E-04	308	3955	1150.00	511.10	662.09	348.59	0.79	0.5	80
			335	3926	1800.00	870.10	1028.72	593.46	1.08	0.5	100
			330	3944	1850.00	880.93	1062.15	600.84	1.09	0.5	100
			330	3945	1810.00	861.88	1039.45	587.85	1.07	0.5	100
average K	1.443E-03	1.456E-04									
stdevp K	3.044E-05	1.267E-06									
C.D.	1.118E-04	4.655E-06									
Error %	7.751	3.198									

353 K

Table I.16: CH_4/CO_2 Shell Side Permeance Mixture Raw Data (353 K)

	Feed Height		Permeate Height		Permeate flow rate	Permeate CH4 Flow	Permeate CO2 Flow	Permeate CH4 Flow	Permeate CH4 Flow	Compo-sition	ΔP
	CH4	CO2	CH4	CO2	(ml/min)	(ml/min)	(ml/min)	umol/s	μmol.m^{-2}.s^{-1}.Pa^{-1}	Fraction CH4	(kPa)
	3418	4242	4532	3792	475.81	299.87	212.49	172.66	1.05	0.5	30
	3737	4298	4759	4066	475.81	314.89	227.84	181.31	1.10	0.5	30
	3647	4198	4629	4046	478.66	308.12	228.08	177.41	1.08	0.5	30
K1	1.463E-04	1.179E-04	4562	4109	718.99	456.12	347.93	262.63	0.96	0.5	50
K2	1.338E-04	1.163E-04	4426	3967	723.33	445.20	337.93	256.34	0.93	0.5	50
K3	1.371E-04	1.191E-04	4503	4004	716.42	448.61	337.83	258.30	0.94	0.5	50
			4649	4033	1238.39	800.61	588.19	460.98	0.93	0.5	90
			4455	3929	1242.24	769.58	574.80	443.11	0.90	0.5	90
			4588	3986	1242.24	792.56	583.14	456.34	0.92	0.5	90
average K	1.391E-04	1.178E-04									
stdevp K	5.283E-06	1.134E-06									
C.D.	1.941E-05	4.165E-06									
Error %	13.961	3.537									

Table I.17: H_2/CH_4 Shell Side Permeance Mixture Raw Data (353 K)

	Feed Height		Permeate Height		Permeate flow rate	Permeate H2	Permeate CH4	Permeate H2	Permeate H2 Flow	Compo-sition	ΔP
	H2	CH4	H2	CH4	(ml/min)	(ml/min)	(ml/min)	umol/s	μmol.m^{-2}.s^{-1}.Pa^{-1}	Fraction H2	(kPa)
	363	3667	364	3930	774.2	405.6	428.9	233.5	1.42	0.5	30
	352	3470	340	3915	768.3	375.9	424.0	216.5	1.31	0.5	30
	329	3510	352	4082	778.7	394.5	448.1	227.1	1.38	0.5	30
K1	1.377E-03	1.364E-04	302	3783	1181.1	513.4	629.8	295.6	1.08	0.5	50
K2	1.420E-03	1.441E-04	271	3777	1182.3	461.1	629.5	265.5	0.97	0.5	50
K3	1.520E-03	1.425E-04	280	3913	1178.8	475.0	650.2	273.5	1.00	0.5	50
			318	3764	2193.8	1004.0	1164.0	578.1	1.17	0.5	90
			310	3897	2193.8	978.8	1205.1	563.6	1.14	0.5	90
			273	3882	2234.6	878.0	1222.8	505.5	1.02	0.5	90
average K	1.439E-03	1.410E-04									
stdevp K	5.961E-05	3.330E-06									
C.D.	2.190E-04	1.224E-05									
Error %	15.219	8.682									

Table I.18: H_2/CO_2 Shell Side Permeance Mixture Raw Data (353 K)

	Feed Height		Permeate Height		Permeate flow rate	Permeate H2	Permeate CO2	Permeate H2	Permeate H2 Flow rate	Compo-sition	ΔP
	H2	CO2	H2	CO2	(ml/min)	(ml/min)	(ml/min)	umol/s	$\mu mol.m^{-2}.s^{-1}.Pa^{-1}$	Fraction H2	(kPa)
	361	3553	335	3782	590.84	266.71	318.36	153.57	0.93	0.5	30
	368	3452	310	4122	592.59	247.54	348.01	142.53	0.86	0.5	30
	385	3525	340	4032	591.72	271.09	339.91	156.09	0.95	0.5	30
K1	1.385E-03	1.407E-04	416	3814	860.83	482.54	467.76	277.84	1.01	0.5	50
K2	1.359E-03	1.448E-04	435	4107	857.14	502.42	501.54	289.28	1.05	0.5	50
K3	1.299E-03	1.418E-04	428	4027	872.73	503.32	500.71	289.81	1.05	0.5	50
			400	3869	1494.40	805.47	823.74	463.78	0.94	0.5	90
			395	3824	1500.00	798.38	817.21	459.70	0.93	0.5	90
			393	3819	1476.01	781.64	803.09	450.05	0.91	0.5	90
average K	1.347E-03	1.425E-04									
stdevp K	3.613E-05	1.738E-06									
C.D.	1.328E-04	6.388E-06									
Error %	**9.853**	**4.484**									

Appendix J

Amorphous Silica Binary Permeance Processed Data

298 K

Table J.1: CH_4/CO_2 Binary Permeance Processed Data (298 K)

50/50 Mixtures										
Pressure Difference (kPa)	Feed Flow (ml/min)		Permeate (ml/min)		Permeate (mol/min)		Permeate Permeance ($\mu mol.m^{-2}.s^{-1}.Pa^{-1}$)		$\alpha_{(CH4/CO2)}$	$\alpha_{(CO2/CH4)}$
	CH4	CO2	CH4	CO2	CH4	CO2	CH4	CO2		
50	1250	1250	359.339	369.691	0.015	0.015	0.747	0.768	0.972	1.029
80	1250	1250	404.252	463.395	0.017	0.019	0.525	0.602	0.872	1.146
100	1250	1250	493.712	523.673	0.020	0.021	0.513	0.544	0.943	1.061
20/80 Mixtures										
Pressure Difference (kPa)	Feed Flow (ml/min)		Permeate (ml/min)		Permeate (mol/min)		Permeate Permeance ($\mu mol.m^{-2}.s^{-1}.Pa^{-1}$)		$\alpha_{(CH4/CO2)}$	$\alpha_{(CO2/CH4)}$
	CH4	CO2	CH4	CO2	CH4	CO2	CH4	CO2		
50	1250	1250	137.776	532.705	0.006	0.022	0.286	1.107	1.035	0.967
80	1250	1250	280.938	1097.429	0.011	0.045	0.365	1.426	1.024	0.977
100	1250	1250	440.626	1727.295	0.018	0.071	0.458	1.795	1.020	0.980
80/20 Mixtures										
Pressure Difference (kPa)	Feed Flow (ml/min)		Permeate (ml/min)		Permeate (mol/min)		Permeate Permeance ($\mu mol.m^{-2}.s^{-1}.Pa^{-1}$)		$\alpha_{(CH4/CO2)}$	$\alpha_{(CO2/CH4)}$
	CH4	CO2	CH4	CO2	CH4	CO2	CH4	CO2		
50	1250	1250	713.621	162.232	0.029	0.007	1.483	0.337	1.100	0.909
80	1250	1250	1400.604	315.355	0.057	0.013	1.819	0.410	1.110	0.901
100	1250	1250	1825.931	401.437	0.075	0.016	1.897	0.417	1.137	0.879
65/35 Mixtures										
Pressure Difference (kPa)	Feed Flow (ml/min)		Permeate (ml/min)		Permeate (mol/min)		Permeate Permeance (μmol/m^2.s.Pa)		$\alpha_{(CH4/CO2)}$	$\alpha_{(CO2/CH4)}$
	CH4	CO2	CH4	CO2	CH4	CO2	CH4	CO2		
50	1250	1250	605.714	302.265	0.025	0.012	1.259	0.628	1.079	0.927
80	1250	1250	937.040	453.784	0.038	0.019	1.217	0.589	1.112	0.899
100	1250	1250	1160.732	568.417	0.047	0.023	1.206	0.591	1.100	0.909
35/65Mixtures										
Pressure Difference (kPa)	Feed Flow (ml/min)		Permeate (ml/min)		Permeate (mol/min)		Permeate Permeance ($\mu mol.m^{-2}.s^{-1}.Pa^{-1}$)		$\alpha_{(CH4/CO2)}$	$\alpha_{(CO2/CH4)}$
	CH4	CO2	CH4	CO2	CH4	CO2	CH4	CO2		
50	1250	1250	247.565	577.837	0.010	0.024	0.515	1.201	0.796	1.257
80	1250	1250	378.094	905.855	0.015	0.037	0.491	1.177	0.775	1.290
100	1250	1250	542.892	1292.260	0.022	0.053	0.564	1.343	0.780	1.282

Table J.2: H_2/CH_4 Binary Permeance Processed Data (298 K)

50/50 Mixtures										
Pressure Difference (kPa)	Feed Flow (ml/min)		Permeate (ml/min)		Permeate (mol/min)		Permeate Permeance ($\mu mol.m^{-2}.s^{-1}.Pa^{-1}$)		$\alpha_{(H2/CH4)}$	$\alpha_{(XH4/H2)}$
	H2	CH4	H2	CH4	H2	CH4	H2	CH4		
50	1250	1250	271.959	213.723	0.011	0.009	0.565	0.444	1.272	0.786
80	1250	1250	694.324	457.945	0.028	0.019	0.902	0.595	1.516	0.660
100	1250	1250	829.481	528.345	0.034	0.022	0.862	0.549	1.570	0.637
20/80 Mixtures										
Pressure Difference (kPa)	Feed Flow (ml/min)		Permeate (ml/min)		Permeate (mol/min)		Permeate Permeance ($\mu mol/m^2.s.Pa$)		$\alpha_{(H2/CH4)}$	$\alpha_{(XH4/H2)}$
	H2	CH4	H2	CH4	H2	CH4	H2	CH4		
50	1250	1250	279.212	811.330	0.011	0.033	0.580	1.686	1.377	0.726
80	1250	1250	170.959	529.064	0.007	0.022	0.222	0.687	1.293	0.774
100	1250	1250	415.500	1326.012	0.017	0.054	0.432	1.378	1.253	0.798
80/20 Mixtures										
Pressure Difference (kPa)	Feed Flow (ml/min)		Permeate (ml/min)		Permeate (mol/min)		Permeate Permeance ($\mu mol.m^{-2}.s^{-1}.Pa^{-1}$)		$\alpha_{(H2/CH4)}$	$\alpha_{(XH4/H2)}$
	H2	CH4	H2	CH4	H2	CH4	H2	CH4		
50	1250	1250	723.112	219.654	0.030	0.009	1.503	0.457	0.823	1.215
80	1250	1250	448.921	144.995	0.018	0.006	0.583	0.188	0.774	1.292
100	1250	1250	1428.893	551.904	0.058	0.023	1.485	0.574	0.647	1.545
65/35 Mixtures										
Pressure Difference (kPa)	Feed Flow (ml/min)		Permeate (ml/min)		Permeate (mol/min)		Permeate Permeance ($\mu mol.m^{-2}.s^{-1}.Pa^{-1}$)		$\alpha_{(H2/CH4)}$	$\alpha_{(XH4/H2)}$
	H2	CH4	H2	CH4	H2	CH4	H2	CH4		
50	1250	1250	1289.424	677.620	0.053	0.028	2.680	1.408	1.025	0.976
80	1250	1250	2012.004	834.874	0.082	0.034	2.614	1.084	1.298	0.771
100	1250	1250	1461.147	854.005	0.060	0.035	1.518	0.887	0.921	1.085
35/65 Mixtures										
Pressure Difference (kPa)	Feed Flow (ml/min)		Permeate (ml/min)		Permeate (mol/min)		Permeate Permeance ($\mu mol.m^{-2}.s^{-1}.Pa^{-1}$)		$\alpha_{(H2/CH4)}$	$\alpha_{(XH4/H2)}$
	H2	CH4	H2	CH4	H2	CH4	H2	CH4		
50	1250	1250	321.193	806.318	0.013	0.033	0.668	1.676	0.740	1.352
80	1250	1250	664.063	1300.445	0.027	0.053	0.863	1.689	0.948	1.054
100	1250	1250	822.729	1644.308	0.034	0.067	0.855	1.709	0.929	1.076

Table J.3: H_2/CO_2 Binary Permeance Processed Data (298 K)

50/50 Mixtures										
Pressure Difference (kPa)	Feed Flow (ml/min)		Permeate (ml/min)		Permeate (mol/min)		Permeate Permeance ($\mu mol.m^{-2}.s^{-1}.Pa^{-1}$)		$\alpha_{(H2/XO2)}$	$\alpha_{(XO2/H2)}$
	H2	CO2	H2	CO2	H2	CO2	H2	CO2		
50	1250	1250	519.227	395.295	0.021	0.016	1.079	0.822	1.314	0.761
80	1250	1250	628.642	452.751	0.026	0.019	0.817	0.588	1.388	0.720
100	1250	1250	777.507	582.195	0.032	0.024	0.808	0.605	1.335	0.749

20/80 Mixtures										
Pressure Difference (kPa)	Feed Flow (ml/min)		Permeate (ml/min)		Permeate (mol/min)		Permeate Permeance ($\mu mol.m^{-2}.s^{-1}.Pa^{-1}$)		$\alpha_{(H2/XO2)}$	$\alpha_{(XO2/H2)}$
	H2	CO2	H2	CO2	H2	CO2	H2	CO2		
50	1250	1250	145.159	517.431	0.006	0.021	0.302	1.075	1.122	0.891
80	1250	1250	364.963	1008.008	0.015	0.041	0.474	1.309	1.448	0.690
100	1250	1250	286.707	852.539	0.012	0.035	0.298	0.886	1.345	0.743
80/20 Mixtures										
Pressure Difference (kPa)	Feed Flow (ml/min)		Permeate (ml/min)		Permeate (mol/min)		Permeate Permeance ($\mu mol.m^{-2}.s^{-1}.Pa^{-1}$)		$\alpha_{(H2/XO2)}$	$\alpha_{(XO2/H2)}$
	H2	CO2	H2	CO2	H2	CO2	H2	CO2		
50	1250	1250	1030.095	298.528	0.042	0.012	2.141	0.620	0.863	1.159
80	1250	1250	1091.019	471.350	0.045	0.019	1.417	0.612	0.579	1.728
100	1250	1250	1150.934	624.069	0.047	0.026	1.196	0.649	0.461	2.169
65/35 Mixtures										
Pressure Difference (kPa)	Feed Flow (ml/min)		Permeate (ml/min)		Permeate (mol/min)		Permeate Permeance ($\mu mol.m^{-2}.s^{-1}.Pa^{-1}$)		$\alpha_{(H2/XO2)}$	$\alpha_{(XO2/H2)}$
	H2	CO2	H2	CO2	H2	CO2	H2	CO2		
50	1250	1250	533.569	374.285	0.022	0.015	1.109	0.778	0.768	1.303
80	1250	1250	1564.037	589.880	0.064	0.024	2.032	0.766	1.428	0.700
100	1250	1250	2016.617	773.923	0.082	0.032	2.096	0.804	1.403	0.713
35/65Mixtures										
Pressure Difference (kPa)	Feed Flow (ml/min)		Permeate (ml/min)		Permeate (mol/min)		Permeate Permeance ($\mu mol.m^{-2}.s^{-1}.Pa^{-1}$)		$\alpha_{(H2/XO2)}$	$\alpha_{(XO2/H2)}$
	H2	CO2	H2	CO2	H2	CO2	H2	CO2		
50	1250	1250	348.267	550.736	0.014	0.023	0.724	1.145	1.174	0.852
80	1250	1250	330.436	805.485	0.014	0.033	0.429	1.046	0.762	1.313
100	1250	1250	609.070	1193.713	0.025	0.049	0.633	1.240	0.948	1.055

328 K

Table J.4: CH_4/CO_2 Binary Permeance Processed Data (328 K)

50/50 Mixtures										
Pressure Difference (kPa)	Feed Flow (ml/min)		Permeate (ml/min)		Permeate (mol/min)		Permeate Permeance ($\mu mol.m^{-2}.s^{-1}.Pa^{-1}$)		$\alpha_{(CH4/CO2)}$	$\alpha_{(CO2/CH4)}$
	CH4	CO2	CH4	CO2	CH4	CO2	CH4	CO2		
30	1250	1250	244.459	238.012	0.010	0.010	0.847	0.824	1.027	0.974
50	1250	1250	362.753	353.640	0.015	0.014	0.754	0.735	1.026	0.975
80	1250	1250	642.319	633.692	0.026	0.026	0.834	0.823	1.014	0.987
20/80 Mixtures										
Pressure Difference (kPa)	Feed Flow (ml/min)		Permeate (ml/min)		Permeate (mol/min)		Permeate Permeance ($\mu mol.m^{-2}.s^{-1}.Pa^{-1}$)		$\alpha_{(CH4/CO2)}$	$\alpha_{(CO2/CH4)}$
	CH4	CO2	CH4	CO2	CH4	CO2	CH4	CO2		
30	1250	1250	111.356	325.489	0.005	0.013	0.386	1.127	1.368	0.731
50	1250	1250	160.675	470.432	0.007	0.019	0.334	0.978	1.366	0.732
80	1250	1250	282.965	818.455	0.012	0.033	0.368	1.063	1.383	0.723

80/20 Mixtures										
Pressure Difference (kPa)	Feed Flow (ml/min)		Permeate (ml/min)		Permeate (mol/min)		Permeate Permeance ($\mu mol.m^{-2}.s^{-1}.Pa^{-1}$)		$\alpha_{(CH4/CO2)}$	$\alpha_{(CO2/CH4)}$
	CH4	CO2	CH4	CO2	CH4	CO2	CH4	CO2		
30	1250	1250	407.142	103.687	0.017	0.004	1.410	0.359	0.982	1.019
50	1250	1250	635.083	158.800	0.026	0.006	1.320	0.330	1.000	1.000
80	1250	1250	1085.693	275.301	0.044	0.011	1.410	0.358	0.986	1.014

Table J.5: H_2/CH_4 Binary Permeance Processed Data (328 K)

50/50 Mixtures										
Pressure Difference (kPa)	Feed Flow (ml/min)		Permeate (ml/min)		Permeate (mol/min)		Permeate Permeance ($\mu mol.m^{-2}.s^{-1}.Pa^{-1}$)		$\alpha_{(H2/CH4)}$	$\alpha_{(H2/CH4)}$
	H2	CH4	H2	CH4	H2	CH4	H2	CH4		
30	1250	1250	299.028	380.017	0.012	0.016	1.036	1.316	0.787	1.271
50	1250	1250	357.811	428.559	0.015	0.018	0.744	0.891	0.835	1.198
80	1250	1250	867.282	919.848	0.035	0.038	1.127	1.195	0.943	1.061
20/80 Mixtures										
Pressure Difference (kPa)	Feed Flow (ml/min)		Permeate (ml/min)		Permeate (mol/min)		Permeate Permeance ($\mu mol.m^{-2}.s^{-1}.Pa^{-1}$)		$\alpha_{(H2/CH4.)}$	$\alpha_{(H2/CH4.)}$
	H2	CH4	H2	CH4	H2	CH4	H2	CH4		
30	1250	1250	59.807	505.727	0.002	0.021	0.207	1.752	0.473	2.114
50	1250	1250	91.522	741.858	0.004	0.030	0.190	1.542	0.493	2.026
80	1250	1250	145.551	1188.042	0.006	0.049	0.189	1.543	0.490	2.041
80/20 Mixtures										
Pressure Difference (kPa)	Feed Flow (ml/min)		Permeate (ml/min)		Permeate (mol/min)		Permeate Permeance ($\mu mol.m^{-2}.s^{-1}.Pa^{-1}$)		$\alpha_{(H2/CH4.)}$	$\alpha_{(H2/CH4.)}$
	H2	CH4	H2	CH4	H2	CH4	H2	CH4		
30	1250	1250	700.332	165.565	0.029	0.007	2.426	0.574	1.057	0.946
50	1250	1250	1154.664	294.768	0.047	0.012	2.400	0.613	0.979	1.021
80	1250	1250	1760.176	424.139	0.072	0.017	2.286	0.551	1.037	0.964

Table J.6: H_2/CO_2 Binary Permeance Processed Data (328 K)

50/50 Mixtures										
Pressure Difference (kPa)	Feed Flow (ml/min)		Permeate (ml/min)		Permeate (mol/min)		Permeate Permeance ($\mu mol.m^{-2}.s^{-1}.Pa^{-1}$)		$\alpha_{(H2/XO2)}$	$\alpha_{(H2/XO2)}$
	H2	CO2	H2	CO2	H2	CO2	H2	CO2		
30	1250	1250	270.598	250.405	0.011	0.010	0.937	0.867	1.081	0.925
50	1250	1250	434.465	402.268	0.018	0.016	0.903	0.836	1.080	0.926
80	1250	1250	581.466	590.245	0.024	0.024	0.755	0.767	0.985	1.015
20/80 Mixtures										
Pressure Difference (kPa)	Feed Flow (ml/min)		Permeate (ml/min)		Permeate (mol/min)		Permeate Permeance ($\mu mol.m^{-2}.s^{-1}.Pa^{-1}$)		$\alpha_{(H2/CO2)}$	$\alpha_{(H2/CO2)}$
	H2	CO2	H2	CO2	H2	CO2	H2	CO2		
30	1250	1250	57.390	330.461	0.002	0.014	0.199	1.145	0.695	1.440
50	1250	1250	66.158	503.815	0.003	0.021	0.138	1.047	0.525	1.904
80	1250	1250	84.509	791.790	0.003	0.032	0.110	1.029	0.427	2.342

80/20 Mixtures										
Pressure Difference (kPa)	Feed Flow (ml/min)		Permeate (ml/min)		Permeate (mol/min)		Permeate Permeance ($\mu mol.m^{-2}.s^{-1}.Pa^{-1}$)		$\alpha_{(H2/CO2)}$	$\alpha_{(H2/CO2)}$
	H2	CO2	H2	CO2	H2	CO2	H2	CO2		
30	1250	1250	1228.178	266.698	0.050	0.011	4.254	0.924	1.151	0.869
50	1250	1250	934.888	204.150	0.038	0.008	1.943	0.424	1.145	0.873
80	1250	1250	435.463	102.836	0.018	0.004	0.566	0.134	1.059	0.945

353 K

Table J.7: CH_4/CO_2 Binary Permeance Processed Data (353 K)

50/50 Mixtures										
Pressure Difference (kPa)	Feed Flow (ml/min)		Permeate (ml/min)		Permeate (mol/min)		Permeate Permeance ($\mu mol.m^{-2}.s^{-1}.Pa^{-1}$)		$\alpha_{(CH4/CO2)}$	$\alpha_{(CO2/CH4)}$
	CH4	CO2	CH4	CO2	CH4	CO2	CH4	CO2		
30	1250	1250	228.931	216.766	0.009	0.009	0.793	0.751	1.056	0.947
50	1250	1250	346.311	324.216	0.014	0.013	0.720	0.674	1.068	0.936
80	1250	1250	512.481	484.954	0.021	0.020	0.666	0.630	1.057	0.946
20/80 Mixtures										
Pressure Difference (kPa)	Feed Flow (ml/min)		Permeate (ml/min)		Permeate (mol/min)		Permeate Permeance ($\mu mol.m^{-2}.s^{-1}.Pa^{-1}$)		$\alpha_{(CH4/CO2)}$	$\alpha_{(CO2/CH4)}$
	CH4	CO2	CH4	CO2	CH4	CO2	CH4	CO2		
30	1250	1250	81.208	282.854	0.003	0.012	0.281	0.980	1.148	0.871
50	1250	1250	148.218	443.160	0.006	0.018	0.308	0.921	1.338	0.747
80	1250	1250	244.147	692.952	0.010	0.028	0.317	0.900	1.409	0.710
80/20 Mixtures										
Pressure Difference (kPa)	Feed Flow (ml/min)		Permeate (ml/min)		Permeate (mol/min)		Permeate Permeance ($\mu mol.m^{-2}.s^{-1}.Pa^{-1}$)		$\alpha_{(CH4/CO2)}$	$\alpha_{(CO2/CH4)}$
	CH4	CO2	CH4	CO2	CH4	CO2	CH4	CO2		
30	1250	1250	416.912	105.104	0.017	0.004	1.444	0.364	0.992	1.008
50	1250	1250	617.155	151.436	0.025	0.006	1.283	0.315	1.019	0.982
80	1250	1250	1046.496	273.149	0.043	0.011	1.359	0.355	0.958	1.044
65/35 Mixtures										
Pressure Difference (kPa)	Feed Flow (ml/min)		Permeate (ml/min)		Permeate (mol/min)		Permeate Permeance ($\mu mol.m^{-2}.s^{-1}.Pa^{-1}$)		$\alpha_{(CH4/CO2)}$	$\alpha_{(CO2/CH4)}$
	CH4	CO2	CH4	CO2	CH4	CO2	CH4	CO2		
30	1250	1250	391.456	188.329	0.016	0.008	1.356	0.652	1.119	0.893
50	1250	1250	569.511	282.833	0.023	0.012	1.184	0.588	1.084	0.922
80	1250	1250	854.557	426.160	0.035	0.017	1.110	0.554	1.080	0.926
35/65Mixtures										
Pressure Difference (kPa)	Feed Flow (ml/min)		Permeate (ml/min)		Permeate (mol/min)		Permeate Permeance ($\mu mol.m^{-2}.s^{-1}.Pa^{-1}$)		$\alpha_{(CH4/CO2)}$	$\alpha_{(CO2/CH4)}$
	CH4	CO2	CH4	CO2	CH4	CO2	CH4	CO2		
30	1250	1250	119.853	192.108	0.005	0.008	0.415	0.665	1.159	0.863
50	1250	1250	248.816	403.956	0.010	0.017	0.517	0.840	1.144	0.874
80	1250	1250	368.817	602.828	0.015	0.025	0.479	0.783	1.136	0.880

Table J.8: H_2/CH_4 Binary Permeance Processed Data (353 K)

50/50 Mixtures										
Pressure Difference (kPa)	Feed Flow (ml/min)		Permeate (ml/min)		Permeate (mol/min)		Permeate Permeance ($\mu mol.m^{-2}.s^{-1}.Pa^{-1}$)		$\alpha_{(H2/CH4)}$	$\alpha_{(H2/CH4)}$
	H2	CH4	H2	CH4	H2	CH4	H2	CH4		
30	1250	1250	400.874	336.461	0.016	0.014	1.389	1.165	1.191	0.839
50	1250	1250	562.886	496.833	0.023	0.020	1.170	1.033	1.133	0.883
80	1250	1250	587.231	524.839	0.024	0.021	0.763	0.682	1.119	0.894

20/80 Mixtures										
Pressure Difference (kPa)	Feed Flow (ml/min)		Permeate (ml/min)		Permeate (mol/min)		Permeate Permeance ($\mu mol.m^{-2}.s^{-1}.Pa^{-1}$)		$\alpha_{(H2/CH4.)}$	$\alpha_{(H2/CH4.)}$
	H2	CH4	H2	CH4	H2	CH4	H2	CH4		
30	1250	1250	89.261	434.022	0.004	0.018	0.309	1.503	0.823	1.216
50	1250	1250	154.218	741.309	0.006	0.030	0.321	1.541	0.832	1.202
80	1250	1250	137.656	710.298	0.006	0.029	0.179	0.923	0.775	1.290
80/20 Mixtures										
Pressure Difference (kPa)	Feed Flow (ml/min)		Permeate (ml/min)		Permeate (mol/min)		Permeate Permeance ($\mu mol.m^{-2}.s^{-1}.Pa^{-1}$)		$\alpha_{(H2/CH4.)}$	$\alpha_{(H2/CH4.)}$
	H2	CH4	H2	CH4	H2	CH4	H2	CH4		
30	1250	1250	653.259	160.920	0.027	0.007	2.263	0.557	1.015	0.985
50	1250	1250	1022.170	266.825	0.042	0.011	2.124	0.555	0.958	1.044
80	1250	1250	1602.981	380.151	0.066	0.016	2.082	0.494	1.054	0.949
65/35 Mixtures										
Pressure Difference (kPa)	Feed Flow (ml/min)		Permeate (ml/min)		Permeate (mol/min)		Permeate Permeance ($\mu mol.m^{-2}.s^{-1}.Pa^{-1}$)		$\alpha_{(H2/CH4.)}$	$\alpha_{(H2/CH4.)}$
	H2	CH4	H2	CH4	H2	CH4	H2	CH4		
30	1250	1250	550.345	286.829	0.023	0.012	1.906	0.994	1.033	0.968
50	1250	1250	614.784	289.929	0.025	0.012	1.278	0.603	1.142	0.876
80	1250	1250	1171.049	706.466	0.048	0.029	1.521	0.918	0.893	1.120
35/65 Mixtures										
Pressure Difference (kPa)	Feed Flow (ml/min)		Permeate (ml/min)		Permeate (mol/min)		Permeate Permeance ($\mu mol.m^{-2}.s^{-1}.Pa^{-1}$)		$\alpha_{(H2/CH4.)}$	$\alpha_{(H2/CH4.)}$
	H2	CH4	H2	CH4	H2	CH4	H2	CH4		
30	1250	1250	233.362	471.261	0.010	0.019	0.808	1.632	0.920	1.087
50	1250	1250	394.193	739.712	0.016	0.030	0.819	1.537	0.990	1.010
80	1250	1250	600.709	1141.591	0.025	0.047	0.780	1.483	0.977	1.023

Table J.9: H_2/CO_2 Binary Permeance Processed Data (353 K)

50/50 Mixtures										
Pressure Difference (kPa)	Feed Flow (ml/min)		Permeate (ml/min)		Permeate (mol/min)		Permeate Permeance ($\mu mol.m^{-2}.s^{-1}.Pa^{-1}$)		$\alpha_{(H2/XO2)}$	$\alpha_{(H2/XO2)}$
	H2	CO2	H2	CO2	H2	CO2	H2	CO2		
30	1250	1250	280.240	230.106	0.011	0.009	0.971	0.797	1.218	0.821
50	1250	1250	361.786	339.048	0.015	0.014	0.752	0.705	1.067	0.937
80	1250	1250	650.695	569.026	0.027	0.023	0.845	0.739	1.144	0.874
20/80 Mixtures										
Pressure Difference (kPa)	Feed Flow (ml/min)		Permeate (ml/min)		Permeate (mol/min)		Permeate Permeance ($\mu mol.m^{-2}.s^{-1}.Pa^{-1}$)		$\alpha_{(H2/CO2)}$	$\alpha_{(H2/CO2)}$
	H2	CO2	H2	CO2	H2	CO2	H2	CO2		
30	1250	1250	81.787	303.470	0.003	0.012	0.283	1.051	1.078	0.928
50	1250	1250	102.333	433.976	0.004	0.018	0.213	0.902	0.943	1.060
80	1250	1250	194.458	673.872	0.008	0.028	0.253	0.875	1.154	0.866
80/20 Mixtures										
Pressure Difference (kPa)	Feed Flow (ml/min)		Permeate (ml/min)		Permeate (mol/min)		Permeate Permeance ($\mu mol.m^{-2}.s^{-1}.Pa^{-1}$)		$\alpha_{(H2/CO2)}$	$\alpha_{(H2/CO2)}$
	H2	CO2	H2	CO2	H2	CO2	H2	CO2		
30	1250	1250	527.097	139.091	0.022	0.006	1.826	0.482	0.947	1.056
50	1250	1250	965.712	207.257	0.040	0.008	2.007	0.431	1.165	0.858
80	1250	1250	1799.530	342.625	0.074	0.014	2.338	0.445	1.313	0.762
65/35 Mixtures										
Pressure Difference (kPa)	Feed Flow (ml/min)		Permeate (ml/min)		Permeate (mol/min)		Permeate Permeance ($\mu mol.m^{-2}.s^{-1}.Pa^{-1}$)		$\alpha_{(H2/CO2)}$	$\alpha_{(H2/CO2)}$
	H2	CO2	H2	CO2	H2	CO2	H2	CO2		
30	1250	1250	1462.218	631.845	0.060	0.026	5.065	2.189	1.246	0.802
50	1250	1250	468.297	217.059	0.019	0.009	0.973	0.451	1.162	0.861
80	1250	1250	1053.244	529.849	0.043	0.022	1.368	0.688	1.070	0.934

372 K

Table J.10: CH_4/CO_2 Binary Permeance Processed Data (372 K)

50/50 Mixtures										
Pressure Difference (kPa)	Feed Flow (ml/min)		Permeate (ml/min)		Permeate (mol/min)		Permeate Permeance ($\mu mol.m^{-2}.s^{-1}.Pa^{-1}$)		$\alpha_{(CH4/CO2)}$	$\alpha_{(CO2/CH4)}$
	CH4	CO2	CH4	CO2	CH4	CO2	CH4	CO2		
30	1250	1250	241.570	237.418	0.010	0.010	0.837	0.822	1.017	0.983
50	1250	1250	332.991	327.186	0.014	0.013	0.692	0.680	1.018	0.983
80	1250	1250	501.841	494.498	0.021	0.020	0.652	0.642	1.015	0.985
20/80 Mixtures										
Pressure Difference (kPa)	Feed Flow (ml/min)		Permeate (ml/min)		Permeate (mol/min)		Permeate Permeance ($\mu mol.m^{-2}.s^{-1}.Pa^{-1}$)		$\alpha_{(CH4/CO2)}$	$\alpha_{(CO2/CH4)}$
	CH4	CO2	CH4	CO2	CH4	CO2	CH4	CO2		
30	1250	1250	195.732	300.838	0.008	0.012	0.678	1.042	2.602	0.384
50	1250	1250	268.567	419.393	0.011	0.017	0.558	0.872	2.561	0.390
80	1250	1250	383.846	584.076	0.016	0.024	0.499	0.759	2.629	0.380
80/20 Mixtures										
Pressure Difference (kPa)	Feed Flow (ml/min)		Permeate (ml/min)		Permeate (mol/min)		Permeate Permeance ($\mu mol.m^{-2}.s^{-1}.Pa^{-1}$)		$\alpha_{(CH4/CO2)}$	$\alpha_{(CO2/CH4)}$
	CH4	CO2	CH4	CO2	CH4	CO2	CH4	CO2		
30	1250	1250	74.741	21.585	0.003	0.001	0.259	0.075	0.866	1.155
50	1250	1250	592.472	173.145	0.024	0.007	1.231	0.360	0.855	1.169
80	1250	1250	914.240	290.584	0.037	0.012	1.188	0.377	0.787	1.271

Table J.11: H_2/CH_4 Binary Permeance Processed Data (372 K)

50/50 Mixtures										
Pressure Difference (kPa)	Feed Flow (ml/min)		Permeate (ml/min)		Permeate (mol/min)		Permeate Permeance ($\mu mol.m^{-2}.s^{-1}.Pa^{-1}$)		$\alpha_{(H2/CH4)}$	$\alpha_{(H2/CH4)}$
	H2	CH4	H2	CH4	H2	CH4	H2	CH4		
30	1250	1250	231.365	345.612	0.009	0.014	0.801	1.197	0.669	1.494
50	1250	1250	358.711	520.551	0.015	0.021	0.746	1.082	0.689	1.451
80	1250	1250	449.259	613.827	0.018	0.025	0.584	0.797	0.732	1.366
20/80 Mixtures										
Pressure Difference (kPa)	Feed Flow (ml/min)		Permeate (ml/min)		Permeate (mol/min)		Permeate Permeance ($\mu mol.m^{-2}.s^{-1}.Pa^{-1}$)		$\alpha_{(H2/CH4.)}$	$\alpha_{(H2/CH4.)}$
	H2	CH4	H2	CH4	H2	CH4	H2	CH4		
30	1250	1250	97.798	439.584	0.004	0.018	0.339	1.523	0.890	1.124
50	1250	1250	148.421	639.567	0.006	0.026	0.308	1.329	0.928	1.077
80	1250	1250	265.500	1023.560	0.011	0.042	0.345	1.330	1.038	0.964
80/20 Mixtures										
Pressure Difference (kPa)	Feed Flow (ml/min)		Permeate (ml/min)		Permeate (mol/min)		Permeate Permeance ($\mu mol.m^{-2}.s^{-1}.Pa^{-1}$)		$\alpha_{(H2/CH4.)}$	$\alpha_{(H2/CH4.)}$
	H2	CH4	H2	CH4	H2	CH4	H2	CH4		
30	1250	1250	525.571	154.100	0.021	0.006	1.821	0.534	0.853	1.173
50	1250	1250	1115.295	252.780	0.046	0.010	2.318	0.525	1.103	0.907
80	1250	1250	1986.188	417.260	0.081	0.017	2.580	0.542	1.190	0.840

Table J.12: H_2/CO_2 Binary Permeance Processed Data (372 K)

50/50 Mixtures										
Pressure Difference (kPa)	Feed Flow (ml/min)		Permeate (ml/min)		Permeate (mol/min)		Permeate Permeance ($\mu mol.m^{-2}.s^{-1}.Pa^{-1}$)		$\alpha_{(H2/XO2)}$	$\alpha_{(H2/XO2)}$
	H2	CO2	H2	CO2	H2	CO2	H2	CO2		
30	1250	1250	319.275	209.951	0.013	0.009	1.106	0.727	1.521	0.658
50	1250	1250	479.756	246.891	0.020	0.010	0.997	0.513	1.943	0.515
80	1250	1250	638.629	466.127	0.026	0.019	0.830	0.605	1.370	0.730

20/80 Mixtures										
Pressure Difference (kPa)	Feed Flow (ml/min)		Permeate (ml/min)		Permeate (mol/min)		Permeate Permeance ($\mu mol.m^{-2}.s^{-1}.Pa^{-1}$)		$\alpha_{(H2/CO2)}$	$\alpha_{(H2/CO2)}$
	H2	CO2	H2	CO2	H2	CO2	H2	CO2		
30	1250	1250	71.124	285.789	0.003	0.012	0.246	0.990	0.995	1.005
50	1250	1250	115.780	443.592	0.005	0.018	0.241	0.922	1.044	0.958
80	1250	1250	185.688	694.533	0.008	0.028	0.241	0.902	1.069	0.935
80/20 Mixtures										
Pressure Difference (kPa)	Feed Flow (ml/min)		Permeate (ml/min)		Permeate (mol/min)		Permeate Permeance ($\mu mol.m^{-2}.s^{-1}.Pa^{-1}$)		$\alpha_{(H2/CO2)}$	$\alpha_{(H2/CO2)}$
	H2	CO2	H2	CO2	H2	CO2	H2	CO2		
30	1250	1250	653.528	133.714	0.027	0.005	2.264	0.463	1.222	0.818
50	1250	1250	1135.627	215.714	0.046	0.009	2.360	0.448	1.316	0.760
80	1250	1250	1642.498	320.228	0.067	0.013	2.134	0.416	1.282	0.780

Shell Side Data

298 K

Table J.13: CH_4/CO_2 Binary Permeance Shell Side Processed Data (298 K)

50/50 Mixtures										
Pressure Difference (kPa)	Feed Flow (ml/min)		Permeate (ml/min)		Permeate (mol/min)		Permeate Permeance ($\mu mol.m^{-2}.s^{-1}.Pa^{-1}$)		$\alpha_{(CH4/CO2)}$	$\alpha_{(CO2/CH4)}$
	CH4	CO2	CH4	CO2	CH4	CO2	CH4	CO2		
50	1250	1250	387.114	343.348	0.016	0.014	0.805	0.714	1.127	0.887
80	1250	1250	483.569	407.563	0.020	0.017	0.628	0.529	1.186	0.843
100	1250	1250	848.896	679.896	0.035	0.028	0.882	0.707	1.249	0.801

Table J.14: H_2/CH_4 Binary Permeance Shell Side Processed Data (298 K)

50/50 Mixtures										
Pressure Difference (kPa)	Feed Flow (ml/min)		Permeate (ml/min)		Permeate (mol/min)		Permeate Permeance ($\mu mol.m^{-2}.s^{-1}.Pa^{-1}$)		$\alpha_{(H2/CH4)}$	$\alpha_{(H2/CH4)}$
	H2	CH4	H2	CH4	H2	CH4	H2	CH4		
50	1250	1250	372.913	450.870	0.015	0.018	0.775	0.937	0.827	1.209
80	1250	1250	726.076	700.538	0.030	0.029	0.943	0.910	1.036	0.965
100	1250	1250	1195.497	1267.939	0.049	0.052	1.242	1.318	0.943	1.061

Table J.15: H_2/CO_2 Binary Permeance Shell Side Processed Data (298 K)

50/50 Mixtures										
Pressure Difference (kPa)	Feed Flow (ml/min)		Permeate (ml/min)		Permeate (mol/min)		Permeate Permeance ($\mu mol.m^{-2}.s^{-1}.Pa^{-1}$)		$\alpha_{(H2/XO2)}$	$\alpha_{(H2/XO2)}$
	H2	CO2	H2	CO2	H2	CO2	H2	CO2		
50	1250	1250	337.245	373.536	0.014	0.015	0.701	0.776	0.903	1.108
80	1250	1250	494.790	650.005	0.020	0.027	0.643	0.844	0.761	1.314
100	1250	1250	870.970	1043.439	0.036	0.043	0.905	1.084	0.835	1.198

353 K

Table J.16: CH_4/CO_2 Binary Permeance Shell Side Processed Data (353 K)

50/50 Mixtures										
Pressure Difference (kPa)	Feed Flow (ml/min)		Permeate (ml/min)		Permeate (mol/min)		Permeate Permeance ($\mu mol.m^{-2}.s^{-1}.Pa^{-1}$)		$\alpha_{(CH4/CO2)}$	$\alpha_{(CO2/CH4)}$
	CH4	CO2	CH4	CO2	CH4	CO2	CH4	CO2		
30	1250	1250	307.623	222.802	0.013	0.009	1.066	0.772	1.381	0.724
50	1250	1250	449.977	341.228	0.018	0.014	0.935	0.709	1.319	0.758
80	1250	1250	787.584	582.043	0.032	0.024	1.023	0.756	1.353	0.739

Table J.17: H_2/CH_4 Binary Permeance Shell Side Processed Data (353 K)

50/50 Mixtures										
Pressure Difference (kPa)	Feed Flow (ml/min)		Permeate (ml/min)		Permeate (mol/min)		Permeate Permeance ($\mu mol.m^{-2}.s^{-1}.Pa^{-1}$)		$\alpha_{(H2/CH4)}$	$\alpha_{(H2/CH4)}$
	H2	CH4	H2	CH4	H2	CH4	H2	CH4		
30	1250	1250	392.001	433.654	0.016	0.018	1.358	1.502	0.904	1.106
50	1250	1250	483.164	636.507	0.020	0.026	1.004	1.323	0.759	1.317
80	1250	1250	953.595	1197.326	0.039	0.049	1.239	1.555	0.796	1.256

Table J.18: H_2/CO_2 Binary Permeance Shell Side Processed Data (353 K)

50/50 Mixtures										
Pressure Difference (kPa)	Feed Flow (ml/min)		Permeate (ml/min)		Permeate (mol/min)		Permeate Permeance ($\mu mol.m^{-2}.s^{-1}.Pa^{-1}$)		$\alpha_{(H2/XO2)}$	$\alpha_{(H2/XO2)}$
	H2	CO2	H2	CO2	H2	CO2	H2	CO2		
30	1250	1250	261.779	335.426	0.011	0.014	0.907	1.162	0.780	1.281
50	1250	1250	496.092	490.004	0.020	0.020	1.031	1.018	1.012	0.988
80	1250	1250	795.162	814.684	0.033	0.033	1.033	1.058	0.976	1.025

Appendix K

Amorphous Silica
Binary Permeance
Statistical Data

HEIGHT STATISTICS

Table K.1: Height Statistics of the Feed Gas (CH_4 and CO_2) at 298 K

		Height			
50/50: CH4/CO2		$\overline{h}$	σ	c.i.	%ε
Feed	CH4	2510.333	56.192	63.587	5.066
	CO2	2147.667	35.226	39.862	3.712
		Height			
20/80:CH4/CO2		$\overline{h}$	σ	c.i.	%ε
Feed	CH4	1516.667	14.974	16.945	2.234
	CO2	2901.000	15.937	18.035	1.243
		Height			
80/20:CH4/CO2		$\overline{h}$	σ	c.i.	%ε
Feed	CH4	3579.333	160.284	181.378	10.135
	CO2	1223.667	1.700	1.923	0.314
		Height			
65/35:CH4/CO2		$\overline{h}$	σ	c.i.	%ε
Feed	CH4	5377.000	76.581	86.660	3.223
	CO2	3603.333	102.477	115.964	6.436
		Height			
35/65:CH4/CO2		$\overline{h}$	σ	c.i.	%ε
Feed	CH4	4410.000	93.091	105.343	4.777
	CO2	4359.000	97.334	110.144	5.054

Table K.2: Height Statistics of the Permeate Gas (CH_4 and CO_2) at 298 K

		Height				Height			
50/50: CH4/CO2		CH4				CO2			
ΔP		$\overline{h}$	σ	c.i.	%ε	$\overline{h}$	σ	c.i.	%ε
Permeate	50	2535.000	46.007	52.062	4.107	2231.667	22.485	25.444	2.280
	80	2784.000	24.055	27.221	1.956	2730.667	61.759	69.887	5.119
	100	3000.000	100.000	138.593	9.240	2725.000	25.000	34.648	2.543
		Height				Height			
20/80:CH4/CO2		CH4				CO2			
ΔP		$\overline{h}$	σ	c.i.	%ε	$\overline{h}$	σ	c.i.	%ε
Permeate	50	1576.333	1.247	1.411	0.179	2914.667	19.602	22.181	1.522
	80	1563.333	8.260	9.347	1.196	2920.333	11.614	13.143	0.900
	100	1484.000	42.000	58.209	7.845	2782.000	76.000	105.331	7.572

		Height				Height			
80/20:CH4/CO2		CH4				CO2			
ΔP		$\overline{h}$	σ	c.i.	%ε	$\overline{h}$	σ	c.i.	%ε
Permeate	50	3605.333	90.408	102.306	5.675	1123.000	17.049	19.293	3.436
	80	3664.000	15.748	17.821	0.973	1130.333	27.146	30.718	5.435
	100	3535.500	16.500	22.868	1.294	1065.000	52.000	72.068	13.534
		Height				Height			
65/35:CH4/CO2		CH4				CO2			
ΔP		$\overline{h}$	σ	c.i.	%ε	$\overline{h}$	σ	c.i.	%ε
Permeate	50	5830.667	28.964	32.775	1.124	3619.000	54.888	62.111	3.433
	80	5855.500	15.000	20.789	0.710	3527.000	16.500	22.868	1.297
	100	5816.000	2.500	3.465	0.119	3542.500	2.500	3.465	0.196
		Height				Height			
35/65:CH4/CO2		CH4				CO2			
ΔP		$\overline{h}$	σ	c.i.	%ε	$\overline{h}$	σ	c.i.	%ε
Permeate	50	4014.333	21.669	24.521	1.222	4986.667	40.574	45.913	1.841
	80	3891.500	11.000	15.245	0.784	4962.000	11.000	15.245	0.614
	100	3922.000	54.500	75.533	3.852	4968.500	54.500	75.533	3.040

Table K.3: Height Statistics of the Feed Gas (CH_4 and H_2) at 298 K

		Height			
50/50: H2/CH4		$\overline{h}$	σ	c.i.	%ε
Feed	H2	322.333	4.784	5.414	3.359
	CH4	6406.333	105.743	119.659	3.736
		Height			
20/80:H2/CH4		$\overline{h}$	σ	c.i.	%ε
Feed	H2	95.333	0.471	0.533	1.119
	CH4	3564.000	45.760	51.783	2.906
		Height			
80/20:H2/CH4		$\overline{h}$	σ	c.i.	%ε
Feed	H2	274.000	9.201	10.412	7.600
	CH4	1298.667	34.989	39.594	6.098
		Height			
65/35:H2/CH4		$\overline{h}$	σ	c.i.	%ε
Feed	H2	392.000	4.320	4.889	2.494
	CH4	3845.667	21.700	24.556	1.277
		Height			
35/65:H2/CH4		$\overline{h}$	σ	c.i.	%ε
Feed	H2	482.000	2.828	3.201	1.328
	CH4	5444.667	81.671	92.420	3.395

Table K.4: Height Statistics of the Permeate Gas (CH_4 and H_2) at 298 K

		Height				Height			
50/50: H2/CH4		**H2**				**CH4**			
ΔP		$\bar{h}$	**σ**	**c.i.**	**%ε**	$\bar{h}$	**σ**	**c.i.**	**%ε**
Permeate	50	162.333	7.587	8.585	**10.577**	2535.333	58.340	66.018	**5.208**
	80	194.667	3.300	3.734	**3.836**	2551.667	48.733	55.146	**4.322**
	100	253.500	1.500	2.079	**1.640**	3209.000	18.000	24.947	**1.555**
		Height				**Height**			
20/80:H2/CH4		**H2**				**CH4**			
ΔP		$\bar{h}$	**σ**	**c.i.**	**%ε**	$\bar{h}$	**σ**	**c.i.**	**%ε**
Permeate	50	140.667	8.731	9.880	**14.047**	3819.667	246.136	278.529	**14.584**
	80	120.667	6.549	7.411	**12.283**	3691.333	16.760	18.965	**1.028**
	100	118.500	0.500	0.693	**1.170**	3534.000	7.000	9.702	**0.549**
		Height				**Height**			
80/20:H2/CH4		**H2**				**CH4**			
ΔP		$\bar{h}$	**σ**	**c.i.**	**%ε**	$\bar{h}$	**σ**	**c.i.**	**%ε**
Permeate	50	257.000	2.449	2.772	**2.157**	1480.667	54.064	61.179	**8.264**
	80	259.333	6.650	7.525	**5.803**	1588.667	49.815	56.371	**7.097**
	100	310.000	4.000	5.544	**3.577**	2271.000	0.000	0.000	**0.000**
		Height				**Height**			
65/35:H2/CH4		**H2**				**CH4**			
ΔP		$\bar{h}$	**σ**	**c.i.**	**%ε**	$\bar{h}$	**σ**	**c.i.**	**%ε**
Permeate	50	519.000	6.976	7.894	**3.042**	4969.667	171.154	193.679	**7.794**
	80	519.000	1.000	1.386	**0.534**	3924.000	84.000	116.418	**5.934**
	100	372.500	12.500	17.324	**9.302**	3967.000	2.000	2.772	**0.140**
		Height				**Height**			
35/65:H2/CH4		**H2**				**CH4**			
ΔP		$\bar{h}$	**σ**	**c.i.**	**%ε**	$\bar{h}$	**σ**	**c.i.**	**%ε**
Permeate	50	371.667	20.950	23.707	**12.757**	5674.000	44.520	50.379	**1.776**
	80	489.500	9.500	13.166	**5.380**	5829.500	4.500	6.237	**0.214**
	100	470.500	18.500	25.640	**10.899**	5718.500	13.500	18.710	**0.654**

Table K.5: Height Statistics of the Feed Gas (CO_2 and H_2) at 298 K

		Height			
50/50: H2/CO2		$\bar{h}$	**σ**	**c.i.**	**%ε**
Feed	**H2**	255.333	6.848	7.749	**6.069**
	CO2	2404.000	47.081	53.278	**4.432**
		Height			
20/80:H2/CO2		$\bar{h}$	**σ**	**c.i.**	**%ε**
Feed	**H2**	104.667	2.494	2.823	**5.394**
	CO2	2845.000	77.567	87.776	**6.171**

		Height			
80/20:H2/CO2		$\overline{h}$	σ	c.i.	%ε
Feed	H2	338.667	8.260	9.347	5.520
	CO2	1072.333	52.105	58.962	10.997
		Height			
65/35:H2/CO2		$\overline{h}$	σ	c.i.	%ε
Feed	H2	344.000	16.083	18.200	10.581
	CO2	3538.333	61.668	69.783	3.944
		Height			
35/65:H2/CO2		$\overline{h}$	σ	c.i.	%ε
Feed	H2	496.667	12.472	14.114	5.683
	CO2	4976.667	118.812	134.448	5.403

Table K.6: Height Statistics of the Permeate Gas ($H_2$and CO_2) at 298 K

		Height				Height			
50/50: H2/CO2		H2				CO2			
ΔP		$\overline{h}$	σ	c.i.	%ε	$\overline{h}$	σ	c.i.	%ε
Permeate	50	311.333	8.380	9.483	6.092	2232.333	13.912	15.743	1.410
	80	302.500	2.500	3.465	2.291	2050.000	50.000	69.296	6.761
	100	308.333	6.236	7.057	4.577	2175.000	57.879	80.216	7.376
		Height				Height			
20/80:H2/CO2		H2				CO2			
ΔP		$\overline{h}$	σ	c.i.	%ε	$\overline{h}$	σ	c.i.	%ε
Permeate	50	113.000	6.683	7.563	13.386	2736.667	22.867	25.876	1.891
	80	149.000	1.000	1.386	1.860	2796.000	13.000	18.017	1.289
	100	137.000	6.683	9.263	13.522	2762.000	26.192	36.300	2.629
		Height				Height			
80/20:H2/CO2		H2				CO2			
ΔP		$\overline{h}$	σ	c.i.	%ε	$\overline{h}$	σ	c.i.	%ε
Permeate	50	381.333	10.656	12.059	6.324	1397.333	80.392	90.972	13.021
	80	254.000	1.000	1.386	1.091	1382.333	7.318	10.142	1.467
	100	209.000	1.000	1.386	1.326	1432.500	5.500	7.623	1.064
		Height				Height			
65/35:H2/CO2		H2				CO2			
ΔP		$\overline{h}$	σ	c.i.	%ε	$\overline{h}$	σ	c.i.	%ε
Permeate	50	256.000	3.559	4.027	3.146	3437.000	52.618	59.543	3.465
	80	487.500	7.500	10.394	4.264	3519.000	22.000	30.490	1.733
	100	492.500	6.500	9.009	3.658	3617.500	135.500	187.793	10.382

35/65:H2/CO2		Height H2				Height CO2			
ΔP		$\overline{h}$	σ	c.i.	%ε	$\overline{h}$	σ	c.i.	%ε
Permeate	50	602.000	2.160	2.994	0.995	5136.667	156.176	176.730	6.881
	80	382.500	5.000	6.930	3.623	5031.000	24.000	33.262	1.322
	100	482.500	2.500	3.465	1.436	5102.500	7.500	10.394	0.407

PERMEANCE STATISTICS

Table K.7: Permeance Statistics (CH_4 and CO_2) at 298 K

50/50: CH4/CO2		Permeance (μmol.m^{-2}.s^{-1}.Pa^{-1}) CH4				Permeance (μmol.m^{-2}.s^{-1}.Pa^{-1}) CO2			
ΔP		$\overline{x}$	σ	c.i.	%ε	$\overline{x}$	σ	c.i.	%ε
Permeate	50	0.747	0.009	0.011	2.827	0.769	0.005	0.006	1.459
	80	0.525	0.003	0.004	1.365	0.602	0.016	0.018	5.845
	100	0.513	0.033	0.045	17.621	0.544	0.021	0.030	10.940
20/80:CH4/CO2		Permeance (μmol.m^{-2}.s^{-1}.Pa^{-1}) CH4				Permeance (μmol.m^{-2}.s^{-1}.Pa^{-1}) CO2			
ΔP		$\overline{x}$	σ	c.i.	%ε	$\overline{x}$	σ	c.i.	%ε
Permea	50	0.286	0.000	0.000	0.179	1.108	0.007	0.008	1.522
	80	0.365	0.001	0.001	0.503	1.426	0.010	0.011	1.561
	100	0.458	0.013	0.018	7.845	1.796	0.049	0.068	7.572
80/20:CH4/CO2		Permeance (μmol.m^{-2}.s^{-1}.Pa^{-1}) CH4				Permeance (μmol.m^{-2}.s^{-1}.Pa^{-1}) CO2			
ΔP		$\overline{x}$	σ	c.i.	%ε	$\overline{x}$	σ	c.i.	%ε
Permea	50	1.484	0.037	0.042	5.675	0.337	0.005	0.006	3.436
	80	1.820	0.008	0.009	0.973	0.410	0.010	0.011	5.435
	100	1.898	0.009	0.012	1.294	0.417	0.020	0.028	13.534
65/35:CH4/CO2		Permeance (μmol.m^{-2}.s^{-1}.Pa^{-1}) CH4				Permeance (μmol.m^{-2}.s^{-1}.Pa^{-1}) CO2			
ΔP		$\overline{x}$	σ	c.i.	%ε	$\overline{x}$	σ	c.i.	%ε
Permea	50	1.260	0.006	0.007	1.124	0.629	0.010	0.011	3.433
	80	1.218	0.006	0.008	1.349	0.590	0.003	0.003	1.179
	100	1.207	0.007	0.009	1.573	0.591	0.000	0.001	0.196
35/65:CH4/CO2		Permeance (μmol.m^{-2}.s^{-1}.Pa^{-1}) CH4				Permeance (μmol.m^{-2}.s^{-1}.Pa^{-1}) CO2			
ΔP		$\overline{x}$	σ	c.i.	%ε	$\overline{x}$	σ	c.i.	%ε
Permea	50	0.515	0.003	0.003	1.222	1.202	0.010	0.011	1.841
	80	0.491	0.004	0.006	2.457	1.177	0.003	0.004	0.614
	100	0.564	0.002	0.002	0.848	1.344	0.015	0.020	3.040

Table K.8: Permeance Statistics ($H_2$and CH_4) at 298 K

		Permeance (μmol.m^{-2}.s^{-1}.Pa^{-1})				Permeance (μmol.m^{-2}.s^{-1}.Pa^{-1})			
50/50: H2/CH4		H2				CH4			
ΔP		$\bar{x}$	σ	c.i.	%ε	$\bar{x}$	σ	c.i.	%ε
Permea	50	0.566	0.026	0.030	10.577	0.444	0.010	0.012	5.208
	80	0.902	0.015	0.017	3.836	0.595	0.011	0.013	4.322
	100	0.862	0.005	0.007	1.640	0.549	0.003	0.004	1.555
		Permeance (μmol.m^{-2}.s^{-1}.Pa^{-1})				Permeance (μmol.m^{-2}.s^{-1}.Pa^{-1})			
20/80:H2/CH4		H2				CH4			
ΔP		$\bar{x}$	σ	c.i.	%ε	$\bar{x}$	σ	c.i.	%ε
Permea	50	0.581	0.036	0.041	14.047	1.687	0.109	0.123	14.584
	80	0.210	0.011	0.013	12.283	0.688	0.003	0.004	1.028
	100	0.432	0.002	0.003	1.170	1.379	0.003	0.004	0.549
		Permeance (μmol.m^{-2}.s^{-1}.Pa^{-1})				Permeance (μmol.m^{-2}.s^{-1}.Pa^{-1})			
80/20:H2/CH4		H2				CH4			
ΔP		$\bar{x}$	σ	c.i.	%ε	$\bar{x}$	σ	c.i.	%ε
Permea	50	1.504	0.014	0.016	2.157	0.457	0.017	0.019	8.264
	80	0.583	0.015	0.017	5.803	0.188	0.006	0.007	7.097
	100	1.486	0.019	0.027	3.577	0.574	0.000	0.000	0.000
		Permeance (μmol.m^{-2}.s^{-1}.Pa^{-1})				Permeance (μmol.m^{-2}.s^{-1}.Pa^{-1})			
65/35:H2/CH4		H2				CH4			
ΔP		$\bar{x}$	σ	c.i.	%ε	$\bar{x}$	σ	c.i.	%ε
Permea	50	2.681	0.036	0.041	3.042	1.409	0.049	0.055	7.794
	80	2.615	0.005	0.007	0.534	1.085	0.023	0.032	5.934
	100	1.519	0.051	0.071	9.302	0.888	0.000	0.001	0.140
		Permeance (μmol.m^{-2}.s^{-1}.Pa^{-1})				Permeance (μmol.m^{-2}.s^{-1}.Pa^{-1})			
35/65:H2/CH4		H2				CH4			
ΔP		$\bar{x}$	σ	c.i.	%ε	$\bar{x}$	σ	c.i.	%ε
Permea	50	0.668	0.038	0.043	12.757	1.677	0.013	0.015	1.776
	80	0.863	0.017	0.023	5.380	1.690	0.001	0.002	0.214
	100	0.855	0.034	0.047	10.899	1.710	0.004	0.006	0.654

Table K.9: Permeance Statistics ($H_2$and CO_2) at 298 K

		Permeance (μmol.m^{-2}.s^{-1}.Pa^{-1})				Permeance (μmol.m^{-2}.s^{-1}.Pa^{-1})			
50/50: H2/CO2		H2				CO2			
ΔP		$\bar{x}$	σ	c.i.	%ε	$\bar{x}$	σ	c.i.	%ε
Permea	50	1.080	0.029	0.033	6.092	0.822	0.005	0.006	1.410
	80	0.808	0.021	0.009	2.145	0.605	0.014	0.019	6.185
	100	0.817	0.053	0.060	14.674	0.588	0.048	0.054	18.305
		Permeance (μmol.m^{-2}.s^{-1}.Pa^{-1})				Permeance (μmol.m^{-2}.s^{-1}.Pa^{-1})			
20/80:H2/CO2		H2				CO2			
ΔP		$\bar{x}$	σ	c.i.	%ε	$\bar{x}$	σ	c.i.	%ε
Permea	50	0.302	0.018	0.020	13.386	1.076	0.009	0.010	1.891
	80	0.298	0.035	0.039	26.458	0.886	0.113	0.128	28.806
	100	0.474	0.003	0.004	1.860	1.310	0.006	0.008	1.289

		Permeance (μmol.m^{-2}.s^{-1}.Pa^{-1})				Permeance (μmol.m^{-2}.s^{-1}.Pa^{-1})			
80/20:H2/CO2		H2				CO2			
ΔP		$\bar{x}$	σ	c.i.	%ε	$\bar{x}$	σ	c.i.	%ε
Permea	50	2.142	0.060	0.068	6.324	0.621	0.036	0.040	13.021
	80	1.418	0.006	0.008	1.091	0.613	0.000	0.000	0.100
	100	1.197	0.025	0.028	4.747	0.649	0.013	0.015	4.627
		Permeance (μmol.m^{-2}.s^{-1}.Pa^{-1})				Permeance (μmol.m^{-2}.s^{-1}.Pa^{-1})			
65/35:H2/CO2		H2				CO2			
ΔP		$\bar{x}$	σ	c.i.	%ε	$\bar{x}$	σ	c.i.	%ε
Permea	50	1.110	0.015	0.017	3.146	0.778	0.012	0.013	3.465
	80	2.033	0.031	0.043	4.264	0.767	0.005	0.007	1.733
	100	2.097	0.028	0.038	3.658	0.805	0.030	0.042	10.382
		Permeance (μmol.m^{-2}.s^{-1}.Pa^{-1})				Permeance (μmol.m^{-2}.s^{-1}.Pa^{-1})			
35/65:H2/CO2		H2				CO2			
ΔP		$\bar{x}$	σ	c.i.	%ε	$\bar{x}$	σ	c.i.	%ε
Permeate	50	0.724	0.003	0.003	0.812	1.145	0.035	0.039	6.881
	80	0.429	0.109	0.152	70.655	1.047	0.005	0.007	1.322
	100	0.633	0.003	0.005	1.436	1.241	0.002	0.003	0.407

SELECTVITY STATISTICS

Table K.10: Selectivity Statistics ($CH_4$and CO_2) at 298 K

		Selectivity			
50/50: CH4/CO2		CH4/CO2			
ΔP		$\bar{x}$	σ	c.i.	%ε
Permeate	50	0.972	0.014	0.016	3.233
	80	0.873	0.026	0.029	6.749
	100	0.942	0.023	0.032	6.699
		Selectivity			
20/80:CH4/CO2		CH4/CO2			
ΔP		$\bar{x}$	σ	c.i.	%ε
Permeate	50	0.259	0.002	0.002	1.697
	80	0.256	0.001	0.001	1.124
	100	0.255	0.000	0.000	0.273
		Selectivity			
80/20:CH4/CO2		CH4/CO2			
ΔP		$\bar{x}$	σ	c.i.	%ε
Permeate	50	4.399	0.085	0.096	4.358
	80	4.444	0.103	0.117	5.255
	100	4.560	0.244	0.338	14.824

		Selectivity			
65/35:CH4/CO2		CH4/CO2			
ΔP		$\bar{x}$	σ	c.i.	%ε
Permeate	50	2.004	0.023	0.026	2.579
	80	2.065	0.019	0.026	2.528
	100	2.042	0.010	0.014	1.377
		Selectivity			
35/65:CH4/CO2		CH4/CO2			
ΔP		$\bar{x}$	σ	c.i.	%ε
Permeate	50	0.428	0.006	0.006	2.980
	80	0.417	0.003	0.004	1.843
	100	0.420	0.006	0.008	3.888

Table K.11: Selectivity Statistics ($H_2$and CH_4) at 298 K

		Selectivity			
50/50: H2/CH4		H2/CH4			
ΔP		$\bar{x}$	σ	c.i.	%ε
Permeate	50	1.272	0.050	0.057	8.949
	80	1.517	0.035	0.040	5.239
	100	1.570	0.000	0.001	0.085
		Selectivity			
20/80:H2/CH4		H2/CH4			
ΔP		$\bar{x}$	σ	c.i.	%ε
Permeate	50	0.344	0.005	0.005	3.046
	80	0.305	0.016	0.019	12.128
	100	0.313	0.001	0.001	0.621
		Selectivity			
80/20:H2/CH4		H2/CH4			
ΔP		$\bar{x}$	σ	c.i.	%ε
Permeate	50	3.297	0.141	0.160	9.708
	80	3.102	0.173	0.196	12.611
	100	2.589	0.033	0.046	3.577
		Selectivity			
65/35:H2/CH4		H2/CH4			
ΔP		$\bar{x}$	σ	c.i.	%ε
Permeate	50	1.905	0.053	0.060	6.302
	80	2.411	0.056	0.078	6.467
	100	1.711	0.058	0.081	9.441

		Selectivity			
35/65:H2/CO2		H2/CO2			
ΔP		$\bar{x}$	σ	c.i.	%ε
Permeate	50	0.633	0.021	0.023	7.345
	80	0.410	0.103	0.142	69.417
	100	0.510	0.002	0.003	1.029

Table K.12: Selectivity Statistics ($H_2$and CO_2) at 298 K

		Selectivity			
50/50: H2/CO2		H2/CO2			
ΔP		$\bar{x}$	σ	c.i.	%ε
Permeate	50	1.314	0.043	0.049	7.472
	80	1.336	0.045	0.051	7.700
	100	1.390	0.022	0.031	4.471
		Selectivity			
20/80:H2/CO2		H2/CO2			
ΔP		$\bar{x}$	σ	c.i.	%ε
Permeate	50	0.281	0.019	0.021	15.124
	80	0.337	0.015	0.017	10.193
	100	0.362	0.004	0.006	3.149
		Selectivity			
80/20:H2/CO2		H2/CO2			
ΔP		$\bar{x}$	σ	c.i.	%ε
Permeat	50	3.465	0.265	0.299	17.279
	80	2.315	0.010	0.014	1.191
	100	1.844	0.130	0.147	15.924
		Selectivity			
65/35:H2/CO2		H2/CO2			
ΔP		$\bar{x}$	σ	c.i.	%ε
Permea	50	1.110	0.033	0.037	6.674
	80	2.033	0.024	0.034	3.302
	100	2.097	0.132	0.183	17.474
		Selectivity			
35/65:H2/CO2		H2/CO2			
ΔP		$\bar{x}$	σ	c.i.	%ε
Permeate	50	0.633	0.021	0.023	7.345
	80	0.410	0.103	0.142	69.417
	100	0.510	0.002	0.003	1.029

HEIGHT STATISTICS

Table K.13: Height Statistics of the feed gas ($CH_4$and CO_2) at 328 K

		Height			
50/50: CH4/CO2		$\overline{h}$	σ	c.i.	%ε
Feed	CH4	2610.000	65.120	73.691	5.647
	CO2	2148.333	16.780	18.988	1.768
		Height			
20/80:CH4/CO2		$\overline{h}$	σ	c.i.	%ε
Feed	CH4	1196.333	74.029	83.771	14.005
	CO2	3002.667	3.859	4.366	0.291
		Height			
80/20:CH4/CO2		$\overline{h}$	σ	c.i.	%ε
Feed	CH4	3566.000	114.668	129.759	7.278
	CO2	973.667	30.214	34.190	7.023

Table K.14: Height Statistics of the feed gas ($H_2$and CH_4) at 328 K

		Height			
50/50: H2/CH4		$\overline{h}$	σ	c.i.	%ε
Feed	H2	212.667	7.134	8.072	7.592
	CH4	2569.667	79.037	89.439	6.961
		Height			
20/80:H2/CH4		$\overline{h}$	σ	c.i.	%ε
Feed	H2	430.667	3.300	3.734	1.734
	CH4	3404.000	58.856	66.602	3.913
		Height			
80/20:H2/CH4		$\overline{h}$	σ	c.i.	%ε
Feed	H2	237.333	15.628	17.684	14.903
	CH4	1505.000	20.461	23.154	3.077

Table K.15: Height Statistics of the feed gas ($H_2$and CO_2) at 328 K

		Height			
50/50: H2/CO2		$\overline{h}$	σ	c.i.	%ε
Feed	H2	255.333	14.384	16.277	12.749
	CO2	2350.000	40.307	45.612	3.882
		Height			
20/80:H2/CO2		$\overline{h}$	σ	c.i.	%ε
Feed	H2	272.000	12.356	13.982	10.281
	CO2	3257.667	121.024	136.952	8.408

		Height			
80/20:H2/CO2		$\bar{h}$	σ	c.i.	%ε
Feed	H2	246.000	14.166	16.030	13.033
	CO2	1454.667	53.878	60.969	8.383

Table K.16: Height Statistics of the permeate gas ($CH_4$and CO_2) at 328 K

		Height				Height			
50/50: CH4/CO2		CH4				CO2			
ΔP		$\bar{h}$	σ	c.i.	%ε	$\bar{h}$	σ	c.i.	%ε
Permeate	30	2643.000	34.419	38.949	2.947	2119.333	7.040	7.966	0.752
	50	2717.667	41.772	47.269	3.479	2182.000	43.336	49.039	4.495
	80	2595.000	0.000	0.000	0.000	2108.500	1.500	2.079	0.197
		Height				Height			
20/80:CH4/CO2		CH4				CO2			
ΔP		$\bar{h}$	σ	c.i.	%ε	$\bar{h}$	σ	c.i.	%ε
Permeate	30	1551.667	26.550	30.044	3.872	2857.000	5.354	6.059	0.424
	50	1571.667	31.095	35.187	4.478	2898.667	33.510	37.920	2.616
	80	1590.000	20.000	27.719	3.487	2897.000	2.000	2.772	0.191
		Height				Height			
80/20:CH4/CO2		CH4				CO2			
ΔP		$\bar{h}$	σ	c.i.	%ε	$\bar{h}$	σ	c.i.	%ε
Permeate	30	3621.333	5.558	6.289	0.347	1007.333	26.887	30.425	6.041
	50	3590.667	32.190	36.427	2.029	980.667	17.518	19.824	4.043
	80	3560.000	2.000	2.772	0.156	986.000	11.000	15.245	3.092

Table K.17: Height Statistics of the permeate gas ($CH_4$and H_2) at 328 K

		Height				Height			
50/50: H2/CH4		H2				CH4			
ΔP		$\bar{h}$	σ	c.i.	%ε	$\bar{h}$	σ	c.i.	%ε
Permeat	30	169.000	6.976	7.894	9.342	2595.667	12.344	13.968	1.076
	50	182.333	8.994	10.177	11.164	2639.333	17.649	19.972	1.513
	80	209.000	2.000	2.772	2.652	2679.000	8.299	11.502	0.859
		Height				Height			
20/80:H2/CH4		H2				CH4			
ΔP		$\bar{h}$	σ	c.i.	%ε	$\bar{h}$	σ	c.i.	%ε
Permea	30	225.000	10.801	12.223	10.865	3758.667	64.830	73.362	3.904
	50	227.667	4.028	4.558	4.004	3645.667	209.559	237.138	13.009
	80	228.000	14.000	19.403	17.020	3676.500	103.500	143.444	7.803
		Height				Height			
80/20:H2/CH4		H2				CH4			
ΔP		$\bar{h}$	σ	c.i.	%ε	$\bar{h}$	σ	c.i.	%ε
Permeat	30	241.667	6.236	7.057	5.840	1455.333	37.044	41.919	5.761
	50	232.000	2.449	2.772	2.390	1508.667	31.383	35.513	4.708
	80	239.000	1.000	1.386	1.160	1467.000	29.000	40.192	5.479

Table K.18: Height Statistics of the permeate gas ($CO_2$and H_2) at 328 K

		Height				Height			
50/50: H2/CO2		H2				CO2			
ΔP		$\bar{h}$	σ	c.i.	%ε	$\bar{h}$	σ	c.i.	%ε
Permeate	30	266.333	12.392	14.023	10.530	2274.667	88.864	100.560	8.842
	50	286.000	15.937	18.035	12.612	2444.000	79.049	89.452	7.320
	80	254.000	4.320	4.889	3.850	2379.667	43.484	49.207	4.136
		Height				Height			
20/80:H2/CO2		H2				CO2			
ΔP		$\bar{h}$	σ	c.i.	%ε	$\bar{h}$	σ	c.i.	%ε
Permeate	30	185.667	4.190	4.741	5.107	3203.000	47.525	53.780	3.358
	50	137.333	7.134	8.072	11.756	3133.333	83.508	94.498	6.032
	80	114.000	1.000	1.386	2.431	3200.000	51.000	70.682	4.418
		Height				Height			
80/20:H2/CO2		H2				CO2			
ΔP		$\bar{h}$	σ	c.i.	%ε	$\bar{h}$	σ	c.i.	%ε
Permeate	30	247.000	12.570	14.224	11.517	1271.000	40.472	45.799	7.207
	50	257.667	15.283	17.294	13.423	1333.333	41.556	47.025	7.054
	80	239.333	4.190	5.807	4.853	1339.333	29.330	40.649	6.070

PERMEANCE STATISTICS

Table K.19: Permeance Statistics ($CH_4$and CO_2) at 328 K

		Permeance ($\mu mol.m^{-2}.s^{-1}.Pa^{-1}$)				Permeance ($\mu mol.m^{-2}.s^{-1}.Pa^{-1}$)			
50/50: CH4/CO2		CH4				CO2			
ΔP		$\bar{x}$	σ	c.i.	%ε	$\bar{x}$	σ	c.i.	%ε
Permeate	50	0.847	0.011	0.012	2.947	0.825	0.003	0.003	0.752
	80	0.754	0.012	0.013	3.479	0.735	0.015	0.017	4.495
	100	0.835	0.000	0.000	0.000	0.824	0.001	0.001	0.197
		Permeance ($\mu mol.m^{-2}.s^{-1}.Pa^{-1}$)				Permeance ($\mu mol.m^{-2}.s^{-1}.Pa^{-1}$)			
20/80:CH4/CO2		CH4				CO2			
ΔP		$\bar{x}$	σ	c.i.	%ε	$\bar{x}$	σ	c.i.	%ε
Permeate	50	0.386	0.007	0.007	3.872	1.128	0.002	0.002	0.424
	80	0.334	0.007	0.007	4.478	0.978	0.011	0.013	2.616
	100	0.368	2.428	3.365	1829.775	1.064	0.001	0.001	0.191
		Permeance ($\mu mol.m^{-2}.s^{-1}.Pa^{-1}$)				Permeance ($\mu mol.m^{-2}.s^{-1}.Pa^{-1}$)			
80/20:CH4/CO2		CH4				CO2			
ΔP		$\bar{x}$	σ	c.i.	%ε	$\bar{x}$	σ	c.i.	%ε
Permeate	50	1.411	0.002	0.002	0.347	0.359	0.010	0.011	6.041
	80	1.321	0.012	0.013	2.029	0.330	0.006	0.007	4.043
	100	1.411	0.001	0.001	0.156	0.358	0.004	0.006	3.092

Table K.20: Permeance Statistics ($H_2$and CH_4) at 328 K

		Permeance (μmol.m^{-2}.s^{-1}.Pa^{-1})				Permeance (μmol.m^{-2}.s^{-1}.Pa^{-1})			
50/50: H2/CH4		H2				CH4			
ΔP		$\bar{x}$	σ	c.i.	%ε	$\bar{x}$	σ	c.i.	%ε
Permea	50	1.036	0.043	0.048	9.342	1.317	0.029	0.033	5.009
	80	0.744	0.037	0.042	11.164	0.891	0.010	0.011	2.447
	100	1.127	0.011	0.015	2.652	1.195	0.029	0.041	6.829
		Permeance (μmol.m^{-2}.s^{-1}.Pa^{-1})				Permeance (μmol.m^{-2}.s^{-1}.Pa^{-1})			
20/80:H2/CH4		H2				CH4			
ΔP		$\bar{x}$	σ	c.i.	%ε	$\bar{x}$	σ	c.i.	%ε
Permea	50	0.207	0.010	0.011	10.865	1.753	0.030	0.034	3.904
	80	0.190	0.003	0.004	4.004	1.543	0.089	0.100	13.009
	100	0.189	0.012	0.016	17.020	1.544	0.043	0.060	7.803
		Permeance (μmol.m^{-2}.s^{-1}.Pa^{-1})				Permeance (μmol.m^{-2}.s^{-1}.Pa^{-1})			
80/20:H2/CH4		H2				CH4			
ΔP		$\bar{x}$	σ	c.i.	%ε	$\bar{x}$	σ	c.i.	%ε
Permea	50	2.427	0.063	0.071	5.840	0.574	0.015	0.017	5.761
	80	2.401	0.025	0.029	2.390	0.613	0.013	0.014	4.708
	100	2.288	0.010	0.013	1.160	0.551	0.011	0.015	5.479

Table K.21: Permeance Statistics ($H_2$and CO_2) at 328 K

		Permeance (μmol.m^{-2}.s^{-1}.Pa^{-1})				Permeance (μmol.m^{-2}.s^{-1}.Pa^{-1})			
50/50: H2/CO2		H2				CO2			
ΔP		$\bar{x}$	σ	c.i.	%ε	$\bar{x}$	σ	c.i.	%ε
Permea	50	0.938	0.044	0.049	10.530	0.868	0.034	0.038	8.842
	80	0.903	0.050	0.057	12.612	0.836	0.027	0.031	7.320
	100	0.756	0.013	0.018	4.715	0.767	0.014	0.019	5.065
		Permeance (μmol.m^{-2}.s^{-1}.Pa^{-1})				Permeance (μmol.m^{-2}.s^{-1}.Pa^{-1})			
20/80:H2/CO2		H2				CO2			
ΔP		$\bar{x}$	σ	c.i.	%ε	$\bar{x}$	σ	c.i.	%ε
Permea	50	0.199	0.004	0.005	5.107	1.145	0.017	0.019	3.358
	80	0.138	0.007	0.008	11.756	1.048	0.028	0.032	6.032
	100	0.110	0.001	0.001	2.431	1.029	0.016	0.023	4.418
		Permeance (μmol.m^{-2}.s^{-1}.Pa^{-1})				Permeance (μmol.m^{-2}.s^{-1}.Pa^{-1})			
80/20:H2/CO2		H2				CO2			
ΔP		$\bar{x}$	σ	c.i.	%ε	$\bar{x}$	σ	c.i.	%ε
Permea	50	4.257	0.217	0.245	11.517	0.924	0.029	0.033	7.207
	80	1.944	0.115	0.130	13.423	0.425	0.013	0.015	7.054
	100	0.566	0.010	0.011	3.962	0.134	0.003	0.003	4.956

SELECTVITY STATISTICS

Table K.22: Selectivity Statistics ($CH_4$and CO_2) at 328 K

		Selectivity			
50/50: CH4/CO2		CH4/CO2			
ΔP		$\bar{x}$	σ	c.i.	%ε
Permeate	50	1.027	0.016	0.019	3.626
	80	1.026	0.005	0.005	1.040
	100	1.014	0.001	0.001	0.197
		Selectivity			
20/80:CH4/CO2		CH4/CO2			
ΔP		$\bar{x}$	σ	c.i.	%ε
Permea	50	0.342	0.005	0.006	3.496
	80	0.342	0.009	0.010	5.681
	100	0.346	0.004	0.005	2.691
		Selectivity			
80/20:CH4/CO2		CH4/CO2			
ΔP		$\bar{x}$	σ	c.i.	%ε
Permea	50	3.929	0.107	0.121	6.136
	80	4.001	0.108	0.122	6.086
	100	3.944	0.046	0.064	3.248

Table K.23: Selectivity Statistics ($H_2$and CH_4) at 328 K

		Selectivity			
50/50: H2/CH4		H2/CH4			
ΔP		$\bar{x}$	σ	c.i.	%ε
Permea	50	0.787	0.033	0.037	9.517
	80	0.835	0.049	0.055	13.209
	100	0.944	0.032	0.045	9.479
		Selectivity			
20/80:H2/CH4		H2/CH4			
ΔP		$\bar{x}$	σ	c.i.	%ε
Permea	50	0.118	0.005	0.005	8.812
	80	0.124	0.005	0.006	9.705
	100	0.122	0.004	0.006	9.233
		Selectivity			
80/20:H2/CH4		H2/CH4			
ΔP		$\bar{x}$	σ	c.i.	%ε
Permea	50	4.231	0.104	0.117	5.539
	80	3.920	0.122	0.138	7.044
	100	4.152	0.099	0.138	6.639

Table K.24: Selectivity Statistics ($H_2$and CO_2) at 328 K

		Selectivity			
50/50: H2/CO2		H2/CO2			
ΔP		$\bar{x}$	σ	c.i.	%ε
Permea	50	1.082	0.064	0.072	13.377
	80	1.079	0.029	0.032	5.989
	100	0.985	0.025	0.028	5.649
		Selectivity			
20/80:H2/CO2		H2/CO2			
ΔP		$\bar{x}$	σ	c.i.	%ε
Permea	50	0.174	0.005	0.006	7.128
	80	0.131	0.005	0.006	9.140
	100	0.107	0.001	0.001	1.986
		Selectivity			
80/20:H2/CO2		H2/CO2			
ΔP		$\bar{x}$	σ	c.i.	%ε
Permea	50	4.617	0.377	0.426	18.459
	80	4.576	0.134	0.151	6.622
	100	4.235	0.053	0.073	3.448

HEIGHT STATISTICS

Table K.25: Height Statistics of the Feed Gas (CH_4 and CO_2) at 353 K

		Height			
50/50: CH4/CO2		$\bar{h}$	σ	c.i.	%ε
Feed	CH4	2470.000	31.633	35.796	2.898
	CO2	2046.667	70.835	80.157	7.833
		Height			
20/80:CH4/CO2		$\bar{h}$	σ	c.i.	%ε
Feed	CH4	733.667	11.898	13.464	3.670
	CO2	3287.333	19.396	21.949	1.335
		Height			
80/20:CH4/CO2		$\bar{h}$	σ	c.i.	%ε
Feed	CH4	3602.667	30.923	34.992	1.943
	CO2	755.667	20.072	22.714	6.012
		Height			
65/35:CH4/CO2		$\bar{h}$	σ	c.i.	%ε
Feed	CH4	5261.000	202.555	229.213	8.714
	CO2	3459.000	150.659	170.486	9.858

		Height			
35/65:CH4/CO2		$\overline{h}$	σ	c.i.	%ε
Feed	CH4	4115.000	283.409	320.707	15.587
	CO2	5824.333	77.616	87.831	3.016

Table K.26: Height Statistics of the Feed Gas (H_2 and CH_4) at 353 K

		Height			
50/50: H2/CH4		$\overline{h}$	σ	c.i.	%ε
Feed	H2	162.000	9.416	10.656	13.155
	CH4	2611.667	43.683	49.432	3.785
		Height			
20/80:H2/CH4		$\overline{h}$	σ	c.i.	%ε
Feed	H2	65.000	3.742	4.234	13.028
	CH4	3681.000	52.783	59.729	3.245
		Height			
80/20:H2/CH4		$\overline{h}$	σ	c.i.	%ε
Feed	H2	212.000	10.708	12.118	11.432
	CH4	1520.667	7.364	8.333	1.096
		Height			
65/35:H2/CH4		$\overline{h}$	σ	c.i.	%ε
Feed	H2	408.667	18.927	21.418	10.482
	CH4	3741.333	94.996	107.498	5.747
		Height			
35/65:H2/CH4		$\overline{h}$	σ	c.i.	%ε
Feed	H2	355.333	12.037	13.621	7.667
	CH4	5521.000	105.322	119.183	4.317

Table K.27: Height Statistics of the Feed Gas (H_2 and CO_2) at 353 K

		Height			
50/50: H2/CO2		$\overline{h}$	σ	c.i.	%ε
Feed	H2	175.667	10.656	12.059	13.729
	CO2	2517.000	75.113	84.999	6.754
		Height			
20/80:H2/CO2		$\overline{h}$	σ	c.i.	%ε
Feed	H2	65.333	3.682	4.166	12.754
	CO2	3247.333	4.922	5.569	0.343
		Height			
80/20:H2/CO2		$\overline{h}$	σ	c.i.	%ε
Feed	H2	218.333	8.654	9.793	8.970
	CO2	1324.333	81.455	92.175	13.920

		Height			
65/35:H2/CO2		$\overline{h}$	σ	c.i.	%ε
Feed	H2	239.333	11.842	13.400	11.198
	CO2	3339.333	42.898	48.543	2.907

Table K.28: Height Statistics of the Permeate Gas (CH_4 and CO_2) at 353 K

		Height				Height			
50/50: CH4/CO2		CH4				CO2			
ΔP		$\overline{h}$	σ	c.i.	%ε	$\overline{h}$	σ	c.i.	%ε
Permeat	50	2699.000	35.590	40.274	2.984	2115.333	45.639	51.645	4.883
	80	2685.000	25.153	28.463	2.120	2080.667	40.144	45.427	4.367
	100	2642.333	13.225	14.965	1.133	2069.667	9.741	11.023	1.065
		Height				Height			
20/80:CH4/CO2		CH4				CO2			
ΔP		$\overline{h}$	σ	c.i.	%ε	$\overline{h}$	σ	c.i.	%ε
Permeat	30	762.667	8.994	10.177	2.669	2976.333	14.291	16.171	1.087
	50	873.333	44.969	50.887	11.654	2925.667	18.625	21.076	1.441
	80	903.333	36.818	41.663	9.224	2872.667	17.988	20.355	1.417
		Height				Height			
80/20:CH4/CO2		CH4				CO2			
ΔP		$\overline{h}$	σ	c.i.	%ε	$\overline{h}$	σ	c.i.	%ε
Permeat	30	3765.667	11.324	12.814	0.681	796.000	17.907	20.264	5.091
	50	3758.667	13.275	15.022	0.799	773.333	25.850	29.252	7.565
	80	3818.333	34.422	38.952	2.040	835.667	37.026	41.898	10.028
		Height				Height			
65/35:CH4/CO2		CH4				CO2			
ΔP		$\overline{h}$	σ	c.i.	%ε	$\overline{h}$	σ	c.i.	%ε
Permeat	30	6032.333	59.365	67.178	2.227	3542.000	64.915	73.459	4.148
	50	5993.333	56.759	64.229	2.143	3632.667	37.633	42.585	2.345
	80	5957.000	2.500	2.829	0.095	3625.667	17.632	19.953	1.101
		Height				Height			
35/65:CH4/CO2		CH4				CO2			
ΔP		$\overline{h}$	σ	c.i.	%ε	$\overline{h}$	σ	c.i.	%ε
Permeat	30	4203.667	39.041	44.179	2.102	5158.000	26.870	30.406	1.179
	50	4186.667	116.511	161.476	7.714	5203.333	45.065	50.996	1.960
	80	4107.667	25.421	35.232	1.715	5139.667	23.907	27.054	1.053

Table K.29: Height Statistics of the Permeate Gas (H_2 and CH_4) at 353 K

		Height				Height			
50/50: H2/CH4		H2				CH4			
ΔP		$\overline{h}$	σ	c.i.	%ε	$\overline{h}$	σ	c.i.	%ε
Permeat	30	193.000	12.832	14.521	15.048	2619.333	2.867	3.245	0.248
	50	182.333	2.625	2.970	3.258	2602.333	18.264	20.667	1.588
	80	180.000	9.899	11.202	12.447	2601.333	5.312	6.012	0.462

		Height				Height			
20/80:H2/CH4		H2				CH4			
ΔP		$\overline{h}$	σ	c.i.	%ε	$\overline{h}$	σ	c.i.	%ε
Permeate	30	55.333	2.055	2.325	8.404	3819.667	246.136	278.529	14.584
	50	56.333	1.247	1.411	5.011	3691.333	16.760	18.965	1.028
	80	52.333	1.886	2.613	9.987	3534.000	7.000	7.921	0.448
		Height				Height			
80/20:H2/CH4		H2				CH4			
ΔP		$\overline{h}$	σ	c.i.	%ε	$\overline{h}$	σ	c.i.	%ε
Permeate	30	210.667	4.784	5.414	5.140	1492.667	6.650	7.525	1.008
	50	198.667	6.799	7.693	7.745	1491.667	17.211	19.476	2.611
	80	218.333	11.671	13.207	12.098	1489.333	5.558	6.289	0.845
		Height				Height			
65/35:H2/CH4		H2				CH4			
ΔP		$\overline{h}$	σ	c.i.	%ε	$\overline{h}$	σ	c.i.	%ε
Permeate	30	413.333	26.043	29.470	14.260	3761.000	15.642	17.700	0.941
	50	459.667	4.497	6.232	2.712	3784.667	55.428	62.722	3.315
	80	369.333	7.040	9.756	5.283	3890.000	44.900	50.809	2.612
		Height				Height			
35/65:H2/CH4		H2				CH4			
ΔP		$\overline{h}$	σ	c.i.	%ε	$\overline{h}$	σ	c.i.	%ε
Permeate	30	341.667	22.485	25.444	14.894	5822.667	47.162	53.368	1.833
	50	369.667	13.671	15.470	8.370	5854.000	19.201	21.728	0.742
	80	365.000	14.720	16.657	9.127	5853.667	13.888	15.716	0.537

Table K.30: Height Statistics of the Permeate Gas (H_2 and CO_2) at 353 K

		Height				Height			
50/50: H2/CO2		H2				CO2			
ΔP		$\overline{h}$	σ	c.i.	%ε	$\overline{h}$	σ	c.i.	%ε
Permeate	30	194.667	6.799	7.693	7.904	2297.000	39.192	44.350	3.862
	50	173.333	11.086	12.544	14.474	2334.333	27.439	31.050	2.660
	80	187.000	6.164	6.976	7.461	2350.000	5.099	5.770	0.491
		Height				Height			
20/80:H2/CO2		H2				CO2			
ΔP		$\overline{h}$	σ	c.i.	%ε	$\overline{h}$	σ	c.i.	%ε
Permeate	30	70.000	3.266	3.696	10.559	3237.667	96.503	109.204	6.746
	50	61.000	2.944	3.331	10.922	3224.667	56.151	63.540	3.941
	80	74.333	3.300	4.573	12.305	3211.000	10.424	11.796	0.735
		Height				Height			
80/20:H2/CO2		H2				CO2			
ΔP		$\overline{h}$	σ	c.i.	%ε	$\overline{h}$	σ	c.i.	%ε
Permeate	30	209.333	8.654	9.793	9.356	1337.333	15.173	17.170	2.568
	50	257.000	4.967	6.883	5.357	1335.333	18.373	20.791	3.114
	80	287.667	5.793	8.028	5.582	1326.000	32.073	36.294	5.474

65/35:H2/CO2		Height H2				Height CO2			
ΔP		$\overline{h}$	σ	c.i.	%ε	$\overline{h}$	σ	c.i.	%ε
Permea	30	290.667	4.922	5.569	3.832	3273.000	34.029	38.508	2.353
	50	276.333	8.055	9.116	6.597	3337.667	62.002	70.162	4.204
	80	268.667	8.179	9.255	6.890	3522.000	1.414	1.600	0.091

PERMEANCE STATISTICS

Table K.31: Permeance Statistics ($CH_4$and CO_2) at 353 K

50/50: CH4/CO2		Permeance (μmol.m^{-2}.s^{-1}.Pa^{-1}) CH4				Permeance (μmol.m^{-2}.s^{-1}.Pa^{-1}) CO2			
ΔP		$\overline{x}$	σ	c.i.	%ε	$\overline{x}$	σ	c.i.	%ε
Permea	50	0.793	0.010	0.012	2.984	0.751	0.016	0.018	4.883
	80	0.720	0.007	0.008	2.120	0.674	0.013	0.015	4.367
	100	0.666	0.003	0.005	1.387	0.630	0.003	0.004	1.305
20/80:CH4/CO2		Permeance (μmol.m^{-2}.s^{-1}.Pa^{-1}) CH4				Permeance (μmol.m^{-2}.s^{-1}.Pa^{-1}) CO2			
ΔP		$\overline{x}$	σ	c.i.	%ε	$\overline{x}$	σ	c.i.	%ε
Permea	50	0.281	0.003	0.004	2.669	0.980	0.005	0.005	1.087
	80	0.308	0.016	0.018	11.654	0.922	0.006	0.007	1.441
	100	0.317	0.013	0.018	11.297	0.901	0.006	0.008	1.736
80/20:CH4/CO2		Permeance (μmol.m^{-2}.s^{-1}.Pa^{-1}) CH4				Permeance (μmol.m^{-2}.s^{-1}.Pa^{-1}) CO2			
ΔP		$\overline{x}$	σ	c.i.	%ε	$\overline{x}$	σ	c.i.	%ε
Permea	50	1.445	0.004	0.005	0.681	0.364	0.008	0.009	5.091
	80	1.283	0.005	0.005	0.799	0.315	0.011	0.012	7.565
	100	1.360	0.012	0.017	2.499	0.355	0.016	0.022	12.281
65/35:CH4/CO2		Permeance (μmol.m^{-2}.s^{-1}.Pa^{-1}) CH4				Permeance (μmol.m^{-2}.s^{-1}.Pa^{-1}) CO2			
ΔP		$\overline{x}$	σ	c.i.	%ε	$\overline{x}$	σ	c.i.	%ε
Permea	50	1.357	0.013	0.015	2.227	0.653	0.012	0.014	4.148
	80	1.184	0.011	0.013	2.143	0.588	0.006	0.007	2.345
	100	1.111	0.006	0.008	1.390	0.554	0.003	0.004	1.348
35/65:CH4/CO2		Permeance (μmol.m^{-2}.s^{-1}.Pa^{-1}) CH4				Permeance (μmol.m^{-2}.s^{-1}.Pa^{-1}) CO2			
ΔP		$\overline{x}$	σ	c.i.	%ε	$\overline{x}$	σ	c.i.	%ε
Permea	50	0.415	0.004	0.004	2.102	0.666	0.003	0.004	1.179
	80	0.517	0.014	0.016	6.298	0.840	0.007	0.008	1.960
	100	0.479	0.003	0.004	1.715	0.783	0.004	0.005	1.289

Table K.32: Permeance Statistics ($CH_4$and H_2) at 353 K

50/50: H2/CH4		Permeance (μmol.m^{-2}.s^{-1}.Pa^{-1}) H2				Permeance (μmol.m^{-2}.s^{-1}.Pa^{-1}) CH4			
ΔP		$\overline{x}$	σ	c.i.	%ε	$\overline{x}$	σ	c.i.	%ε
Permea	50	1.389	0.092	0.105	15.048	1.166	0.001	0.001	0.248
	80	1.170	0.017	0.019	3.258	1.033	0.007	0.008	1.588
	100	0.763	0.042	0.058	15.244	0.682	0.001	0.002	0.586

		Permeance (μmol.m^{-2}.s^{-1}.Pa^{-1})				Permeance (μmol.m^{-2}.s^{-1}.Pa^{-1})			
20/80:H2/CH4		H2				CH4			
ΔP		$\bar{x}$	σ	c.i.	%ε	$\bar{x}$	σ	c.i.	%ε
Permea	50	0.309	0.011	0.013	8.404	1.504	0.005	0.006	0.804
	80	0.321	0.007	0.008	5.011	1.542	0.009	0.011	1.378
	100	0.179	0.006	0.009	9.987	0.923	0.003	0.004	0.901
		Permeance (μmol.m^{-2}.s^{-1}.Pa^{-1})				Permeance (μmol.m^{-2}.s^{-1}.Pa^{-1})			
80/20:H2/CH4		H2				CH4			
ΔP		$\bar{x}$	σ	c.i.	%ε	$\bar{x}$	σ	c.i.	%ε
Permea	50	2.264	0.051	0.058	5.140	0.558	0.002	0.003	1.008
	80	2.126	0.073	0.082	7.745	0.555	0.006	0.007	2.611
	100	2.083	0.111	0.154	14.818	0.494	0.002	0.003	1.034
		Permeance (μmol.m^{-2}.s^{-1}.Pa^{-1})				Permeance (μmol.m^{-2}.s^{-1}.Pa^{-1})			
65/35:H2/CH4		H2				CH4			
ΔP		$\bar{x}$	σ	c.i.	%ε	$\bar{x}$	σ	c.i.	%ε
Permea	50	1.907	0.120	0.136	14.260	0.994	0.004	0.005	0.941
	80	1.278	0.013	0.014	2.214	0.603	0.009	0.010	3.315
	100	1.522	0.029	0.040	5.283	0.918	0.011	0.015	3.199
		Permeance (μmol.m^{-2}.s^{-1}.Pa^{-1})				Permeance (μmol.m^{-2}.s^{-1}.Pa^{-1})			
35/65:H2/CH4		H2				CH4			
ΔP		$\bar{x}$	σ	c.i.	%ε	$\bar{x}$	σ	c.i.	%ε
Permea	50	0.809	0.053	0.060	14.894	1.633	0.013	0.015	1.833
	80	0.820	0.030	0.034	8.370	1.538	0.005	0.006	0.742
	100	0.781	0.031	0.044	11.178	1.484	0.004	0.005	0.658

Table K.33: Permeance Statistics ($H_2$and CO_2) at 353 K

		Permeance (μmol.m^{-2}.s^{-1}.Pa^{-1})				Permeance (μmol.m^{-2}.s^{-1}.Pa^{-1})			
50/50: H2/CO2		H2				CO2			
ΔP		$\bar{x}$	σ	c.i.	%ε	$\bar{x}$	σ	c.i.	%ε
Permea	50	0.971	0.034	0.038	7.904	0.797	0.014	0.015	3.862
	80	0.752	0.048	0.054	14.474	0.705	0.008	0.009	2.660
	100	0.846	0.028	0.039	9.137	0.740	0.002	0.002	0.601
		Permeance (μmol.m^{-2}.s^{-1}.Pa^{-1})				Permeance (μmol.m^{-2}.s^{-1}.Pa^{-1})			
20/80:H2/CO2		H2				CO2			
ΔP		$\bar{x}$	σ	c.i.	%ε	$\bar{x}$	σ	c.i.	%ε
Permea	50	0.283	0.013	0.015	10.559	1.052	0.031	0.035	6.746
	80	69.797	0.010	0.012	0.033	0.902	0.016	0.018	3.941
	100	0.253	0.011	0.016	12.305	0.876	0.003	0.004	0.900
		Permeance (μmol.m^{-2}.s^{-1}.Pa^{-1})				Permeance (μmol.m^{-2}.s^{-1}.Pa^{-1})			
80/20:H2/CO2		H2				CO2			
ΔP		$\bar{x}$	σ	c.i.	%ε	$\bar{x}$	σ	c.i.	%ε
Permea	50	1.827	0.076	0.085	9.356	0.482	0.005	0.006	2.568
	80	2.008	0.039	0.044	4.374	0.431	0.006	0.007	3.114
	100	2.339	0.047	0.065	5.582	0.445	0.011	0.015	6.704

65/35:H2/CO2		Permeance (μmol.m^{-2}.s^{-1}.Pa^{-1}) H2				Permeance (μmol.m^{-2}.s^{-1}.Pa^{-1}) CO2			
ΔP		$\bar{x}$	σ	c.i.	%ε	$\bar{x}$	σ	c.i.	%ε
Permea	50	5.066	0.086	0.097	3.832	2.196	0.023	0.026	2.353
	80	0.973	0.028	0.032	6.597	0.453	0.008	0.010	4.204
	100	1.368	0.042	0.058	8.438	0.691	0.000	0.000	0.111

SELECTVITY STATISTICS

Table K.34: Selectivity Statistics ($CH_4$and CO_2) at 353 K

50/50: CH4/CO2		Selectivity CH4/CO2			
ΔP		$\bar{x}$	σ	c.i.	%ε
Permea	50	1.057	0.037	0.042	7.941
	80	1.068	0.012	0.014	2.638
	100	1.057	0.002	0.002	0.432

20/80:CH4/CO2		Selectivity CH4/CO2			
ΔP		$\bar{x}$	σ	c.i.	%ε
Permea	50	0.287	0.002	0.003	1.909
	80	0.335	0.019	0.022	13.024
	100	0.352	0.013	0.019	10.583

80/20:CH4/CO2		Selectivity CH4/CO2			
ΔP		$\bar{x}$	σ	c.i.	%ε
Permea	50	3.968	0.076	0.086	4.356
	80	4.080	0.146	0.165	8.077
	100	3.840	0.198	0.275	14.310

65/35:CH4/CO2		Selectivity CH4/CO2			
ΔP		$\bar{x}$	σ	c.i.	%ε
Permea	50	2.079	0.018	0.020	1.934
	80	2.014	0.034	0.038	3.819
	100	2.005	0.015	0.021	2.130

35/65:CH4/CO2		Selectivity CH4/CO2			
ΔP		$\bar{x}$	σ	c.i.	%ε
Permea	50	0.624	0.007	0.008	2.522
	80	0.616	0.013	0.014	4.690
	100	0.612	0.003	0.005	1.494

Table K.35: Selectivity Statistics ($H_2$and CH_4) at 353 K

		Selectivity			
50/50: H2/CH4		**H2/CH4**			
ΔP		$\bar{x}$	**σ**	**c.i.**	**%ε**
Permea	50	1.191	0.080	0.091	15.202
	80	1.133	0.021	0.024	4.238
	100	1.119	0.064	0.088	15.799
		Selectivity			
20/80:H2/CH4		**H2/CH4**			
ΔP		$\bar{x}$	**σ**	**c.i.**	**%ε**
Permea	50	0.206	0.008	0.009	9.188
	80	0.208	0.004	0.005	4.799
	100	0.194	0.007	0.010	10.196
		Selectivity			
80/20:H2/CH4		**H2/CH4**			
ΔP		$\bar{x}$	**σ**	**c.i.**	**%ε**
Permea	50	4.059	0.086	0.097	4.778
	80	3.830	0.089	0.100	5.241
	100	4.216	0.212	0.293	13.912
		Selectivity			
65/35:H2/CH4		**H2/CH4**			
ΔP		$\bar{x}$	**σ**	**c.i.**	**%ε**
Permea	50	1.919	0.126	0.143	14.895
	80	2.121	0.031	0.035	3.298
	100	1.658	0.051	0.070	8.445
		Selectivity			
35/65:H2/CH4		**H2/CH4**			
ΔP		$\bar{x}$	**σ**	**c.i.**	**%ε**
Permea	50	0.495	0.029	0.033	13.251
	80	0.533	0.020	0.022	8.427
	100	0.526	0.020	0.028	10.699

Table K.36: Selectivity Statistics ($H_2$and CO_2) at 353 K

		Selectivity			
50/50: H2/CO2		**H2/CO2**			
ΔP		$\bar{x}$	**σ**	**c.i.**	**%ε**
Permea	50	1.218	0.023	0.026	4.286
	80	1.066	0.056	0.064	11.942
	100	1.144	0.038	0.052	9.092
		Selectivity			
20/80:H2/CO2		**H2/CO2**			
ΔP		$\bar{x}$	**σ**	**c.i.**	**%ε**
Permea	50	0.270	0.021	0.023	17.342
	80	0.236	0.008	0.009	7.245
	100	0.289	0.014	0.019	13.189

		Selectivity			
80/20:H2/CO2		H2/CO2			
ΔP		$\bar{x}$	σ	c.i.	%ε
Permea	50	3.791	0.171	0.194	10.217
	80	4.661	0.144	0.163	6.996
	100	5.255	0.154	0.214	8.128
		Selectivity			
65/35:H2/CO2		H2/CO2			
ΔP		$\bar{x}$	σ	c.i.	%ε
Permea	50	2.306	0.025	0.029	2.502
	80	2.151	0.087	0.098	9.126
	100	1.981	0.060	0.083	8.401

HEIGHT STATISTICS

Table K.37: Height Statistics of the Feed Gas (CH_4 and CO_2) at 372 K

		Height			
50/50: CH4/CO2		$\bar{h}$	σ	c.i.	%ε
Feed	CH4	2561.667	59.331	67.140	5.242
	CO2	2023.667	125.359	141.857	14.020
		Height			
20/80:CH4/CO2		$\bar{h}$	σ	c.i.	%ε
Feed	CH4	717.000	36.688	41.516	11.581
	CO2	3280.667	48.992	55.440	3.380
		Height			
80/20:CH4/CO2		$\bar{h}$	σ	c.i.	%ε
Feed	CH4	3834.667	66.244	74.962	3.910
	CO2	665.333	27.645	31.283	9.404

Table K.38: Height Statistics of the Feed Gas (H_2 and CH_4) at 372 K

		Height			
50/50: H2/CH4		$\bar{h}$	σ	c.i.	%ε
Feed	H2	161.667	6.182	6.996	8.655
	CH4	2442.000	81.343	92.048	7.539
		Height			
20/80:H2/CH4		$\bar{h}$	σ	c.i.	%ε
Feed	H2	53.333	0.943	1.067	4.001
	CH4	3977.333	40.925	46.311	2.329
		Height			
80/20:H2/CH4		$\bar{h}$	σ	c.i.	%ε
Feed	H2	207.667	10.965	12.408	11.950
	CH4	1515.000	24.345	27.549	3.637

Table K.39: Height Statistics of the Feed Gas (H_2 and CO_2) at 372 K

		Height			
50/50: H2/CO2		$\overline{h}$	σ	c.i.	%ε
Feed	H2	149.667	8.957	10.135	13.544
	CO2	2702.000	39.098	44.244	3.275
		Height			
20/80:H2/CO2		$\overline{h}$	σ	c.i.	%ε
Feed	H2	73.333	2.055	2.325	6.342
	CO2	3320.000	200.205	226.553	13.648
		Height			
80/20:H2/CO2		$\overline{h}$	σ	c.i.	%ε
Feed	H2	205.333	4.110	4.650	4.530
	CO2	1345.333	18.190	20.584	3.060

Table K.40: Height Statistics of the Permeate Gas (CH_4 and CO_2) at 372 K

		Height				Height			
50/50: CH4/CO2		CH4				CO2			
ΔP		$\overline{h}$	σ	c.i.	%ε	$\overline{h}$	σ	c.i.	%ε
Permeate	30	2765.000	8.165	9.240	0.668	2139.667	23.171	26.220	2.451
	50	2752.333	30.728	34.772	2.527	2129.333	9.031	10.219	0.960
	80	2730.333	22.395	25.343	1.856	2118.333	24.226	27.414	2.588
		Height				Height			
20/80:CH4/CO2		CH4				CO2			
ΔP		$\overline{h}$	σ	c.i.	%ε	$\overline{h}$	σ	c.i.	%ε
Permeate	30	1675.667	5.793	6.555	0.782	2953.333	75.464	85.396	5.783
	50	1699.333	58.790	66.527	7.830	3043.000	38.401	43.455	2.856
	80	1629.333	12.120	13.715	1.683	2843.000	106.116	120.082	8.448
		Height				Height			
80/20:CH4/CO2		CH4				CO2			
ΔP		$\overline{h}$	σ	c.i.	%ε	$\overline{h}$	σ	c.i.	%ε
Permea	30	3772.333	15.434	17.466	0.926	755.000	26.470	29.954	7.935
	50	3746.000	22.642	25.622	1.368	758.667	15.063	17.045	4.493
	80	3809.000	37.851	42.832	2.249	839.000	40.274	45.574	10.864

Table K.41: Height Statistics of the Permeate Gas (CH_4 and H_2) at 372 K

		Height				Height			
50/50: H2/CH4		H2				CH4			
ΔP		$\overline{h}$	σ	c.i.	%ε	$\overline{h}$	σ	c.i.	%ε
Permeate	30	117.667	2.055	2.325	3.952	2656.000	26.981	30.532	2.299
	50	120.667	3.300	3.734	6.189	2646.000	3.559	4.027	0.304
	80	128.000	0.816	0.924	1.444	2642.667	11.898	13.464	1.019

20/80:H2/CH4		Height H2				Height CH4			
ΔP		$\overline{h}$	σ	c.i.	%ε	$\overline{h}$	σ	c.i.	%ε
Permeat	30	47.667	2.055	2.325	9.756	3995.333	8.957	10.135	0.507
	50	49.667	2.625	2.970	11.960	3991.000	28.178	31.886	1.598
	80	55.000	2.449	2.772	10.079	3954.000	41.785	47.284	2.392
80/20:H2/CH4		**Height H2**				**Height CH4**			
ΔP		$\overline{h}$	σ	c.i.	%ε	$\overline{h}$	σ	c.i.	%ε
Permeat	30	177.333	3.091	3.498	3.945	1521.000	3.559	4.027	0.530
	50	237.000	13.638	15.433	13.024	1571.333	23.443	26.528	3.376
	80	256.667	9.672	10.945	8.529	1577.333	38.003	43.004	5.453

Table K.42: Height Statistics of the Permeate Gas (H_2 and CO_2) at 372 K

50/50: H2/CO2		Height H2				Height CO2			
ΔP		$\overline{h}$	σ	c.i.	%ε	$\overline{h}$	σ	c.i.	%ε
Permeat	30	190.000	6.532	7.392	7.781	2263.000	24.055	27.221	2.406
	50	244.000	2.160	2.445	2.004	2274.333	11.557	13.078	1.150
	80	172.667	10.274	11.626	13.467	2282.667	33.250	37.626	3.297
20/80:H2/CO2		**Height H2**				**Height CO2**			
ΔP		$\overline{h}$	σ	c.i.	%ε	$\overline{h}$	σ	c.i.	%ε
Permeat	30	73.333	4.714	5.334	14.548	3325.000	4.572	5.174	0.311
	50	77.333	2.494	2.823	7.300	3343.333	3.735	4.226	0.253
	80	79.333	2.867	3.245	8.180	3348.333	49.802	56.356	3.366
80/20:H2/CO2		**Height H2**				**Height CO2**			
ΔP		$\overline{h}$	σ	c.i.	%ε	$\overline{h}$	σ	c.i.	%ε
Permeat	30	255.000	10.033	11.354	8.905	1367.667	10.143	11.478	1.679
	50	274.000	12.570	14.224	10.383	1364.333	11.813	13.368	1.960
	80	280.000	5.099	5.770	4.121	1431.000	18.055	20.432	2.856

PERMEANCE STATISTICS

Table K.43: Permeance Statistics ($CH_4$and CO_2) at 372 K

50/50: CH4/CO2		Permeance (μmol.m^{-2}.s^{-1}.Pa^{-1}) CH4				Permeance (μmol.m^{-2}.s^{-1}.Pa^{-1}) CO2			
ΔP		$\overline{x}$	σ	c.i.	%ε	$\overline{x}$	σ	c.i.	%ε
Permea	50	0.837	0.002	0.003	0.668	0.823	0.009	0.010	2.451
	80	0.692	0.008	0.009	2.527	0.680	0.003	0.003	0.960
	100	0.652	0.005	0.007	2.274	0.643	0.007	0.010	3.170

20/80:CH4/CO2		Permeance (μmol.m^{-2}.s^{-1}.Pa^{-1}) CH4				Permeance (μmol.m^{-2}.s^{-1}.Pa^{-1}) CO2			
ΔP		$\bar{x}$	σ	c.i.	%ε	$\bar{x}$	σ	c.i.	%ε
Permea	50	0.678	0.002	0.003	0.782	1.043	0.027	0.030	5.783
	80	0.558	0.019	0.022	7.830	0.872	0.011	0.012	2.856
	100	0.499	0.004	0.005	2.062	0.759	0.028	0.039	10.346
80/20:CH4/CO2		Permeance (μmol.m^{-2}.s^{-1}.Pa^{-1}) CH4				Permeance (μmol.m^{-2}.s^{-1}.Pa^{-1}) CO2			
ΔP		$\bar{x}$	σ	c.i.	%ε	$\bar{x}$	σ	c.i.	%ε
Permea	50	0.259	0.001	0.001	0.926	0.075	0.003	0.003	7.935
	80	1.232	0.007	0.008	1.368	0.360	0.007	0.008	4.493
	100	1.188	0.012	0.016	2.754	0.378	0.018	0.025	13.306

Table K.44: Permeance Statistics ($H_2$and CH_4) at 372 K

50/50: H2/CH4		Permeance (μmol.m^{-2}.s^{-1}.Pa^{-1}) H2				Permeance (μmol.m^{-2}.s^{-1}.Pa^{-1}) CH4			
ΔP		$\bar{x}$	σ	c.i.	%ε	$\bar{x}$	σ	c.i.	%ε
Permea	50	0.802	0.014	0.016	3.952	1.198	0.012	0.014	2.299
	80	0.746	0.020	0.023	6.189	1.082	0.001	0.002	0.304
	100	0.584	0.004	0.005	1.768	0.798	0.004	0.005	1.248
20/80:H2/CH4		Permeance (μmol.m^{-2}.s^{-1}.Pa^{-1}) H2				Permeance (μmol.m^{-2}.s^{-1}.Pa^{-1}) CH4			
ΔP		$\bar{x}$	σ	c.i.	%ε	$\bar{x}$	σ	c.i.	%ε
Permea	50	0.339	0.015	0.017	9.756	1.523	0.003	0.004	0.507
	80	0.309	0.016	0.018	11.960	1.330	0.009	0.011	1.598
	100	0.345	0.015	0.021	12.345	1.330	0.014	0.019	2.929
80/20:H2/CH4		Permeance (μmol.m^{-2}.s^{-1}.Pa^{-1}) H2				Permeance (μmol.m^{-2}.s^{-1}.Pa^{-1}) CH4			
ΔP		$\bar{x}$	σ	c.i.	%ε	$\bar{x}$	σ	c.i.	%ε
Permea	50	1.821	0.032	0.036	3.945	0.534	0.001	0.001	0.530
	80	2.319	0.133	0.151	13.024	0.526	0.008	0.009	3.376
	100	2.581	0.097	0.135	10.446	0.542	0.013	0.018	6.678

Table K.45: Permeance Statistics ($H_2$and CO_2) at 372 K

50/50: H2/CO2		Permeance (μmol.m^{-2}.s^{-1}.Pa^{-1}) H2				Permeance (μmol.m^{-2}.s^{-1}.Pa^{-1}) CO2			
ΔP		$\bar{x}$	σ	c.i.	%ε	$\bar{x}$	σ	c.i.	%ε
Permea	50	1.107	0.038	0.043	7.781	0.728	0.008	0.009	2.406
	80	0.998	0.009	0.010	2.004	0.680	0.003	0.003	0.868
	100	0.830	0.049	0.068	16.493	0.606	0.009	0.012	4.038
20/80:H2/CO2		Permeance (μmol.m^{-2}.s^{-1}.Pa^{-1}) H2				Permeance (μmol.m^{-2}.s^{-1}.Pa^{-1}) CO2			
ΔP		$\bar{x}$	σ	c.i.	%ε	$\bar{x}$	σ	c.i.	%ε
Permea	50	0.246	0.016	0.018	14.548	0.990	0.003	0.003	0.586
	80	0.241	0.008	0.009	7.300	0.922	0.007	0.008	1.640
	100	0.241	0.009	0.012	10.019	0.903	0.013	0.019	4.123

80/20:H2/CO2		Permeance (μmol.m^{-2}.s^{-1}.Pa^{-1}) H2				Permeance (μmol.m^{-2}.s^{-1}.Pa^{-1}) CO2			
ΔP		$\bar{x}$	σ	c.i.	%ε	$\bar{x}$	σ	c.i.	%ε
Permea	50	2.265	0.089	0.101	8.905	0.463	0.003	0.004	1.679
	80	2.361	0.108	0.123	10.383	0.449	0.004	0.004	1.960
	100	2.135	0.039	0.054	5.048	0.416	0.005	0.007	3.497

SELECTIVITY STATISTICS

Table K.46: Selectivity Statistics ($Ch_4$and CO_2) at 372 K

50/50: CH4/CO2		Selectivity CH4/CO2			
ΔP		$\bar{x}$	σ	c.i.	%ε
Permea	50	1.018	0.010	0.012	2.317
	80	1.018	0.007	0.008	1.596
	100	1.015	0.010	0.014	2.730
20/80:CH4/CO2		**Selectivity CH4/CO2**			
ΔP		$\bar{x}$	σ	c.i.	%ε
Permea	50	0.651	0.018	0.020	6.240
	80	0.640	0.015	0.016	5.131
	100	0.658	0.029	0.040	12.113
80/20:CH4/CO2		**Selectivity CH4/CO2**			
ΔP		$\bar{x}$	σ	c.i.	%ε
Permea	50	3.467	0.136	0.154	8.859
	80	3.424	0.087	0.098	5.743
	100	3.154	0.172	0.239	15.124

Table K.47: Selectivity Statistics ($H_2$and CH_4) at 372 K

50/50: H2/CH4		Selectivity H2/CH4			
ΔP		$\bar{x}$	σ	c.i.	%ε
Permea	50	0.670	0.018	0.020	6.059
	80	0.689	0.019	0.022	6.314
	100	0.732	0.008	0.011	3.011
20/80:H2/CH4		**Selectivity H2/CH4**			
ΔP		$\bar{x}$	σ	c.i.	%ε
Permea	50	0.222	0.010	0.011	10.211
	80	0.232	0.014	0.016	13.407
	100	0.259	0.013	0.018	13.515

		Selectivity			
80/20:H2/CH4		H2/CH4			
ΔP		$\bar{x}$	σ	c.i.	%ε
Permea	50	3.411	0.056	0.063	3.723
	80	4.415	0.292	0.330	14.962
	100	4.767	0.285	0.394	16.551

Table K.48: Selectivity Statistics ($H_2$and CO_2) at 372 K

		Selectivity			
50/50: H2/CO2		H2/CO2			
ΔP		$\bar{x}$	σ	c.i.	%ε
Permea	50	1.521	0.056	0.063	8.274
	80	1.943	0.008	0.009	0.922
	100	1.370	0.083	0.115	16.837
		Selectivity			
20/80:H2/CO2		H2/CO2			
ΔP		$\bar{x}$	σ	c.i.	%ε
Permea	50	0.249	0.015	0.017	14.051
	80	0.261	0.007	0.007	5.684
	100	0.267	0.008	0.011	8.312
		Selectivity			
80/20:H2/CO2		H2/CO2			
ΔP		$\bar{x}$	σ	c.i.	%ε
Permea	50	4.889	0.216	0.244	9.999
	80	5.267	0.278	0.315	11.950
	100	5.129	0.085	0.118	4.589

Appendix L

Extra Graphs based On Amorphous Silica Data and Results

L-1: OPERATING TEMPERATURE OF 353 K

INFLUENCE OF MEMBRANE ORIENTATION:

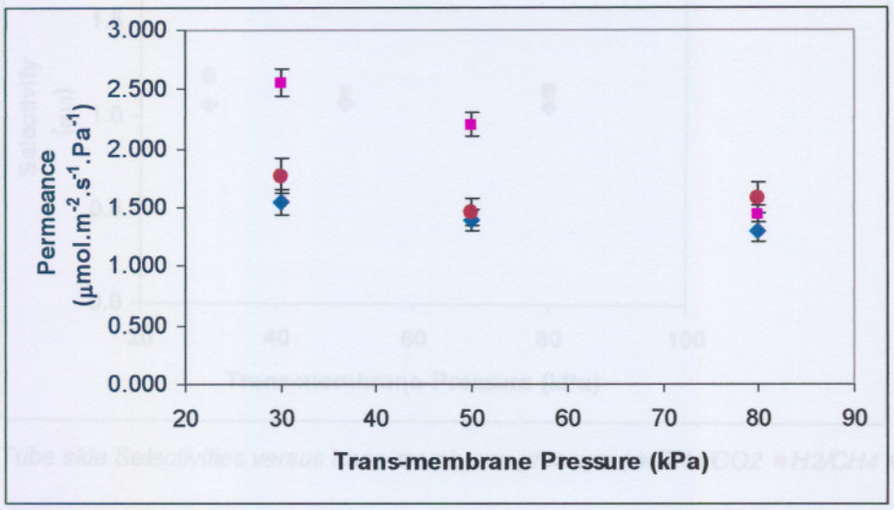

Figure L.1: Tube side permeances versus trans-membrane pressure (◆ CH4/CO2 ■ H2/CH4 ● H2/CO2)

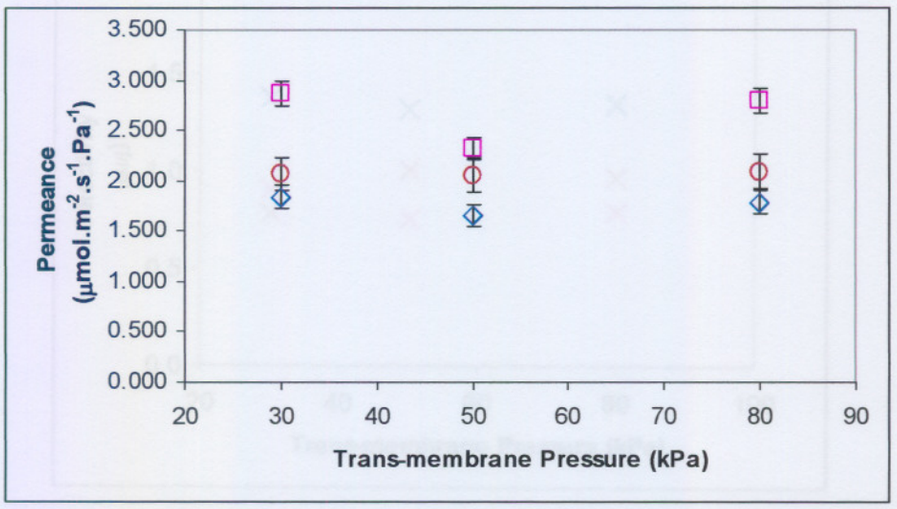

Figure L.2: Shell side permeances versus trans-membrane pressure (◇ CH4/CO2 □ H2/CH4 ○ H2/CO2)

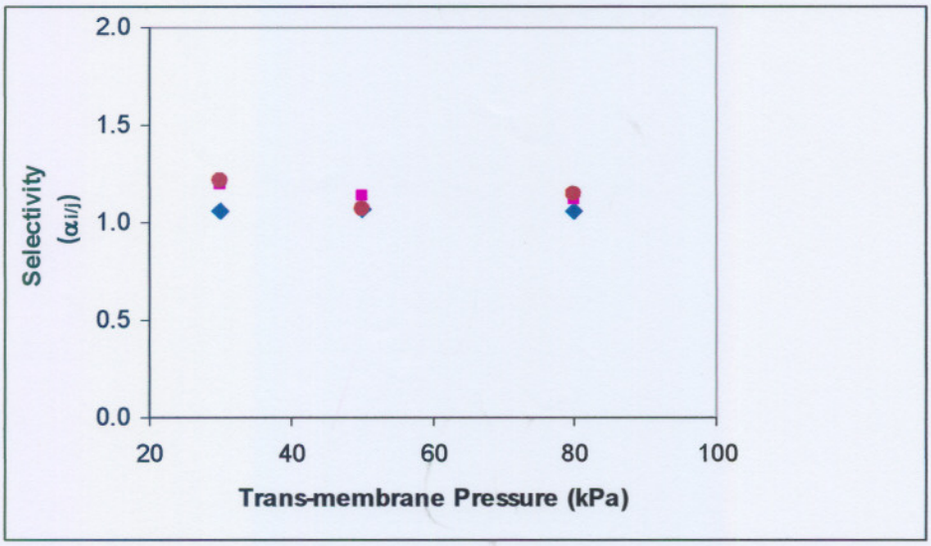

Figure L.3: Tube side Selectivities versus trans-membrane pressure (◆ CH4/CO2 ■ H2/CH4 ● H2/CO2)

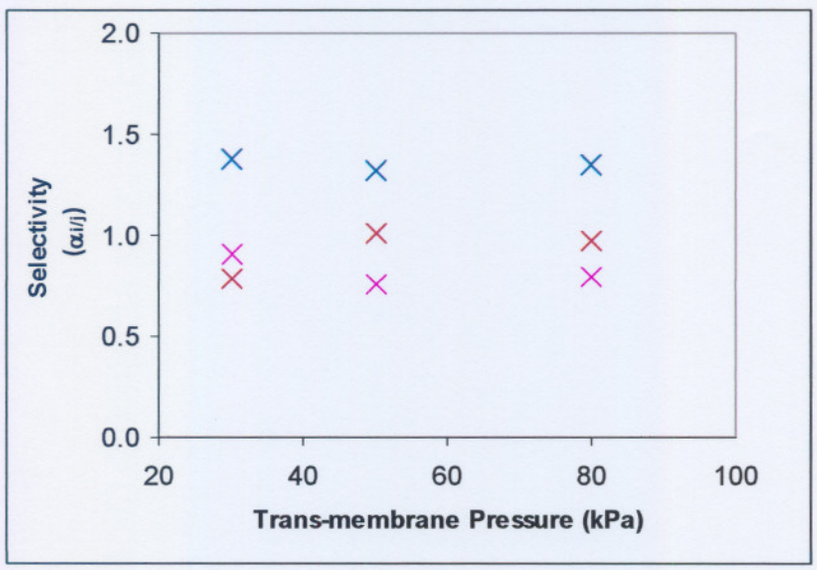

Figure L.4: Shell side Selectivities versus trans-membrane pressure (× CH4/CO2 × H2/CH4 × H2/CO2)

KNUDSEN FLOW FITTED MODEL AND EXPERIMENTAL DATA:

The model equation used: [Lee *et al.*, 2004]

$$J_{knudsen} = \frac{2\varepsilon_{sup} r_p}{3\tau} \sqrt{\frac{8}{\pi MRT}} \frac{\Delta P}{\delta_{sup}}$$

Table L.1: Knudsen Transport Model Parameters

$J_{knudsen}$ Model Values (Gamma layer)	
Property	**Values**
rp	3.50E-09
esup	0.325
t	3.08
T	298
visc	8.96E-06
delta	3.90E-05
k	1.38E-23
R	8.31E+00
phi	1.00E-10
$M_{w\text{-}Hydrogen}$	2.00E-03
$M_{w\text{-}Methane}$	0.016
$M_{w\text{-}Carbon\ dioxide}$	0.044

Table L.2: Knudsen Transport Flux Model and Experimental Values

	J_{model}	$J_{experimental}$	ΔP (Pa)	ΔP (kPa)
Hydrogen	1.13E-01	9.40E-02	2.50E+04	25
	2.26E-01	1.71E-01	5.00E+04	50
	3.39E-01	2.54E-01	7.50E+04	75
	4.07E-01	3.00E-01	9.00E+04	90
Methane	4.00E-02	4.70E-02	2.50E+04	25
	8.00E-02	8.10E-02	5.00E+04	50
	1.20E-01	1.19E-01	7.50E+04	75
	1.60E-01	1.58E-01	1.00E+05	100
Carbon dioxide	2.41E-02	3.60E-02	2.50E+04	25
	4.82E-02	5.50E-02	5.00E+04	50
	7.24E-02	7.80E-02	7.50E+04	75
	9.65E-02	1.04E-01	1.00E+05	100

References

- ALGIERI, C, BERNARDO, P, GOLEMME, G, BARBIERI, G & DRIOLI, E. 2003. Permeation properties of a thin silicalite-1 (MFI) membrane. *Journal of Membrane Science*, 222: 181–190, June. 2.
- ASAEDA, M., YAMASAKI, S. 2001. Separation of inorganic/organic gas mixtures by porous silica membranes. *Separation and purification technology.* 25: 151-159.
- BAI, C., JIA, M.D., FALCONER, L. & NOBLE, R.D. 1995. Preparation and separation properties of silicalite composite membranes. *Journal of Membrane Science.* 165: 79-87.
- BAKKER, W.J.W., KAPTEIJN, F., POPPE, J. & MOULIJN, J.A. 1996. Permeation characteristics of a metal-supported silicalite-1 zeolite membrane. *Journal of Membrane Science.* 117: 57-78.
- BENES, N.E. 2000. Mass transport in thin supported silica membranes. (Thesis-phD) 161p.
- BIESHEUVAL, P.M., NIJMEIJER, A. & VERWIEJ, H. 1998. Theory of batch wise centrifugal casting. *AICHE Journal.* 44: 1914-1922.
- BURGGRAAF, A.J. 1999. Single gas permeation of thin zeolite (MFI) membranes: theory and analysis of experimental observations. *Journal of Membrane Science.* 155: 45-65.
- CHEN, X., YANG, W., LIU, J. & LIN, L. 2005. Synthesis of zeolite NaA membranes with high permeance under microwave radiation on mesoporous-layer-modified macroporous substrates for gas separation. *Journal of Membrane Science*: 1-11, Jan. 21.
- CHOI, G.G., DO, D.D. AND DO, H.D. 2001, Surface diffusion of adsorbed molecules in porous media: Monolayer, multilayer and capillary condensation regimes, *Industrial Engineering Chemistry Research*, 40:4005-4031
- DE LANGE, R.S.A. & BURGGRAAF, A.J. 1995. Analysis and theory of gas transport in microporous sol-gel derived ceramic membranes. *Journal of Membrane Science.* 104: 81-100.
- DE VOS, R.M., MAIER, W.F. & VERWEIJ, H. 1999. Hydrophobic silica membrane for gas separation. *Journal of Membrane Science.* 158: 277-288.
- DE VOS, R.M. & VERWEIJ, H. 1998. Improvement performance of silica membrane for gas separation. *Journal of Membrane Science.* 143: 37-51

- FAUSI, A.F., RIDZUAN, I.N & RAHMAN, S.A. 2003. Latest development on the membrane formation for gas separation. *Songklanakarin Journal of Science and Technology*, 24 (Suppl.): 1025-1043, Apr. 23.
- FUNKE, H, ARGO, A.M, BAERTSCH, C.D, FALCONER, J.L & NOBLE, R.D. 1996. Separation of close boiling hydrocarbons with silicalite zeolite membranes. *Journal of chemical society, Faraday transport*, 92(13): 2499-2502, Jan.23.
- FUNKE, H., KOVALCHICK, M.G., FALCONER, J.L. & NOBLE, R.D. 1996. Separation of hydrocarbon isomer vapours with silicalite zeolite membranes. *Journal of industrial engineering and chemical research*. 35 (5): 1575-1582, Jan.31.
- HSIEH, H.P. 1996. Inorganic Membranes for separation and reaction. 3rd ed. Netherlands: *Elsevier Science B.V.* 582 p.
- IEA CLEAN COAL CENTRE, 2003. Prospects for hydrogen from coal. London, U.K. Dec. Internet: http://www.iea-coal.org.uk.
- IWAMOTO, Y., SATO, K., INADA, T & KUBO, Y. 2005. A hydrogen-permselective amorphous silica membrane derived from polysilazane. *Journal of the European Ceramic Society.* 25: 257-264.
- KAPTEIJN, F, BAKKER, W.J.W, ZHENG, G, POPPE, J & MOULIJN, J.A. 1995. Permeation and separation of light hydrocarbons through a silicalite-1 membrane: Application of the generalized Maxwell-Stefan equations. *The Chemical Engineering journal*, 57: 145-153.
- KAPTEIJN, F, VAN DE GRAAF, J & MOULIJN, J.A. 1998. The Delft silicalite-1 membrane: peculiar permeation and counter-intuitive separation phenomena. *Journal of molecular catalysis A: Chemical,* 134 201-208.
- KAKPTEIJN,F., RAKKA, W.J.W., VAN DE GRAAF,J., ZHENG, G., POPPE,J. & MOULIJN,J.A. 1995. Permeation and separation behaviour of a silicalite-1 membrane. *Catalysis Today*, 25: 213-218.
- KAPTEIJN, F, VAN DE GRAAF, J.M. & MOULIJN, J. 2000. One-component permeation maximum: diagnostic tool for silicalite-1 membranes? *AICHE Journal,* 46 (5): 1096-1100, May.
- KIM, Y.S, KUSAKABE, K, MOROOKA, S & YANG, S.M. 2000. Preparation of microporous silica membranes for gas separation. *Korean Journal of Chemical engineering,* 18(1): 101-112, Nov.
- KOUKOU, M.K., PAPAYANNAKOS, N., MARKATOS, N.C., BRACHT, M., VAN VEEN, H.M. & ROSKAM, A. 1999. Performance of ceramic membranes at elevated pressures and

temperatures: effect of non-ideal pressure conditions in a pilot scale membrane separator. *Journal of Membrane Science*. 155: 241-259.

- KRISHNA, R. & PASCHEK, D. 2000. Separation of hydrocarbon mixtures using zeolite membranes: a modelling approach combining molecular simulations with the Maxwell-Stefan theory. *Journal of separation and purification technology*, 21: 111-136, May.29.
- KRISHNA, R & VAN DEN BROEKE, L.P.J. 1995. The Maxwell-Stefan description of mass transport across zeolite membranes. *The chemical engineering journal*, 57: 155-162.
- LEE, D., ZHANG, L., OYAMA, S.T., NIU, S. & SARAF, R.F. 2004. Synthesis, characterization and gas permeation properties of a hydrogen permeable silica membrane supported on porous alumina. *Journal of Membrane Science*. 231: 117-126. Oct. 30.
- MULDER, M. 1998. Basic principles of membrane technology. 2nd ed. Dordrecht: Kluwer academic publishers. 564 p.
- NAIR, S, LAI, Z, NIKOLAKIS, V, XOMERITAKIS, G, BONILLA, G & TSAPATSIS, M. 2001. Separation of close-boiling hydrocarbon mixtures by MFI and FAU membranes made by secondary growth. *Microporous and Mesoporous Materials*, 48: 219-228, Jan. 17.
- NUNES, D. 2003. The removal of water from n-octane/water mixtures using a supported zeolite membrane. (Dissertation – M.Eng.) 115 p.
- PETERS, T.A., FONTALVO, J., VORSTMAN, M.A.G., BENES, N.E., VAN SOEST-VERCAMMEN, E.L.J. & KEURENTJIES, J.T.F. 2005. Hollow fibre microporous silica membranes for gas separation and pervaporation Synthesis performance and stability. *Journal of Membrane Science*. 248: 73-80.
- PRESENT, R.D.& DEBETHUNE, A.J. 1948. Separation of a gas mixture flowing through a long tube at low pressure. *Phys. Rev.* 75: 1050-1057.
- SCHURING, D. 2002. Diffusion in zeolites: Towards a microscopic understanding. (Thesis – D.Tech).
- SEADER, J.D. & HENLEY, E.J. 1998. Separation Process Principles. *John Wiley & Sons, Inc.* New York. 713-777
- SO, J., YANG H.S., & PARK, S.B. 1998. Preparation of silica-alumina composite membranes for hydro separation by multi-step pore modifications. *Journal of Membrane Science*. 147: 147-158
- SOMMER, S % MELIN, T. 2005. Performance evaluation of microporous inorganic membranes in the dehydration of industrial solvents. *Chemical Engineering and Processing* 44: 138-1156

- STEENKAMP, G.C. 2000. Centrifugal casting and coating of tubular ceramic membrane supports. (Dissertation – M.Eng.)
- TOMITA, T, NAKAYAMA, K & SAKAI, H. 2004. Gas separation characteristics of DDR type zeolite membrane. *Microporous and Mesoporous materials*, 68: 71-75, Nov.29.
- TSAI, C.Y, TAM, S, LU, Y & BRINKER C.J. 1999. Dual-layer asymmetric microporous silica membranes. University of New Mexico/NSF Centre for Micro-engineering materials. U.S.A.
- UHLHORN, R.J.R. 1990. Ceramic membranes for gas separation. Synthesis and transport properties. (thesis-PhD) University of Twente, Netherlands.
- VAN BEKKUM, H, FLANIGEN, E.M & JANSEN, J.C. 1991. Introduction to zeolite science and practice. *Elsevier.*
- VAN DEN BROEKE, L.J.P, KAPTEIJN, F & MOULIJN, J.A. 1998. Transport and separation properties of a silicalite-1 membrane –II. Variable Separation Factor. *Chemical Engineering Science*, 54: 259-269, Aug.14.
- VAN DE GRAAF, J.M. 1999. Permeation and Separation Properties of Supported Silicalite-1 Membranes: A Modelling Approach. (Thesis – PhD) 208 p.
- VROON, Z.A.E.P, KEIZER, K, GILDE, M.J., VERWEIJ, H & BURGGRAAF, A.J. 1996. Transport Properties of alkanes through ceramic thin zeolite MFI membranes. *Journal of Membrane Science*, 113: 293-300, Apr. 3.
- VROON, Z.A.E.P. 1995. Synthesis and transport studies of thin ceramic supported zeolite (MFI) membranes. (Thesis – PhD)
- XU, X., BAO, Y., SONG, C., YANG, W., LIU, J. & LIN, L. 2004. Synthesis, characterisation and single gas permeation properties of NaA zeolite membrane. *Journal of Membrane Science*. 249 p. 51 – 64.
- XU, X, WEISHEN, Y, LIU, J &LIN, L. 2001. Synthesis of NaA zeolite membranes from clear solution. *Microporous and Mesoporous Materials*. 43: 299 – 311, Jan 10.
- XU, X., YANG, W., LIU, J. & LIN, L. 2001. Synthesis of NaA zeolite membrane from clear solution. *Microporous and Mesoporous Materials.* 43: 299-311.
- Zah, J. 2005.

INTERNET SITES:

- http://www.colorado.edu/che/FalcGrp/research/zeolite.html